

NASA Technical Paper 1243



LOAN COPY: RETURN TO
AFWL TECHNICAL LIBRARY
KIRTLAND AFB, N.M.

Characteristics of Mach 10 Transitional and Turbulent Boundary Layers

Ralph D. Watson

NOVEMBER 1978

NASA



NASA Technical Paper 1243

Characteristics of Mach 10
Transitional and Turbulent
Boundary Layers

Ralph D. Watson
*Langley Research Center
Hampton, Virginia*



National Aeronautics
and Space Administration

**Scientific and Technical
Information Office**

1978

CONTENTS

SUMMARY	1
INTRODUCTION	1
SYMBOLS	3
EXPERIMENTAL APPARATUS AND TECHNIQUES	6
Facility and Test Conditions	6
Models	6
Heat-Transfer Measurements	7
Pressure Measurements	8
Skin-Friction Measurements	8
Survey Probes	9
Pitot probes	10
Static-pressure probe	10
Total-temperature probes	11
RESULTS AND DISCUSSION	11
Schlieren Photographs	11
Tabulated Data	12
Combined-data test cases	12
Heat-transfer data	12
Skin-friction data	12
Surface-pressure data	12
Pitot-pressure data	13
Total-temperature data	13
Free-Stream and Local Flow Properties	13
Model 1	15
Model 2	15
Heat-Transfer Distributions	16
Surface-Pressure Distributions	18
Skin-Friction Data	18
Mean Velocity Profiles	19
Total-Temperature Profiles	21
Static-Pressure Surveys	23
Reynolds Analogy and Recovery Factor	23
DERIVED TURBULENCE PARAMETERS	25
COMPARISONS WITH FINITE-DIFFERENCE CALCULATIONS	29
CONCLUDING REMARKS	33
APPENDIX A - PROBE EFFECTS ON WALL PRESSURE	34
APPENDIX B - PITOT PRESSURE CORRECTIONS IN RAREFIED HELIUM FLOW	36
REFERENCES	38
TABLES	44
FIGURES	236

SUMMARY

Measurements of the mean flow properties of transitional and turbulent boundary layers in helium on 4° and 5° wedges have been made for flows with edge Mach numbers from 9.5 to 11.3, ratios of wall temperature to total temperature of 0.4 to 0.95, and maximum length Reynolds numbers of 100×10^6 . The data include pitot and total-temperature surveys and measurements of heat transfer and surface shear. In addition, with the assumption of local similarity, turbulence quantities such as the mixing length were derived from the mean flow profiles. Low Reynolds number and precursor transition effects were significant factors at these test conditions and were included in finite-difference boundary-layer predictions.

The skin-friction data could be reasonably well predicted; however, heat-transfer and total-temperature survey data at a wall temperature slightly above the adiabatic wall value could not. Peaks in the distributions of wall heating, surface shear, and surface pressure did not occur at the same locations, the discrepancy being a function of the ratio of wall temperature to total temperature.

INTRODUCTION

The optimum structural and aerodynamic design of hypersonic aircraft will rely on accurate predictions of the mean flow characteristics of transitional and turbulent boundary layers at flight conditions. The prediction of these characteristics at Mach numbers above 5 is uncertain in many cases. For example, the widely used methods of Spalding and Chi (ref. 1) and Van Driest (ref. 2) for predicting turbulent flat-plate skin friction differ by 10 percent at Mach 11 in helium at $T_w/T_t = 0.3$. Unfortunately, the difference increases as the ratio of wall temperature to total temperature T_w/T_t decreases, and it is the cold wall conditions which are of practical interest at high Mach numbers. Future vehicle design codes will probably utilize finite-difference boundary-layer predictive methods to determine boundary-layer induced effects on the flow field as well as to determine shear drag and heating loads. Only finite-difference methods, compared with integral methods, offer the potential to expand into fully three-dimensional field calculations. (See ref. 3.)

In the finite-difference calculation of turbulent boundary layers, assumptions must be made for closure of the equations. Various degrees of complexity in the resulting algorithm depend on the type of assumptions made for closure. (See refs. 4 and 5.) The simplest method utilizing mean field closure relates the turbulent shear stress to the mean velocity field through either a mixing length or eddy viscosity model (ref. 6) and turbulent heat flux to the turbulent shear stress through the turbulent Prandtl number. Thus, the mixing length, viscosity, and turbulent Prandtl number must be specified. Mixing length and eddy viscosity distributions through turbulent boundary layers have

been found to be almost invariant functions of y/δ at high Reynolds numbers from incompressible to supersonic flow. In the initial stages of turbulent flow the turbulence length scales are functions of the local Reynolds number even for incompressible flow (ref. 7). This phenomenon, known as the "low Reynolds number effect," becomes of increasing importance at high Mach numbers where large extents of transitional and low Reynolds number flow can exist. Reference 8 demonstrates that the outer mixing length variation can be broadly classified into "nozzle flows" and "flat plate flows," that is, turbulent flows having a previous history of large negative pressure gradient, and those without such a history. For each type the effect of compressibility on the correlation with Reynolds number does not appear to be too large.

Similarly, at low Reynolds numbers, the turbulent Prandtl number has been shown to be a function of the Reynolds number. (See refs. 9 and 10.) At low speeds and high Reynolds numbers in air, the commonly assumed turbulent Prandtl number of 0.9 works well; however, supersonic flat-plate flow and total-temperature profiles could not be predicted by use of a constant turbulent Prandtl number in reference 9.

In addition to possible Mach number influences on low Reynolds number effects for mixing length and turbulent Prandtl number, transition itself may not occur in the same way at high Mach numbers as at low Mach numbers. Disturbances indicative of boundary-layer transition occur near the outer edge of the boundary layer in high-speed flow (ref. 11) and spread toward the surface at a shallow angle (ref. 12). At the surface the heat-transfer rate begins to deviate from laminar heat transfer near where the disturbances reach the surface (ref. 13). Inclusion of this "precursor transition effect" was shown in references 14 and 15 to improve agreement between calculated and measured boundary-layer properties. Most boundary-layer prediction schemes do not incorporate this effect since little data exist on which to model it.

Finally, intermittency factors in compressible flow, both streamwise in the transition region and normal to the flow in the turbulent region, have seldom been measured. A measurement at Mach 7 in reference 16 has shown that streamwise intermittency is similar to the incompressible distribution which is used in many finite-difference prediction methods (e.g., ref. 5). Intermittency normal to the surface at Mach 9.37 is shown to be very different from the incompressible distribution in reference 17. The effect of surface normal intermittency on mean flow quantities calculated by a finite-difference solution is examined in this report.

The experiments described in this report were undertaken to better define the effects discussed previously in a highly compressible (high Mach number) boundary layer at high length Reynolds numbers. This was accomplished by comparing mean flow data from transitional and turbulent boundary-layer flow with finite-difference calculations in which each effect could be incorporated independently. Measurements were made in a boundary layer having a nominal edge Mach number of 10 on sharp flat plates at 4° and 5° incidence to the flow. Ratios of wall temperature to total temperature ranged from 0.4 to 1 at a maximum length Reynolds number of 100×10^6 . Data from two separate investigations, reported in part in references 15 and 18, have been compiled and tabulated, together with additional data which could not be included in those references

because of space limitations. In terms of the density variation across the boundary layer, the Mach 10 helium boundary layer corresponds to an air boundary layer at Mach 13. (See ref. 19.)

The following boundary-layer characteristics were measured: surface heat-transfer distributions, pressure distributions, skin friction (direct measurements by skin-friction balance), pitot surveys, and total-temperature surveys at several stations along the models. In addition, mixing length, eddy viscosity, and turbulent Prandtl number distributions were derived from the data by assuming local similarity.

Appendix A discusses the increase in wall pressure measured beneath the tip of survey probes as the probes approached the wall. The magnitude of rarefaction effects on pitot-pressure boundary-layer survey data was investigated by Leonard Weinstein and included as appendix B to this report. No rarefaction correction was necessary for the present data.

SYMBOLS

C	constant in equation (3)
c_f	local skin-friction coefficient, $2\tau_w/\rho_e u_e^2$
c_p	specific heat at constant pressure
d	probe diameter
F_T	$= \frac{T_t - T_w}{T_{t,e} - T_w}$
G_1, G_2	gradient quantities defined in equation (11)
H	total enthalpy
h	probe tip thickness
I_1, I_2, I_3	integral quantities defined in equation (11)
k	slope of mixing length at wall
l	mixing length
M	Mach number
N	velocity profile exponent
N_{Pr}	molecular Prandtl number
$N_{Pr,t}$	static turbulent Prandtl number

N_{St}	Stanton number, $q_w/\rho_e u_e c_p (T_{aw} - T_w)$
p	pressure
p_s	static probe pressure
Q	total heat-transfer rate, see equation (10)
q	heat-transfer rate
R	Reynolds number
R_p	Reynolds number based on x at peak value of recovery factor
R_T	Reynolds number based on total temperature and probe thickness
S	Reynolds analogy factor
T	temperature
$T_{support}$	temperature of needles supporting fine wire on total-temperature probe
T_{wire}	temperature of fine wire of total-temperature probe
u	velocity
u^*	generalized velocity, see equation (2)
u_τ	shear velocity, $(\tau_w/\rho_w)^{1/2}$
x, y	model coordinates, see figure (2)
x_T	beginning of transition from q measurements
$x_{T,e}$	peak heating location
y^+	$= \frac{y u_\tau}{\nu_w}$
Γ	intermittency
γ	ratio of specific heat
δ	derived boundary-layer thickness
δ_p	pitot boundary-layer thickness
δ_u	velocity boundary-layer thickness

δ^* displacement thickness, $\int_0^\delta \left(1 - \frac{\rho u}{\rho_e u_e}\right) dy$

$$\delta_I^* = \int_0^\delta \left(1 - \frac{u}{u_e}\right) dy$$

$$\delta^+ = \frac{\delta u_\tau}{\nu_w}$$

ϵ eddy viscosity

η recovery factor

θ momentum thickness, $\int_0^\delta \frac{\rho u}{\rho_e u_e} \left(1 - \frac{u}{u_e}\right) dy$

μ molecular viscosity

ν kinematic viscosity

ρ density

τ shear stress

$$\phi = \frac{T_t - T_{\text{wire}}}{T_{\text{wire}} - T_{\text{support}}}$$

Subscripts:

aw adiabatic wall value

e at edge of boundary layer

L laminar value

max maximum value

min minimum value

T turbulent value

t total value

w wall value

x,y based on x,y coordinates

- 1 free-stream value
- 2 value behind model shock wave
- θ based on momentum thickness

Primes denote a quantity transformed to equivalent incompressible value.

EXPERIMENTAL APPARATUS AND TECHNIQUES

Facility and Test Conditions

Tests were run in the Mach 20 leg of the high Reynolds number helium tunnel complex, described in detail in reference 20. The free-stream Mach number varies from 16.3 to 18.5 as a function of the tunnel stagnation pressure and location in the test section. The Mach number gradient in the test section region is 0.125 per meter, and the inviscid core size is approximately 40 cm in diameter. Tunnel run time is approximately 5 sec, including an initial 1 sec of starting transients. During starting transients the stagnation pressure rises smoothly to the desired level with little or no overshoot. The total temperature momentarily peaks at about 370 K and decreases rapidly to slightly above the initial temperature in the storage tanks. It then decreases linearly as the reservoir helium is depleted. Total temperature for the tests was approximately 305 K. Free-stream unit Reynolds numbers ranged from 9.8×10^6 to 46.0×10^6 per meter, obtained by operating at stagnation pressures from 2760 to 13 800 kPa.

For the first series of tests the leading edge of the model was located 12.7 cm below the tunnel center line and 42.5 cm downstream of the nozzle test section joint. An estimate of the Mach number at the leading edge of the model was made from the tunnel calibration of reference 20 and checked against the Mach number which was obtained from the ratio of pitot pressure measured on the model center line below the leading edge to the tunnel stagnation pressure. Estimated and measured Mach numbers are shown in figure 1 to be in excellent agreement; thus, the model blockage did not alter the free-stream flow. For the second series of tests the model leading edge was 10.2 cm below the tunnel center line and 17.1 cm from the nozzle test section joint.

Models

Data were obtained on two models, designated "model 1" and "model 2" shown in the sketches of figure 2. Model 1 was used to study the characteristics of transitional and turbulent boundary layers at near-adiabatic wall conditions. The results from the investigation of model 1 clearly demonstrated the need for additional data at cold wall conditions. Therefore, to investigate the effect of T_w/T_t , model 2 was designed to be cooled internally with liquid nitrogen.

Model 1 was a sharp flat plate at 5° incidence to the flow, 101.5 cm wide by 236 cm long. The leading-edge thickness was 0.013 cm with the underside beveled at 17° . The top surface consisted of type 347 stainless-steel plates

0.476 cm thick supported by an aluminum frame mounted on six floor struts. (See figs. 2(a) and 2(b).) Interchangeable sections along the model center line contained the instrumentation. End plates were required to prevent flow divergence over the upper surface of the model since the ratio of wedge to free-stream static pressure was approximately 7.5. The end plates were 12.9 cm high at the base of the model, and located 30.5 cm from and parallel to the model center line. From oil-flow measurements with end plates attached, no discernible surface flow divergence was present over the 15.24-cm-wide instrumentation strip. Without end plates, divergence angles of up to 2° were measured. Skin-friction balances were fitted to an interchangeable surface plate at stations 74.2, 99.6, 125.0, and 211.2 cm from the leading edge of the model.

Model 2, shown in figure 2(c), was a flat plate at 4° incidence 61 cm by 229 cm and having a sharp leading edge of 0.1-mm maximum thickness. It was constructed of type 347 stainless steel to withstand cryogenic temperatures and an internal pressure of 410 kPa. It consisted of three sections: the leading edge, a forebody, and an afterbody with two chambers along the center line in the forebody and afterbody sections which contained the instrumentation. A manifold under the model distributed liquid nitrogen to each section and exhausted gaseous nitrogen outside the tunnel. The model was sealed with annealed copper and stainless-steel O-rings to prevent contamination of the test gas with nitrogen.

End plates extended to the height of the calculated inviscid shock to diminish end effects over the surface. Oil-flow tests at near-adiabatic wall conditions showed that the flow was two-dimensional over the center instrumentation strip and most of the surface for the range of free-stream test conditions covered in the investigation. Small corner effects were observed at the juncture of the end plates and the model surface.

Mean flow surveys and skin-friction measurements were made at seven center-line stations: 50.5, 75.9, 101.3, 136.9 (131.2 for skin friction), 165.1, 190.5, and 215.9 cm from the leading edge. Additional surveys were made 35.6 cm from the leading edge.

Heat-Transfer Measurements

Surface heating rates on both models were measured by using thermocouples and standard thin-skin calorimeter assumptions. (See ref. 21.) The surface material for both models was type 347 stainless steel having a specific heat of 458.1 J/kg-K at 311 K and a density of 7.9 g/cm³ at room temperature. The variation of these properties with temperature, taken from reference 22, was used in the data reduction program.

The skin thickness on model 1 varied from 0.0152 to 0.0160 cm, and heating rates ranged from near zero to a maximum of about 0.159 W/cm². The low heating rates were due to the small thermal potential over the model; in fact, T_{aw} approached T_w in certain regions of transitional flow as the recovery factor changed from the laminar to the turbulent value. Scatter in the data is attributed to the inherent inaccuracy involved in measuring low heating rates by the thin-skin method. The 36-gage iron-constantan thermocouples used to instrument

the model produced negligible conduction errors: calculations of spanwise and chordwise conduction errors also showed these to be negligible.

On model 2 the skin thickness was approximately 0.051 cm with 30-gage iron-constantan thermocouples spot-welded to the underside. Thermocouple conduction errors were calculated to be insignificant, and the error due to the local non-uniformity in surface temperature caused by the thin skin was estimated to be less than 1 percent. For some cold wall cases to be presented the distribution of T_w/T_t was nonuniform; however, the magnitude of surface conduction errors due to the nonuniformity was not estimated for each case.

Pressure Measurements

A variety of pressure-measuring devices was used to cover the wide range of pressures encountered in the investigation. Tunnel stagnation pressures were measured with bonded strain-gage transducers accurate to 0.25 percent of full-scale output. A range of transducers was used that gave stagnation pressures accurate to better than 1 percent.

Model surface pressures were measured with variable capacitance transducers having a manufacturer's quoted accuracy of 0.5 percent of the reading. Static-pressure probe data were taken with a miniature variable capacitance transducer accurate to 0.5 percent of its rated full scale of 6.9 kPa.

Pitot pressures were measured with two types of transducers, a miniature "integrated sensor" transducer and an unbonded strain-gage transducer of low internal volume. Combined nonlinearity and hysteresis of the integrated sensor transducer was 1 percent of its listed full range of 34.5 kPa. It is estimated that hysteresis was the dominant source of error in this transducer and produced a maximum error in pressure measurement of 350 Pa. The unbonded strain-gage transducer was accurate to 0.5 percent of its full-scale output of 172.4 kPa.

The integrated sensor transducer was found to be extremely sensitive to temperature change whereas the strain-gage transducer was not. For surveys on model 2 with an integrated sensor transducer, the transducer was maintained at $306\text{ K} \pm 3\text{ K}$ by wrapping the transducer with platinum resistance wire to form a heater. The heater was controlled automatically by use of a thermocouple bonded to the transducer.

Skin-Friction Measurements

Skin friction was measured with commercially available floating element balances of the self-nulling type. The drag elements were 0.94 cm in diameter surrounded by a gap of 0.064 mm. Prior to the skin-friction tests, measurements of transient pressures on the surface of model 1 during tunnel start and shutdown showed the loads to be well within the safe operating range of the balances. The balances were calibrated before and after a series of runs, and the change in sensitivity was no more than 0.05 percent; thus, the output of the balances did not change from run to run. The balances were carefully fitted to interchangeable instrumentation plates (see fig. 2(a)) so that they

were no more than 0.03 mm below the surface. The error on the measured force due to protrusion and gap size is estimated to be less than 5 percent, based on figure 7 of reference 23.

On model 2 balances were required to operate at cryogenic temperature as well as under tunnel vacuum. The operation and calibration of several balances were checked in a vacuum chamber at a pressure of 670 Pa and near liquid nitrogen temperature. Two balances were found to be suitable for use at these conditions. After calibration, the balances were carefully fitted to cases which were installed in the instrumentation chambers as shown in figure 3.

Before each cold wall run, model 2 was cooled to liquid nitrogen temperature (≈ 77 K) in the tunnel at a pressure between 1000 and 2000 Pa. A slight haze formed on the surface of the model at these conditions. The model surface in the vicinity of the skin-friction balance was kept free of haze by a jet of pure helium. (See fig. 3.) Prior to the run, the jet mechanism was retracted to avoid flow-field interference. Intermediate T_w/T_t runs were made by letting the model warm up uniformly to the desired temperature.

Survey Probes

Surveys on model 1 were made by mounting the probe on a pneumatic mechanism under the model with the probe extending through the surface of the model. Figure 4 shows the mounting arrangement. Transducers were located as close as practical to the tip of the probe to minimize pressure lag effects (about 20.3 cm). A pressure transducer was also mounted under the model in a shielded instrumentation channel to measure surface pressures beneath the tip of the probes.

Because of the rather large increases in surface pressure on model 1 as the probes approached the wall, the survey probes for model 2 were mounted on a mechanism above the model with the stem of the probe extending upward instead of through the surface of the model. Probe effects on the wall pressure, discussed in appendix A, were found to be approximately the same for both mounting arrangements. The probes were mounted on a hydraulic mechanism automatically controlled to survey the boundary layer in a series of steps. The stepping rate frequency and dwell time at each step could be independently controlled to survey a desired height within the available run time. It was found that very high stepping rates with short dwell times could be used. The data were recorded continuously at 40 frames per second per channel and, for some early surveys, data points between steps were discarded. In later surveys all data points were retained; thus, some plots were given the appearance of a "noisy" electrical signal. This is due to probe movements with a small but finite pressure lag time.

The probe position for both models was measured with a potentiometer specified to be linear within 0.2 percent of its maximum travel of 16.5 cm. Calibrations over a limited range of travel further reduced this error. On model 2 with the probe mounted above the model, errors due to movement of the survey mechanism under run loads were minimized by using a foul indication when a needle attached to the probe touched the surface. The maximum error in height mea-

surement occurred because of the error involved in measuring the height of the probe at foul. This error is estimated to be about 0.013 cm.

Pitot probes.- A sketch of the pitot probe used on model 1 is shown in figure 5(a). A flattened tip rather than a round tip of the same height was used to provide a larger face area and thus minimize pressure lag effects. Surveys at different traverse speeds showed no discernible lag effects, and data were recorded while the probe traversed the boundary layer at a constant slow speed.

The same probe was initially used on model 2 to determine whether mounting the probe above the model instead of through the surface (as for model 1) would decrease probe interference effects. When it was found that the effects were about the same in both cases, smaller probes designed to reduce probe interference effects were tested. A probe having a circular orifice diameter of 0.51 mm was the smallest which could be tested without excessive pressure lag effects. A sketch of this probe is shown in figure 5(b). This probe decreased the pressure rise at the wall by almost a factor of 2.

It was anticipated that pitot pressure readings might be influenced by rarefaction effects in the boundary layer close to the model wall. Accordingly, a study of these effects was made by Leonard Weinstein and is included in appendix B of this report. For the range of conditions covered by the present data, the rarefaction corrections of appendix B were significant only for the $R_1/m = 7.8 \times 10^6$ case of model 1 deep within the boundary layer. For this reason no rarefaction corrections were made to the data.

Static-pressure probe.- In reference 5, it is shown that in a turbulent boundary layer at Mach 10, the wall pressure should be about 10 percent higher than the edge static pressure. An attempt was made to measure the static-pressure distribution through the boundary layer on model 1 by using the flow-aligned cone-cylinder probe shown in figure 5(a). The probe had a 42.5° half-angle conical tip attached to a cylindrical afterbody in which four orifices were drilled circumferentially to minimize pressure lag effects.

Pressure measurements on simple bodies, if little affected by self-induced viscous effects, can be nondimensionalized by the local pitot pressure to uniquely determine the local Mach number and thus the local static pressure. On a cone or wedge small enough to survey the boundary layer, orifices would have been prohibitively small for the run time of the helium tunnel. A cone-cylinder probe having a 42.5° half-angle cone tip was chosen based on the results of reference 24, where it was shown that the pressure on the cylindrical afterbody 3.8 diameters downstream of the tip is almost independent of Reynolds number. Inviscid calculations by the method of characteristics were used to relate $P_s/P_{t,2}$ to M_1 as shown in figure 6. Since errors in machining probes of this size are likely, calculations were made for noses of 40° and 42.5° to estimate the effect which a 2.5° variation in the cone tip would have on the calibration curve. Analysis of the pressure measured at the outer edge of the boundary layer showed the 40° inviscid calibration curve to be more nearly correct for the probe used in these surveys.

The calibration curve of figure 6 shows that for a constant error in the ratio $P_s/P_{t,2}$, the error in indicated Mach number increases as M_1 increases.

At a Mach number of 10 for this probe in helium, a ± 2 -percent error in P_s/P_t ,² results in a ± 5 -percent error in Mach number and a corresponding ± 9 -percent error in static pressure. Also, above Mach 4, the tip geometry becomes of increasing importance as the Mach number increases.

Total-temperature probes.- Total-temperature surveys were made on model 1 at station 4 using a shielded fine wire resistance probe described in reference 25. See figure 5(a) for a sketch of the probe. The probe was calibrated in the 3-inch Mach 20 calibration apparatus at the Langley Research Center hypersonic helium tunnel and in a low density supersonic nozzle using the techniques described in reference 25. The resulting calibration is shown in figure 7. The faired curve used for data reduction was within 8 percent of the calibrated data, except for one point which was evidently in error. Data from the probe during a survey consisted of the wire resistance, which was converted to temperature, and the temperature of one support needle, which was measured with a thermocouple. It was necessary to combine the fine wire data with a pitot survey at the same conditions which, with the assumption of constant static pressure through the boundary layer, provided Mach number and total-pressure distributions through the boundary layer. With the Mach number, total pressure, wire temperature, and support temperature known at a point, the unknown true total temperature was obtained from the fairing of figure 7 by iteration. The total temperature at the edge of the boundary layer at the same x-location as the survey probe was measured with a conventional shielded thermocouple probe of 0.32-cm outside diameter.

For model 2 the total-temperature probe shown in figure 5(b) was used. This probe, described in reference 26, differed from the probe used on model 1 in that the sensing element was a coiled tungsten wire with a length-to-diameter ratio of approximately 800 which effectively eliminated end loss corrections. A tunnel calibration covering a range of Mach numbers and Reynolds numbers, necessary for the shielded straight wire probe, was not needed. Oven calibrations relating wire resistance to temperature were used in reducing the data. A current of approximately 1 ma was used to measure wire resistance without appreciably heating the wire. The total temperature at the edge of the boundary layer was measured with a similar coiled-wire probe having a tip thickness of 0.1 mm. The time constant for the coiled-wire probe was much smaller than that for a shielded thermocouple probe, a significant factor which will be discussed in the presentation of the total-temperature data.

RESULTS AND DISCUSSION

Schlieren Photographs

Spark schlieren photographs of a 10° half-angle cone in the tunnel used for the present investigation showed distinct turbulent "bursts" occurring before heat-transfer data indicated transition (ref. 27), whereas schlierens on a 2.87° cone in the same tunnel showed only a wavy boundary-layer structure ahead of transition with no bursts (ref. 28). For the 10° cone, the boundary-layer edge Mach number was 7.6; for the 2.87° cone, it was about 14. Schlieren photographs were made to determine whether bursts could be detected at the present boundary-layer edge Mach numbers of 10 to 11. Spark schlieren photographs

of model 1 with end plates removed are shown in figure 8 for a range of free-stream Reynolds numbers from 5.48×10^6 to 42.33×10^6 per meter. The spark duration of 1/4 microsecond stopped large-scale disturbances moving at the free-stream velocity of 1758 m/sec.

The interpretation of schlierens on a two-dimensional body is different from that on an axisymmetric body. For the wedge the schlieren presents an integrated view in the spanwise direction, whereas for a cone, the view is a vertical section of the flow field. Large-scale disturbances are visible in the photographs of figure 8; however, it has been concluded that they are due to an interaction between the model shock wave and the tunnel-wall boundary layer. No features which could be identified as bursts were detected in the present photographs. The width of model 1 was 101.5 cm whereas the inviscid core size is approximately 50.8 cm. The shock system of the model extended well into the tunnel-wall boundary layer. Schlieren photographs of model 2 were taken; however, they are similar to the photographs of figure 8 and are not presented.

Tabulated Data

Since the amount of tabulated data presented in this report is large, a brief description of the organization of tables 1 to 6 is given. In table 1 the data from subsequent tables are referred to by case number, rather than run number. In tables 2 to 5 cases composed of one or two runs are listed in a logical sequence determined by the test conditions. Contents of the tables are as follows:

Combined-data test cases.- Pitot survey, total-temperature survey, skin friction, and surface pressure data obtained at approximately the same free-stream unit Reynolds number were combined to produce a test case. For model 1 five test cases are listed in part (a) of table 1 at nominal R_1/m from 9.8×10^6 to 44.9×10^6 . For model 2, three test cases are listed in part (b) of table 1 at $R_1/m = 46 \times 10^6$ for $T_w/T_t = 0.4, 0.5, \text{ and } 0.95$. Included in table 1 are the integral thicknesses θ and δ^* as well as δ_u and δ_p for each profile.

Heat-transfer data.- Tunnel stagnation conditions for models 1 and 2 are summarized in part (a) of table 2. Part (b) of table 2 lists values of q , T_w , and T_w/T_t at each thermocouple location for both models.

Skin-friction data.- For model 1, measurements are listed in table 3 at four stations for five free-stream test conditions. For model 2 the data are listed at one free-stream test condition for $T_w/T_t \approx 0.92, 0.5, \text{ and } 0.35$. Two additional measurements at station 8 are listed for $Re_x \approx 150 \times 10^6$ and $T_w/T_t = 0.92$ and 0.35 .

Surface-pressure data.- Surface-pressure data on model 1 are listed in part (a) of table 4, nondimensionalized by the free-stream static pressure. Surface pressures were interpolated from these data for table 1 at the test conditions of table 1. Data on model 2 are listed in part (b) of table 4 for R_1/m from 14.1×10^6 to 46.2×10^6 and $T_w/T_t = 0.99$ and 0.35 .

Pitot-pressure data.- Part (a) of table 5 is a summary of tunnel stagnation chamber conditions at which the listings of part (b) of the table were taken. For the model 2 listings in part (b), the listings consist of measured pitot pressures corrected to a nominal constant tunnel stagnation pressure. Each point has been multiplied by the ratio of p_t (in kPa)/13 789.6.

Total-temperature data.- Part (a) of table 6 is a summary of stagnation chamber conditions for the listings of part (b). In part (b) the point at which the wall pressure rise began is marked for the data of model 1. For model 2 the survey data at station 1, $T_w/T_t = 0.5$ contained large discrepancies and were discarded.

Free-Stream and Local Flow Properties

Since model blockage did not alter the free-stream Mach number, measurement of the tunnel stagnation pressure uniquely determined the free-stream Mach number. Real-gas correction factors from reference 29 were used in conjunction with the ideal gas relations of reference 30 to calculate the properties of the flow. For Reynolds number calculations, the low-temperature quantum effect on the molecular viscosity of helium was included. Reference 31 shows that below about 8 K, the power-law viscosity-temperature relation is inaccurate. The following equation was found to predict the low temperature data presented in reference 31, while approaching the power-law relation at temperatures above 8 K:

$$\mu = 5.023 \left(\frac{T^{1.647}}{T + 0.83} \right) \quad (1)$$

where the unit for μ is micro poise and for T is kelvins. Equation (1) was used in the data reduction except as noted in tables 1 and 3. Values of T_t quoted in this report are as measured in the free stream and require no real-gas corrections. Stagnation chamber total pressures should be corrected by the factors of reference 29.

Accurate determination of the boundary-layer edge flow properties is difficult at hypersonic wind-tunnel conditions on slender bodies since the "inviscid" flow external to the boundary layer is rotational. For the free-stream Mach number - Reynolds number environment encountered in these investigations, the boundary layer on a slender body is thick enough to induce large shock curvature at the nose of the body. As a result, the Mach number as well as total and static pressures at the edge of the boundary layer vary along the body, and finite vorticity exists at the edge of the boundary layer. Near the leading edge where the shock curvature is very strong, it is difficult to distinguish a boundary-layer edge since the boundary layer merges with the shock layer. Similar problems in defining the boundary-layer edge on a flat plate at Mach 20 are discussed in reference 32.

Determination of the Mach number must be made by independently measuring two quantities such as the pitot pressure and the static pressure. Unfortunately, it was not possible to obtain accurate static-pressure boundary-layer

surveys at the present test conditions. There are indications that the static pressure at the wall may be about 10 percent higher than that at the edge of the boundary layer in the case of high-speed turbulent flat-plate boundary layers (see ref. 5); however, the exact distribution of pressure through the boundary layer is not accurately known at present. Without accurate static-pressure measurements, the measured wall pressure was assumed to be constant throughout the boundary layer in the reduction of the present data - a technique in general use for pitot boundary-layer reduction.

In the present analysis the Mach number and an effective local total pressure at the edge of the boundary layer were calculated from the experimental value of pitot pressure at the boundary-layer edge and the local surface static pressure using the ideal gas relations for helium from reference 30. The edge of the boundary layer was found by plotting pitot pressure against y and determining the point where deviation from the shock-layer pitot-pressure decay occurred. The trend characteristic of the shock-layer pitot-pressure decay was established from characteristics calculations of the flow field.

In order to estimate the variations in boundary-layer edge conditions with x which could be expected on the model 1 tests, inviscid calculations by the method of characteristics were made for the flow fields corresponding to the highest and lowest test unit Reynolds numbers. Since the calculations were made before flow field surveys had been completed, the boundary-layer edge conditions were estimated by finding an effective surface wedge angle which would give a surface pressure equal to the averaged measured surface pressure. The boundary-layer edge Mach numbers and Reynolds numbers were calculated from oblique shock relations using this effective wedge angle. Boundary-layer displacement thicknesses, calculated by the finite-difference method of reference 6 by assuming $dp/dx = 0$, were added to the 5° wedge surface. The resulting coordinates were used as body inputs to the method of characteristics program described in reference 33. Some details of the calculated flow fields for free-stream unit Reynolds numbers of 34.5×10^6 and 7.8×10^6 are shown in figure 9. Note the large expansion of the y -coordinate relative to the x -coordinate.

In the flow-field cross section shown in figure 9, a shock inflection point caused by the self-induced bluntness (the blast wave effect, see ref. 24) produces a point of minimum entropy at the shock, and results in a line of maximum local total pressure within the flow field almost parallel to the edge of the displacement thickness. The line of maximum total pressure appeared as a distinct peak in pitot pressure in the boundary-layer surveys. In the laminar region near the leading edge, the y -location of the peak pitot pressure is well above the displacement thickness; however, far downstream it is engulfed by the growing boundary layer and eventually disappears. Another feature is the line of minimum flow deflection angle within the flow field. The viscous-inviscid interaction produces a favorable pressure gradient near the beginning of transition. Within the transition region, δ^* decreases because of the rapid filling out of the velocity profile and then resumes growth in the turbulent flow. The expansion of the outer flow followed by a compression is evident in calculated and measured surface pressure distributions to be presented in a following section. A consequence of the expansion-compression process is that Mach lines tend to coalesce near the line of minimum flow deflection. For the

lowest Reynolds number case, a shock within the flow field limited the downstream extent to which calculations could be made.

In order to define the mean flow properties of the boundary layer, it was necessary to combine a large amount of data. Since the total temperature of the tunnel and the model wall temperature with no cooling depended on the ambient temperature, variations in T_w/T_t occurred from run to run. Pitot and total-temperature surveys were combined with wall pressure, skin friction, and heat-transfer data by these procedures.

Model 1.- Static-pressure survey data on this model were found to contain probe interference errors and were discarded. For the final data reduction, surface pressures measured at each probe tip location were plotted as a function of tunnel stagnation pressure. A wall pressure corresponding to the tunnel stagnation pressure at which pitot surveys were taken was interpolated from a plot and used as the local static pressure.

The local boundary-layer edge Mach numbers and Reynolds numbers varied with x at a constant nominal free-stream Mach number (or equivalently, nominal tunnel stagnation pressure). Local boundary-layer edge properties, listed in table 1, were used to reduce surface shear data to skin-friction coefficients. Average Mach numbers and Reynolds numbers representative of the edge conditions at the five nominal test stagnation pressures are as follows:

P_t , kPa	M_1	R_1/m	M_e	Re/m
2.76×10^3	16.88	9.80×10^6	9.5	9.62×10^6
5.45	17.38	18.86	9.7	18.75
7.93	17.60	27.49	9.7	27.50
10.48	17.70	36.32	10.0	37.06
13.10	18.05	44.87	10.1	46.57

Model 2.- Pitot pressures were corrected to a stagnation pressure of 13 790 kPa. Surface pressures were measured at hot and cold wall conditions; however, the variation of p_w with T_w/T_t was found to be so slight that a single local value of p_w/p_1 was used at each station for all values of T_w/T_t . Total-temperature surveys were combined with pitot surveys at slightly different values of T_w/T_t . The values of T_w/T_t quoted in table 1 are for the total-temperature surveys. Local values of q_w were required at each survey location to determine Reynolds analogy factors and as inputs for the calculation of turbulent Prandtl numbers. At each survey location, q_w/T_t from the heat-transfer data were plotted as functions of T_w/T_t at a nominal $R_1/m = 46 \times 10^6$. Values of q_w/T_t were interpolated from these plots at the value of T_w/T_t for the survey. Skin-friction coefficients were weak functions of T_w/T_t and R_x ; therefore, directly measured values of c_f were used.

As for model 1, the local edge conditions obtained from the survey data are listed in table 1. Nominal test conditions and average test conditions for which most data were taken are as follows:

$$p_t = 13\ 790\ \text{kPa}$$

$$T_t = 311\ \text{K}$$

$$M_1 = 18.05$$

$$M_e = 11.3$$

$$T_w/T_t = 0.40, 0.51, \text{ and } 0.95$$

$$R_1/m = 46 \times 10^6$$

$$R_e/m = 54 \times 10^6$$

Calculated displacement thicknesses were found to be insensitive to the choice of δ ; however, momentum thicknesses were very sensitive, especially at the most upstream survey stations. Thus, in some instances when δ may be somewhat arbitrary, an inviscid contribution can be present in the integrated values of θ in table 1, depending on the value of δ used in the data reduction.

Heat-Transfer Distributions

Measurements of surface heating rates were made on model 1 at free-stream unit Reynolds numbers from 9.9×10^6 to 43.2×10^6 at $T_w/T_t = 0.94$, and on model 2 for variable R_1/m and T_w/T_t . Based on the results of these measurements, stations were selected for surveying the boundary layer. The data are listed in table 2.

Heating rates on model 1 are shown in figure 10. A negative heating rate $-q$ denotes heat transfer from the surface to the flow, caused by the wall temperature being higher than the adiabatic wall temperature. The data were not reduced to Stanton numbers since the recovery factor was not known in transitional and turbulent flow for the present conditions. At a typical $T_w/T_t = 0.94$, a 5-percent error in recovery factor would result in a 73-percent error in Stanton number.

The hot wall data characteristically show a heating-rate decrease below the laminar value in the transition region, an effect which has been measured for hot wall heat transfer on a 10° wedge in reference 34 and on slender cones in reference 35, and has been attributed to a rapid increase in the recovery

factor in the transition region. Reference 36 shows that the recovery factor peaks in the transition region before decaying to the turbulent level downstream.

Heating rates on model 2 are presented in figure 11. At R_1/m about 40×10^6 and variable wall temperature (figs. 11(a) to 11(f)), no laminar heating region was measured, with the possible exception of the hot wall case ($T_w/T_t = 0.92$) shown in figure 11(f). At R_1/m about 20×10^6 , perhaps a short length of laminar heating can be discerned in figures 11(g) and 11(h). In figures 10 and 11 the point of maximum heating $x_{T,e}$ for each run is marked with the exception of figures 10(h), 10(i), and 11(t) where peak turbulent heating was not reached on the models.

Transition Reynolds numbers based on $x_{T,e}$ are shown in figure 12 along with data at a lower edge Mach number from reference 34. Two salient points are evident for the present data: the $T_w/T_t = 1$ data of model 2 show a definite increase in transition Reynolds number over cold wall transition at the same edge unit Reynolds number; and the peak heating transition Reynolds numbers on model 2 (4° wedge) are lower than those on model 1 (5° wedge).

The effect of wall temperature on hypersonic transition has been examined in references 37 and 38. In both references, an increase in transition Reynolds number was measured when T_w was greater than T_{aw} . For $T_w < T_{aw}$, a stabilizing effect in transition was found as T_w/T_t decreased at $M_e = 6.8$ in reference 37. At M_e above 8.8, wall cooling was found to have little, if any, effect on transition in reference 38. No clearly defined trend can be discerned in the present data at $R_1/m \approx 40 \times 10^6$ (figs. 11(a) to 11(e)) or at $R_1/m \approx 20 \times 10^6$ (figs. 11(g) to 11(l)); however, there is some uncertainty in the location of $x_{T,e}$.

The unit Reynolds number effect on peak heating Reynolds numbers is the same for the present data and the 10° wedge data of reference 34, as shown in figure 12. Slender cone transition exhibits a smaller unit Reynolds number effect in the Langley high Reynolds number helium tunnel complex (facility for present data) than in the 22-inch aerodynamics leg of Langley hypersonic helium tunnel facility (facility for data of ref. 34), an effect which has been attributed to the fact that the free-stream disturbance levels are different functions of the free-stream unit Reynolds number in the two tunnels. In reference 35 measured free-stream noise levels and their relation to cone transition in the two tunnels are discussed. The reason for the differences in cone and wedge transition behavior in the two tunnels is not known at present, nor is it clear why transition on model 1 (5° wedge) should be higher than that on model 2 (4° wedge). The leading-edge thickness was measured on model 1 and found to be 0.127 mm after the heat-transfer tests. After remachining the leading edge to 0.076 mm, check runs showed no change in the transition location. The leading edge on model 2 was 0.076 mm, whereas that on the 10° wedge of reference 34 was 0.051 mm. Bluntness Reynolds numbers, based on the free-stream unit Reynolds numbers, should not have been greatly different in all three cases.

Surface-Pressure Distributions

For model 1 the surface pressures along an equivalent body (δ^* added to the 5° wedge surface) were available from the method of characteristics solution discussed previously. These pressures, assumed to be the pressures on the surface of the model, are plotted in figure 13. A dip in the pressure distribution occurs as δ^* decreases in the transition region. It is followed by an increase to a peak pressure caused by compression of the flow as δ^* grows rapidly through the transition region.

Detailed measurements of the surface pressure on model 2 at $T_w/T_t = 0.99$ and 0.3 to 0.4 confirming the trend of the theoretical calculations are shown in figure 14. The data for R_1/m from 46.2×10^6 to 14.1×10^6 (fig. 14) show that at all test unit Reynolds numbers, the differences in both the level and position of the p/p_1 distribution between hot and cold wall conditions are small.

Also shown in figure 14 are the locations of peak heating from figure 11, designated with an arrow and marked with the figure number from which the location was read. For the cases so marked, the location of peak heating occurs upstream of the peak in surface pressure at $T_w/T_t = 0.4$. When $T_w/T_t \approx 1$, the location of peak heating moves downstream, coinciding with the peak pressure at $R_1/m = 40.8 \times 10^6$. The correspondence between peak heating and peak pressure locations for $T_w/T_t \approx 1$ is not as clear at $R_1/m = 19.9 \times 10^6$; however, the location of $x_{T,e}$ is uncertain, as can be seen in figure 11(m).

Skin-Friction Data

On model 1 skin-friction measurements were made at locations 74.24, 99.64, 125.04, and 211.50 cm from the leading edge. Data at five different unit Reynolds numbers for the four test locations are shown in figure 15(a). A baseline $dp/dx = 0$ laminar skin-friction calculation (method of ref. 39) is shown for Reynolds numbers between 4×10^6 and 40×10^6 . At station 1 for each test unit Reynolds number, that is, the most nearly laminar data points, the measured skin-friction coefficients are higher than the flat-plate laminar values. The effect of self-induced pressure gradients on skin friction was calculated by use of the weak interaction T' method of reference 40 for the pressure distribution and the method of reference 41 for correcting hypersonic flat-plate skin friction for pressure gradient effects. Calculations made for the five test Reynolds numbers merged into the single line shown in the figure. The effect of finite vorticity external to the boundary layer has been shown in reference 42 to increase skin friction. Since both effects are present at the present test conditions, the station 1 data points may not be unreasonably high. For comparison of skin-friction data with turbulent theory, the theory of Spalding and Chi from reference 1 is shown for transition Reynolds numbers based on a length of 80 percent of $x_{T,e}$, as recommended in reference 43. Peak heating values from figure 10 are also shown in the figure.

On model 2 skin-friction measurements were made at locations 50.5, 75.9, 101.3, 131.2, 165.1, 190.5, and 215.9 cm from the leading edge. Because of

physical constraints the balances could not be mounted at station 1 (35.6 cm from the leading edge), and the balance had to be installed at the fifth boundary layer survey station upstream 5.7 cm. Data taken at one nominal unit Reynolds number and three values of T_w/T_t are shown in figure 15(b). Additional data were obtained at station 8 by running at $R_l/m = 73.7 \times 10^6$ for $T_w/T_t = 0.35$ and 0.92. Boundary-layer edge conditions were extrapolated from the data at lower stagnation pressures since no surveys were made at this test condition. The most upstream measured skin-friction point at each unit Reynolds number appears to be transitional, as might be expected from the heat-transfer data of figure 11. As in figure 15(a), the laminar flat-plate theory of reference 39 is shown for $M_e = 11$ and $T_w/T_t = 0.3$ and 0.9 along with the effect of induced pressures on skin friction at $T_w/T_t = 0.9$ by the method of references 40 and 41. The turbulent skin-friction theories of references 1 and 2 (with $\gamma = 5/3$) are shown for $T_w/T_t = 0.3$, and of reference 1 for $T_w/T_t = 0.9$ since both theories give about the same results at near-adiabatic wall conditions.

Both the model 1 data and the model 2 data appear lower than turbulent theory when plotted against length Reynolds number in figure 15. Transformed to incompressible values and plotted as a function of R_θ , the turbulent data agree well with the incompressible Karman-Schoenherr skin-friction equation (see ref. 44), as shown in figure 16. The Spalding-Chi transformation factors of reference 1 were used to calculate the theoretical curve shown in figures 15 and 16; however, when the data are plotted as a function of R_θ , it is not necessary to specify a virtual origin for the turbulent boundary layer.

Mean Velocity Profiles

As previously stated, velocity profiles were calculated from pitot survey data by assuming constant static pressure through the boundary layer. In addition to the assumption of constant static pressure through the boundary layer, the total temperature must be known to calculate a velocity profile from a Mach number profile. Total-temperature profiles on model 1 were measured only at station 4 in turbulent flow. The profiles were different from the linear Crocco relation typical of most flat-plate data and were also different from the quadratic relation typical of nozzle wall data. (See ref. 45.) At the slightly hot wall conditions of model 1, it was found in reference 15 that the profile parameters were not sensitive to the choice of assumed total-temperature distribution. Integral values of δ^* and θ reduced by using both the linear Crocco relation and an assumed constant total temperature showed only slight differences. In this report the model 1 velocity profiles were reduced by using the linear Crocco relation; the reason for using this relation is discussed in a later section. The integral boundary-layer properties listed in table 1 were obtained by this method.

For many years, attempts have been made to reduce turbulent compressible profiles to an equivalent incompressible form. Van Driest in reference 46, applying the mixing length hypothesis in compressible flow, derived a compressible law of the wall. Maise and McDonald applied the compressible law of the wall in reference 47 to calculate generalized velocities by using the Crocco energy relation. In its most general form, the generalized velocity is

$$u^* = \int_0^u \sqrt{\rho/\rho_w} du \quad (2)$$

Generalized velocity defects were examined in reference 47 for Mach numbers in the range 1.47 to 4.93 at adiabatic wall conditions and were found to correlate with an incompressible velocity defect. At Mach 5 with heat transfer, the correlation was poor, the degree of discrepancy being a function of T_w/T_t . In reference 48 the complete wall-wake region was examined for isoenergetic turbulent boundary layers at Mach numbers as high as 3.78, and generalized velocities were found to effectively reduce the data to incompressible form. In reference 49 Danberg examined 45 adiabatic wall profiles at Mach numbers from 2 to 6 and Re from 2300 to 7500. He concluded that the data could be adequately fit to the law of the wall in the form

$$\frac{u^*}{u_\tau} = \frac{1}{k} \log_e y^+ + C \quad (3)$$

with $k = 0.43$. His generalized velocity was arbitrarily defined to be that of equation (2) and the constants were found by a best fit to data technique.

Mean velocity profiles on model 1 reduced to generalized velocities for the five different test cases listed in table 1 are shown in figure 17. In this figure, profiles at each of the four survey stations demonstrate the transition from near-laminar to turbulent flow. The profiles at station 4 appear to be turbulent even at the lowest Reynolds numbers.

The incompressible law of the wall (eq. (3)), is also shown for two values of k , 0.4 and 0.43, and a value of C of 5.5. Although 0.4 is the most usual value of k to be found in the literature, a value of 0.43 was more representative of the present data, in agreement with the results of reference 49. Some authors have found k to be a function of the local Reynolds number; however, this has been disputed by others, and the consensus appears to be that k is a universal constant. (See ref. 5.) Turbulent profiles on model 1 are compared with equation (3) in figure 18. The good agreement with the incompressible law of the wall suggests that skin friction could be found from velocity profiles by fitting generalized velocities to the law of the wall by a trial-and-error procedure, where

$$\left(\frac{u_\tau}{u_e} \right)^2 = \frac{c_f}{2} \frac{\rho_e}{\rho_w} \quad (4)$$

This procedure was followed in reference 18 where inferred and measured values of the skin friction on model 2 were compared. It was found that at hot wall conditions, the difference in measured and inferred skin friction was small, but as T_w/T_t decreased, the difference increased. Inferred skin-friction values were always higher than measured values in turbulent flow. Measured total-temperature distributions were used in reference 18 to find u^* .

Despite the fact that skin-friction values inferred from velocity profiles are in error at cold wall conditions, the velocity profile can be reduced to incompressible form. Selected turbulent profiles on model 2 plotted in the law-of-the-wall form using inferred skin-friction values are shown in figure 19.

Total-Temperature Profiles

Total-temperature profiles on model 1 were measured at station 4 (turbulent flow) at four free-stream unit Reynolds numbers. The fine-wire resistance probe used for the surveys (see fig. 5(a)) had a tip thickness of 0.16 cm, slightly larger than the 0.10-cm-thick pitot probe used on this model. Figure 20 shows the measured total-temperature distributions nondimensionalized by the measured boundary-layer edge total temperature plotted as a function of y/δ_p . As the probe approached the wall, the total temperature dropped below the measured wall temperature and then began to increase. Closer to the wall, the indicated total temperature again decreased, the decrease beginning near where the wall pressure measured beneath the tip of the probe began to increase. The second decrease in total temperature appears to be an erroneous result and may be due to the probe not being aspirated properly. Shown in figure 20 and also marked in the data listing of table 6 are the values of $T_w/T_{t,e}$ and y/δ_p at which the wall pressure first began to rise. No indication of an overshoot in T_t above $T_{t,e}$ can be discerned in the data.

On model 2 a shielded coiled-wire probe was used for total-temperature surveys at eight stations for three nominal values of T_w/T_t . The data at station 1 ($T_w/T_t \approx 0.5$) were found to contain large errors and were discarded. Preliminary measurements of $T_{t,e}$ were made by using a conventional shielded thermocouple probe, and, as for the model 1 data, no overshoot in T_t at above adiabatic wall conditions was measured. By using a coiled-wire probe for $T_{t,e}$, an overshoot was measured; this overshoot should occur when $T_w > T_{aw}$. The absence of an overshoot in T_t when the thermocouple probe was used to measure $T_{t,e}$ was attributed to the relatively large thermal inertia of the shielded thermocouple probe compared with the thermal inertia of the coiled-wire probe. It was apparently of critical importance to record T_t within the boundary layer at the same instant that $T_{t,e}$ was recorded.

Total-temperature data on model 2 at station 5 are shown in figure 21 with the value of δ_p from corresponding pitot surveys marked. Total temperatures are presented in terms of F_T or $(T_t - T_w)/(T_{t,e} - T_w)$. A small but finite overshoot appears for the $T_w/T_t = 0.94$ case in figure 21(c). At above-adiabatic wall conditions, F_T becomes negative near $y = 0$; however, in the data reduction, points thought to be influenced by probe interference effects were discarded and the first good data point was faired to $F_T = 0$ at $y = 0$.

The total-temperature data of models 1 and 2 as functions of u/u_e are shown in figure 22. For comparison the relations which are often used in turbulent flow for theoretical predictions and data reduction are shown,

$$F_T = \frac{u}{u_e} \tag{5a}$$

and

$$F_T = \left(\frac{u}{u_e} \right)^2 \quad (5b)$$

Much turbulent flat-plate data follow the linear relation, whereas nozzle wall data tend to follow the quadratic relation. (See refs. 45 and 50.) In supersonic and hypersonic flow large departures from both relations occur, especially at near-adiabatic wall conditions. The data of model 1 and data from reference 51 on a nozzle wall at $M_1 \approx 20$ agree in the outer flow, as seen in figure 22(a). The theory of reference 52 is also shown by use of an effective turbulent Prandtl number of 0.9 and a velocity profile exponent of 10 (values typical of the present data). Although this method does not predict the present data accurately, it predicts the trends and would more closely approach the data if a lower value of the effective Prandtl number, or a higher value of the velocity exponent were used. As T_w approaches T_{aw} , errors in the measurement of T_t , $T_{t,e}$, and T_w are increasingly magnified when presented in terms of F_T . For the present data, the correlation in the outer data at different test conditions implies that measurement errors are not large. The data of model 2 shown in figure 22(b) are similar to the data of model 1 at $T_w/T_t = 0.9$. At cold wall conditions, the data follow the linear relation of equation (5a) except for points near the wall which may contain probe interference errors.

It has been shown in reference 9 that the T_t distribution in flat-plate turbulent boundary layers from $M_e = 2.5$ to $M_e = 4.5$ could be predicted by use of a turbulent Prandtl number derived by a mixing-length approach for the eddy conductivity. Finite-difference calculations by the method of reference 53 were made using the $N_{Pr,t}$ distribution of reference 9 and a similar $N_{Pr,t}$ distribution from reference 10, and neither predicted the present data. In figure 23 the resulting T_t distribution using the $N_{Pr,t}$ from reference 10 is compared with a profile from a laminar similar solution by the method described in reference 39. A slight dip in F_T appears in the turbulent profile near the outer edge of the boundary layer, while the overshoot in T_t above $T_{t,e}$ has moved toward the wall.

A factor which affects T_t distributions is the local uneven addition or removal of energy from the boundary layer, that is, the history effect due to nonuniform wall temperature. In reference 54 the removal of energy near the leading edge of a model has been shown to strongly affect the profile measured downstream and to persist for extremely long distances. At the slightly hot wall conditions of the present tests, some nonuniformity in T_w was present; however, it was typically small, as can be seen in the data listing of table 2. In hypersonic flow the degree of nonuniformity in T_w required to produce significant effects in T_t profiles is not known. Other data at near-adiabatic wall conditions from references 55 and 56 exhibiting the same trends as the present data are shown in figure 24.

Since the present hot wall data could not be predicted, the profile data on model 1 at stations 1, 2, and 3 were reduced by assuming the linear relation of equations (5). It has been shown in reference 15 that at near-adiabatic wall conditions, the exact form of the T_t distribution used in reducing data is not

a significant factor in determining the velocity profile or integrated boundary-layer properties. For consistency, and because the present cold wall data follow the linear relation, all data listed in table 1 were reduced the same way. In the following cases the measured T_t profiles were used in data reduction: for reducing some profiles to incompressible form through generalized velocities, for presenting $F_T - (u/u_e)$ relations, and for deriving $N_{Pr,t}$ distributions from the data.

Static-Pressure Surveys

On model 1 an attempt to measure the static-pressure distribution through the boundary layer was made by using the cone-cylinder probe shown in figure 5(a). Details of the probe construction and calibration as well as the reason for using this type of probe have been discussed previously. Mach numbers reduced by using the static-pressure probe and pitot-probe data are shown in figure 25 along with the wall pressure measured beneath the tip of the static-pressure probe as it traversed the boundary layer. For comparison, Mach numbers are shown reduced from the pitot data by assuming a constant static pressure through the boundary layer equal to the undisturbed value of p_w .

Below the edge of the boundary layer noted in figure 25, the wall pressure increased as the probe approached the wall, reached a peak value, and then decreased. Within the wall pressure rise region, the Mach numbers indicated by the pitot-static probe reduction rapidly increased to a level above that in the shock layer. Since the pitot data reduced for a constant static pressure do not indicate a similar behavior, the blunt probe data are assumed to be in error.

Also shown in figure 25 is the Mach number distribution at this location from the flow field calculations by the method of characteristics (ref. 33). The constant-static-pressure Mach number reduction agrees well with the theoretical distribution; however, the static-pressure probe-pitot probe reduction gives a Mach number about 10 percent low. Edge Mach numbers at other stations usually agreed within about 2 to 5 percent; however, the pressure rise at the wall and rapid departure from the true Mach number distribution were not as pronounced as for the case presented.

The four static orifices on the probe were aligned top to bottom and side to side so that flow separation beneath the probe would have strongly affected the bottom orifice. A three-hole configuration with no orifice on the bottom would have been a better arrangement.

Reynolds Analogy and Recovery Factor

Engineering estimates of skin friction are sometimes required from heat-transfer measurements, or conversely, the prediction of heating loads may be required based on calculated or measured skin friction. This can be done by applying Reynolds analogy

$$S = \frac{N_{St}}{c_f/2} \quad (6)$$

where

$$N_{St} = \frac{q_w}{\rho_e u_e c_p (T_{aw} - T_w)} \quad (7)$$

and

$$T_{aw} = \eta (T_t - T_e) + T_e \quad (8)$$

Since the Stanton number is a function of the adiabatic wall temperature, which, in turn, is a function of the recovery factor, both recovery factor and Reynolds analogy factor must be known with some confidence if accurate predictions are to be made.

The uncertainty in Reynolds analogy factor is reflected as an error in the desired value of N_{St} or c_f . The uncertainty in recovery factor can produce large errors in N_{St} as T_w approaches T_{aw} . At $T_w = T_{aw}$, the Stanton number is not defined, although it should approach a limiting value as T_w approaches T_{aw} from either higher or lower values. In addition, as T_w approaches T_{aw} , q approaches zero, and errors in the measurement of q can become large. Thus, N_{St} as a measure of heating rate may be subject to large errors at T_w near T_{aw} .

The short run time of the Mach 20 leg of the Langley high Reynolds number helium tunnels prevented a direct measurement of T_{aw} by running until the model reached equilibrium temperature. Instead, T_{aw} was found by plotting q/T_t as a function of T_w/T_t as illustrated in figure 26. When $T_w = T_{aw}$, $q = 0$. This method can be used as long as the transition location is not a strong function of T_w/T_t , which the present heat-transfer data show to be true. The heat-transfer data from parts (a) to (m) of figure 11, for free-stream unit Reynolds numbers of about 40×10^6 and 20×10^6 over a range of T_w/T_t were used to determine q/T_t at the eight survey locations of model 2.

In figure 27 recovery factors are compared with data from reference 36 at $M_e = 6.8$ on a 10° half-angle wedge in helium. The data are plotted as a function of Reynolds number based on distance from the peak in recovery factor, which, for the present data, corresponds closely to the peak heating location at cold wall conditions. The square root of the Prandtl number ($N_{Pr} = 0.688$ for helium) sometimes used for the laminar recovery factor, and the cube root of the Prandtl number used for the turbulent recovery factor are also shown. The present recovery factors are lower than those for the data of reference 36, whereas the length Reynolds numbers are much higher. The peak recovery factor is the same in both sets of data, approximately 0.92.

By using the recovery factors shown in figure 27, Stanton numbers at stations 2 to 8 were calculated from the heat-transfer data to determine Reynolds analogy factors which are shown in figure 28 for three nominal values of T_w/T_t

and a nominal Re/m of 54×10^6 . The data at $x = 50.5$ cm are in transitional flow, as is evident from the skin-friction data shown in figure 15(b).

DERIVED TURBULENCE PARAMETERS

It was concluded in reference 15 that the accurate prediction of the measured mean flow properties could not be made in the turbulent boundary layer immediately following transition, that is, the region of low Reynolds number effects. (See ref. 8.) In an effort to better understand the reason of the discrepancy between experimental results and predictions by finite-difference calculations, turbulence parameters which are inputs to finite-difference calculation methods were derived from the turbulent mean profiles of model 2 at stations 5 to 8. The skin-friction data of figure 15(b) show that these locations are in turbulent flow. The derived quantities consist of the mixing-length, turbulent Prandtl number, and eddy viscosity distributions through the boundary layer.

The derivation of these turbulent quantities requires either a sufficient quantity of data to accurately define derivatives of the mean flow velocity and temperature in the streamwise direction or the assumption that the profiles are similar. The four surveys in the turbulent region of the boundary layer on model 2 were not sufficient to accurately determine these streamwise derivatives; therefore, the similarity assumption was applied. Similarity of the velocity and temperature profiles in terms of y/δ occurs at sufficiently large Reynolds numbers that most of the profile is the wakelike outer portion. At $\delta^+ = 1000$, departure from the law of the wall occurs at y^+ near 100 (see fig. 19); thus, approximately 90 percent of the profile is similar. Values of δ^+ for the turbulent data of model 2 lie between 500 and 1000.

The following equations for two-dimensional flow, derived by assuming local similarity (see refs. 57 and 58), were used to calculate the total shear stress and energy flux distributions through the boundary layer:

$$\frac{\tau}{\tau_w} = 1 + \frac{1}{c_f/2} \left(I_1 G_1 - I_2 G_2 \frac{u}{u_e} + \frac{\delta}{\rho_e u_e^2} \frac{y}{\delta} \frac{dp_e}{dx} \right) \quad (9)$$

$$\frac{Q}{q_w} = 1 - \left(1 - \frac{1}{N_{Pr}} \right) \frac{\tau_L}{\tau_w} \frac{u_e \tau_w}{q_w} \frac{u}{u_e} + \frac{\rho_e u_e H_e}{q_w} G_2 \left(I_3 - I_2 \frac{T_t}{T_{t,e}} \right) \quad (10)$$

where

$$I_1 = \int_0^{y/\delta} \frac{\rho}{\rho_e} \left(\frac{u}{u_e} \right)^2 d \left(\frac{y}{\delta} \right) \quad (11a)$$

$$I_2 = \int_0^{y/\delta} \frac{\rho}{\rho_e} \left(\frac{u}{u_e} \right) d \left(\frac{y}{\delta} \right) \quad (11b)$$

$$I_3 = \int_0^{y/\delta} \frac{\rho}{\rho_e} \left(\frac{u}{u_e} \right) \frac{T_t}{T_{t,e}} d\left(\frac{y}{\delta}\right) \quad (11c)$$

$$G_1 = \frac{\delta}{\rho_e u_e^2} \frac{d}{dx} (\rho_e u_e^2) + \frac{d\delta}{dx} \quad (11d)$$

$$G_2 = \frac{\delta}{\rho_e u_e} \frac{d}{dx} (\rho_e u_e) + \frac{d\delta}{dx} \quad (11e)$$

To calculate mixing lengths, eddy viscosities, and turbulent Prandtl numbers, the following relations for shear stress and heat flux were used:

For shear stress,

$$\tau = \tau_L + \tau_T \quad (12a)$$

where

$$\tau_L = \mu \frac{\partial u}{\partial y} \quad (12b)$$

$$\tau_T = \rho \varepsilon \frac{\partial u}{\partial y} \quad \text{or} \quad \rho l^2 \left| \frac{\partial u}{\partial y} \right| \frac{\partial u}{\partial y} \quad (12c)$$

The total shear stress τ is found by quadrature from equation (9), τ_L is obtained from the input similar profile, and τ_T is the difference between τ and τ_L . Values of ε and l are found from τ_T .

For heat flux,

$$Q = Q_L + Q_T \quad (13a)$$

where

$$Q_L = k \frac{\partial T_t}{\partial y} \quad (13b)$$

$$Q_T = q_T + u\tau_T \quad (13c)$$

The total heat flux Q is found from equation (10), Q_L is obtained from the input similar profile, and Q_T is the difference between Q and Q_L . With τ_T , Q_T , and u known, q_T is found from equation (13c). The static turbulent Prandtl number $N_{Pr,t}$ is found by the following equation:

$$N_{Pr,t} = c_p \frac{\tau_w}{q_T} \frac{\partial T / \partial y}{\partial u / \partial y} \quad (14)$$

Mass-flow and dynamic-pressure gradient terms in equations (9) and (10) are evaluated by assuming isentropic flow at the edge of the boundary layer. The gradients are related to the static-pressure gradient term by the following equations:

$$\frac{\delta}{\rho_e u_e} \frac{d}{dx} (\rho_e u_e) = \frac{\delta}{\gamma} \frac{1}{p_e} \left(1 - \frac{1}{M_e^2} \right) \frac{dp_e}{dx} \quad (15a)$$

$$\frac{\delta}{\rho_e u_e^2} \frac{d}{dx} (\rho_e u_e^2) = \frac{\delta}{\gamma} \frac{1}{p_e} \left(1 - \frac{2}{M_e^2} \right) \frac{dp_e}{dx} \quad (15b)$$

Also

$$\frac{\delta}{\rho_e u_e^2} \frac{dp_e}{dx} = \frac{\delta}{\gamma} \frac{1}{p_e} \frac{1}{M_e^2} \frac{dp_e}{dx} \quad (15c)$$

For the present data, as for other high-speed data, the velocity edge δ_v and the pitot edge of the boundary layer δ_p do not coincide. (See refs. 58 and 59, for example.) In the present data at the most upstream survey station, the thicknesses differ (see table 1) and suggest that the difference may be a feature of the initial laminar boundary layer. The flow field near the leading edge contains two mechanisms which might produce different thicknesses: the favorable pressure gradient (neglecting the immediate tip region) which persists until transition occurs; and vorticity in the shock layer produced by the δ^* -induced shock curvature. Laminar similar solutions using the equations of reference 39, a 0.647 viscosity-temperature power law, and a Prandtl number of 0.688 for helium show that at $M_e = 11$, $\delta_u / \delta_p = 0.91$ to 0.94 for $T_w / T_t = 0.3$ to 0.9 and, in general, as M_e increases, $\delta_u / \delta_p \rightarrow 1$. The effect of favorable pressure gradients on similar solutions was examined, and it was found that increasing the similarity pressure gradient parameter for favorable pressure gradients (see ref. 39) slightly decreased δ_u / δ_p ; however, it could not account for the low ratios observed in the present data. The other most probable cause of the difference in thicknesses is finite vorticity external to the boundary layer caused by viscous-induced shock curvature. This has been suggested in reference 60 as the cause of a similar effect in the data of Fischer and Maddalon from reference 59.

When a difference between δ_u and δ_p occurs, neither thickness is a correct similarity parameter since the total temperature, density, and velocity thicknesses do not coincide. For example, when the turbulence modeling parameters were derived from the presentation data by using δ_p as the similarity thickness, τ / τ_w from equation (9) went to zero about halfway through the boundary layer and thereafter became negative. With δ_u as the similarity

thickness τ/τ_w approached zero at the outer edge of the boundary layer. Note that the gradient terms G_1 and G_2 contain δ explicitly.

Since the profiles are not truly similar, a suitably derived thickness must be used to insure that the momentum and heat flux balances through the boundary layer are retained and that calculated negative shear stresses do not appear in the outer region of the boundary layer. There can be two such thicknesses, one for shear stress and one for heat flux. Only the shear stress thickness δ was considered here, although the same thickness produced reasonable matches in integrated heat flux with measured surface values, except for the hot wall cases.

The δ to be used in the similarity equations was taken to be the value of y beyond which there was an insignificant contribution to the value of the momentum thickness. This point was found by plotting $\left[\int_0^{y'} \frac{\rho u}{\rho_e u_e} \left(1 - \frac{u}{u_e} \right) dy \right] / y$ against $1/y$, as shown in figure 29. As y increases without limit, both the ordinate and abscissa approach zero. Initial deviation of the integrated quantity from a straight line through the origin, although somewhat arbitrary, was taken to be δ . The resulting values, which lie between the velocity and pitot thicknesses, are listed in table 1.

In addition to the turbulence quantities, values of the power-law exponent N were calculated for each profile. The value of N is defined by the following equation:

$$\frac{u}{u_e} = \left(\frac{y}{\delta_u} \right)^{1/N} \quad (16)$$

The power-law velocity profile is correctly scaled by δ_u rather than by δ_p when there are significant differences in the two thicknesses. Values of N derived for the present data are listed in table 1.

Examples of mixing-length and eddy viscosity distributions derived from the similarity relations and mean profile data are shown in figure 30. In figure 30(a) representative mixing-length distributions are compared with the incompressible distribution, that is, $k = 0.4$ and $(l/\delta)_{\max} = 0.09$. (See ref. 54.) The derived mixing lengths and the y -coordinate are shown nondimensionalized by δ_u . If δ_p had been used instead of δ_u , the shape of the mixing-length distributions shown would not change; however, the values of l/δ_p would be below the incompressible distribution. If the derived δ had been used, the overall level of l/δ would have been slightly lower than the incompressible, but not as low as it would be if δ_p were used. Thus, the mixing length scale appears to be determined by the velocity field from incompressible flow to the present hypersonic conditions. Significant increases in l/δ_u in the outer region of the boundary layer occur as δ_u^+ decreases. This trend is typical of flatplate turbulent boundary layers, although not of nozzle wall boundary layers. (See ref. 8.) Values of $(l/\delta)_{\max}$ from reference 57 derived from mean flow profiles are compared with the present data and the faired curve

of reference 14 in figure 30(b). The scatter in the data suggests that parameters other than δ_u^+ might also be necessary in correlating $(l/\delta_u)_{\max}$.

Eddy viscosity distributions also increase in level as δ_u^+ decreases. The present data are shown in figure 30(c) along with an incompressible calculated eddy viscosity distribution from reference 47. The eddy viscosities are nondimensionalized by δ_I^* , a parameter determined only from the velocity field which has been shown to remove compressibility effects up to Mach 5 in reference 47. The distributions are plotted as functions of y/δ_u , and it can be seen that the peak in each distribution is at a smaller y/δ_u than that of the incompressible distribution. Since ϵ should approach zero when γ approaches zero, the correct similarity thickness with which to nondimensionalize y in the present data should be the derived δ . As for the mixing lengths, the peak values of nondimensional eddy viscosities increase as δ_u^+ decreases.

Total shear stress profiles for the present data are shown in figure 31 along with a curve of the incompressible data of reference 61. The present results are higher than the incompressible results; however, they are in general agreement with the body of data presented in reference 62, which tend to lie on or slightly above the incompressible curve at higher values of y/δ . The derived similarity thickness δ has been used in plotting the present shear stress distributions.

Turbulent Prandtl number distributions were found from equation (14) by the method previously outlined. Fairings of the present data are shown in figure 32 along with experimental flat-plate data from Mach 2.5 and 4.5 from reference 9. All data are characterized by a peak near the wall, decaying to an almost constant value above a y^+ value of about 100, probably in the wake region for the present profiles. (See fig. 19.) No trend either in the location of the peak value of $N_{Pr,t}$, the level of the peak, or the level in the outer region is obvious from the data shown in figure 32. Theoretical predictions from references 9 and 10, also shown in the figure, increase toward the wall. The accuracy of the experimental $N_{Pr,t}$ distributions decrease with decreasing y^+ because of possible probe interference effects near the wall. The present data cannot resolve the question of whether the turbulent Prandtl number actually decreases within the sublayer and buffer region.

COMPARISONS WITH FINITE-DIFFERENCE CALCULATIONS

Data on model 1 at $R_l/m = 44.9 \times 10^6$ were compared with finite-difference calculations in which low Reynolds number effects, precursor transition effects, and various intermittency distributions could be incorporated. The finite-difference program was that used for the calculations of reference 14, adapted from the mean field closure solution of reference 54 utilizing physical rather than transformed coordinates to more easily handle precursor transition effects. Measured surface pressures were used as inputs for deriving the boundary-layer edge conditions. Calculations made with and without the experimental values of dp/dx in the equations for shear stress showed these effects to be insignificant. A mixing length proportional to y/δ was used in calculating the turbulent shear stress throughout the boundary layer, rather than the two-layer mixing-length-eddy viscosity model (see ref. 6), and a static turbulent Prandtl

number related the turbulent heat flux to the turbulent shear stress. The transition region was calculated by using the incompressible longitudinal intermittency relation of Dawhan and Narasimha from reference 63. Details of the transition calculation can be found in reference 6 where high-speed turbulent boundary-layer data have been successfully predicted. (See also ref. 64.) Data at Mach 7 from reference 16 tend to confirm the agreement of compressible and incompressible flow longitudinal intermittency distributions.

First, the variation of intermittency normal to the surface Γ_y was examined to determine how the calculated values of the skin-friction coefficient would be affected at the present test conditions. In incompressible flow, reference 63 shows that the variation in Γ_y has little effect on mean flow properties. To determine the effect that it might have in hypersonic flow, calculations were made with various Γ_y distributions for $k = 0.4$, $(l/\delta)_{\max} = 0.09$, and $N_{Pr,t} = 0.9$. For one calculation $\Gamma_y = 1$ was used; for another calculation the measured incompressible distribution from reference 65, described by the following equation was used:

$$\Gamma_y = 0.5 \left\{ 1 - \operatorname{erf} \left[4.714 \left(\frac{y}{\delta} - 0.8 \right) \right] \right\} \quad (17)$$

In reference 62 Sandborn compared incompressible measurements with the hypersonic measurements of Laderman and Demetriades and found them to be very different. The hypersonic Γ_y , shown in figure 33 and described by the following equation, was used for the third calculation:

$$\Gamma_y = \operatorname{erf} \left(16 \frac{y}{\delta} \right) \quad \left(\frac{y}{\delta} < 0.7 \right) \quad (18)$$

$$\Gamma_y = 0.5 \left\{ 1 - \operatorname{erf} \left[10 \left(\frac{y}{\delta} - 0.97 \right) \right] \right\} \quad \left(\frac{y}{\delta} > 0.7 \right)$$

The results obtained by using the various intermittency distributions are compared with the c_f data of model 1 in figure 34.

The beginning of transition was input at $x = 86.4$ cm, based on the beginning of the heat-transfer rise shown in figure 10(a). The end of transition ($\Gamma_x = 0.99$) was at $x = 165$ cm, corresponding to the heat-transfer peak. It can be seen that the effect of Γ_y on skin friction is not large at these conditions. The hypersonic distribution described by equations (18) produces results intermediate in value between that of the incompressible relation and that of $\Gamma_y = 1$. The major discrepancy in results between equations (17) and (18) occurs upstream in the transition region. Since this comparison was not conclusive in showing the hypersonic intermittency to be more nearly correct at the present test conditions, the widely used incompressible Γ_y from equation (17) was retained for calculations made to examine low Reynolds number and precursor transition effects.

Next, the effect of the increase in the outer mixing length at low Reynolds numbers was examined. In figure 35 the model 1 skin-friction data are compared with predictions: (a) in which $(l/\delta)_{\max}$ was held fixed at 0.09, (b) using the data fairing of reference 14 (see fig. 30(b)), and (c) in which the method of Pletcher as applied in reference 66 was used.

It is evident that inclusion of the low Reynolds number effect is extremely important for this test condition. Throughout the transition region and into the fully turbulent region, the calculated c_f including low Reynolds number effects is much larger than that resulting from a fixed (equilibrium) value of $(l/\delta)_{\max}$. The range of δ^+ taken from the calculations is shown at several points in figure 35, the lower of two values being from the calculation with fixed $(l/\delta)_{\max}$. Pletcher's method produces better agreement with the present data than the correlation of reference 14; however, the data point at 120 cm is not predicted by either method. In order for the calculations to agree with data, transition would have to be moved upstream. Accordingly, precursor transition effects were examined by using Pletcher's low Reynolds number effect on the outer mixing length and the incompressible Γ_y distribution.

An estimate of the effect which precursor transition has on calculated skin friction was made by using two transition models. The most often used transition model, described in reference 6, assumes the local intermittency to be the product of the x-intermittency multiplied by the y-intermittency. The precursor model assumes that turbulence originates at a point away from the surface and spreads at shallow angles toward both the surface and the outer edge. (See ref. 14.) At a given x-position within the precursor region the turbulent shear is calculated only inside the bounds of the spreading region, as shown in the sketch of figure 36. In order to separate the precursor transition effect from low Reynolds number effects, three calculations were made by using the average edge conditions measured on model 1 at $R_2/m = 44.9 \times 10^6$. In all three calculations the Pletcher low Reynolds number variation of $(l/\delta)_{\max}$ with δ^+ , a value of $k = 0.4$, and Γ_y from equation (17) were used. The input profile was laminar and was calculated by the method of reference 39.

Transition for the first calculation was assumed to begin at $x = 86.4$ cm based on the heat-transfer rise location shown in figure 10(a). For the second calculation precursor transition was assumed at $x = 61$ cm by using the criterion from reference 14 that precursor transition should begin at about 70 percent of the heat-transfer indicated transition. Precursor transition was initiated at the height in the laminar boundary layer where Rouse's parameter was a maximum. (See ref. 67.) The spreading angle calculated from this point to the surface at $x = 86.4$ cm is 1.36° , in agreement with the data compiled in reference 12. A final calculation was made for transition initiating at $x = 61$ cm to match the x-intermittency of the precursor calculation. The results of these three calculations are shown in figure 36 along with skin-friction measurements on model 1.

It is evident that for the case considered, the transition input to the finite-difference calculation should be taken upstream of the heat-transfer indicated transition. It is also evident that the effect of spreading is not large in this case. The precursor spreading effect delays the skin-friction

rise slightly and steepens it when it does occur. Downstream of transition the effect is insignificant.

The prediction of heating rates at near-adiabatic wall conditions, unlike skin-friction predictions, was found to be sensitive to all parameters examined. By using low Reynolds number and precursor transition effects for the best agreement with c_f data and with a Γ_y from equation (17), several turbulent Prandtl number distributions were incorporated into the finite-difference program. The turbulent Prandtl numbers examined included the theoretical distributions of Cebeci (ref. 10) and Meier and Rotta (ref. 9), the empirical relation of Shang (ref. 68), the experimental distribution of reference 10, and a $N_{Pr,t} = 0.9$. The theoretical distributions of references 9 and 10, derived as functions of y^+ , are shown in figure 37(a) as functions of y/δ for three values of δ^+ to compare with the data envelope of reference 68. At low values of δ^+ the overall levels of both the reference 9 and reference 10 distributions are well above the data envelope of Shang. A fairing of the experimental data of reference 9 for flat plates at Mach numbers from 2.5 to 4.5 is compared with the theoretical distributions in figure 37(b). The only significant difference between the experimental distribution and the theoretical distributions is the fact that the experimental distribution peaks at a y^+ about 30 and then decreases toward $N_{Pr,t} = 1$ as y^+ decreases, whereas for the theoretical distributions, $N_{Pr,t}$ continually increases as y^+ decreases.

With these five static turbulent Prandtl number variations input to the finite-difference boundary-layer program, wide variations in calculated q values were obtained, as shown in figure 38. The value of δ^+ at $x = 85$ cm was approximately 210 and made making the $N_{Pr,t}$ distributions of Cebeci and Meier and Rotta greater than 1 throughout the inner 25 percent of the boundary layer at this location. (See fig. 37(b).) Values of q calculated by using both distributions change from negative to positive before the end of transition is reached. Both a constant $N_{Pr,t} = 0.9$ and the Shang average produce the correct trends in the negative heat-transfer rate, although not the correct level. The experimental distribution of Meier and Rotta produces a q intermediate in value between the empirical distributions and the theoretical distributions.

None of the $N_{Pr,t}$ distributions predicted the large deficit in the Crocco function characteristic of the T_t profiles at hot wall conditions shown in figure 22. The $N_{Pr,t} = 0.9$ produced a Crocco function always above the linear relation in the outer part of the boundary layer, whereas the other distributions produced a dip near the outer edge similar to that of the data but far less in magnitude. (See fig. 23.) In view of the wide disparity in q calculated by the different methods, no further attempt was made to predict heat transfer rates.

A best fit prediction of the skin-friction data on model 2 was made by locating the initiation of precursor transition at 34 cm, the point where precursor spreading reaches the wall at 48 cm, and the end of transition ($\Gamma_x = 0.99$) at 89 cm. The calculations are compared with the data of model 2 in figure 39 by using the same transition locations for both hot and cold wall cases. The calculations contain low Reynolds number and precursor transition effects, $N_{Pr,t} = 0.9$, $k = 0.4$, the experimental pressure distribution, and both incompressible (eq. (17)) and hypersonic (eqs. (18)) Γ_y distributions.

The effect of Γ_y is small, except for the cold wall case at high Reynolds numbers. The hot wall data are underpredicted by about 8 to 10 percent in the turbulent region.

Allowing k to vary as a function of the Reynolds number, as some authors have suggested, might improve the prediction of the present data. The consensus at present is that k is invariant for flat-plate flows (see ref. 5), and its variation with δ^+ was not examined here. It is evident that the present data at $M_e = 9.5$ to 11.3 and relatively low values of δ^+ provide difficult test cases for predictive methods.

CONCLUDING REMARKS

Extensive measurements of surface pressure, heat transfer, local surface shear stresses, and pitot and total-temperature surveys have been made in transitional and turbulent boundary layers at edge Mach numbers near 10 in helium. The data were obtained on two sharp flat-plate models at angles of 4° and 5° to the flow for ratios of wall temperature to total temperature from about 0.3 to 1 and maximum length Reynolds numbers of about 110×10^6 . Additional skin friction data were obtained at a length Reynolds number of about 150×10^6 . The data were compared with calculations from a mean field closure finite-difference boundary-layer method to examine the magnitude of precursor transition, low Reynolds number effects, and the effects of incompressible and hypersonic surface normal intermittency distributions at the present test conditions.

Analysis of the data has shown that the present boundary layers, even at length Reynolds numbers as high as 100×10^6 are subject to strong low Reynolds number amplification of the outer layer scales (mixing lengths and eddy viscosities). In addition, it was found that peak values of heating, skin friction, and surface pressure do not coincide, the disparity being a function of the ratio of wall temperature to total temperature.

Local similarity was assumed in order to derive turbulent mixing lengths, eddy viscosities, and Prandtl numbers from the present data. Because the thermal, or pitot, boundary layer was thicker than the velocity boundary layer, the calculated shear stress was found to approach zero before the edge of the boundary layer was reached unless a derived boundary-layer thickness was used in non-dimensionalizing the total temperature and velocity profiles. The derived thickness was intermediate in value between the velocity and pitot thickness of the boundary layer.

The present skin-friction data could be adequately predicted from finite-difference calculations only if low Reynolds number effects and precursor transition effects were included. Heating rates and total-temperature profiles at above-adiabatic wall conditions could not be predicted.

Langley Research Center
National Aeronautics and Space Administration
Hampton, VA 23665
June 13, 1978

APPENDIX A

PROBE EFFECTS ON WALL PRESSURE

Measurement of the wall pressure beneath the tip of the survey probes on model 1 was made as the probes traversed the boundary layer. Wall pressures are shown in figure 40 as a function of y/δ_p for the probe. Values of Γ_x were estimated by the method of reference 63 by assuming $\Gamma_x = 0$ at x_T and $\Gamma_x = 0.99$ at $x_{T,e}$ from the heat-transfer data of figure 10. In part (a) of figure 10 data at 3 different values of Γ_x illustrate the effect which the "degree of turbulence" had on the characteristic shape of the pressure rise. For the most nearly laminar case, the pressure rise peaked when the probe was slightly less than halfway through the boundary layer and then decreased as the probe approached the wall. For the most nearly turbulent case, the pressure increased monotonically as the probe approached the wall. In part (b) of figure 10, data at approximately the same value of Γ_x are shown for different unit Reynolds numbers. As the unit Reynolds number increased, h/δ decreased and the level of the pressure peak increased accordingly.

The phenomenon which produced the increase in wall pressure was not determined, although it might have been flow separation between the probe and the wall, as has been observed in reference 69 at $M_e = 1.72$ for laminar flow. A factor which possibly could have contributed to a separation beneath the probe was the mounting arrangement whereby the probe support extended down through the surface of the model, as shown in figure 4. Because of this, the support for the survey probes used on model 2 extended up into the shock layer.

When surveys were begun on model 2, the probe was positioned at station 2, 50.5 cm from the leading edge of the model, to check for probe interference effects. Runs were made at a $R_e/m = 54 \times 10^6$ with no wall cooling. At this condition the boundary layer was in an early transition state as can be seen in the data of figures 11(f), 14, and 15(b). The probe was constructed of 0.23-cm outside diameter tubing flattened to a tip height of 0.96 mm, having approximately the same dimensions as the pitot probe used for model 1 surveys. The wall pressure rise measured beneath the tip of the probe was approximately the same as that on model 1 at corresponding edge conditions; thus, mounting through the surface was no worse than mounting above the boundary layer.

A check was made to see whether visual evidence of probe interference such as boundary-layer thickening or flow separation beneath the probe could be observed in schlieren photographs as the probe traversed the boundary layer. Two frames from a video tape record of a schlieren are shown in figure 41. In figure 41(a), where the probe is at about twice the boundary-layer height, the shock from the probe is distinct. At the outer edge of the boundary layer (fig. 41(b)), the shock beneath the probe disappears as it penetrates the boundary layer. As the probe descended farther, no shock was visible beneath the probe, possibly because of decreased schlieren sensitivity as the density within the boundary layer decreased. The dark band parallel to the surface of the model may be disturbances at the edges of the model originating near the leading edge.

APPENDIX A

It is evident that the probe tip produces a strong disturbance within the boundary layer impinging on the surface downstream of the tip of the probe. As the probe descends, the impingement area moves forward, disturbing the pressure beneath the tip to a greater degree. In an early transitional boundary layer, the density or mass flow may become so low that below a certain height the probe disturbance begins to lessen and creates the type of pressure rise shown in figure 40. In a turbulent boundary layer, the mean flow properties are such that the disturbance increases until the wall is reached.

In order to keep the shock from the probe tip weak, an axisymmetric design having as small a tip thickness as possible without introducing significant pressure lag effects was tried. This configuration which was used for the surveys on model 2 is shown in figure 5(b). A schlieren record of this probe showed no discernible shock, even outside the boundary layer, and only a slight increase in pressure beneath the tip of the probe during a boundary-layer traverse.

The effect of finite probe size on the y -displacement of the Mach number profile in turbulent boundary layers is shown to be a strong function of the local Mach number in reference 70, based on the analysis of data at $M_e = 4.6$. There is no question that there is a strong effect of at least the edge Mach number on profile distortion for a fixed value of h/δ ; however, it is not possible to extrapolate the data of reference 70 to the present test conditions.

Disturbances in the wall pressure tend to be small when the probe is above δ_u , that is, above $y/\delta_p \approx 0.5$ in figure 40. Peak disturbances occur when the probe is within the velocity boundary layer, which suggests that the velocity gradient may be primarily responsible for the errors incurred because of finite probe size. If this is true, correlations of probe effects based on the velocity thickness of the boundary layer would appear to be more consistent than that based on the pitot thickness, especially at high Mach numbers. It is evident that additional high Mach number data on probe interference are required before the present data can be corrected with any degree of confidence. For this reason, no further attempt was made to estimate errors in y or to correct the present data.

APPENDIX B

PITOT PRESSURE CORRECTIONS IN RAREFIED HELIUM FLOW

Leonard M. Weinstein
Langley Research Center

The symbols used for the corrections made in rarefied helium flow are as follows:

h	probe tip thickness
M	Mach number
N_{Kn}	Knudsen number
p	pressure
p_p	pitot pressure
R_T	Reynolds number based on probe tip thickness and total temperature
T	temperature
T_p	probe temperature
ρ	density

Subscripts:

l	local value
m	measured value
R	Rayleigh value
T	stagnation value
∞	free-stream value
$1,2$	upstream and behind a normal shock, respectively

Frequently, in hypersonic flow studies the density levels are so low that the measured pitot pressure may be different from the Rayleigh, or continuum, impact pressure. Studies in air and nitrogen in references 71 and 72 illustrate the trends and magnitudes of these differences, and in reference 73 a possible explanation of the phenomena is given. It was expected that similar effects would occur in helium, and exact quantitative corrections were needed to apply to data obtained in hypersonic helium tunnels.

APPENDIX B

With decreasing density the pressure measured by pitot probes first drops below the Rayleigh value and then rises to over twice the Rayleigh value in free molecule flow. (See refs. 71 and 72.) The initial drop has been shown

to be a function of the parameter $[\overline{R_T}(\rho_2/\rho_1)^{1/2}]^{-1}$ in references 71 and 73, whereas, the rise is more correctly correlated by the Knudsen number. It will be shown that for the data of this report, the density is so high that the measured pressure never rises above the Rayleigh pressure. Thus, only the correlating parameter $[\overline{R_T}(\rho_2/\rho_1)^{1/2}]^{-1}$ is examined here. Probe geometry is known to affect the measured pressure level (ref. 71); however, for the present study, a single probe geometry typical of the type "c" probe of reference 71 was used.

In order to estimate the range of $[\overline{R_T}(\rho_2/\rho_1)^{1/2}]^{-1}$ against M_1 which would be encountered in surveying boundary layers in a $M_\infty = 19$ helium tunnel, the variation of these parameters through the boundary layer of a 5.9° wedge and through the tunnel-wall boundary layer was calculated by assuming a tunnel stagnation pressure of 6.9 MPa. Also the wall to total-temperature ratio was assumed to be one for both the tunnel wall and wedge boundary-layer flow, and T_T was assumed to be constant through the boundary layers. Conditions at the edge of the boundary layer on the wedge were calculated from the inviscid oblique shock relations given in reference 30. The results are shown in figure 42.

Note that larger values of the parameter $[\overline{R_T}(\rho_2/\rho_1)^{1/2}]^{-1}$ correspond to lower Mach numbers.

Measurements were made in a $M_\infty \approx 20$ helium calibration tunnel. Pitot probes from 0.013 to 0.318 cm high were examined with a width-height ratio of about 4, except for the smallest and largest probes which were 10 and 1, respectively. Test conditions are given in the following table:

$P_T, \text{ Pa}$	M_∞	N_{Kn}	$h, \text{ cm}$	$[\overline{R_T}(\rho_2/\rho_1)^{1/2}]^{-1}$
$3.4 \times 10^2 \text{ to } 3.4 \times 10^4$	3.1 to 3.9	0.002 to 0.29	0.013 to 0.318	0.00055 to 0.084
$2.4 \times 10^4 \text{ to } 1.03 \times 10^7$	17.2 to 19.6	0.0007 to 0.028	0.023 to 0.318	0.00014 to 0.0064

The results of these tests are given in figure 43. The range of

$[\overline{R_T}(\rho_2/\rho_1)^{1/2}]^{-1}$ exceeds the typical cases of figure 42, and, in fact, the lower M_∞ range corresponds to larger values of the parameter. This results

in a representative variation of $[\overline{R_T}(\rho_2/\rho_1)^{1/2}]^{-1}$ with Mach number compared with probable survey values. Thus, the fairing given by the solid line in figure 43 is probably the best to use if data are corrected. The fact that the probe was cooled by flow to $T_p/T_t = 0.85$ could change the pitot pressure (ref. 71), so a probe heated to $T_p/T_t = 1$ was also examined. The results shown by the solid symbols in figure 43 indicate that this effect is not important here.

REFERENCES

1. Spalding, D. B.; and Chi, S. W.: The Drag of a Compressible Turbulent Boundary Layer on a Smooth Flat Plate With and Without Heat Transfer. *J. Fluid Mech.*, vol. 18, pt. 1, Jan. 1964, pp. 117-143.
2. Van Driest, E. R.: The Problem of Aerodynamic Heating. *Aeronaut. Eng. Rev.*, vol. 15, no. 10, Oct. 1956, pp. 26-41.
3. Morkovin, M. V.; and Kline, S. J.: Calculation of Incompressible Turbulent Boundary Layers - A Review of the AFOSR-IFP-Stanford 1968 Conference. *Compressible Turbulent Boundary Layers*, NASA SP-216, 1968, pp. 15-26.
4. Reynolds, W. C.: Computation of Turbulent Flows - State-of-the-Art, 1970. Rep. MD-27 (Grants NSF-GK-10034 and NASA-Ngr-05-020-420), Dep. Mech. Eng., Stanford Univ., Oct. 1970. (Available as NASA CR-128372.)
5. Bushnell, Dennis M.; Cary, Aubrey M., Jr.; and Harris, Julius E.: Calculation Methods for Compressible Turbulent Boundary Layers - 1976. NASA SP-422, 1977.
6. Harris, Julius E.: Numerical Solution of the Equations for Compressible Laminar, Transitional, and Turbulent Boundary Layers and Comparisons With Experimental Data. NASA TR-368, 1971.
7. Coles, D. E.: The Turbulent Boundary Layer in a Compressible Fluid. U.S. Air Force Proj. RAND Rep. R-403-PR (DDC Doc. No. AD 285 651), RAND Corp., Sept. 1962.
8. Bushnell, D. M.; Cary, A. M., Jr.; and Holley, B. B.: Mixing Length in Low Reynolds Number Compressible Turbulent Boundary Layers. *AIAA J.*, vol. 13, no. 8, Aug. 1975, pp. 1119-1121.
9. Meier, H. U.; and Rotta, J. C.: Temperature Distributions in Supersonic Turbulent Boundary Layers. *AIAA J.*, vol. 9, no. 11, Nov. 1971, pp. 2149-2156.
10. Cebeci, T.: A Model for Eddy Conductivity and Turbulent Prandtl Number. *J. Trans. ASME, Ser. C: Heat Transfer*, vol. 95, no. 2, May 1973, pp. 227-234.
11. Henderson, A.; Rogallo, R. S.; Woods, W. C.; and Spitzer, C. R.: Exploratory Hypersonic Boundary-Layer Transition Studies. *AIAA J.*, vol. 3, no. 7, July 1965, pp. 1363-1364.
12. Fischer, Michael C.: Spreading of a Turbulent Disturbance. *AIAA J.*, vol. 10, no. 7, July 1972, pp. 957-959.
13. LaGraff, John E.: Observations of Hypersonic Boundary-Layer Transition Using Hot Wire Anemometry. *AIAA J.*, vol. 10, no. 6, June 1972, pp. 762-769.

14. Bushnell, D. M.; and Alston, D. W.: Calculation of Transitional Boundary-Layer Flows. AIAA J., vol. 11, no. 4, Apr. 1973, pp. 554-556.
15. Watson, Ralph D.; Harris, Julius E.; and Anders, John B., Jr.: Measurements in a Transitional/Turbulent Mach 10 Boundary Layer at High-Reynolds Numbers. AIAA Paper No. 73-165, Jan. 1973.
16. Owen, F. K.; and Horstman, C. C.: Hypersonic Transitional Boundary Layers. AIAA J., vol. 10, no. 6, June 1972, pp. 769-775.
17. Laderman, A. J.; and Demetriades, A.: Measurements of the Mean and Turbulent Flow in a Cooled-Wall Boundary Layer at Mach 9.37. AIAA Paper No. 72-73, Jan. 1972.
18. Watson, Ralph D.: Wall Cooling Effects on Hypersonic Transitional/Turbulent Boundary Layers at High Reynolds Numbers. AIAA Paper No. 75-834, June 1975.
19. Matting, Fred W.; Chapman, Dean R.; Nyholm, Jack R.; and Thomas, Andrew G.: Turbulent Skin Friction at High Mach Numbers and Reynolds Numbers in Air and Helium. NASA TR R-82, 1961.
20. Watson, Ralph D.; and Bushnell, Dennis M.: Calibration of the Langley Mach 20 High Reynolds Number Helium Tunnel Including Diffuser Measurements. NASA TM X-2353, 1971.
21. Weinstein, Leonard M.: Effects of Two-Dimensional Sinusoidal Waves on Heat Transfer and Pressure Over a Plate at Mach 8.0. NASA TN D-5937, 1970.
22. Lucks, C. F.; and Deem, H. W.: Thermal Properties of Thirteen Metals. Spec. Tech. Publ. No. 227, American Soc. Testing Mater., 1958.
23. Allen, Jerry M.: Systematic Study of Error Sources in Supersonic Skin-Friction Balance Measurements. NASA TN D-8291, 1976.
24. Wagner, Richard D., Jr.; and Watson, Ralph: Reynolds Number Effects on the Induced Pressures of Cylindrical Bodies With Different Nose Shapes and Nose Drag Coefficients in Helium at a Mach Number of 24. NASA TR R-182, 1963.
25. Weinstein, Leonard M.: A Shielded Fine-Wire Probe for Rapid Measurement of Total Temperature in High-Speed Flows. J. Spacecr. & Rockets, vol. 8, no. 4, Apr. 1971, pp. 425-428.
26. Weinstein, Leonard M.: Hot-Wire Coil Probe for High-Speed Flows. AIAA J., vol. 11, no. 12, Dec. 1973, pp. 1772-1773.
27. Fischer, Michael C.: Turbulent Bursts and Rings on a Cone in Helium at $M_e = 7.6$. AIAA J., vol. 10, no. 10, Oct. 1972, pp. 1387-1389.

28. Fischer, Michael C.; and Weinstein, Leonard M.: Cone Transitional Boundary-Layer Structure at $M_e = 14$. AIAA J., vol. 10, no. 5, May 1972, pp. 699-701.
29. Erickson, Wayne D.: Real-Gas Correction Factors for Hypersonic Flow Parameters in Helium. NASA TN D-462, 1960.
30. Mueller, James N.: Equations, Tables, and Figures for Use in the Analysis of Helium Flow at Supersonic and Hypersonic Speeds. NACA TN 4063, 1957.
31. Maddalon, Dal V.; and Jackson, Willis E.: A Survey of the Transport Properties of Helium at High Mach Number Wind-Tunnel Conditions. NASA TM X-2020, 1970.
32. Arrington, James P.: Heat-Transfer and Pressure Distributions Due to Sinusoidal Distortions on a Flat Plate at Mach 20 in Helium. NASA TN D-4907, 1968.
33. Inouye, Mamoru; Rakich, John V.; and Lomax, Harvard: A Description of Numerical Methods and Computer Programs for Two-Dimensional and Axisymmetric Supersonic Flow Over Blunt-Nosed and Flared Bodies. NASA TN D-2970, 1965.
34. Wagner, R. D., Jr.; Maddalon, D. V.; and Weinstein, L. M.: Influence of Measured Freestream Disturbances on Hypersonic Boundary-Layer Transition. AIAA J., vol. 8, no. 9, Sept. 1970, pp. 1664-1670.
35. Fischer, M. C.; and Wagner, R. D.: Transition and Hot-Wire Measurements in Hypersonic Helium Flow. AIAA J., vol. 10, no. 10, Oct. 1972, pp. 1326-1332.
36. Rudy, David H.; and Weinstein, Leonard M.: Investigation of Turbulent Recovery Factor in Hypersonic Helium Flow. AIAA J., vol. 8, no. 12, Dec. 1970, pp. 2286-2287.
37. Maddalon, Dal V.: Effect of Varying Wall Temperature and Total Temperature on Transition Reynolds Number at Mach 6.8. AIAA J. (Tech. Notes), vol. 7, no. 12, Dec. 1969, pp. 2355-2357.
38. Fischer, Michael C.: Influence of Moderate Wall Cooling on Cone Transition at $M_e = 13.7$ in Helium. J. Spacecr. & Rockets, vol. 10, no. 4, Apr. 1973, pp. 282-283.
39. Beckwith, Ivan E.; and Cohen, Nathaniel B.: Application of Similar Solutions to Calculation of Laminar Heat Transfer on Bodies With Yaw and Large Pressure Gradient in High-Speed Flow. NASA TN D-625, 1961.
40. Bertram, Mitchel H.; and Blackstock, Thomas A.: Some Simple Solutions to the Problem of Predicting Boundary-Layer Self-Induced Pressures. NASA TN D-798, 1961.

41. Bertram, Mitchel H.; and Feller, William V.: A Simple Method for Determining Heat Transfer, Skin Friction, and Boundary-Layer Thickness for Hypersonic Laminar Boundary-Layer Flows in a Pressure Gradient. NASA MEMO 5-24-59L, 1959.
42. Lewis, Clark Houston: Comparison of a First-Order Treatment of Higher-Order Boundary-Layer Effects With Second-Order Theory and Experimental Data. AEDC-TR-68-148, U.S. Air Force, Oct. 1968. (Available from DDC as AD 676 003.)
43. Cary, Aubrey M., Jr.; and Bertram, Mitchel H.: Engineering Prediction of Turbulent Skin Friction and Heat Transfer in High-Speed Flow. NASA TN D-7507, 1974.
44. Peterson, John B., Jr.: A Comparison of Experimental and Theoretical Results for the Compressible Turbulent-Boundary-Layer Skin Friction With Zero Pressure Gradient. NASA TN D-1795, 1963.
45. Bushnell, Dennis M.; Johnson, Charles B.; Harvey, William D.; and Feller, William V.: Comparison of Prediction Methods and Studies of Relaxation in Hypersonic Turbulent Nozzle-Wall Boundary Layers. NASA TN D-5433, 1969.
46. Van Driest, E. R.: Turbulent Boundary Layer in Compressible Fluids. J. Aeronaut. Sci., vol. 18, no. 3, Mar. 1951, pp. 145-160, 216.
47. Maise, George; and McDonald, Henry: Mixing Length and Kinematic Eddy Viscosity in a Compressible Boundary Layer. AIAA J., vol. 6, no. 1, Jan. 1968, pp. 73-80.
48. Sun, Chen-Chih; and Childs, Morris E.: A Wall-Wake Velocity Profile for Turbulent Compressible Boundary Layers With Heat Transfer. NASA CR-119131, 1975.
49. Danberg, James E.: A Re-Evaluation of Zero Pressure Gradient Compressible Turbulent Boundary Layer Measurements. Turbulent Shear Flows, AGARD-CP-93, Jan. 1972, pp. 1-1 - 1-11.
50. Hopkins, Edward J.; Rubesin, Morris W.; Inouye, Mamoru; Keener, Earl R.; Mateer, George C.; and Polek, Thomas E.: Summary and Correlation of Skin-Friction and Heat-Transfer Data for a Hypersonic Turbulent Boundary Layer on Simple Shapes. NASA TN D-5089, 1969.
51. Bertram, Mitchel H.; and Neal, Luther, Jr.: Recent Experiments in Hypersonic Turbulent Boundary Layers. Presented at the AGARD Specialists' Meeting on Recent Developments in Boundary-Layer Research (Naples, Italy), May 1965. (Available as NASA TM X-56335.)
52. Whitfield, D. L.; and High, M. D.: Velocity-Temperature Relations in Turbulent Boundary Layers With Non-Unity Prandtl Numbers. AIAA Paper No. 76-411, July 1976.

53. Hixon, Barbara A.; Beckwith, Ivan E.; and Bushnell, Dennis M.: Computer Program for Compressible Laminar or Turbulent Nonsimilar Boundary Layers. NASA TM X-2140, 1971.
54. Gates, David F.: Measurements of Upstream History Effects in Compressible Turbulent Boundary Layers. NOLTR 73-152, U.S. Navy, July 26, 1973. (Available from DDC as AD 772 483.)
55. Sturek, W. B.: An Experimental Investigation of the Supersonic Turbulent Boundary Layer in a Moderate Adverse Pressure Gradient. Part II. Analysis of the Experimental Data. BRL Rep. No. 1543, U.S. Army, June 1971. (Available from DDC as AD 729 325.)
56. Mabey, D. G.; and Sawyer, W. G.: Experimental Studies of the Boundary Layer on a Flat Plate at Mach Numbers From 2.5 to 4.5. R. & M. No. 3784, British A.R.C., 1976.
57. Bushnell, Dennis M.; and Morris, Dana J.: Shear-Stress, Eddy-Viscosity, and Mixing-Length Distributions in Hypersonic Turbulent Boundary Layers. NASA TM X-2310, 1971.
58. Horstman, C. C.; and Owen, F. K.: Turbulent Properties of a Compressible Boundary Layer. AIAA J., vol. 10, no. 11, Nov. 1972, pp. 1418-1424.
59. Fischer, Michael C.; and Maddalon, Dal V.: Experimental Laminar, Transitional, and Turbulent Boundary-Layer Profiles on a Wedge at Local Mach Number 6.5 and Comparisons With Theory. NASA TN D-6462, 1971.
60. Sullivan, P. A.; and Koziak, W. W.: Entropy Layer Effects in Constant Pressure Hypersonic Boundary Layers. AIAA J., vol. 11, no. 5, May 1973, pp. 730-731.
61. Tetervin, Neal: A Semi-Empirical Derivation of Friction, Heat-Transfer, and Mass-Transfer Coefficients for the Constant Property Turbulent Boundary Layer on a Flat Plate. NOLTR 63-77, U.S. Navy, Oct. 1963. (Available from DDC as AD 422 359.)
62. Sandborn, V. A.: A Review of Turbulence Measurements in Compressible Flow. NASA TM X-62,337, 1974.
63. Dhawan, S.; and Narasimha, R.: Some Properties of Boundary Layer Flow During the Transition From Laminar to Turbulent Motion. J. Fluid Mech., vol. 3, pt. 4, Jan. 1958, pp. 418-436.
64. Albers, James A.; and Gregg, John L.: Computer Program for Calculating Laminar, Transitional, and Turbulent Boundary Layers for a Compressible Axisymmetric Flow. NASA TN D-7521, 1974.
65. Kovaszny, Leslie S. G.; Kibens, Valdis; and Blackwelder, Ron F.: Large-Scale Motion in the Intermittent Region of a Turbulent Boundary Layer. J. Fluid Mech., vol. 41, pt. 2, Apr. 13, 1970, pp. 283-325.

66. Watson, Ralph D.: Prediction of Outer Layer Mixing Lengths in Turbulent Boundary Layers. AIAA J., vol. 15, no. 4, Apr. 1977, pp. 591-592.
67. Stainback, P. Calvin: Use of Rouse's Stability Parameter in Determining the Critical Layer Height of a Laminar Boundary Layer. AIAA J., vol. 8, no. 1, Jan. 1970, pp. 173-175.
68. Shang, J. S.; Hankey, W. L.; and Dwoyer, D. L.: Numerical Analysis of Eddy Viscosity Models in Supersonic Turbulent Boundary Layers. AIAA Paper No. 73-164, Jan. 1973.
69. Morkovin, M. V.; and Bradfield, W. S.: Probe Interference Measurements in Supersonic Laminar Boundary Layers. J. Aeronaut. Sci. (Readers' Forum), vol. 21, no. 11, Nov. 1954, pp. 785-787.
70. Allen, Jerry M.: Effects of Mach Number on Pitot-Probe Displacement in a Turbulent Boundary Layer. NASA TN D-7466, 1974.
71. Rogers, Kenneth W.; Wainright, John B.; and Touryan, Kenell J.: Impact and Static Pressure Measurements in High Speed Flows With Transitional Knudsen Numbers. Volume II of Advances in Applied Mechanics, J. H. de Leeuw, ed., Academic Press, Inc., 1966, pp. 151-174.
72. Beckwith, Ivan E.; Harvey, William D.; and Clark, Frank L. (Appendix A by Ivan E. Beckwith, William D. Harvey, and Christine M. Darden and appendix B by William D. Harvey, Lemuel E. Forrest, and Frank L. Clark): Comparisons of Turbulent-Boundary-Layer Measurements at Mach Number 19.5 With Theory and an Assessment of Probe Errors. NASA TN D-6192, 1971.
73. White, Richard B.: Hypersonic Viscous-Interaction and Rarefaction Effects on Impact Probes. AIAA Stud. J., vol. 5, no. 2, Apr. 1967, pp. 46-49.

TABLE 1.- COMBINED DATA TEST CASES

(a) Model 1 at $T_w/T_t = 0.94$; nominal $T_t = 305.6$ K

Station	x, cm	$P_{t,1}$, kPa	M_e	R_e/m (a)	Pitot case from table 5	T_t survey case from table 6	P_w , kPa (b)	c_f (b)	δ_p pitot, cm	δ_u velocity, cm	δ^* , cm (c)	θ , cm (c)	R_θ (a,c)
1	74.2	1.276×10^4	10.05	41.02×10^6	1	---	0.931	1.248×10^{-4}	2.032	0.874	0.8056	0.9827×10^{-2}	4 028
2	99.6	1.344	9.80	38.02	2	---	.872	3.060	2.032	1.039	.8656	1.0851	4 123
3	125.0	1.296	10.20	43.34	3	---	.900	3.358	2.032	1.339	1.0099	1.3256	5 741
4	211.2	1.317	10.24	48.93	4	---	.979	2.476	4.064	2.692	2.0755	2.7102	13 252
1	74.2	1.020	9.90	32.60	5	---	.749	1.279	2.032	.904	.8367	1.0030	3 268
2	99.6	1.062	9.68	30.26	6	---	.725	2.983	2.032	1.067	.8512	1.0942	3 308
3	125.0	1.020	10.00	33.17	7	---	.739	3.629	2.286	1.389	1.0351	1.3637	4 521
4	211.2	1.076	10.00	37.90	8	1	.739	2.779	4.064	2.850	2.1201	2.8905	10 947
1	74.2	.779	9.85	25.45	9	---	.591	1.344	2.286	1.041	.9276	1.1420	2 904
2	99.6	.765	9.74	23.40	10	---	.576	2.655	2.286	1.214	.9931	1.2832	3 000
3	125.0	.779	9.77	23.88	11	---	.577	3.788	2.540	1.402	1.0617	1.5337	3 659
4	211.2	.814	9.85	28.41	12	2	.632	3.075	4.064	2.939	2.1547	3.0861	8 760
1	74.2	.531	9.73	17.57	13	---	.420	1.538	2.286	1.128	.9957	1.1923	2 094
2	99.6	.531	9.57	16.23	14	---	.420	2.299	2.540	1.321	1.1209	1.4514	2 354
3	125.0	.531	9.69	16.69	15	---	.410	3.440	3.048	1.727	1.3668	1.5024	2 505
4	211.2	.558	9.76	19.76	16	3	.456	3.384	5.080	3.376	2.5159	3.4417	6 795
1	74.2	.276	9.32	8.31	17	---	.228	2.023	2.540	1.598	1.3391	1.7419	1 447
2	99.6	.255	8.94	7.53	18	---	.248	2.236	2.794	1.913	1.5931	2.3099	1 737
3	125.0	.255	9.70	8.54	19	---	.214	2.586	3.048	2.007	1.6784	2.3650	2 019
4	211.2	.290	9.16	9.06	20	4	.249	4.413	5.080	3.658	2.6251	3.9776	3 620

^aBased on power law temperature-viscosity relation.^bInterpolated from plotted data.^cLinear Crocco T_t relation assumed.

TABLE 1.- Concluded

(b) Model 2 at $P_{t,1} = 13\ 790\ \text{kPa}$

Station	x, cm	T_t , K (a,b)	M_e	R_e/m	T_w/T_t (b)	Pitot case from table 5	T_t survey case from table 6	P_w , kPa (c)	Skin friction case from table 3	δ_p pitot, cm	δ_u velocity, cm	δ derived, cm	δ^* , cm (d)	θ , cm (d)	$R\theta$ (d)	N
1	35.6	294.4	11.1	59.4×10^6	.987	21	5	0.665	---	1.03	0.62	----	0.54	4.7×10^{-3}	2.32×10^3	----
2	50.5	312.8	11.2	46.0	.948	22	6	.636	21	1.27	.90	----	.76	8.2	3.77	----
3	75.9	316.7	11.0	47.8	.946	23	7	.728	22	1.91	1.00	----	.74	10.9	5.21	----
4	101.3	313.9	11.0	51.6	.933	24	8	.757	23	2.40	1.44	----	1.18	1.6×10^{-2}	8.33	----
5	136.9	314.4	11.1	52.3	.935	25	9	.754	24	2.96	1.74	2.03	1.49	1.9	1.01×10^4	10.0
6	165.1	320.0	11.2	51.9	.925	26	10	.732	25	3.18	2.46	2.12	1.73	2.1	1.10	12.0
7	190.5	310.6	11.4	55.4	.957	27	11	.717	26	4.00	2.39	3.39	2.18	2.6	1.43	9.0
8	215.9	310.6	11.6	57.8	.950	28	12	.711	27	4.57	2.70	2.99	2.39	2.8	1.61	9.0
1	35.6	286.1	11.1	61.6	.379	29	13	.665	---	.90	.55	----	.46	6.3×10^{-3}	3.22×10^3	----
2	50.5	310.6	11.3	47.7	.429	30	14	.636	29	1.14	.66	----	.49	7.0	3.32	----
3	75.9	311.1	11.1	51.7	.521	31	15	.728	30	1.78	.97	----	.79	10.0	5.15	----
4	101.3	310.6	10.9	50.7	.370	32	16	.757	31	1.80	1.17	----	.85	1.9×10^{-2}	9.49	----
5	136.9	316.7	11.2	52.9	.400	33	17	.754	32	2.50	1.79	1.96	1.15	2.6	1.35×10^4	11.0
6	165.1	311.7	11.2	52.4	.387	34	18	.732	33	2.74	1.98	2.12	1.39	2.6	1.38	11.0
7	190.5	318.9	11.5	54.9	.392	35	19	.717	34	3.50	1.98	2.54	1.68	2.5	1.36	10.0
8	215.9	322.8	11.5	53.2	.343	36	20	.711	35	3.63	2.67	2.42	1.80	3.1	1.63	10.0
1	35.6	288.3	10.9	48.6	.534	37	---	.665	---	.90	.58	----	.43	7.7×10^{-3}	3.73×10^3	----
2	50.5	304.4	11.3	49.4	.557	38	21	.636	36	1.27	.74	----	.58	7.3	3.63	----
3	75.9	307.8	11.2	54.3	.588	39	22	.728	37	2.03	.99	----	.81	9.9	5.37	----
4	101.3	307.2	10.9	51.2	.468	40	23	.757	38	2.00	1.18	----	.96	1.3×10^{-2}	6.78	----
5	136.9	313.9	11.2	53.2	.508	41	24	.754	39	2.82	1.66	2.03	1.30	2.1	1.09×10^4	11.0
6	165.1	312.8	11.2	52.7	.488	42	25	.732	40	2.67	1.93	2.12	1.46	2.5	1.30	10.0
7	190.5	317.2	11.5	54.9	.473	43	26	.717	41	4.00	2.39	2.54	1.96	2.4	1.29	10.0
8	215.9	320.6	11.8	60.1	.463	44	27	.711	42	3.94	2.81	2.82	2.05	3.0	1.80	10.0

^aMeasured in free stream. No real gas correction required.

^bFrom total-temperature survey data.

^cInterpolated from plotted data.

^dLinear Crocco T_t assumed.

TABLE 2.- HEAT-TRANSFER DATA

(a) Data summary

Case	Model	Run	Pt, 1, kPa	T _t , K	M ₁	R ₁ /m
Test 8						
1	1	11	13 238.0	305.9	18.05	43.18 × 10 ⁶
2	↓	12	11 859.1	299.3	18.0	39.91
3		13	10 583.5	297.6	17.85	36.24
4		17	9 225.2	301.8	17.77	31.07
5		15	7 929.0	298.2	17.65	27.31
6		18	6 543.2	299.2	17.51	22.63
7		20	5 433.1	296.9	17.31	19.25
8		21	4 054.1	298.7	17.13	14.43
9	↓	22	2 709.7	298.2	16.85	9.86
Test 34						
10	2	8	13 238.0	299.8	18.04	44.65 × 10 ⁶
11	↓	19	13 389.7	303.0	18.04	44.28
12		20	13 417.3	304.3	18.04	44.17
13		44	13 141.5	303.4	18.02	43.47
14		24	13 327.6	297.0	18.04	45.38
15		26	13 244.9	300.4	18.02	44.43
16		16	6 691.4	294.3	17.55	23.19
17		9	6 550.1	309.8	17.55	21.57
18		21	6 619.0	302.2	17.55	22.53
19		23	6 688.0	310.0	17.55	22.01
20		45	6 515.6	305.5	17.54	21.88
21		25	6 550.1	303.4	17.55	22.21
22		29	6 494.9	304.8	17.54	21.89
23		11	11 997.0	299.8	17.95	40.44
24		13	10 721.4	291.5	17.90	37.64
25		14	9 383.8	288.2	17.80	33.66
26		15	8 053.1	287.6	17.68	29.16
27		17	5 671.0	291.7	17.44	20.42
28		18	4 240.3	291.9	17.22	15.48
29	↓	30	4 067.9	305.4	17.26	13.92

TABLE 2.- Continued

(b) Case 1: test 8, run 11, $M_1 = 18.05$

x, cm	q, W/cm ²	T _w , K	T _w /T _t
20.65	-.1074E+00	289.01	.915
23.83	-.1067E+00	289.11	.915
27.00	-.1030E+00	289.00	.915
30.18	-.9643E-01	289.09	.915
33.35	-.9243E-01	289.07	.915
36.53	-.8698E-01	289.30	.916
39.70	-.8079E-01	289.29	.916
42.88	-.8180E-01	289.16	.915
58.75	-.7065E-01	289.47	.916
61.93	-.7224E-01	289.64	.917
65.10	-.7388E-01	289.36	.916
68.28	-.7491E-01	289.59	.917
71.45	-.6938E-01	289.63	.917
74.63	-.6252E-01	289.73	.917
80.98	-.6583E-01	289.81	.917
84.15	-.4694E-01	290.35	.919
90.50	-.4970E-01	290.46	.919
96.85	-.4834E-01	290.85	.921
100.03	-.4059E-01	291.24	.922
106.38	-.6407E-01	291.54	.923
109.55	-.8155E-01	291.32	.922
112.73	-.9330E-01	291.46	.923
114.63	-.9188E-01	291.30	.922
122.25	-.1121E+00	291.41	.922
125.43	-.1107E+00	291.24	.922
131.78	-.1336E+00	290.82	.921
134.95	-.1401E+00	290.47	.920
138.13	-.1394E+00	290.23	.919
141.30	-.1492E+00	290.18	.919
144.48	-.1425E+00	290.06	.918
147.65	-.1462E+00	290.08	.918
150.83	-.1394E+00	290.09	.918
160.35	-.1370E+00	290.25	.919
163.53	-.1469E+00	289.96	.918
166.70	-.1551E+00	289.81	.917
173.05	-.1503E+00	290.04	.918
176.23	-.1357E+00	290.07	.918
182.58	-.1226E+00	290.35	.919
185.75	-.1433E+00	290.19	.919
188.93	-.1475E+00	289.93	.918
192.10	-.1455E+00	289.82	.917
195.28	-.1266E+00	290.04	.918
201.63	-.1203E+00	290.17	.919
207.98	-.1059E+00	290.29	.919
211.15	-.1254E+00	290.08	.918
214.33	-.1442E+00	289.84	.918
217.50	-.1459E+00	289.58	.917
220.68	-.1299E+00	289.86	.918
223.85	-.1412E+00	289.83	.918

TABLE 2.- Continued

(c) Case 2: test 8, run 12, $M_1 = 18.0$

x, cm	q, W/cm ²	T _w , K	T _w /T _t
20.65	-.1150E+00	288.09	.934
23.83	-.1129E+00	288.24	.935
27.00	-.1111E+00	288.18	.934
30.18	-.1025E+00	288.31	.935
33.35	-.1010E+00	288.36	.935
36.53	-.9853E-01	288.62	.936
39.70	-.9271E-01	288.64	.936
42.88	-.8829E-01	288.49	.935
58.75	-.8087E-01	288.84	.936
61.93	-.8499E-01	288.97	.937
65.10	-.8414E-01	288.69	.936
68.28	-.8324E-01	288.91	.937
71.45	-.8497E-01	288.98	.937
74.63	-.7189E-01	289.05	.937
80.98	-.8091E-01	289.02	.937
84.15	-.5655E-01	289.77	.939
90.50	-.6272E-01	289.52	.939
96.85	-.5955E-01	289.67	.939
100.03	-.5613E-01	290.07	.940
106.38	-.7097E-01	290.18	.941
109.55	-.8397E-01	289.95	.940
112.73	-.9070E-01	290.04	.940
114.63	-.9337E-01	289.88	.940
122.25	-.1149E+00	289.93	.940
125.43	-.1151E+00	289.79	.940
131.78	-.1383E+00	289.43	.938
134.95	-.1503E+00	289.09	.937
138.13	-.1537E+00	288.93	.937
141.30	-.1570E+00	288.80	.936
144.48	-.1551E+00	288.69	.936
147.65	-.1580E+00	288.72	.936
150.83	-.1506E+00	288.72	.936
160.35	-.1462E+00	288.81	.936
163.53	-.1568E+00	288.53	.935
166.70	-.1614E+00	288.33	.935
173.05	-.1584E+00	288.53	.935
176.23	-.1496E+00	288.62	.936
182.58	-.1378E+00	288.99	.937
185.75	-.1561E+00	288.68	.936
188.93	-.1549E+00	288.44	.935
192.10	-.1489E+00	288.27	.935
195.28	-.1480E+00	288.68	.936
201.63	-.1326E+00	288.78	.936
207.98	-.1228E+00	289.02	.937
211.15	-.1416E+00	288.69	.936
214.33	-.1461E+00	288.36	.935
217.50	-.1526E+00	288.14	.934
220.68	-.1413E+00	288.48	.935
223.85	-.1439E+00	288.39	.935

TABLE 2.- Continued

(d) Case 3: test 8, run 13, $M_1 = 17.85$

x, cm	q, W/cm ²	T _w , K	T _w /T _t
20.65	-.1117E+00	287.66	.941
23.83	-.1104E+00	287.81	.941
27.00	-.1063E+00	287.78	.941
30.18	-.1031E+00	287.95	.942
33.35	-.9617E-01	287.97	.942
36.53	-.9552E-01	288.21	.942
39.70	-.8929E-01	288.24	.942
42.88	-.8299E-01	288.08	.942
58.75	-.7740E-01	288.34	.943
61.93	-.7871E-01	288.45	.943
65.10	-.8281E-01	288.21	.942
68.28	-.8293E-01	288.41	.943
71.45	-.7998E-01	288.43	.943
74.63	-.7508E-01	288.56	.944
80.98	-.7667E-01	288.47	.943
84.15	-.5362E-01	289.42	.946
90.50	-.7040E-01	288.94	.945
96.85	-.5835E-01	289.02	.945
100.03	-.4841E-01	289.38	.946
106.38	-.6718E-01	289.67	.947
109.55	-.7103E-01	289.40	.946
112.73	-.7635E-01	289.54	.947
114.63	-.7699E-01	289.37	.946
122.25	-.9789E-01	289.43	.946
125.43	-.1003E+00	289.32	.946
131.78	-.1211E+00	288.91	.945
134.95	-.1371E+00	288.62	.944
138.13	-.1325E+00	288.34	.943
141.30	-.1396E+00	288.21	.942
144.48	-.1368E+00	288.07	.942
147.65	-.1428E+00	288.13	.942
150.83	-.1360E+00	288.12	.942
160.35	-.1376E+00	288.24	.942
163.53	-.1459E+00	287.92	.941
166.70	-.1518E+00	287.72	.941
173.05	-.1504E+00	287.91	.941
176.23	-.1397E+00	288.01	.942
182.58	-.1268E+00	288.36	.943
185.75	-.1412E+00	288.04	.942
188.93	-.1435E+00	287.79	.941
192.10	-.1445E+00	287.67	.941
195.28	-.1382E+00	288.08	.942
201.63	-.1240E+00	288.14	.942
207.98	-.1161E+00	288.43	.943
211.15	-.1306E+00	288.10	.942
214.33	-.1387E+00	287.77	.941
217.50	-.1463E+00	287.59	.940
220.68	-.1333E+00	287.88	.941
223.85	-.1353E+00	287.82	.941

TABLE 2.- Continued

(e) Case 4: test 8, run 17, $M_1 = 17.77$

x, cm	q, W/cm ²	T _w , K	T _w /T _t
20.65	-.9317E-01	289.30	.936
23.83	-.9134E-01	289.45	.936
27.00	-.8729E-01	289.38	.936
30.18	-.8669E-01	289.51	.936
33.35	-.8203E-01	289.49	.936
36.53	-.8246E-01	289.75	.937
39.70	-.7776E-01	289.79	.937
42.88	-.7518E-01	289.68	.937
58.75	-.6896E-01	289.90	.938
61.93	-.6725E-01	290.08	.938
65.10	-.7811E-01	289.96	.938
68.28	-.7221E-01	290.08	.938
71.45	-.6624E-01	290.20	.939
74.63	-.5778E-01	290.22	.939
80.98	-.5993E-01	290.24	.939
84.15	-.4459E-01	291.06	.941
90.50	-.5215E-01	290.78	.941
96.85	-.3945E-01	290.97	.941
100.03	-.3633E-01	291.21	.942
106.38	-.4377E-01	291.49	.943
109.55	-.4591E-01	291.36	.942
112.73	-.5244E-01	291.61	.943
114.63	-.5651E-01	291.57	.943
122.25	-.7074E-01	291.65	.943
125.43	-.6851E-01	291.48	.943
131.78	-.9291E-01	291.37	.942
134.95	-.1076E+00	291.22	.942
138.13	-.1064E+00	291.03	.941
141.30	-.1108E+00	290.98	.941
144.48	-.1115E+00	290.94	.941
147.65	-.1141E+00	290.94	.941
150.83	-.1117E+00	290.91	.941
160.35	-.1129E+00	291.01	.941
163.53	-.1278E+00	290.88	.941
166.70	-.1326E+00	290.71	.940
173.05	-.1271E+00	290.83	.941
176.23	-.1191E+00	290.81	.941
182.58	-.1102E+00	291.03	.941
185.75	-.1281E+00	290.84	.941
188.93	-.1252E+00	290.69	.940
192.10	-.1257E+00	290.62	.940
195.28	-.1135E+00	290.88	.941
201.63	-.1049E+00	290.99	.941
207.98	-.9660E-01	291.09	.942
211.15	-.1092E+00	290.93	.941
214.33	-.1225E+00	290.76	.940
217.50	-.1266E+00	290.53	.940
220.68	-.1141E+00	290.80	.941
223.85	-.1242E+00	290.79	.941

TABLE 2.- Continued

(f) Case 5: test 8, run 15, $M_1 = 17.65$

x, cm	q , W/cm ²	T_w , K	T_w/T_t
20.65	-.1055E+00	288.27	.946
23.83	-.9916E-01	288.37	.946
27.00	-.1041E+00	288.43	.946
30.18	-.9827E-01	288.53	.946
33.35	-.9131E-01	288.52	.946
36.53	-.8852E-01	288.73	.947
39.70	-.8581E-01	288.73	.947
42.88	-.7669E-01	288.51	.946
58.75	-.7785E-01	288.66	.947
61.93	-.7493E-01	288.73	.947
65.10	-.7220E-01	288.41	.946
68.28	-.7608E-01	288.62	.947
71.45	-.7376E-01	288.64	.947
74.63	-.6895E-01	288.69	.947
80.98	-.7173E-01	288.62	.947
84.15	-.4866E-01	289.57	.950
90.50	-.5929E-01	288.83	.947
96.85	-.5639E-01	288.80	.947
100.03	-.4861E-01	289.15	.948
106.38	-.4996E-01	289.43	.949
109.55	-.4529E-01	289.21	.949
112.73	-.4471E-01	289.44	.949
114.63	-.4386E-01	289.39	.949
122.25	-.5412E-01	289.59	.950
125.43	-.5129E-01	289.56	.950
131.78	-.7582E-01	289.46	.949
134.95	-.8477E-01	289.27	.949
138.13	-.9002E-01	289.02	.948
141.30	-.9946E-01	288.97	.948
144.48	-.1076E+00	288.94	.948
147.65	-.1060E+00	288.86	.947
150.83	-.1041E+00	288.79	.947
160.35	-.1080E+00	288.83	.947
163.53	-.1168E+00	288.63	.947
166.70	-.1203E+00	288.42	.946
173.05	-.1224E+00	288.56	.946
176.23	-.1164E+00	288.58	.947
182.58	-.1124E+00	288.84	.947
185.75	-.1219E+00	288.69	.947
188.93	-.1221E+00	288.46	.946
192.10	-.1201E+00	288.33	.946
195.28	-.1187E+00	288.63	.947
201.63	-.1074E+00	288.64	.947
207.98	-.9517E-01	288.77	.947
211.15	-.1099E+00	288.57	.946
214.33	-.1179E+00	288.40	.946
217.50	-.1218E+00	288.23	.945
220.68	-.1117E+00	288.42	.946
223.85	-.1182E+00	288.38	.946

TABLE 2.- Continued

(g) Case 6: test 8, run 18, $M_1 = 17.51$

x , cm	q , W/cm ²	T_w , K	T_w/T_t
20.65	-.1030E+00	288.49	.946
23.83	-.1005E+00	288.64	.947
27.00	-.9960E-01	288.61	.946
30.18	-.9440E-01	288.69	.947
33.35	-.8734E-01	288.65	.947
36.53	-.8490E-01	288.84	.947
39.70	-.8239E-01	288.87	.947
42.88	-.8207E-01	288.72	.947
58.75	-.7173E-01	288.74	.947
61.93	-.7013E-01	288.89	.947
65.10	-.7227E-01	288.63	.947
68.28	-.7169E-01	288.78	.947
71.45	-.6911E-01	288.83	.947
74.63	-.6124E-01	288.81	.947
80.98	-.6062E-01	288.74	.947
84.15	-.4737E-01	289.48	.949
90.50	-.5644E-01	288.97	.948
96.85	-.4508E-01	289.00	.948
100.03	-.4464E-01	289.18	.948
106.38	-.4287E-01	289.37	.949
109.55	-.4120E-01	289.23	.948
112.73	-.3831E-01	289.47	.949
114.63	-.3407E-01	289.42	.949
122.25	-.3983E-01	289.65	.950
125.43	-.3548E-01	289.57	.950
131.78	-.5718E-01	289.72	.950
134.95	-.5953E-01	289.47	.949
138.13	-.6431E-01	289.32	.949
141.30	-.7414E-01	289.32	.949
144.48	-.7446E-01	289.23	.948
147.65	-.8257E-01	289.26	.949
150.83	-.7951E-01	289.15	.948
160.35	-.8436E-01	289.16	.948
163.53	-.9477E-01	289.03	.948
166.70	-.1039E+00	288.90	.947
173.05	-.1028E+00	288.90	.947
176.23	-.1007E+00	288.93	.947
182.58	-.9319E-01	289.09	.948
185.75	-.1025E+00	288.88	.947
188.93	-.1027E+00	288.74	.947
192.10	-.1040E+00	288.66	.947
195.28	-.1005E+00	288.88	.947
201.63	-.9125E-01	288.94	.948
207.98	-.8061E-01	289.07	.948
211.15	-.9592E-01	288.89	.947
214.33	-.1041E+00	288.77	.947
217.50	-.1054E+00	288.55	.946
220.68	-.9914E-01	288.77	.947
223.85	-.1044E+00	288.77	.947

TABLE 2.- Continued

(h) Case 7: test 8, run 20, $M_1 = 17.31$

x , cm	q , W/cm ²	T_w , K	T_w/T_t
20.65	-.9862E-01	287.99	.954
23.83	-.9291E-01	288.16	.955
27.00	-.9414E-01	288.15	.955
30.18	-.8858E-01	288.28	.955
33.35	-.8771E-01	288.30	.955
36.53	-.8241E-01	288.50	.956
39.70	-.8031E-01	288.51	.956
42.88	-.7832E-01	288.39	.955
58.75	-.6543E-01	288.48	.956
61.93	-.6605E-01	288.62	.956
65.10	-.7267E-01	288.40	.955
68.28	-.6614E-01	288.50	.956
71.45	-.6270E-01	288.49	.956
74.63	-.6366E-01	288.56	.956
80.98	-.6148E-01	288.47	.956
84.15	-.4441E-01	289.26	.958
90.50	-.5226E-01	288.68	.956
96.85	-.4644E-01	288.64	.956
100.03	-.4290E-01	288.84	.957
106.38	-.4179E-01	289.06	.958
109.55	-.3667E-01	288.86	.957
112.73	-.3996E-01	289.19	.958
114.63	-.3547E-01	289.13	.958
122.25	-.3728E-01	289.37	.959
125.43	-.2681E-01	289.33	.959
131.78	-.4239E-01	289.46	.959
134.95	-.4711E-01	289.31	.959
138.13	-.5022E-01	289.15	.958
141.30	-.5946E-01	289.13	.958
144.48	-.6037E-01	289.03	.958
147.65	-.6601E-01	289.07	.958
150.83	-.6426E-01	288.94	.957
160.35	-.6679E-01	288.86	.957
163.53	-.7953E-01	288.74	.957
166.70	-.8707E-01	288.59	.956
173.05	-.9142E-01	288.58	.956
176.23	-.8624E-01	288.59	.956
182.58	-.8274E-01	288.75	.957
185.75	-.9158E-01	288.53	.956
188.93	-.9788E-01	288.39	.955
192.10	-.9528E-01	288.27	.955
195.28	-.9088E-01	288.48	.956
201.63	-.8532E-01	288.51	.956
207.98	-.7957E-01	288.74	.957
211.15	-.9045E-01	288.53	.956
214.33	-.9562E-01	288.32	.955
217.50	-.9971E-01	288.14	.955
220.68	-.9058E-01	288.32	.955
223.85	-.9274E-01	288.18	.955

TABLE 2.- Continued

(i) Case 8: test 8, run 21, $M_1 = 17.13$

x, cm	q, W/cm ²	T _w , K	T _w /T _t
20.65	-.8922E-01	289.20	.956
23.83	-.8591E-01	289.34	.957
27.00	-.8621E-01	289.38	.957
30.18	-.7993E-01	289.46	.957
33.35	-.7676E-01	289.47	.957
36.53	-.7124E-01	289.64	.958
39.70	-.7375E-01	289.71	.958
42.88	-.6863E-01	289.58	.958
58.75	-.5907E-01	289.74	.958
61.93	-.5766E-01	289.87	.959
65.10	-.6229E-01	289.63	.958
68.28	-.5832E-01	289.74	.958
71.45	-.5826E-01	289.79	.958
74.63	-.5369E-01	289.83	.958
80.98	-.5162E-01	289.74	.958
84.15	-.4027E-01	290.18	.960
90.50	-.4607E-01	289.87	.959
96.85	-.4523E-01	289.81	.958
100.03	-.3811E-01	289.93	.959
106.38	-.3764E-01	290.07	.959
109.55	-.4032E-01	289.94	.959
112.73	-.3178E-01	290.11	.959
114.63	-.2800E-01	290.02	.959
122.25	-.3377E-01	290.34	.960
125.43	-.3329E-01	290.39	.960
131.78	-.2797E-01	290.58	.961
134.95	-.3722E-01	290.57	.961
138.13	-.3501E-01	290.39	.960
141.30	-.3959E-01	290.45	.960
144.48	-.4324E-01	290.45	.960
147.65	-.4039E-01	290.45	.960
150.83	-.4106E-01	290.37	.960
160.35	-.4726E-01	290.37	.960
163.53	-.4842E-01	290.22	.960
166.70	-.5497E-01	290.09	.959
173.05	-.5984E-01	290.08	.959
176.23	-.5919E-01	290.05	.959
182.58	-.5775E-01	290.12	.959
185.75	-.6601E-01	289.97	.959
188.93	-.6601E-01	289.78	.958
192.10	-.7045E-01	289.69	.958
195.28	-.6606E-01	289.79	.958
201.63	-.6792E-01	289.83	.958
207.98	-.5998E-01	289.91	.959
211.15	-.7072E-01	289.77	.958
214.33	-.7540E-01	289.62	.958
217.50	-.7834E-01	289.46	.957
220.68	-.7623E-01	289.62	.958
223.85	-.7561E-01	289.47	.957

TABLE 2.- Continued

(j) Case 9: test 8, run 22, $M_1 = 16.85$

x, cm	q, W/cm ²	T _w , K	T _w /T _t
20.65	-.7780E-01	289.79	.963
23.83	-.7679E-01	289.94	.963
27.00	-.7598E-01	289.95	.963
30.18	-.7086E-01	290.02	.964
33.35	-.6820E-01	290.06	.964
36.53	-.6852E-01	290.28	.965
39.70	-.6289E-01	290.29	.965
42.88	-.6109E-01	290.00	.964
58.75	-.5189E-01	290.34	.965
61.93	-.5103E-01	290.48	.965
65.10	-.5302E-01	290.25	.964
68.28	-.4592E-01	290.33	.965
71.45	-.4867E-01	290.39	.965
74.63	-.4483E-01	290.45	.965
80.98	-.4437E-01	290.38	.965
84.15	-.3680E-01	290.81	.966
90.50	-.4007E-01	290.46	.965
96.85	-.4112E-01	290.33	.965
100.03	-.3280E-01	290.43	.965
106.38	-.3792E-01	290.57	.966
109.55	-.3425E-01	290.34	.965
112.73	-.3260E-01	290.56	.965
114.63	-.3292E-01	290.48	.965
122.25	-.2835E-01	290.64	.966
125.43	-.2340E-01	290.63	.966
131.78	-.2992E-01	290.92	.967
134.95	-.3147E-01	290.84	.966
138.13	-.2593E-01	290.71	.966
141.30	-.2996E-01	290.81	.966
144.48	-.3196E-01	290.83	.966
147.65	-.2578E-01	290.81	.966
150.83	-.2985E-01	290.92	.967
160.35	-.2129E-01	290.98	.967
163.53	-.2817E-01	290.97	.967
166.70	-.3002E-01	290.92	.967
173.05	-.3416E-01	290.93	.967
176.23	-.3339E-01	290.96	.967
182.58	-.3563E-01	291.02	.967
185.75	-.3728E-01	290.91	.967
188.93	-.3674E-01	290.73	.966
192.10	-.3637E-01	290.62	.966
195.28	-.3744E-01	290.71	.966
201.63	-.3674E-01	290.65	.966
207.98	-.3368E-01	290.69	.966
211.15	-.4097E-01	290.57	.966
214.33	-.4650E-01	290.51	.965
217.50	-.4845E-01	290.38	.965
220.68	-.4947E-01	290.48	.965
223.85	-.4806E-01	290.37	.965

TABLE 2.- Continued

(k) Case 10: test 34, run 8, $M_1 = 18.04$

x, cm	q, W/cm ²	T _w , K	T _w /T _t
42.33	.4100E+00	124.70	.402
45.77	.5108E+00	124.70	.402
49.20	.6000E+00	123.51	.398
52.64	.7119E+00	122.91	.396
56.08	.8154E+00	122.62	.395
59.52	.9750E+00	122.91	.396
62.95	.9918E+00	121.13	.391
66.39	.1224E+01	122.91	.396
69.83	.1269E+01	123.81	.399
73.27	.1260E+01	123.51	.398
76.71	.1343E+01	124.40	.401
80.14	.1264E+01	122.02	.393
83.58	.1303E+01	123.21	.397
87.02	.1226E+01	122.32	.394
90.45	.1169E+01	122.02	.393
93.89	.1236E+01	124.10	.400
97.33	.1248E+01	123.81	.399
100.77	.1178E+01	124.10	.400
104.20	.1158E+01	123.51	.398
107.64	.1139E+01	125.00	.403
111.08	.1148E+01	125.59	.405
112.03	.1085E+01	125.59	.405
114.52	.9917E+00	127.38	.411
117.95	.1089E+01	125.59	.405
119.67	.1014E+01	122.32	.394
121.39	.8103E+00	132.73	.428
124.83	.9151E+00	129.76	.418
128.26	.7496E+00	134.52	.434
131.70	.8023E+00	133.92	.432
132.40	.7666E+00	130.35	.420
135.14	.8405E+00	135.11	.436
154.94	.7899E+00	138.98	.448
156.65	.7524E+00	137.20	.442
158.37	.7069E+00	136.31	.440
160.09	.7644E+00	137.79	.444
161.81	.7468E+00	137.20	.442
163.53	.7695E+00	135.71	.438
165.25	.7638E+00	135.11	.436
166.97	.6984E+00	134.22	.433
168.69	.7659E+00	134.52	.434
170.40	.7129E+00	132.14	.426
172.12	.7430E+00	132.73	.428
173.84	.7523E+00	131.25	.423
175.56	.7385E+00	132.14	.426
177.28	.7251E+00	130.06	.419
179.00	.6905E+00	129.46	.417
180.72	.6932E+00	129.16	.417
182.44	.7018E+00	129.76	.418
184.16	.7179E+00	128.27	.414

TABLE 2.- Continued

(k) Concluded

x , cm	q , W/cm ²	T_w , K	T_w/T_t
185.87	.6947E+00	128.57	.415
189.31	.5537E+00	164.88	.532
191.03	.5871E+00	121.42	.392
192.75	.7485E+00	126.48	.408
194.46	.6261E+00	125.29	.404
196.18	.7228E+00	125.29	.404
197.90	.7185E+00	123.81	.399
199.62	.7671E+00	126.78	.409
201.34	.6853E+00	124.70	.402
203.06	.6553E+00	123.81	.399
204.78	.6421E+00	122.02	.393
206.50	.6172E+00	124.40	.401
208.22	.6060E+00	127.67	.412
209.93	.6485E+00	124.40	.401
211.63	.6115E+00	122.62	.395
213.37	.7619E+00	124.70	.402
215.09	.6674E+00	124.40	.401
216.81	.6555E+00	121.13	.391
218.53	.7465E+00	121.72	.393
220.25	.7648E+00	123.21	.397
221.97	.7070E+00	122.32	.394
223.69	.7174E+00	123.81	.399

TABLE 2.- Continued

(1) Case 11: test 34, run 19, $M_1 = 18.04$

x, cm	q, W/cm ²	T _w , K	T _w /T _t
42.33	.2844E+00	146.55	.468
45.77	.3551E+00	146.24	.467
49.20	.4426E+00	144.67	.462
52.64	.5422E+00	143.11	.457
56.08	.6535E+00	142.17	.454
59.52	.7554E+00	141.23	.451
62.95	.7594E+00	139.35	.445
66.39	.9306E+00	139.66	.446
69.83	.9489E+00	139.98	.447
73.27	.9295E+00	139.04	.444
76.71	.1022E+01	139.35	.445
80.14	.9314E+00	137.47	.439
83.58	.9649E+00	138.72	.443
87.02	.9337E+00	137.16	.438
90.45	.8866E+00	137.47	.439
93.89	.9162E+00	139.35	.445
97.33	.8941E+00	139.66	.446
100.77	.8854E+00	140.29	.448
104.20	.8695E+00	140.91	.450
107.64	.8273E+00	143.11	.457
111.08	.8444E+00	144.67	.462
112.03	.7971E+00	146.86	.469
114.52	.8100E+00	145.93	.466
117.95	.8205E+00	145.61	.465
119.67	.7677E+00	142.17	.454
121.39	.7065E+00	151.87	.485
124.83	.7588E+00	150.94	.482
128.26	.6154E+00	156.26	.499
131.70	.6844E+00	156.26	.499
132.40	.5955E+00	155.63	.497
135.14	.6063E+00	160.02	.511
154.94	.3792E+00	189.77	.606
156.65	.3575E+00	189.14	.604
158.37	.3945E+00	187.57	.599
160.09	.4144E+00	186.01	.594
161.81	.4074E+00	186.01	.594
163.53	.4370E+00	184.75	.590
165.25	.4511E+00	182.25	.582
166.97	.4816E+00	178.18	.569
168.69	.5101E+00	178.49	.570
170.40	.5152E+00	175.99	.562
172.12	.5421E+00	173.48	.554
173.84	.5667E+00	169.10	.540
175.56	.5607E+00	169.72	.542
177.28	.5695E+00	167.85	.536
179.00	.5514E+00	165.03	.527
180.72	.5713E+00	162.21	.518
182.44	.5758E+00	162.52	.519
184.16	.5821E+00	161.27	.515

TABLE 2.- Continued

(1) Concluded

x, cm	q, W/cm ²	T _w , K	T _w /T _t
185.87	.5736E+00	159.70	.510
189.31	.4635E+00	186.63	.596
191.03	.5355E+00	153.75	.491
192.75	.6285E+00	155.32	.496
194.46	.5370E+00	152.81	.488
196.18	.5996E+00	154.69	.494
197.90	.5997E+00	155.32	.496
199.62	.6460E+00	154.69	.494
201.34	.5634E+00	152.50	.487
203.06	.5502E+00	154.07	.492
204.78	.4951E+00	154.69	.494
206.50	.5086E+00	154.38	.493
208.22	.5490E+00	154.07	.492
209.93	.5062E+00	155.01	.495
211.63	.4787E+00	155.95	.498
213.37	.6039E+00	156.26	.499
215.09	.5609E+00	155.01	.495
216.81	.5404E+00	155.32	.496
218.53	.5586E+00	156.57	.500
220.25	.5696E+00	156.57	.500
221.97	.5577E+00	155.63	.497
223.69	.5129E+00	157.82	.504

TABLE 2.- Continued

(m) Case 12: test 34, run 20, $M_1 = 18.04$

x, cm	q, W/cm ²	T _w , K	T _w /T _t
42.33	.2051E+00	179.27	.571
45.77	.2750E+00	178.95	.570
49.20	.3349E+00	176.72	.563
52.64	.4319E+00	175.13	.558
56.08	.5238E+00	173.21	.552
59.52	.6167E+00	171.62	.547
62.95	.6160E+00	169.38	.540
66.39	.7739E+00	169.70	.541
69.83	.8087E+00	169.38	.540
73.27	.8017E+00	168.75	.538
76.71	.8521E+00	168.75	.538
80.14	.7690E+00	167.79	.535
83.58	.7958E+00	169.06	.539
87.02	.7594E+00	168.75	.538
90.45	.7112E+00	169.38	.540
93.89	.7408E+00	170.98	.545
97.33	.7309E+00	170.98	.545
100.77	.7033E+00	171.62	.547
104.20	.7012E+00	171.62	.547
107.64	.6858E+00	172.57	.550
111.08	.7032E+00	172.89	.551
112.03	.6396E+00	174.17	.555
114.52	.6564E+00	173.53	.553
117.95	.6619E+00	172.89	.551
119.67	.6288E+00	170.66	.544
121.39	.5538E+00	177.04	.564
124.83	.6192E+00	176.08	.561
128.26	.4763E+00	181.19	.577
131.70	.4996E+00	183.10	.583
132.40	.4956E+00	180.23	.574
135.14	.5027E+00	187.57	.598
154.94	.2631E+00	213.72	.681
156.65	.2609E+00	212.77	.678
158.37	.2575E+00	213.09	.679
160.09	.2660E+00	212.77	.678
161.81	.2745E+00	212.45	.677
163.53	.2856E+00	211.17	.673
165.25	.3008E+00	209.90	.669
166.97	.3033E+00	207.66	.662
168.69	.3383E+00	207.02	.660
170.40	.3293E+00	205.75	.656
172.12	.3552E+00	204.47	.651
173.84	.3759E+00	201.28	.641
175.56	.3681E+00	201.28	.641
177.28	.3771E+00	199.69	.636
179.00	.3631E+00	197.45	.629
180.72	.3836E+00	194.58	.620
182.44	.3889E+00	194.90	.621
184.16	.4079E+00	193.31	.616

TABLE 2.- Continued

(m) Concluded

x, cm	q, W/cm ²	T _w , K	T _w /T _t
185.87	.4090E+00	191.71	.611
189.31	.3263E+00	211.17	.673
191.03	.3567E+00	186.61	.595
192.75	.4232E+00	186.93	.596
194.46	.3389E+00	185.65	.591
196.18	.4069E+00	185.33	.590
197.90	.4441E+00	184.38	.587
199.62	.4186E+00	185.97	.592
201.34	.3667E+00	186.29	.594
203.06	.3632E+00	185.65	.591
204.78	.3948E+00	183.42	.584
206.50	.3825E+00	187.88	.599
208.22	.3106E+00	192.99	.615
209.93	.3923E+00	188.84	.602
211.63	.3770E+00	185.65	.591
213.37	.4069E+00	186.93	.596
215.09	.3675E+00	187.57	.598
216.81	.3695E+00	184.38	.587
218.53	.3834E+00	87.08	.277
220.25	.4022E+00	184.06	.586
221.97	.3810E+00	184.38	.587
223.69	.3848E+00	184.70	.588

TABLE 2.- Continued

(n) Case 13: test 34, run 44, $M_1 = 18.02$

x , cm	q , W/cm ²	T_w , K	T_w/T_t
42.33	.1090E+00	204.90	.654
45.77	.1541E+00	205.84	.657
49.20	.1967E+00	205.21	.655
52.64	.2672E+00	204.90	.654
56.08	.3399E+00	204.27	.652
59.52	.3904E+00	203.33	.649
62.95	.4206E+00	201.46	.643
66.39	.5132E+00	201.77	.644
69.83	.5278E+00	201.14	.642
73.27	.5288E+00	200.20	.639
76.71	.5550E+00	199.89	.638
80.14	.5150E+00	198.95	.635
83.58	.5119E+00	199.58	.637
87.02	.4912E+00	199.26	.636
90.45	.4558E+00	199.58	.637
93.89	.4682E+00	200.52	.640
97.33	.4653E+00	201.14	.642
100.77	.4336E+00	201.77	.644
104.20	.4401E+00	202.08	.645
107.64	.4148E+00	203.02	.648
111.08	.4175E+00	203.33	.649
112.03	.3791E+00	204.59	.653
114.52	.3921E+00	204.27	.652
117.95	.4060E+00	204.27	.652
119.67	.3825E+00	202.71	.647
121.39	.2982E+00	208.03	.664
124.83	.3371E+00	208.03	.664
128.26	.2354E+00	212.11	.677
131.70	.2611E+00	214.30	.684
132.40	.2815E+00	212.11	.677
135.14	.2334E+00	217.43	.694
154.94	.1911E+00	224.01	.715
156.65	.1939E+00	224.33	.716
158.37	.2058E+00	224.95	.718
160.09	.2037E+00	225.27	.719
161.81	.2007E+00	226.21	.722
163.53	.1951E+00	225.89	.721
165.25	.2063E+00	225.89	.721
166.97	.1967E+00	224.95	.718
168.69	.2118E+00	225.58	.720
170.40	.2098E+00	224.95	.718
172.12	.2267E+00	224.64	.717
173.84	.2203E+00	223.39	.713
175.56	.2064E+00	224.01	.715
177.28	.2303E+00	222.76	.711
179.00	.2163E+00	222.45	.710
180.72	.2311E+00	221.19	.706
182.44	.2258E+00	221.51	.707
184.16	.2272E+00	219.94	.702

TABLE 2.- Continued

(n) Concluded

x, cm	q, W/cm ²	T _w , K	T _w /T _t
185.87	.2364E+00	219.94	.702
189.31	.1940E+00	234.35	.748
191.03	.2277E+00	215.55	.688
192.75	.2290E+00	217.43	.694
194.46	.2052E+00	217.75	.695
196.18	.1938E+00	217.43	.694
197.90	.2259E+00	215.24	.687
199.62	.2406E+00	217.12	.693
201.34	.2087E+00	218.69	.698
203.06	.1811E+00	218.69	.698
204.78	.5196E+00	217.43	.694
206.50	.1355E+00	221.82	.708
208.22	.1682E+00	221.82	.708
209.93	.1546E+00	222.13	.709
211.63	.1700E+00	219.63	.701
213.37	.2162E+00	219.94	.702
215.09	.2092E+00	219.63	.701
216.81	.2175E+00	217.12	.693
218.53	.2248E+00	214.93	.686
220.25	.2264E+00	216.18	.690
221.97	.2278E+00	215.55	.688
223.69	.2375E+00	214.93	.686

TABLE 2.- Continued

(o) Case 14: test 34, run 24, $M_1 = 18.04$

x, cm	q, W/cm ²	T _w , K	T _w /T _t
42.33	.1805E-02	238.85	.778
45.77	.4387E-01	239.46	.780
49.20	.7563E-01	239.46	.780
52.64	.1174E+00	239.77	.781
56.08	.1477E+00	239.77	.781
59.52	.1931E+00	239.46	.780
62.95	.2081E+00	238.54	.777
66.39	.2540E+00	238.23	.776
69.83	.2518E+00	237.93	.775
73.27	.2492E+00	237.00	.772
76.71	.2469E+00	236.39	.770
80.14	.2507E+00	235.16	.766
83.58	.2620E+00	234.86	.765
87.02	.2456E+00	234.24	.763
90.45	.2298E+00	233.93	.762
93.89	.2335E+00	233.93	.762
97.33	.2174E+00	233.93	.762
100.77	.2119E+00	233.93	.762
104.20	.1990E+00	233.93	.762
107.64	.1926E+00	234.55	.764
111.08	.1944E+00	234.86	.765
112.03	.1716E+00	235.78	.768
114.52	.1592E+00	235.47	.767
117.95	.1740E+00	235.16	.766
119.67	.1862E+00	233.93	.762
121.39	.1183E+00	237.31	.773
124.83	.1530E+00	237.00	.772
128.26	.9815E-01	238.85	.778
131.70	.1185E+00	239.46	.780
132.40	.1298E+00	239.15	.779
135.14	.1168E+00	241.00	.785
154.94	.5951E-01	248.36	.809
156.65	.5650E-01	248.98	.811
158.37	.5505E-01	249.28	.812
160.09	.4982E-01	249.59	.813
161.81	.4531E-01	250.51	.816
163.53	.4253E-01	250.51	.816
165.25	.4506E-01	250.51	.816
166.97	.3925E-01	250.21	.815
168.69	.5149E-01	250.51	.816
170.40	.5443E-01	250.51	.816
172.12	.6044E-01	250.21	.815
173.84	.6257E-01	249.28	.812
175.56	.6239E-01	249.59	.813
177.28	.5303E-01	249.28	.812
179.00	.5112E-01	248.67	.810
180.72	.7284E-01	247.44	.806
182.44	.7320E-01	247.75	.807
184.16	.8105E-01	247.44	.806

TABLE 2.- Continued

(o) Concluded

x, cm	q, W/cm ²	T _w , K	T _w /T _t
185.87	.8062E-01	246.83	.804
189.31	.6977E-01	255.12	.831
191.03	.9173E-01	244.99	.798
192.75	.9310E-01	244.68	.797
194.46	.9361E-01	243.45	.793
196.18	.1032E+00	243.14	.792
197.90	.8202E-01	243.45	.793
199.62	.9848E-01	243.76	.794
201.34	.9820E-01	242.22	.789
203.06	.1095E+00	242.22	.789
204.78	.8669E-01	242.22	.789
206.50	.9400E-01	242.22	.789
208.22	.8206E-01	241.61	.787
209.93	.1021E+00	241.92	.788
211.63	.9011E-01	241.92	.788
213.37	.9376E-01	241.00	.785
215.09	.9906E-01	240.38	.783
216.81	.1241E+00	240.07	.782
218.53	.9797E-01	239.77	.781
220.25	.1211E+00	239.77	.781
221.97	.1145E+00	239.15	.779
223.69	.9945E-01	239.46	.780

TABLE 2.- Continued

(p) Case 15: test 34, run 26, $M_1 = 18.02$

x, cm	q, W/cm ²	T _w , K	T _w /T _t
42.33	-.7224E-01	283.79	.915
45.77	-.6509E-01	283.79	.915
49.20	-.5520E-01	284.10	.916
52.64	-.4457E-01	284.10	.916
56.08	-.3284E-01	284.72	.918
59.52	-.1134E-01	284.10	.916
62.95	.5244E-02	284.41	.917
66.39	.1975E-02	284.41	.917
69.83	-.8955E-02	284.41	.917
73.27	-.1357E-01	284.41	.917
76.71	-.4061E-01	284.41	.917
80.14	-.3642E-01	284.41	.917
83.58	-.6107E-01	284.41	.917
87.02	-.6346E-01	284.10	.916
90.45	-.8164E-01	284.10	.916
93.89	-.9695E-01	284.10	.916
97.33	-.1076E+00	284.10	.916
100.77	-.1168E+00	284.10	.916
104.20	-.1160E+00	284.10	.916
107.64	-.1188E+00	284.10	.916
111.08	-.1184E+00	284.10	.916
112.03	-.1173E+00	284.10	.916
114.52	-.1274E+00	284.10	.916
117.95	-.1150E+00	284.10	.916
119.67	-.9224E-01	284.10	.916
121.39	-.1491E+00	284.41	.917
124.83	-.1261E+00	284.10	.916
128.26	-.1484E+00	284.41	.917
131.70	-.1285E+00	284.10	.916
132.40	-.1135E+00	284.10	.916
135.14	-.1312E+00	284.10	.916
154.94	-.1081E+00	284.10	.916
156.65	-.9365E-01	284.10	.916
158.37	-.7543E-01	284.10	.916
160.09	-.1122E+00	284.41	.917
161.81	-.1098E+00	284.41	.917
163.53	-.1168E+00	284.41	.917
165.25	-.9480E-01	284.41	.917
166.97	-.9615E-01	284.41	.917
168.69	-.1120E+00	284.41	.917
170.40	-.1053E+00	284.41	.917
172.12	-.9855E-01	284.41	.917
173.84	-.1012E+00	284.41	.917
175.56	-.1105E+00	284.41	.917
177.28	-.1062E+00	284.41	.917
179.00	-.9899E-01	284.41	.917
180.72	-.9805E-01	284.41	.917
182.44	-.1007E+00	284.41	.917
184.16	-.1049E+00	284.10	.916

TABLE 2.- Continued

(p) Concluded

x, cm	q, W/cm ²	T _w , K	T _w /T _t
185.87	-.9999E-01	284.41	.917
189.31	-.7391E-01	285.34	.920
191.03	-.7123E-01	284.41	.917
192.75	-.9703E-01	284.10	.916
194.46	-.7543E-01	284.10	.916
196.18	-.9617E-01	284.10	.916
197.90	-.1088E+00	284.41	.917
199.62	-.1019E+00	284.10	.916
201.34	-.7892E-01	284.10	.916
203.06	-.7175E-01	283.79	.915
204.78	-.1045E+00	283.79	.915
206.50	-.8385E-01	283.79	.915
208.22	-.9533E-01	283.79	.915
209.93	-.7755E-01	283.79	.915
211.63	-.1003E+00	284.10	.916
213.37	-.9103E-01	283.79	.915
215.09	-.6186E-01	283.79	.915
216.81	-.7141E-01	283.79	.915
218.53	-.1004E+00	283.79	.915
220.25	-.8467E-01	283.79	.915
221.97	-.7669E-01	283.79	.915
223.69	-.8850E-01	283.79	.915

TABLE 2.- Continued

(q) Case 16: test 34, run 16, $M_1 = 17.55$

x, cm	q, W/cm ²	T _w , K	T _w /T _t
42.33	.2118E+00	108.57	.362
45.77	.2400E+00	109.17	.364
49.20	.2303E+00	108.27	.361
52.64	.2251E+00	107.67	.359
56.08	.2428E+00	107.37	.358
59.52	.2471E+00	107.07	.357
62.95	.2390E+00	106.47	.355
66.39	.2944E+00	107.37	.358
69.83	.3515E+00	107.67	.359
73.27	.3858E+00	107.97	.360
76.71	.4330E+00	108.57	.362
80.14	.4608E+00	107.97	.360
83.58	.5344E+00	109.17	.364
87.02	.5489E+00	109.17	.364
90.45	.5543E+00	109.47	.365
93.89	.6119E+00	111.26	.371
97.33	.6225E+00	111.56	.372
100.77	.6338E+00	112.46	.375
104.20	.6401E+00	112.76	.376
107.64	.6365E+00	113.66	.379
111.08	.6546E+00	114.56	.382
112.03	.6539E+00	114.56	.382
114.52	.6292E+00	115.46	.385
117.95	.6491E+00	114.26	.381
119.67	.5921E+00	113.06	.377
121.39	.5903E+00	118.76	.396
124.83	.6194E+00	116.66	.389
128.26	.5267E+00	119.96	.400
131.70	.5681E+00	119.96	.400
132.40	.5517E+00	118.76	.396
135.14	.5817E+00	120.56	.402
154.94	.5768E+00	109.47	.365
156.65	.5633E+00	108.27	.361
158.37	.5447E+00	108.87	.363
160.09	.5566E+00	110.66	.369
161.81	.5540E+00	110.36	.368
163.53	.5847E+00	108.87	.363
165.25	.5672E+00	110.07	.367
166.97	.5118E+00	111.26	.371
168.69	.5424E+00	111.26	.371
170.40	.5541E+00	107.97	.360
172.12	.5531E+00	110.96	.370
173.84	.5468E+00	111.26	.371
175.56	.5356E+00	111.26	.371
177.28	.5611E+00	108.87	.363
179.00	.5207E+00	110.36	.368
180.72	.5133E+00	112.76	.376
182.44	.5249E+00	112.16	.374
184.16	.5547E+00	109.47	.365

TABLE 2.- Continued

(q) Concluded

x, cm	q, W/cm ²	T _w , K	T _w /T _t
185.87	.5396E+00	112.46	.375
189.31	.4043E+00	152.65	.509
191.03	.4266E+00	108.57	.362
192.75	.5196E+00	113.06	.377
194.46	.4033E+00	115.16	.384
196.18	.4995E+00	116.06	.387
197.90	.5033E+00	113.06	.377
199.62	.5192E+00	115.46	.385
201.34	.4411E+00	118.16	.394
203.06	.4328E+00	116.66	.389
204.78	.4460E+00	114.86	.383
206.50	.4274E+00	120.26	.401
208.22	.3965E+00	124.76	.416
209.93	.4328E+00	121.76	.406
211.63	.4152E+00	119.36	.398
213.37	.4792E+00	120.26	.401
215.09	.4379E+00	120.26	.401
216.81	.4217E+00	116.66	.389
218.53	.4542E+00	114.86	.383
220.25	.4580E+00	116.06	.387
221.97	.4340E+00	115.46	.385
223.69	.4360E+00	115.46	.385

TABLE 2.- Continued

(r) Case 17: test 34, run 9, $M_1 = 17.55$

x, cm	q, W/cm ²	T _w , K	T _w /T _t
42.33	.1271E+00	177.09	.562
45.77	.1463E+00	176.46	.560
49.20	.1652E+00	175.20	.556
52.64	.1526E+00	173.94	.552
56.08	.1447E+00	173.00	.549
59.52	.1616E+00	172.05	.546
62.95	.1623E+00	171.11	.543
66.39	.1957E+00	170.48	.541
69.83	.2166E+00	170.48	.541
73.27	.2367E+00	169.84	.539
76.71	.2751E+00	170.16	.540
80.14	.2945E+00	169.84	.539
83.58	.3353E+00	170.48	.541
87.02	.3516E+00	170.79	.542
90.45	.3610E+00	171.74	.545
93.89	.4190E+00	173.31	.550
97.33	.4428E+00	174.57	.554
100.77	.4292E+00	175.83	.558
104.20	.4245E+00	177.09	.562
107.64	.4459E+00	178.98	.568
111.08	.4322E+00	180.24	.572
112.03	.3957E+00	181.50	.576
114.52	.3858E+00	181.19	.575
117.95	.4030E+00	180.87	.574
119.67	.3840E+00	178.67	.567
121.39	.3432E+00	183.08	.581
124.83	.3910E+00	182.13	.578
128.26	.3258E+00	184.02	.584
131.70	.3604E+00	183.71	.583
132.40	.3531E+00	184.02	.584
135.14	.3868E+00	183.08	.581
154.94	.4110E+00	171.11	.543
156.65	.3952E+00	171.11	.543
158.37	.3540E+00	171.74	.545
160.09	.3757E+00	174.26	.553
161.81	.3677E+00	173.94	.552
163.53	.3811E+00	173.63	.551
165.25	.3646E+00	174.89	.555
166.97	.3419E+00	176.15	.559
168.69	.3587E+00	175.83	.558
170.40	.3478E+00	174.89	.555
172.12	.3544E+00	176.78	.561
173.84	.3537E+00	177.72	.564
175.56	.3386E+00	177.41	.563
177.28	.3533E+00	176.46	.560
179.00	.3243E+00	177.41	.563
180.72	.3269E+00	178.67	.567
182.44	.3290E+00	178.35	.566
184.16	.3296E+00	177.41	.563

TABLE 2.- Continued

(r) Concluded

x, cm	q, W/cm ²	T _w , K	T _w /T _t
185.87	.3190E+00	178.98	.568
189.31	.2637E+00	203.25	.645
191.03	.2648E+00	177.41	.563
192.75	.3049E+00	180.56	.573
194.46	.2345E+00	181.82	.577
196.18	.2821E+00	183.08	.581
197.90	.2998E+00	181.19	.575
199.62	.3069E+00	181.82	.577
201.34	.2491E+00	184.66	.586
203.06	.2526E+00	184.34	.585
204.78	.2510E+00	183.71	.583
206.50	.2432E+00	186.55	.592
208.22	.2174E+00	190.64	.605
209.93	.2647E+00	187.81	.596
211.63	.2458E+00	186.23	.591
213.37	.2669E+00	188.44	.598
215.09	.2256E+00	190.01	.603
216.81	.2216E+00	187.81	.596
218.53	.2412E+00	186.86	.593
220.25	.2427E+00	189.07	.600
221.97	.2168E+00	190.96	.606
223.69	.2261E+00	190.33	.604

TABLE 2.- Continued

(s) Case 18: test 34, run 21, $M_1 = 17.55$

x, cm	q, W/cm ²	T _w , K	T _w /T _t
42.33	.1088E+00	177.92	.578
45.77	.1174E+00	177.30	.576
49.20	.1244E+00	175.76	.571
52.64	.1300E+00	173.92	.565
56.08	.1502E+00	172.38	.560
59.52	.1560E+00	170.22	.553
62.95	.1650E+00	168.38	.547
66.39	.2109E+00	167.76	.545
69.83	.2332E+00	167.14	.543
73.27	.2498E+00	166.84	.542
76.71	.3065E+00	166.84	.542
80.14	.3225E+00	166.53	.541
83.58	.3707E+00	167.76	.545
87.02	.3849E+00	168.07	.546
90.45	.3962E+00	168.68	.548
93.89	.4312E+00	170.22	.553
97.33	.4409E+00	171.15	.556
100.77	.4302E+00	172.07	.559
104.20	.4321E+00	172.68	.561
107.64	.4344E+00	174.22	.566
111.08	.4265E+00	175.15	.569
112.03	.3928E+00	178.53	.580
114.52	.3978E+00	176.38	.573
117.95	.4116E+00	176.69	.574
119.67	.3845E+00	173.92	.565
121.39	.3187E+00	180.69	.587
124.83	.3495E+00	181.61	.590
128.26	.2774E+00	186.54	.606
131.70	.2828E+00	189.61	.616
132.40	.2843E+00	187.77	.610
135.14	.2962E+00	193.92	.630
154.94	.1790E+00	208.70	.678
156.65	.1841E+00	208.70	.678
158.37	.1779E+00	209.01	.679
160.09	.1766E+00	209.01	.679
161.81	.1867E+00	209.01	.679
163.53	.1893E+00	208.39	.677
165.25	.2057E+00	207.78	.675
166.97	.1961E+00	206.24	.670
168.69	.2077E+00	205.93	.669
170.40	.2141E+00	204.39	.664
172.12	.2207E+00	203.77	.662
173.84	.2272E+00	201.00	.653
175.56	.2325E+00	201.31	.654
177.28	.2350E+00	200.08	.650
179.00	.2238E+00	198.54	.645
180.72	.2373E+00	196.39	.638
182.44	.2349E+00	196.39	.638
184.16	.2490E+00	194.85	.633

TABLE 2.- Continued

(s) Concluded

x , cm	q , W/cm ²	T_w , K	T_w/T_t
185.87	.2480E+00	194.23	.631
189.31	.1996E+00	213.32	.693
191.03	.2256E+00	190.23	.618
192.75	.2496E+00	190.85	.620
194.46	.2230E+00	190.85	.620
196.18	.2452E+00	190.85	.620
197.90	.2540E+00	189.00	.614
199.62	.2560E+00	190.54	.619
201.34	.2196E+00	192.39	.625
203.06	.2146E+00	192.08	.624
204.78	.2314E+00	190.23	.618
206.50	.2091E+00	195.46	.635
208.22	.1691E+00	199.77	.649
209.93	.2197E+00	196.39	.638
211.63	.2071E+00	193.31	.628
213.37	.2349E+00	193.62	.629
215.09	.2177E+00	194.23	.631
216.81	.2169E+00	190.54	.619
218.53	.2327E+00	188.08	.611
220.25	.2403E+00	189.31	.615
221.97	.2308E+00	189.00	.614
223.69	.2273E+00	188.69	.613

TABLE 2.- Continued

(t) Case 19: test 34, run 23, $M_1 = 17.55$

x , cm	q , W/cm ²	T_w , K	T_w/T_t
42.33	.3134E-01	220.82	.700
45.77	.2168E-01	221.77	.703
49.20	.2831E-01	222.08	.704
52.64	.3655E-01	222.08	.704
56.08	.4143E-01	222.08	.704
59.52	.4514E-01	221.77	.703
62.95	.6837E-01	221.14	.701
66.39	.8228E-01	221.14	.701
69.83	.1016E+00	220.82	.700
73.27	.1427E+00	220.82	.700
76.71	.1439E+00	220.51	.699
80.14	.1652E+00	220.19	.698
83.58	.1934E+00	219.88	.697
87.02	.2058E+00	219.56	.696
90.45	.2160E+00	218.93	.694
93.89	.2357E+00	218.61	.693
97.33	.2448E+00	217.67	.690
100.77	.2498E+00	217.04	.688
104.20	.2526E+00	215.46	.683
107.64	.2503E+00	214.51	.680
111.08	.2598E+00	211.99	.672
112.03	.2657E+00	209.78	.665
114.52	.2514E+00	211.99	.672
117.95	.2662E+00	210.10	.666
119.67	.2436E+00	211.67	.671
121.39	.2176E+00	210.10	.666
124.83	.2927E+00	207.26	.657
128.26	.2327E+00	207.57	.658
131.70	.2692E+00	205.37	.651
132.40	.2821E+00	203.16	.644
135.14	.2988E+00	204.42	.648
154.94	.1943E+00	214.51	.680
156.65	.1953E+00	214.51	.680
158.37	.1765E+00	215.78	.684
160.09	.1865E+00	216.41	.686
161.81	.1835E+00	217.04	.688
163.53	.1874E+00	216.72	.687
165.25	.1798E+00	217.67	.690
166.97	.1764E+00	217.67	.690
168.69	.1820E+00	217.98	.691
170.40	.1781E+00	217.35	.689
172.12	.1878E+00	217.98	.691
173.84	.1834E+00	217.67	.690
175.56	.1810E+00	217.98	.691
177.28	.1854E+00	217.04	.688
179.00	.1739E+00	217.04	.688
180.72	.1738E+00	217.35	.689
182.44	.1781E+00	217.04	.688
184.16	.1779E+00	216.09	.685

TABLE 2.- Continued

(t) Concluded

x, cm	q, W/cm ²	T _w , K	T _w /T _t
185.87	.1851E+00	216.09	.685
189.31	.1563E+00	230.92	.732
191.03	.1738E+00	213.57	.677
192.75	.1754E+00	214.20	.679
194.46	.1575E+00	213.88	.678
196.18	.1769E+00	212.31	.673
197.90	.1832E+00	212.31	.673
199.62	.1933E+00	213.25	.676
201.34	.1754E+00	212.31	.673
203.06	.1704E+00	211.04	.669
204.78	.1769E+00	209.78	.665
206.50	.1819E+00	209.78	.665
208.22	.1533E+00	211.67	.671
209.93	.1824E+00	209.15	.663
211.63	.1862E+00	208.20	.660
213.37	.1941E+00	209.78	.665
215.09	.1694E+00	211.04	.669
216.81	.1653E+00	209.15	.663
218.53	.1701E+00	208.84	.662
220.25	.1799E+00	210.10	.666
221.97	.1781E+00	211.04	.669
223.69	.1683E+00	211.04	.669

TABLE 2.- Continued

(u) Case 20: test 34, run 45, $M_1 = 17.54$

x, cm	q, W/cm ²	T _w , K	T _w /T _t
42.33	.4833E-01	206.10	.663
45.77	.4774E-01	206.72	.665
49.20	.5891E-01	206.41	.664
52.64	.6657E-01	206.10	.663
56.08	.8095E-01	205.17	.660
59.52	.9700E-01	204.55	.658
62.95	.1076E+00	202.99	.653
66.39	.1283E+00	202.68	.652
69.83	.1436E+00	202.37	.651
73.27	.1642E+00	201.44	.648
76.71	.1888E+00	201.13	.647
80.14	.2119E+00	200.82	.646
83.58	.2410E+00	201.44	.648
87.02	.2431E+00	201.44	.648
90.45	.2622E+00	202.06	.650
93.89	.2743E+00	202.99	.653
97.33	.2782E+00	203.92	.656
100.77	.2785E+00	204.86	.659
104.20	.2754E+00	206.10	.663
107.64	.2636E+00	207.03	.666
111.08	.2519E+00	208.28	.670
112.03	.2108E+00	211.39	.680
114.52	.2202E+00	209.83	.675
117.95	.2177E+00	210.45	.677
119.67	.2485E+00	207.66	.668
121.39	.1790E+00	213.25	.686
124.83	.2004E+00	214.49	.690
128.26	.1586E+00	218.22	.702
131.70	.1675E+00	221.33	.712
132.40	.1466E+00	217.60	.700
135.14	.1889E+00	221.95	.714
154.94	.1538E+00	222.58	.716
156.65	.1543E+00	223.20	.718
158.37	.1424E+00	223.82	.720
160.09	.1237E+00	224.13	.721
161.81	.1429E+00	225.06	.724
163.53	.1299E+00	225.06	.724
165.25	.1428E+00	225.37	.725
166.97	.1361E+00	225.06	.724
168.69	.1492E+00	225.37	.725
170.40	.1528E+00	224.75	.723
172.12	.1473E+00	225.06	.724
173.84	.1397E+00	224.13	.721
175.56	.1512E+00	224.44	.722
177.28	.1509E+00	223.51	.719
179.00	.1504E+00	223.20	.718
180.72	.1494E+00	222.58	.716
182.44	.1536E+00	222.89	.717
184.16	.1529E+00	221.64	.713

TABLE 2.- Continued

(u) Concluded

x, cm	q, W/cm ²	T _w , K	T _w /T _t
185.87	0.	222.27	.715
189.31	.1260E+00	236.88	.762
191.03	.1473E+00	219.47	.706
192.75	.1524E+00	221.33	.712
194.46	.1270E+00	221.64	.713
196.18	.1544E+00	221.95	.714
197.90	.1522E+00	220.09	.708
199.62	.1446E+00	221.33	.712
201.34	.1286E+00	222.27	.715
203.06	.1290E+00	223.20	.718
204.78	.1268E+00	222.89	.717
206.50	.1122E+00	226.00	.727
208.22	.1014E+00	225.06	.724
209.93	.1357E+00	225.37	.725
211.63	.1331E+00	223.51	.719
213.37	.1110E+00	224.13	.721
215.09	.1280E+00	223.20	.718
216.81	.1346E+00	222.27	.715
218.53	.1346E+00	220.71	.710
220.25	.1478E+00	221.64	.713
221.97	.1475E+00	221.02	.711
223.69	.1367E+00	220.71	.710

TABLE 2.- Continued

(v) Case 21: test 34, run 25, $M_1 = 17.55$

x , cm	q , W/cm ²	T_w , K	T_w/T_t
42.33	.1083E-01	239.37	.775
45.77	.1269E-01	239.99	.777
49.20	.1031E-01	239.99	.777
52.64	.1591E-01	239.99	.777
56.08	.1714E-01	239.68	.776
59.52	.2856E-01	239.37	.775
62.95	.4463E-01	238.44	.772
66.39	.5079E-01	238.14	.771
69.83	.6018E-01	237.52	.769
73.27	.7713E-01	236.59	.766
76.71	.9944E-01	235.97	.764
80.14	.9659E-01	235.36	.762
83.58	.1320E+00	235.05	.761
87.02	.1437E+00	234.74	.760
90.45	.1478E+00	234.43	.759
93.89	.1543E+00	234.74	.760
97.33	.1771E+00	234.74	.760
100.77	.1524E+00	235.05	.761
104.20	.1598E+00	235.36	.762
107.64	.1585E+00	235.97	.764
111.08	.1492E+00	236.59	.766
112.03	.1374E+00	237.83	.770
114.52	.1340E+00	237.21	.768
117.95	.1459E+00	237.21	.768
119.67	.1478E+00	235.97	.764
121.39	.1073E+00	239.06	.774
124.83	.1240E+00	239.06	.774
128.26	.8736E-01	240.61	.779
131.70	.1024E+00	241.22	.781
132.40	.1120E+00	240.92	.780
135.14	.1042E+00	242.46	.785
154.94	.6818E-01	247.71	.802
156.65	.7316E-01	248.02	.803
158.37	.4541E-01	248.33	.804
160.09	.6086E-01	248.95	.806
161.81	.5828E-01	249.56	.808
163.53	.5569E-01	249.87	.809
165.25	.6518E-01	249.87	.809
166.97	.6154E-01	249.56	.808
168.69	.6085E-01	249.87	.809
170.40	.4870E-01	250.18	.810
172.12	.6844E-01	249.87	.809
173.84	.7086E-01	249.25	.807
175.56	.5759E-01	249.56	.808
177.28	.5803E-01	249.25	.807
179.00	.6759E-01	248.64	.805
180.72	.7355E-01	248.02	.803
182.44	.7019E-01	248.02	.803
184.16	.7524E-01	247.71	.802

TABLE 2.- Continued

(v) Concluded

x, cm	q, W/cm ²	T _w , K	T _w /T _t
185.87	.7280E-01	247.40	.801
189.31	.5601E-01	255.74	.828
191.03	.6758E-01	245.86	.796
192.75	.8305E-01	245.86	.796
194.46	.7485E-01	244.93	.793
196.18	.6408E-01	244.62	.792
197.90	.7156E-01	244.93	.793
199.62	.8620E-01	244.93	.793
201.34	.7045E-01	244.00	.790
203.06	.7656E-01	244.00	.790
204.78	.7247E-01	243.70	.789
206.50	.7587E-01	244.31	.791
208.22	.7010E-01	243.70	.789
209.93	.8350E-01	243.70	.789
211.63	.6717E-01	243.39	.788
213.37	.8627E-01	243.08	.787
215.09	.7910E-01	242.46	.785
216.81	.8160E-01	242.15	.784
218.53	.6298E-01	241.84	.783
220.25	.6697E-01	241.84	.783
221.97	.9047E-01	241.53	.782
223.69	.7555E-01	241.53	.782

TABLE 2.- Continued

(w) Case 22: test 34, run 29, $M_1 = 17.54$

x , cm	q , W/cm ²	T_w , K	T_w/T_t
42.33	-.4417E-01	286.55	.924
45.77	-.5266E-01	286.55	.924
49.20	-.6962E-01	286.55	.924
52.64	-.5253E-01	286.55	.924
56.08	-.4365E-01	286.55	.924
59.52	-.5046E-01	286.55	.924
62.95	-.4147E-01	286.55	.924
66.39	-.4002E-01	286.55	.924
69.83	-.3001E-01	286.55	.924
73.27	-.2447E-01	286.55	.924
76.71	-.1196E-01	286.55	.924
80.14	-.9125E-02	286.55	.924
83.58	-.1286E-01	286.55	.924
87.02	-.8819E-02	286.55	.924
90.45	-.7786E-02	286.55	.924
93.89	-.1011E-01	286.55	.924
97.33	-.4767E-02	286.55	.924
100.77	-.1317E-02	286.55	.924
104.20	.7684E-02	286.55	.924
107.64	-.1429E-01	286.55	.924
111.08	-.1836E-01	286.55	.924
112.03	-.2471E-01	286.55	.924
114.52	-.2906E-01	286.87	.925
117.95	-.2806E-01	286.55	.924
119.67	-.1149E-01	286.55	.924
121.39	-.5397E-01	287.18	.926
124.83	-.4133E-01	286.87	.925
128.26	-.6346E-01	286.87	.925
131.70	-.4104E-01	286.87	.925
132.40	-.3637E-01	286.87	.925
135.14	-.5489E-01	286.87	.925
154.94	-.5281E-01	286.87	.925
156.65	-.5257E-01	286.87	.925
158.37	-.3047E-01	286.87	.925
160.09	-.5405E-01	286.87	.925
161.81	-.4826E-01	287.18	.926
163.53	-.5659E-01	286.87	.925
165.25	-.4308E-01	286.87	.925
166.97	-.4554E-01	286.87	.925
168.69	-.5650E-01	286.87	.925
170.40	-.5989E-01	286.87	.925
172.12	-.5815E-01	286.87	.925
173.84	-.5832E-01	287.18	.926
175.56	-.5438E-01	287.18	.926
177.28	-.4039E-01	286.87	.925
179.00	-.4302E-01	286.87	.925
180.72	-.5573E-01	286.87	.925
182.44	-.4846E-01	287.18	.926
184.16	-.6280E-01	286.87	.925

TABLE 2.- Continued

(w) Concluded

x , cm	q , W/cm ²	T_w , K	T_w/T_t
185.87	-.5807E-01	287.18	.926
189.31	-.4692E-01	288.43	.930
191.03	-.4234E-01	286.87	.925
192.75	-.4764E-01	287.18	.926
194.46	-.3361E-01	286.87	.925
196.18	-.6225E-01	287.18	.926
197.90	-.5622E-01	286.87	.925
199.62	-.4755E-01	286.87	.925
201.34	-.4574E-01	286.87	.925
203.06	-.5272E-01	286.24	.923
204.78	-.6471E-01	286.24	.923
206.50	-.4836E-01	286.55	.924
208.22	-.5136E-01	286.24	.923
209.93	-.4739E-01	286.24	.923
211.63	-.5964E-01	286.24	.923
213.37	-.4745E-01	286.24	.923
215.09	-.4014E-01	286.55	.924
216.81	-.4179E-01	286.24	.923
218.53	-.4516E-01	286.24	.923
220.25	-.5597E-01	286.24	.923
221.97	-.4776E-01	286.24	.923
223.69	-.4407E-01	286.24	.923

TABLE 2.- Continued

(x) Case 23: test 34, run 11, $M_1 = 17.95$

x, cm	q, W/cm ²	T _w , K	T _w /T _t
42.33	.3156E+00	114.64	.371
45.77	.3779E+00	114.95	.372
49.20	.4298E+00	113.40	.367
52.64	.4851E+00	112.48	.364
56.08	.5876E+00	112.48	.364
59.52	.7190E+00	111.55	.361
62.95	.7598E+00	110.62	.358
66.39	.1006E+01	112.48	.364
69.83	.1123E+01	114.02	.369
73.27	.1160E+01	114.02	.369
76.71	.1285E+01	115.57	.374
80.14	.1209E+01	114.02	.369
83.58	.1278E+01	115.88	.375
87.02	.1211E+01	114.95	.372
90.45	.1137E+01	114.95	.372
93.89	.1212E+01	117.11	.379
97.33	.1199E+01	117.42	.380
100.77	.1163E+01	118.04	.382
104.20	.1139E+01	118.04	.382
107.64	.1133E+01	119.58	.387
111.08	.1150E+01	119.89	.388
112.03	.1086E+01	118.04	.382
114.52	.1076E+01	120.51	.390
117.95	.1108E+01	118.35	.383
119.67	.1009E+01	117.42	.380
121.39	.9386E+00	124.22	.402
124.83	.1053E+01	119.89	.388
128.26	.8977E+00	123.91	.401
131.70	.1023E+01	121.13	.392
132.40	.9628E+00	120.51	.390
135.14	.1056E+01	122.06	.395
154.94	.9890E+00	118.35	.383
156.65	.9275E+00	116.18	.376
158.37	.9085E+00	115.57	.374
160.09	.9360E+00	116.80	.378
161.81	.9006E+00	116.49	.377
163.53	.9860E+00	114.95	.372
165.25	.9409E+00	114.64	.371
166.97	.8717E+00	113.40	.367
168.69	.9470E+00	114.64	.371
170.40	.9281E+00	111.86	.362
172.12	.9529E+00	113.40	.367
173.84	.9529E+00	111.86	.362
175.56	.9429E+00	113.71	.368
177.28	.9434E+00	111.55	.361
179.00	.8385E+00	111.55	.361
180.72	.8791E+00	112.17	.363
182.44	.9052E+00	113.09	.366
184.16	.9369E+00	111.24	.360

TABLE 2.- Continued

(x) Concluded

x, cm	q, W/cm ²	T _w , K	T _w /T _t
185.87	.9062E+00	112.48	.364
189.31	.7091E+00	154.19	.499
191.03	.7127E+00	105.99	.343
192.75	.8851E+00	111.55	.361
194.46	.7308E+00	110.93	.359
196.18	.8920E+00	112.79	.365
197.90	.8900E+00	111.24	.360
199.62	.9177E+00	112.79	.365
201.34	.8059E+00	112.17	.363
203.06	.7976E+00	111.24	.360
204.78	.7374E+00	111.24	.360
206.50	.6421E+00	110.93	.359
208.22	.7497E+00	117.11	.379
209.93	.8696E+00	115.57	.374
211.63	.7073E+00	112.17	.363
213.37	.9402E+00	113.09	.366
215.09	.8099E+00	111.55	.361
216.81	.7492E+00	108.77	.352
218.53	.8465E+00	109.39	.354
220.25	.8233E+00	110.00	.356
221.97	.7914E+00	109.70	.355
223.69	.8090E+00	111.24	.360

TABLE 2.- Continued

(y) Case 24: test 34, run 13, $M_1 = 17.90$

x, cm	q, W/cm ²	T _w , K	T _w /T _t
42.33	.3145E+00	107.64	.359
45.77	.3694E+00	107.94	.360
49.20	.4215E+00	107.03	.357
52.64	.4897E+00	106.43	.355
56.08	.5782E+00	106.73	.356
59.52	.6648E+00	106.43	.355
62.95	.6960E+00	105.52	.352
66.39	.9294E+00	107.64	.359
69.83	.1020E+01	108.85	.363
73.27	.1049E+01	109.46	.365
76.71	.1173E+01	110.67	.369
80.14	.1098E+01	109.16	.364
83.58	.1164E+01	110.97	.370
87.02	.1115E+01	110.07	.367
90.45	.1050E+01	110.67	.369
93.89	.1116E+01	112.79	.376
97.33	.1105E+01	112.79	.376
100.77	.1049E+01	113.40	.378
104.20	.1040E+01	113.70	.379
107.64	.1011E+01	115.22	.385
111.08	.1026E+01	115.83	.387
112.03	.9674E+00	115.22	.385
114.52	.9780E+00	117.04	.391
117.95	.9886E+00	115.22	.385
119.67	.9120E+00	113.40	.378
121.39	.8541E+00	121.28	.405
124.83	.9577E+00	118.25	.395
128.26	.8002E+00	123.10	.411
131.70	.8312E+00	120.98	.404
132.40	.6389E+00	120.37	.402
135.14	.8202E+00	122.19	.408
154.94	.8435E+00	120.98	.404
156.65	.8019E+00	118.56	.396
158.37	.7588E+00	117.04	.391
160.09	.8292E+00	118.25	.395
161.81	.8144E+00	117.04	.391
163.53	.8394E+00	115.22	.385
165.25	.8124E+00	114.92	.383
166.97	.7686E+00	114.01	.380
168.69	.8397E+00	114.31	.381
170.40	.8149E+00	112.19	.374
172.12	.8438E+00	113.10	.377
173.84	.8449E+00	111.88	.373
175.56	.8303E+00	113.70	.379
177.28	.8287E+00	112.49	.375
179.00	.7800E+00	112.19	.374
180.72	.7859E+00	112.19	.374
182.44	.7964E+00	113.70	.379
184.16	.8080E+00	112.79	.376

TABLE 2.- Continued

(y) Concluded

x, cm	q, W/cm ²	T _w , K	T _w /T _t
185.87	.7835E+00	114.01	.380
189.31	.6047E+00	155.55	.519
191.03	.6250E+00	110.37	.368
192.75	.7451E+00	114.31	.381
194.46	.6269E+00	112.49	.375
196.18	.7297E+00	116.74	.390
197.90	.7166E+00	116.13	.388
199.62	.7565E+00	115.83	.387
201.34	.6690E+00	115.22	.385
203.06	.6204E+00	117.34	.392
204.78	.5420E+00	118.56	.396
206.50	.5371E+00	120.68	.403
208.22	.6213E+00	120.07	.401
209.93	.5740E+00	122.50	.409
211.63	.5424E+00	122.19	.408
213.37	.7517E+00	121.59	.406
215.09	.6778E+00	117.34	.392
216.81	.6551E+00	117.65	.393
218.53	.6950E+00	118.56	.396
220.25	.7104E+00	117.65	.393
221.97	.6601E+00	115.52	.386
223.69	.6810E+00	118.25	.395

TABLE 2.- Continued

(z) Case 25: test 34, run 14, $M_1 = 17.80$

x, cm	q, W/cm ²	T _w , K	T _w /T _t
42.33	.2572E+00	115.38	.390
45.77	.3150E+00	115.98	.392
49.20	.3023E+00	115.08	.389
52.64	.3545E+00	114.49	.387
56.08	.3983E+00	114.19	.386
59.52	.4770E+00	113.59	.384
62.95	.4993E+00	112.70	.381
66.39	.6423E+00	114.19	.386
69.83	.7299E+00	114.78	.388
73.27	.7934E+00	115.38	.390
76.71	.9213E+00	116.27	.393
80.14	.8841E+00	115.38	.390
83.58	.9819E+00	116.87	.396
87.02	.9307E+00	116.57	.395
90.45	.8939E+00	117.17	.397
93.89	.9624E+00	119.26	.404
97.33	.9540E+00	119.55	.405
100.77	.9121E+00	120.75	.409
104.20	.9081E+00	121.34	.411
107.64	.8730E+00	122.83	.416
111.08	.8978E+00	123.73	.419
112.03	.8417E+00	124.62	.422
114.52	.8290E+00	124.92	.423
117.95	.8566E+00	124.03	.420
119.67	.7797E+00	122.24	.414
121.39	.6287E+00	129.39	.438
124.83	.7205E+00	127.90	.433
128.26	.5714E+00	131.78	.446
131.70	.6009E+00	131.48	.445
132.40	.4965E+00	131.78	.446
135.14	.6145E+00	132.08	.447
154.94	.7583E+00	122.24	.414
156.65	.7293E+00	120.45	.408
158.37	.7010E+00	119.85	.406
160.09	.4608E+00	121.04	.410
161.81	.7329E+00	120.45	.408
163.53	.7582E+00	119.26	.404
165.25	.7354E+00	119.26	.404
166.97	.6890E+00	118.36	.401
168.69	.7479E+00	119.26	.404
170.40	.7187E+00	117.17	.397
172.12	.7419E+00	118.36	.401
173.84	.7530E+00	116.87	.396
175.56	.7367E+00	118.96	.403
177.28	.7275E+00	118.06	.400
179.00	.6955E+00	117.77	.399
180.72	.6916E+00	117.77	.399
182.44	.6998E+00	119.55	.405
184.16	.7056E+00	118.96	.403

TABLE 2.- Continued

(z) Concluded

x , cm	q_r , W/cm ²	T_w , K	T_w/T_t
185.87	.7004E+00	119.85	.406
189.31	.4713E+00	159.80	.541
191.03	.5474E+00	117.77	.399
192.75	.6725E+00	121.04	.410
194.46	.5565E+00	119.26	.404
196.18	.6389E+00	124.92	.423
197.90	.6305E+00	124.03	.420
199.62	.6693E+00	123.13	.417
201.34	.6026E+00	123.13	.417
203.06	.5237E+00	126.71	.429
204.78	.4027E+00	128.80	.436
206.50	.4087E+00	131.18	.444
208.22	.4502E+00	129.69	.439
209.93	.4323E+00	132.97	.450
211.63	.4139E+00	132.97	.450
213.37	.5515E+00	130.88	.443
215.09	.5817E+00	125.81	.426
216.81	.5399E+00	127.01	.430
218.53	.5275E+00	127.90	.433
220.25	.6149E+00	126.41	.428
221.97	.5886E+00	123.43	.418
223.69	.5713E+00	126.71	.429

TABLE 2.- Continued

(aa) Case 26: test 34, run 15, $M_1 = 17.68$

x, cm	q, W/cm ²	T _w , K	T _w /T _t
42.33	.2334E+00	123.33	.419
45.77	.2576E+00	123.92	.421
49.20	.2533E+00	122.73	.417
52.64	.2906E+00	122.14	.415
56.08	.3014E+00	121.84	.414
59.52	.3407E+00	120.96	.411
62.95	.3578E+00	120.07	.408
66.39	.4507E+00	121.25	.412
69.83	.5118E+00	121.55	.413
73.27	.5636E+00	122.14	.415
76.71	.6569E+00	123.03	.418
80.14	.6619E+00	122.44	.416
83.58	.7559E+00	124.22	.422
87.02	.7563E+00	124.22	.422
90.45	.7392E+00	125.11	.425
93.89	.7307E+00	127.18	.433
97.33	.6895E+00	128.07	.436
100.77	.6491E+00	129.26	.440
104.20	.6526E+00	129.85	.442
107.64	.6234E+00	131.33	.447
111.08	.6238E+00	132.22	.450
112.03	.6062E+00	133.70	.455
114.52	.6006E+00	133.41	.454
117.95	.6131E+00	132.81	.452
119.67	.5848E+00	131.04	.446
121.39	.5274E+00	137.26	.467
124.83	.5827E+00	136.37	.464
128.26	.4821E+00	139.63	.475
131.70	.5126E+00	139.93	.476
132.40	.4571E+00	141.11	.480
135.14	.5185E+00	140.23	.477
134.94	.6679E+00	125.11	.425
156.65	.6409E+00	123.92	.421
158.37	.6061E+00	123.62	.420
160.09	.6363E+00	124.51	.423
161.81	.6421E+00	124.51	.423
163.53	.6599E+00	123.62	.420
165.25	.6370E+00	124.22	.422
166.97	.6003E+00	123.33	.419
168.69	.6482E+00	124.22	.422
170.40	.6283E+00	122.73	.417
172.12	.6408E+00	124.22	.422
173.84	.6337E+00	122.73	.417
175.56	.6339E+00	124.81	.424
177.28	.6343E+00	124.22	.422
179.00	.5812E+00	124.22	.422
180.72	.6036E+00	123.92	.421
182.44	.6132E+00	125.70	.427
184.16	.5987E+00	125.40	.426

TABLE 2.- Continued

(aa) Concluded

x, cm	q, W/cm ²	T _w , K	T _w /T _t
185.87	.5946E+00	126.59	.430
189.31	.4021E+00	163.94	.558
191.03	.4625E+00	125.11	.425
192.75	.4990E+00	128.07	.436
194.46	.4678E+00	126.59	.430
196.18	.4676E+00	132.22	.450
197.90	.4714E+00	131.04	.446
199.62	.4885E+00	130.15	.443
201.34	.4481E+00	130.44	.444
203.06	.3930E+00	134.30	.457
204.78	.3605E+00	136.96	.466
206.50	.3563E+00	139.34	.474
208.22	.3874E+00	136.96	.466
209.93	.3675E+00	141.41	.481
211.63	.3547E+00	141.71	.482
213.37	.4627E+00	138.74	.472
215.09	.4263E+00	133.41	.454
216.81	.4060E+00	135.19	.460
218.53	.4350E+00	135.78	.462
220.25	.4500E+00	134.30	.457
221.97	.4318E+00	131.33	.447
223.69	.4266E+00	134.00	.456

TABLE 2.- Continued

(bb) Case 27: test 34, run 17, $M_1 = 17.44$

x, cm	q, W/cm ²	T _w , K	T _w /T _t
42.33	.1811E+00	118.12	.398
45.77	.2051E+00	119.01	.401
49.20	.1912E+00	118.12	.398
52.64	.1840E+00	117.53	.396
56.08	.1931E+00	116.93	.394
59.52	.2119E+00	116.64	.393
62.95	.1946E+00	116.04	.391
66.39	.2254E+00	116.64	.393
69.83	.2625E+00	116.64	.393
73.27	.2730E+00	116.93	.394
76.71	.3213E+00	117.23	.395
80.14	.3220E+00	116.93	.394
83.58	.3973E+00	118.12	.398
87.02	.4106E+00	118.12	.398
90.45	.4141E+00	118.71	.400
93.89	.4914E+00	120.49	.406
97.33	.5095E+00	121.09	.408
100.77	.5213E+00	122.57	.413
104.20	.5361E+00	123.16	.415
107.64	.5470E+00	124.35	.419
111.08	.5512E+00	125.54	.423
112.03	.5529E+00	126.73	.427
114.52	.5267E+00	126.43	.426
117.95	.5549E+00	125.84	.424
119.67	.5318E+00	124.06	.418
121.39	.4386E+00	129.69	.437
124.83	.4626E+00	128.21	.432
128.26	.3826E+00	130.88	.441
131.70	.4163E+00	131.47	.443
132.40	.4114E+00	130.58	.440
135.14	.4412E+00	131.47	.443
154.94	.5260E+00	115.45	.389
156.65	.4941E+00	114.26	.385
158.37	.4829E+00	115.45	.389
160.09	.5160E+00	117.23	.395
161.81	.5083E+00	117.23	.395
163.53	.5278E+00	115.45	.389
165.25	.5147E+00	117.82	.397
166.97	.4915E+00	119.01	.401
168.69	.5146E+00	119.01	.401
170.40	.4993E+00	115.45	.389
172.12	.5209E+00	119.01	.401
173.84	.5239E+00	119.60	.403
175.56	.4921E+00	119.31	.402
177.28	.4968E+00	116.34	.392
179.00	.4727E+00	118.71	.400
180.72	.4610E+00	121.38	.409
182.44	.4795E+00	120.79	.407
184.16	.4873E+00	117.53	.396

TABLE 2.- Continued

(bb) Concluded

x, cm	q, W/cm ²	T _w , K	T _w /T _t
185.87	.4906E+00	121.38	.409
189.31	.3190E+00	159.97	.539
191.03	.3724E+00	117.82	.397
192.75	.4711E+00	122.87	.414
194.46	.3661E+00	125.24	.422
196.18	.4241E+00	127.02	.428
197.90	.4462E+00	122.87	.414
199.62	.4538E+00	126.13	.425
201.34	.3287E+00	129.40	.436
203.06	.3278E+00	128.51	.433
204.78	.3940E+00	125.84	.424
206.50	.2981E+00	132.07	.445
208.22	.3003E+00	135.63	.457
209.93	.3246E+00	133.85	.451
211.63	.3156E+00	130.88	.441
213.37	.3478E+00	132.07	.445
215.09	.3259E+00	132.07	.445
216.81	.3279E+00	128.51	.433
218.53	.3957E+00	126.13	.425
220.25	.3713E+00	127.62	.430
221.97	.3865E+00	127.02	.428
223.69	.3831E+00	126.73	.427

TABLE 2.- Continued

(cc) Case 28: test 34, run 18, $M_1 = 17.22$

x, cm	q , W/cm ²	T_w , K	T_w/T_t
42.33	.1418E+00	126.02	.426
45.77	.1517E+00	126.61	.428
49.20	.1565E+00	126.02	.426
52.64	.1534E+00	125.43	.424
56.08	.1268E+00	124.83	.422
59.52	.1446E+00	124.24	.420
62.95	.1365E+00	123.65	.418
66.39	.1502E+00	123.95	.419
69.83	.1497E+00	123.65	.418
73.27	.1791E+00	123.65	.418
76.71	.1830E+00	123.95	.419
80.14	.1809E+00	123.65	.418
83.58	.1946E+00	124.24	.420
87.02	.2160E+00	124.54	.421
90.45	.2192E+00	125.13	.423
93.89	.2486E+00	126.31	.427
97.33	.2714E+00	127.20	.430
100.77	.2618E+00	128.68	.435
104.20	.2606E+00	129.57	.438
107.64	.2792E+00	130.75	.442
111.08	.2949E+00	131.93	.446
112.03	.3357E+00	133.71	.452
114.52	.3164E+00	132.82	.449
117.95	.3178E+00	132.53	.448
119.67	.3099E+00	130.75	.442
121.39	.3107E+00	135.48	.458
124.83	.3376E+00	134.89	.456
128.26	.2912E+00	137.55	.465
131.70	.3104E+00	138.74	.469
132.40	.3224E+00	137.55	.465
135.14	.3351E+00	138.44	.468
154.94	.4298E+00	119.21	.403
156.65	.4242E+00	118.33	.400
158.37	.3822E+00	119.51	.404
160.09	.4181E+00	121.28	.410
161.81	.4315E+00	121.28	.410
163.53	.4384E+00	119.51	.404
165.25	.4099E+00	121.88	.412
166.97	.3828E+00	123.36	.417
168.69	.4165E+00	123.36	.417
170.40	.4110E+00	119.81	.405
172.12	.4104E+00	123.65	.418
173.84	.4262E+00	124.54	.421
175.56	.4201E+00	124.24	.420
177.28	.4154E+00	120.99	.409
179.00	.3835E+00	123.95	.419
180.72	.3816E+00	126.61	.428
182.44	.3916E+00	126.61	.428
184.16	.3875E+00	123.06	.416

TABLE 2.- Continued

(cc) Concluded

x, cm	q, W/cm ²	T _w , K	T _w /T _t
185.87	.3778E+00	127.20	.430
189.31	.2643E+00	163.59	.553
191.03	.3111E+00	123.95	.419
192.75	.3294E+00	128.68	.435
194.46	.2628E+00	131.05	.443
196.18	.2953E+00	133.12	.450
197.90	.3096E+00	128.98	.436
199.62	.3136E+00	131.93	.446
201.34	.2857E+00	135.48	.458
203.06	.2615E+00	134.89	.456
204.78	.2714E+00	132.53	.448
206.50	.2627E+00	138.74	.469
208.22	.2483E+00	142.58	.482
209.93	.2460E+00	140.81	.476
211.63	.2595E+00	137.55	.465
213.37	.3003E+00	139.33	.471
215.09	.2600E+00	139.03	.470
216.81	.2584E+00	135.78	.459
218.53	.2831E+00	133.12	.450
220.25	.2946E+00	134.60	.455
221.97	.2683E+00	160.33	.542
223.69	.2540E+00	133.41	.451

TABLE 2.- Continued

(dd) Case 29: test 34, run 30, $M_1 = 17.26$

x, cm	q, W/cm ²	T _w , K	T _w /T _t
42.33	-.4964E-01	286.50	.927
45.77	-.4988E-01	286.50	.927
49.20	-.4234E-01	286.50	.927
52.64	-.4037E-01	286.50	.927
56.08	-.4885E-01	286.50	.927
59.52	-.4140E-01	286.50	.927
62.95	-.3876E-01	286.20	.926
66.39	-.3001E-01	286.20	.926
69.83	-.3034E-01	286.50	.927
73.27	-.3294E-01	286.20	.926
76.71	-.3075E-01	286.20	.926
80.14	-.1931E-01	286.20	.926
83.58	-.1750E-01	286.20	.926
87.02	-.2362E-01	286.20	.926
90.45	-.1084E-01	286.20	.926
93.89	-.1272E-01	286.20	.926
97.33	-.6799E-02	286.20	.926
100.77	-.1835E-01	286.50	.927
104.20	-.1135E-01	286.20	.926
107.64	-.8694E-02	286.50	.927
111.08	-.1147E-01	286.50	.927
112.03	-.3133E-02	286.20	.926
114.52	-.7843E-02	286.50	.927
117.95	-.5675E-02	286.20	.926
119.67	-.1078E-02	286.20	.926
121.39	-.1458E-01	286.81	.928
124.83	-.9795E-02	286.50	.927
128.26	-.1042E-01	286.50	.927
131.70	-.1158E-01	286.50	.927
132.40	-.2542E-02	286.50	.927
135.14	-.2100E-02	286.50	.927
154.94	-.7695E-02	286.81	.928
156.65	-.4529E-02	286.81	.928
158.37	-.5312E-02	286.81	.928
160.09	-.1511E-01	286.81	.928
161.81	-.1915E-01	286.81	.928
163.53	-.1743E-01	286.81	.928
165.25	-.1580E-01	286.81	.928
166.97	-.1821E-01	286.81	.928
168.69	-.2113E-01	286.81	.928
170.40	-.1914E-01	286.81	.928
172.12	-.2124E-01	286.81	.928
173.84	-.2971E-01	286.81	.928
175.56	-.2222E-01	286.81	.928
177.28	-.2716E-01	286.81	.928
179.00	-.2307E-01	286.81	.928
180.72	-.2317E-01	286.81	.928
182.44	-.2405E-01	286.81	.928
184.16	-.3001E-01	286.81	.928

TABLE 2.- Concluded

(dd) Concluded

x, cm	q, W/cm ²	T _w , K	T _w /T _t
185.87	-.2885E-01	287.12	.929
189.31	-.1438E-01	288.05	.932
191.03	-.2505E-01	286.81	.928
192.75	-.2575E-01	286.81	.928
194.46	-.1680E-01	286.81	.928
196.18	-.2902E-01	286.81	.928
197.90	-.3458E-01	286.81	.928
199.62	-.3145E-01	286.81	.928
201.34	-.1931E-01	286.50	.927
203.06	-.2721E-01	286.20	.926
204.78	-.3066E-01	286.20	.926
206.50	-.2608E-01	286.20	.926
208.22	-.3390E-01	285.89	.925
209.93	-.2281E-01	286.20	.926
211.63	-.3407E-01	286.20	.926
213.37	-.3221E-01	286.20	.926
215.09	-.2177E-01	286.20	.926
216.81	-.2393E-01	286.20	.926
218.53	-.3412E-01	285.89	.925
220.25	-.3444E-01	286.20	.926
221.97	-.2532E-01	285.89	.925
223.69	-.2838E-01	285.89	.925

TABLE 3.- SKIN-FRICTION DATA

(a) Model 1

Case	Station	x, cm	Run	Pt, l, kPa	τ , Pa	c_f	$R_{x,e}$ (a)	M_e
1	1	74.2	24	13 148	9.467	1.248×10^{-4}	31.28×10^6	10.09
2	2	99.6	8	12 031	19.622	3.060	34.13	9.71
3	3	125.0	13	13 190	26.393	3.358	55.63	10.24
4	4	211.2	19	13 210	21.339	2.476	102.25	10.23
5	1	74.2	25	10 583	7.846	1.279	24.85	9.92
6	2	99.6	7	10 652	17.071	2.983	30.21	9.68
7	3	125.0	14	10 583	22.270	3.629	42.34	9.98
8	4	211.2	20	10 542	18.395	2.779	77.31	9.98
9	1	74.2	26	7 922	6.299	1.344	18.71	9.85
10	2	99.6	9	7 998	11.625	2.655	22.75	9.73
11	3	125.0	15	7 908	16.975	3.788	30.03	9.78
12	4	211.2	21	7 929	15.306	3.075	56.53	9.83
13	1	74.2	27	5 454	4.984	1.538	13.00	9.78
14	2	99.6	11	5 488	7.212	2.299	16.08	9.47
15	3	125.0	16	5 440	10.790	3.440	20.92	9.67
16	4	211.2	22	5 454	12.018	3.384	40.32	9.73
17	1	74.2	28	2 758	3.208	2.023	6.29	9.33
18	2	99.6	12	2 758	3.238	2.236	7.85	8.95
19	3	125.0	17	2 674	3.923	2.586	10.58	9.69
20	4	211.2	23	2 723	7.302	4.413	16.63	9.14

^aBased on power law μ -T relation.

TABLE 3.- Concluded

(b) Model 2

Case	Station	x, cm	Run	T_w/T_t	τ , Pa	c_f	$R_{x,e}$	M_e	$P_{t,1}$, kPa	T_t , K
21	2	50.5	2	0.931	9.804	1.477×10^{-4}	20.8×10^6	11.2	13 651.7	300.9
22	3	75.9	13	.927	22.063	3.075	31.8	11.0	13 755.1	312.1
23	4	101.3	18	.937	23.173	2.993	46.4	11.0	13 734.4	308.2
24	5	131.2	21	.917	21.877	2.834	58.1	11.1	13 741.3	320.4
25	6	165.1	30	.902	19.809	2.542	72.8	11.2	13 789.6	328.2
26	7	190.5	9	.919	17.926	2.326	88.8	11.4	13 651.7	314.8
27	8	215.9	26	.920	16.858	2.134	104.5	11.6	13 817.2	317.1
28	8	215.9	25	.920	21.477	1.817	156.0	11.6	20 684.4	313.2
29	2	50.5	34	.485	12.231	1.812	21.0	11.3	13 734.4	310.4
30	3	75.9	15	.488	26.028	3.362	35.2	11.2	13 734.4	308.7
31	4	101.3	20	.493	26.055	3.439	45.3	10.9	13 755.1	305.4
32	5	131.2	23	.465	23.814	3.095	60.2	11.2	13 762.0	312.1
33	6	165.1	32	.480	21.263	2.785	74.8	11.2	13 762.0	313.7
34	7	190.5	11	.500	19.464	2.528	95.1	11.5	13 655.5	300.9
35	8	215.9	29	.470	19.312	2.303	116.4	11.8	13 796.5	309.3
36	2	50.5	33	.355	10.694	1.584	20.1	11.3	13 741.3	318.7
37	3	75.9	14	.402	34.729	4.600	34.3	11.1	13 706.9	307.9
38	4	101.3	19	.345	27.538	3.622	44.3	10.9	13 741.3	312.6
39	5	131.2	22	.337	23.573	3.036	59.1	11.2	13 775.8	320.4
40	6	165.1	31	.334	21.201	2.819	71.5	11.2	13 720.7	322.6
41	7	190.5	12	.371	21.822	2.801	93.4	11.5	13 606.2	303.7
42	8	215.9	28	.312	19.712	2.561	103.1	11.5	13 775.8	310.4
43	8	215.9	27	.346	25.097	2.170	152.2	11.6	20 698.2	306.8

TABLE 4.- SURFACE PRESSURES

(a) Model 1

Case	$P_{t,1}$, kPa	x , cm	P/P_1	M_1
1	2 798	74.24	6.827	16.88
2	2 861	74.24	6.589	16.90
3	2 620	99.64	8.133	16.83
4	2 689	99.64	8.077	16.85
5	2 689	125.04	7.281	16.85
6	2 551	125.04	7.372	16.82
7	2 620	211.15	7.901	16.83
8	5 447	74.24	7.950	17.4
9	5 240	74.24	8.168	17.35
10	5 240	99.64	7.620	17.35
11	5 309	99.64	7.698	17.37
12	5 275	125.04	7.570	17.35
13	5 378	125.04	7.443	17.36
14	5 378	211.15	8.605	17.36
15	7 860	74.14	8.144	17.60
16	7 653	74.14	8.265	17.60
17	7 860	99.64	7.765	17.60
18	7 791	99.64	7.704	17.60
19	7 653	125.04	7.301	17.60
20	7 929	125.04	7.679	17.60
21	7 860	211.15	8.655	17.60
22	10 239	74.14	8.265	17.82
23	10 756	74.14	8.191	17.87
24	10 687	99.64	7.981	17.85
25	10 480	99.64	7.891	17.83
26	10 135	125.04	8.084	17.80
27	10 480	125.04	8.468	17.83
28	12 928	74.24	8.236	18.05
29	12 893	74.24	8.390	18.05
30	13 583	99.64	7.919	18.11
31	13 100	99.64	8.106	18.07
32	12 893	125.04	7.942	18.05
33	13 100	211.15	8.948	18.07

TABLE 4.- Continued

(b) Model 2

x, cm	p/p ₁ for -							
	Case 34	Case 35	Case 36	Case 37	Case 38	Case 39	Case 40	Case 41
41.61	5.61	5.85	5.98	5.91	6.20	6.22	6.36	6.82
45.42	5.51	5.96	6.10	5.79	6.34	6.04	6.49	6.54
50.50	5.56	5.69	5.82	5.81	6.00	6.04	6.14	6.58
55.58	5.51	5.41	5.51	5.64	5.59	5.80	5.71	6.20
60.66	5.72	5.66	5.70	5.68	5.69	5.80	5.78	6.25
65.74	5.97	5.88	5.88	5.82	5.80	5.95	5.89	6.54
70.82	6.18	6.15	6.15	5.90	5.98	5.81	6.01	6.32
75.90	6.28	6.14	6.09	5.91	5.84	5.82	5.78	6.14
80.98	6.28	6.21	6.16	5.93	5.87	5.77	5.74	6.03
86.06	6.42	6.32	6.29	6.07	5.97	5.77	5.73	5.81
91.14	6.58	6.68	6.69	6.39	6.39	6.13	6.12	6.24
96.22	6.52	6.71	6.72	6.34	6.44	6.09	6.13	6.27
101.30	6.50	6.74	6.76	6.38	6.49	6.03	6.13	5.99
106.38	6.52	6.73	6.75	6.38	6.49	6.05	6.09	5.94
111.46	6.49	6.53	6.56	6.40	6.34	6.10	5.99	5.93
116.54	6.64	6.85	6.89	6.61	6.73	6.47	6.44	6.56
136.86	6.56	6.79	6.84	6.56	6.77	6.57	6.64	6.67
165.10	6.32	6.54	6.59	6.34	6.60	6.47	6.60	6.72
190.50	6.22	6.49	6.58	6.29	6.65	6.57	6.73	7.09
215.90	6.13	6.40	6.46	6.16	6.52	6.54	6.62	7.26
P _t , l, kPa . .	13 624	12 259	10 887	9 487	8 294	6 771	6 240	4 116
*T _t , K . . .	307.2	310.1	306.1	309.8	312.8	310.1	305.5	311.2
M ₁	18.05	17.96	17.90	17.80	17.70	17.57	17.50	17.28
R ₁ /m	46.3 × 10 ⁶	41.1 × 10 ⁶	37.1 × 10 ⁶	31.8 × 10 ⁶	27.5 × 10 ⁶	22.8 × 10 ⁶	21.5 × 10 ⁶	13.9 × 10 ⁶
T _w /T _t	0.97	0.97	0.98	0.97	0.96	0.97	0.98	0.96

*Measured in free stream. No real gas correction required.

TABLE 4.- Concluded

(b) Concluded

x, cm	p/p ₁ for -							
	Case 42	Case 43	Case 44	Case 45	Case 46	Case 47	Case 48	Case 49
41.61	5.69	5.81	5.75	5.74	5.85	6.06	6.26	6.40
45.42	5.72	5.87	5.85	5.87	6.43	6.25	6.35	6.48
50.50	5.58	5.67	5.63	5.65	5.58	5.76	5.87	6.38
55.58	5.66	5.73	5.69	5.69	5.65	5.79	5.87	5.95
60.66	5.76	5.79	5.70	5.66	5.59	5.67	5.74	5.87
65.74	5.98	5.99	5.84	5.76	5.68	5.75	5.84	6.01
70.82	6.10	6.12	5.96	5.88	5.69	5.75	5.82	5.94
75.90	6.36	6.33	6.15	6.00	5.75	5.79	5.80	5.83
80.98	6.37	6.36	6.19	6.06	5.83	5.81	5.77	5.80
86.06	6.52	6.51	6.39	6.27	6.01	5.90	5.79	5.78
91.14	6.48	6.49	6.40	6.34	6.13	6.01	5.87	5.84
96.22	6.52	6.57	6.51	6.47	6.25	6.14	5.97	5.99
101.30	6.60	6.63	6.60	6.57	6.49	6.35	6.11	5.94
106.38	6.65	6.64	6.61	6.60	6.49	6.32	6.07	5.92
111.46	----	----	----	----	6.40	6.23	6.04	5.91
116.54	6.51	6.42	6.40	6.46	6.41	6.28	6.18	6.13
136.86	6.58	6.35	6.30	6.42	6.45	6.20	6.33	6.37
165.10	6.35	6.28	6.21	6.25	6.22	6.21	6.28	6.38
190.50	6.22	6.12	6.16	6.27	6.27	6.28	6.41	6.61
215.90	6.20	6.13	6.14	6.23	6.26	6.24	6.35	6.59
P _t , kPa . . .	13 355	12 066	10 735	9604	8350	6957	5550	4171
*T _t , K . . .	303.3	301.0	299.0	298.2	309.1	307.8	307.8	309.5
M ₁	18.03	17.96	17.86	17.80	17.70	17.58	17.45	17.28
R ₁ /m	46.2 × 10 ⁶	42.2 × 10 ⁶	37.9 × 10 ⁶	34.0 × 10 ⁶	28.1 × 10 ⁶	23.6 × 10 ⁶	18.9 × 10 ⁶	14.2 × 10 ⁶
T _w /T _t	0.38	0.33	0.33	0.39	0.36	0.28	0.27	0.31

*Measured in free stream. No real gas correction required.

TABLE 5.- PITOT SURVEY DATA

[Average values of $p_{t,1}$ are listed; pitot data corrected to $p_{t,1} = 13\,789.6$ kPa]

(a) Data summary

[For model 1, Nominal $T_t = 305.6$ K; for model 2, T_t is measured in free stream and no real gas correction is required]

Case	Station	Test-Run	$p_{t,1}$, kPa	T_t , K	T_w/T_t
Model 1					
1	1	11-6	12 755.4		
2	2	11-36	13 444.9		
3	3	11-62	12 962.2		
4	4	15-11	13 169.1		
5	1	11-5	10 204.3		
6	2	11-37	10 618.0		
7	3	11-63	10 204.3		
8	4	15-10	10 755.9		
9	1	11-5	7 791.1		
10	2	11-39	7 653.2		
11	3	11-64	7 791.1		
12	4	15-9	8 135.9		
13	1	11-8	5 309.0		
14	2	11-40	5 309.0		
15	3	11-65	5 309.0		
16	4	15-8	5 584.8		
17	1	11-4	2 757.9		
18	2	11-41	2 551.1		
19	3	11-66	2 551.1		
20	4	15-7	2 895.8		
Model 2					
21	1	42-13	13 720.7	303.9	0.952
22	2	39-12	13 617.2	311.1	.959
23	3	39-31	13 720.7	309.4	.943
24	4	42-10	13 720.7	308.9	.944
25	5	42-7	13 789.6	322.2	.899
26	6	39-36, 40	13 734.5	309.7	.966
27	7	42-3, 4	13 672.4	318.3	.916
28	8	39-48, 49	13 651.7	302.5	.985
29	1	42-15	13 824.1	303.5	.495
30	2	39-27	13 720.7	307.8	.542
31	3	39-33	13 706.9	302.2	.524
32	4	42-12	13 762.0	303.3	.465
33	5	42-9	13 789.6	312.2	.488
34	6	39-45, 46	13 686.2	306.4	.558
35	7	42-6	13 706.9	311.1	.459
36	8	39-56, 60	13 582.8	309.5	.501
37	1	42-14	13 824.1	318.3	.331
38	2	39-26	13 755.1	306.7	.362
39	3	39-32	13 741.3	308.3	.306
40	4	42-11	13 603.4	305.8	.376
41	5	42-8	13 779.6	310.6	.364
42	6	39-43, 44	13 651.7	314.7	.358
43	7	42-5	13 693.1	311.1	.330
44	8	39-54, 55	13 669.0	308.1	.334

TABLE 5.- Continued

(b) Pitot profiles: Case 1; station 1; test 11; run 6;
 $P_{t,1} = 12\ 755.4$ kPa; $T_t = 305.6$ K

y, cm	p, N/cm ²
.1277	.176
.1966	.253
.3024	.408
.3759	.562
.4220	.769
.4732	.912
.5186	1.239
.5569	1.642
.5797	2.163
.5965	2.533
.6278	2.990
.6494	3.489
.6712	3.979
.6886	4.359
.7147	4.935
.7250	5.717
.7547	6.532
.7754	7.205
.7959	7.901
.8261	8.639
.8375	9.215
.8734	9.781
.9197	10.216
.9560	10.695
1.0370	11.023
1.1081	11.372
1.1951	11.602
1.2631	11.865
1.3163	12.116
1.4099	12.227
1.5186	12.456
1.5982	12.601
1.6941	12.690
1.7743	12.855
2.0239	13.133
2.1462	13.169
2.2577	13.226
2.3921	13.262
2.4845	13.221
2.6254	13.182
2.7500	13.217
2.8593	13.274
3.0015	13.452
3.1999	13.598
3.3735	13.787
3.5544	13.857
3.7609	14.068
3.9960	14.172
4.2038	14.058
4.4639	14.142
4.7298	14.160
4.8340	11.906
4.8898	6.806
5.0441	5.117
5.1485	5.155
5.3542	5.217

TABLE 5.- Continued

(c) Pitot profiles: Case 2; station 2; test 11; run 36;
 $P_{t,1} = 13\ 444.9$ kPa; $T_t = 305.6$ K

y , cm	p , N/cm ²
.1569	.140
.3113	.628
.3987	.953
.4797	1.333
.5747	1.898
.6134	2.550
.6514	3.170
.7016	3.866
.7396	4.475
.7833	5.019
.7907	5.421
.8289	6.074
.8665	6.585
.9060	7.324
.9332	7.737
.9600	8.183
.9942	8.607
1.0151	9.042
1.0359	9.445
1.0889	9.690
1.1287	10.249
1.1815	10.651
1.2724	11.053
1.3169	11.270
1.3726	11.530
1.4557	11.801
1.5497	12.050
1.6465	12.212
1.7456	12.364
1.8513	12.548
1.9960	12.622
2.2015	12.696
2.4256	12.748
2.6237	12.790
2.7677	12.940
2.8991	13.200
2.9518	13.330
3.0113	13.547
3.0916	13.720
3.1760	13.785
3.2476	13.610
3.4983	13.487
3.7621	13.462
4.0822	13.480
4.2592	13.500
4.4619	13.465
4.7159	13.429
4.8760	13.351
4.9991	13.198
5.1286	13.022
5.2284	12.912
5.3274	12.944
5.4409	13.062
5.5529	13.203
5.6484	13.332

TABLE 5.- Continued

(c) Concluded

$y, \text{ cm}$	$p, \text{ N/cm}^2$
5.7259	13.440
5.8033	13.526
6.0227	13.622
6.1024	13.033
6.1040	11.760
6.1354	11.074
6.1637	9.626
6.1668	8.723
6.1847	6.438
6.2078	5.382
6.2608	4.957
6.3211	4.945
6.4106	4.933
6.5336	4.942
6.6637	4.919
6.7929	4.917
6.8562	4.894
6.9044	4.915

TABLE 5.- Continued

(d) Pitot profiles: Case 3; station 3; test 11; run 62;
 $P_{t,1} = 12\ 962\pm 2$ kPa; $T_t = 305\pm 6$ K

y, cm	p, N/cm ²
.1288	.755
.1629	.848
.2259	1.127
.2772	1.303
.3885	1.654
.5185	2.161
.6172	2.637
.6796	3.113
.7646	3.579
.8160	4.159
.8604	4.709
.9046	5.238
.9491	5.797
.9925	6.201
1.0521	6.605
1.0994	7.082
1.1465	7.517
1.1750	8.046
1.2230	8.637
1.2462	9.363
1.3232	9.954
1.3562	10.379
1.4066	11.146
1.4930	11.653
1.6029	12.285
1.7137	12.823
1.7781	13.092
1.8733	13.339
1.9431	13.546
2.0470	13.721
2.1874	13.802
2.3307	13.852
2.5241	13.891
2.7125	13.909
2.8764	13.928
3.0342	14.029
3.1659	14.152
3.2935	14.171
3.4107	14.138
3.5716	14.063
3.7177	13.968
3.8422	13.893
4.0135	13.808
4.1510	13.817
4.3710	13.772
4.4678	13.698
4.6460	13.613
4.7635	13.580
4.9399	13.536
5.0460	13.555
5.1240	13.606
5.1949	13.636
5.2914	13.676
5.3975	13.747
5.4729	13.912

TABLE 5.- Continued

(d) Concluded

y, cm	p, N/cm ²
5.5726	13.963
5.6900	14.055
5.7906	14.095
5.9244	14.104
6.0347	14.092
6.1957	14.069
6.3658	14.098
6.5446	14.105
6.6867	14.093
6.9233	14.048
7.1653	13.942
7.2832	13.878
7.3296	11.739
7.3825	9.362
7.4438	6.393
7.5017	5.168
7.6787	5.167
7.8853	5.155
7.9016	5.154
7.9046	5.142
7.9213	5.140
7.9300	5.138
7.9391	5.137
7.9484	5.136

TABLE 5.- Continued

(e) Pitot profiles: Case 4; station 4; test 15; run 11;
 $P_{t,1} = 13\ 169.1$ kPa; $T_t = 305.6$ K

y , cm	p , N/cm ²
.2221	.471
.2580	.576
.3211	.733
.4054	.951
.6215	1.253
.7191	1.366
.7931	1.546
.9209	1.806
1.0130	2.129
1.1367	2.463
1.2909	2.878
1.3880	3.138
1.4500	3.429
1.5182	3.783
1.5905	4.230
1.7151	4.635
1.8578	5.196
1.9377	5.612
1.9956	5.923
2.0613	6.371
2.1166	6.745
2.2019	7.399
2.3273	8.147
2.3690	8.842
2.4833	9.413
2.5446	9.984
2.5838	10.369
2.6368	10.774
2.6894	11.170
2.7617	11.564
2.9020	12.333
2.9939	12.977
3.1004	13.351
3.1894	13.913
3.3205	14.287
3.5392	14.558
3.6793	14.786
3.9243	15.081
4.1718	15.196
4.3205	15.302
4.6857	15.314
4.9331	15.306

TABLE 5.- Continued

(f) Pitot profiles: Case 5; station 1; test 11; run 5;
 $P_{t,1} = 10\ 204.3$ kPa; $T_t = 305.6$ K

y, cm	p, N/cm ²
.1333	.102
.2443	.257
.3695	.424
.4933	.841
.5678	1.386
.6489	2.203
.6781	2.856
.7165	3.553
.7462	4.140
.7661	4.760
.7907	5.391
.8152	5.880
.8253	6.380
.8478	6.968
.8781	7.686
.9357	8.166
.9916	8.558
1.0636	8.919
1.1791	9.150
1.2627	9.370
1.3377	9.599
1.4147	9.820
1.5293	9.976
1.6641	10.164
1.7137	10.274
1.8301	10.473
1.9770	10.532
2.0462	10.632
2.1392	10.624
2.2339	10.769
2.3319	10.707
2.4327	10.916
2.5370	10.778
2.6324	10.716
2.7222	10.795
2.8476	10.820
2.9760	10.824
3.0873	10.872
3.1901	10.961
3.3294	11.085
3.5003	11.101
3.6436	11.204
3.7920	11.263
3.9482	11.311
4.1215	11.392
4.3017	11.397
4.4810	11.372
4.6704	11.324
4.8767	11.125
4.9203	11.128
5.0100	8.788
5.0198	6.312
5.0860	4.218
5.1847	4.166
5.2319	4.190
5.2507	4.181
5.2660	4.182

TABLE 5.- Continued

(g) Pitot profiles: Case 6; station 2; test 11; run 37;
 $P_{t,1} = 10.618 \pm 0$ kPa; $T_t = 305.6$ K

y, cm	p, N/cm ²
.2620	.426
.3949	.775
.4923	1.103
.5589	1.408
.5897	1.799
.6138	2.223
.6583	2.485
.6763	2.811
.7009	3.148
.7508	3.627
.7809	4.170
.8252	4.475
.8546	5.030
.8864	5.682
.9119	6.476
1.0725	7.999
1.1230	8.304
1.1623	8.554
1.1971	8.740
1.2501	8.990
1.3391	9.230
1.4102	9.438
1.4576	9.580
1.5117	9.700
1.6742	9.952
1.7621	10.105
1.8966	10.161
1.9908	10.162
2.0714	10.174
2.1375	10.262
2.1662	10.306
2.2816	10.319
2.3969	10.342
2.5485	10.355
2.6526	10.422
2.7566	10.510
2.8583	10.609
2.9554	10.762
3.0176	10.883
3.1009	11.003
3.1637	11.134
3.2071	11.222
3.2635	11.179
3.3449	11.115
3.4201	11.062
3.4765	11.030
3.5237	11.020
3.5768	11.010
3.6153	11.032
3.6926	11.044
3.9190	11.036
3.9903	10.993
4.1000	11.006
4.1884	11.018
4.3178	11.095

TABLE 5.- Continued

(g) Concluded

y , cm	p , N/cm ²
4.4199	11.064
4.6459	11.067
4.7795	10.982
4.8795	10.896
4.9638	10.799
5.0275	10.670
5.0848	10.573
5.1869	10.498
5.3007	10.467
5.3777	10.457
5.4753	10.491
5.5631	10.557
5.6454	10.645
5.7204	10.766
5.8222	10.887
6.0313	10.997
6.0904	11.063
6.1897	11.141
6.2691	11.152
6.2725	10.446
6.3059	8.947
6.3222	7.589
6.3380	6.308
6.3518	5.373
6.3958	4.874
6.4073	4.320
6.4244	4.125
6.4466	4.028
6.4769	3.985
6.6120	3.998
6.7110	3.999
6.7929	4.012
6.8347	4.003
6.8905	3.993

TABLE 5.- Continued

(h) Pitot profiles: Case 7; station 3; test 11; run 63;
 $P_{t,1} = 10\ 204.3$ kPa; $T_t = 305.6$ K

y , cm	p , N/cm ²
.2067	.688
.2414	.844
.3051	1.103
.3860	1.341
.4384	1.558
.5076	1.714
.5634	1.869
.6193	2.128
.6611	2.304
.6692	2.522
.7381	2.771
.8081	3.206
.8435	3.580
.8925	4.140
.9476	4.492
.9751	4.627
1.0237	5.104
1.0723	5.602
1.1274	5.954
1.1756	6.244
1.2168	6.441
1.2378	6.732
1.2663	7.126
1.3015	7.437
1.3298	7.769
1.3860	8.173
1.4283	8.567
1.4844	8.982
1.5403	9.262
1.5961	9.510
1.6241	9.687
1.6664	9.936
1.7422	10.174
1.8180	10.381
1.8936	10.547
1.9616	10.671
2.1003	10.805
2.2282	10.929
2.3518	10.980
2.4904	10.969
2.6697	10.968
2.8631	11.009
3.0266	11.091
3.1099	11.184
3.1901	11.267
3.2568	11.308
3.3168	11.297
3.4232	11.203
3.5209	11.130
3.6709	11.047
3.7862	11.015
3.9774	11.035
4.1151	11.034
4.2231	11.013
4.3328	10.992

TABLE 5.- Continued

(h) Concluded

y, cm	p, N/cm ²
4.4728	10.981
4.6460	10.938
4.8792	10.875
5.0711	10.874
5.2922	10.883
5.4799	10.955
5.6998	11.058
5.8082	11.140
5.8858	11.264
5.9866	11.388
6.0558	11.492
6.1782	11.471
6.3257	11.470
6.5040	11.407
6.6158	11.396
6.7169	11.406
6.8456	11.436
6.9469	11.457
7.0762	11.518
7.2259	11.538
7.3002	11.497
7.3916	11.434
7.5487	11.350
7.6316	10.748
7.6900	9.690
7.7169	7.179
7.7292	5.747
7.8398	4.419
7.9171	4.242
7.9862	4.242
8.0180	4.241
8.0233	4.250
8.0238	4.230

TABLE 5.- Continued

(i) Pitot profiles: Case 8; station 4; test 15; run 10;
 $P_{t,1} = 10\ 755.9$ kPa; $T_t = 305.6$ K

y, cm	p, N/cm ²
.2533	.485
.3112	.606
.3546	.747
.4802	.886
.6417	1.089
.7254	1.221
.8424	1.363
.9491	1.576
1.0168	1.768
1.1538	1.939
1.2824	2.215
1.4314	2.523
1.4992	2.841
1.5643	3.208
1.6222	3.433
1.7642	3.835
1.9286	4.330
2.0493	4.814
2.1321	5.277
2.1777	5.584
2.2323	5.870
2.3149	6.105
2.3559	6.540
2.4601	7.036
2.5776	7.625
2.6604	8.068
2.7324	8.292
2.7990	8.569
2.8411	8.857
2.8802	9.270
2.9736	9.755
3.0696	10.115
3.1482	10.507
3.2302	10.804
3.3235	10.986
3.4235	11.220
3.5265	11.497
3.6161	11.712
3.7910	11.843
3.8210	11.841
3.8785	11.826
3.9411	11.895
4.0731	12.026
4.3338	12.136
4.3999	12.183
4.4725	12.209
4.6632	12.201
4.9302	12.197
5.0518	12.212
5.1607	12.172
5.5320	12.194
5.6443	12.175
5.9431	12.145
6.2383	12.168

TABLE 5.- Continued

(j) Pitot profiles: Case 9; station 1; test 11; run 5;
 $P_{t,1} = 7791.1$ kPa; $T_t = 305.6$ K

y, cm	p, N/cm ²
.1276	.071
.2044	.126
.2506	.159
.3073	.203
.3844	.291
.4608	.411
.5227	.574
.5701	.749
.6031	.955
.6477	1.173
.6852	1.379
.7226	1.672
.7472	1.987
.7589	2.378
.7930	2.748
.8200	3.084
.8285	3.475
.8460	3.920
.8730	4.268
.8906	4.572
.9085	4.985
.9171	5.321
.9662	5.702
1.0110	6.104
1.0446	6.386
1.1010	6.647
1.1718	6.821
1.2478	7.083
1.3383	7.290
1.4066	7.442
1.5021	7.573
1.5763	7.704
1.6239	7.802
1.7094	7.923
1.7806	8.021
1.9074	8.142
2.0129	8.229
2.1296	8.263
2.2026	8.307
2.2831	8.351
2.3878	8.439
2.4954	8.538
2.5987	8.484
2.6913	8.485
2.7958	8.388
2.9106	8.368
2.9999	8.379
3.1112	8.446
3.1987	8.457
3.3208	8.534
3.4491	8.611
3.6061	8.613
3.7536	8.669
3.8805	8.681

TABLE 5.- Continued

(j) Concluded

y , cm	p , N/cm ²
4.0338	8.736
4.1662	8.737
4.2503	8.738
4.3130	8.750
4.4157	8.716
4.5368	8.719
4.6463	8.742
4.7214	8.667
4.8364	8.668
4.9254	8.647
5.0041	8.615
5.0692	8.595
5.1289	8.520
5.1800	8.488
5.2054	7.913
5.2155	6.817
5.2506	5.569
5.2983	4.245
5.3387	3.171
5.4565	3.151
5.5219	3.141
5.5811	3.142

TABLE 5.- Continued

(k) Pitot profiles: Case 10; station 2; test 11; run 39;
 $P_{t,1} = 7653.2$ kPa; $T_t = 305.6$ K

y, cm	p, N/cm ²
.2607	.250
.3728	.405
.5130	.560
.6023	.860
.6616	1.223
.6979	1.419
.7462	1.792
.7944	2.103
.8291	2.424
.8572	2.839
.9122	3.150
.9656	3.450
.9787	3.865
1.0105	4.446
1.0420	4.839
1.1044	5.326
1.1544	5.772
1.2161	6.083
1.3111	6.559
1.3822	6.818
1.4532	7.025
1.5535	7.190
1.6460	7.366
1.7598	7.531
1.8438	7.634
2.1176	7.820
2.3034	7.933
2.4024	7.953
2.5069	7.963
2.5462	8.046
2.6638	8.055
2.7523	8.117
2.9278	8.189
3.0462	8.209
3.2708	8.353
3.3389	8.436
3.3758	8.394
3.4068	8.425
3.4440	8.508
3.4995	8.487
3.5860	8.517
3.6785	8.537
3.8234	8.568
3.9576	8.557
4.1131	8.577
4.2884	8.586
4.5047	8.564
4.6951	8.542
4.8509	8.479
5.0626	8.437
5.2408	8.405
5.3947	8.290
5.4994	8.196

TABLE 5.- Continued

(k) Concluded

y, cm	p, N/cm ²
5.5898	8.123
5.7149	8.143
5.8329	8.225
5.9465	8.328
5.9828	8.400
6.0997	8.514
6.3852	8.617
6.5337	8.690
6.6036	8.699
6.6684	8.585
6.7133	8.315
6.7439	7.744
6.7659	5.618
6.7785	4.643
6.8279	3.461
6.9231	3.139
7.0177	3.116
7.0558	3.107
7.0741	3.117
7.0810	3.137
7.0885	3.106

TABLE 5.- Continued

(1) Pitot profiles: Case 11; station 3; test 11; run 64;
 $P_{t,1} = 7791.1$ kPa; $T_t = 305.6$ K

y, cm	p, N/cm ²
.1113	.326
.1567	.440
.2216	.595
.2666	.636
.3114	.781
.3560	.905
.3876	.967
.4320	1.050
.5082	1.225
.5720	1.433
.6422	1.681
.6993	1.857
.7507	2.044
.7804	2.210
.8245	2.386
.8698	2.750
.9069	2.968
.9658	3.207
1.0138	3.549
1.0802	3.933
1.1471	4.401
1.2202	4.816
1.2409	5.076
1.3082	5.376
1.3716	5.688
1.4011	6.020
1.4649	6.373
1.5631	6.736
1.6678	7.026
1.7449	7.243
1.8843	7.512
1.9872	7.867
2.0813	7.759
2.2076	7.841
2.3371	7.933
2.4883	8.024
2.6488	8.033
2.8455	8.082
3.0613	8.132
3.2369	8.192
3.3647	8.263
3.5455	8.292
3.7167	8.279
3.8773	8.287
3.9789	8.286
4.1020	8.264
4.2222	8.272
4.3703	8.261
4.4649	8.269
4.6227	8.267
4.7766	8.234
4.9633	8.201
5.1355	8.157
5.2890	8.134
5.4624	8.142

TABLE 5.- Continued

(1) Concluded

y, cm	p, N/cm ²
5.6648	8.129
5.8120	8.179
5.9196	8.271
6.0375	8.342
6.1353	8.435
6.2769	8.527
6.4556	8.587
6.6270	8.595
6.8378	8.603
6.9926	8.622
7.1343	8.599
7.3668	8.575
7.7175	8.520
7.8806	8.517
7.9730	8.504
8.0151	7.691
8.1142	5.496
8.1989	3.903
8.2886	3.143
8.4287	3.131
8.4441	3.130
8.4557	3.118
8.4627	3.138
8.4671	3.126
8.4711	3.135

TABLE 5.- Continued

(m) Pitot profiles: Case 12; station 4; test 15; run 9;
 $P_{t,1} = 8135.9$ kPa; $T_t = 305.6$ K

y , cm	p , N/cm ²
.1926	.420
.2336	.453
.2869	.559
.3992	.665
.5366	.802
.6463	.940
.7321	1.026
.6637	1.206
1.0091	1.375
1.0780	1.513
1.1402	1.610
1.1965	1.747
1.3045	1.936
1.4070	2.155
1.5140	2.314
1.6019	2.431
1.6388	2.663
1.7335	2.831
1.8390	3.010
1.9469	3.312
2.0163	3.563
2.0976	3.772
2.1706	3.951
2.2345	4.109
2.2896	4.382
2.3599	4.633
2.4799	5.030
2.6066	5.312
2.6725	5.612
2.7344	6.073
2.8011	6.189
2.8474	6.325
2.9069	6.525
2.9405	6.756
3.0218	7.007
3.1299	7.362
3.2270	7.550
3.2750	7.811
3.3388	8.009
3.3890	8.105
3.4368	8.180
3.4715	8.275
3.5346	8.360
3.5966	8.518
3.7267	8.654
3.8482	8.771
3.9095	8.856
3.9462	8.899
4.0100	8.923
4.0603	8.998
4.1967	9.073
4.4527	9.129
4.5061	9.162
4.5836	9.156

TABLE 5.- Continued

(m) Concluded

y, cm	p, N/cm ²
4.6416	9.191
4.8315	9.204
5.0234	9.197
5.1301	9.210
5.1616	9.212
5.2401	9.216
5.2944	9.199
5.3882	9.149
5.6106	9.120

TABLE 5.- Continued

(n) Pitot profiles: Case 13; station 1; test 11; run 8;
 $P_{t,1} = 5309.0$ kPa; $T_t = 305.6$ K

y, cm	p, N/cm ²
.2073	.060
.2734	.088
.3360	.122
.4302	.177
.4941	.232
.5513	.325
.5911	.413
.6105	.538
.6421	.647
.6672	.811
.7106	.958
.7198	1.115
.7530	1.370
.7819	1.658
.8128	1.935
.8734	2.245
.9115	2.495
.9316	2.739
.9519	2.967
.9833	3.254
.9961	3.564
1.0166	3.781
1.0428	4.020
1.0839	4.221
1.1068	4.395
1.1507	4.520
1.2245	4.662
1.2724	4.793
1.3345	4.973
1.4109	5.126
1.4803	5.257
1.5445	5.324
1.6099	5.433
1.6944	5.510
1.7605	5.592
1.8500	5.643
1.9203	5.747
2.0428	5.765
2.1488	5.816
2.2788	5.904
2.3567	5.960
2.4425	5.983
2.5576	5.996
2.6719	6.019
2.7735	6.010
2.8621	5.969
2.9916	5.954

TABLE 5.- Continued

(n) Concluded

y, cm	p, N/cm ²
3.1151	5.940
3.2109	5.963
3.3113	6.014
3.4166	6.059
3.4968	6.136
3.6214	6.165
3.7050	6.145
3.8047	6.174
3.9075	6.186
3.9934	6.204
4.1190	6.228
4.2017	6.234
4.3117	6.209
4.4143	6.233
4.5326	6.219
4.6759	6.211
4.8025	6.219
4.9950	6.200
5.0629	6.192
5.1986	6.184
5.2854	6.159
5.3793	6.047
5.4678	5.919
5.4878	5.643
5.5089	5.232
5.5117	4.896
5.5501	4.462
5.5514	4.051
5.5561	3.699
5.5658	3.325
5.5680	2.828
5.6012	2.309
5.6673	2.186
5.7628	2.171
5.9039	2.173
5.9682	2.196

TABLE 5.. Continued

(o) Pitot profiles: Case 14; station 2; test 11; run 40;
 $P_{t,1} = 5309.0$ kPa; $T_t = 305.6$ K

y, cm	p, N/cm ²
.1518	.046
.1775	.046
.2751	.099
.3391	.140
.4151	.212
.5340	.305
.6311	.428
.6898	.552
.7166	.687
.7600	.832
.8054	.976
.8567	1.225
.9023	1.442
.9311	1.691
.9678	1.939
1.0298	2.292
1.0646	2.592
1.0993	2.882
1.1270	3.089
1.1682	3.286
1.2026	3.472
1.2372	3.721
1.2650	3.939
1.3131	4.187
1.3814	4.363
1.4750	4.538
1.5434	4.693
1.6181	4.848
1.6973	4.983
1.8136	5.116
1.9309	5.209
2.0787	5.270
2.2126	5.383
2.3297	5.455
2.4575	5.485
2.6157	5.556
2.7408	5.586
2.8604	5.637
2.9959	5.678
3.0907	5.677
3.2116	5.718
3.2886	5.738
3.3383	5.789
3.4539	5.861
3.5145	5.902
3.6443	5.963
3.8144	5.993
3.9951	6.023
4.2005	6.001
4.3268	5.990
4.4947	5.999
4.6347	5.998
4.7924	5.976
4.9294	5.954
5.1020	5.943
5.2429	5.952

TABLE 5.- Continued

(o) Concluded

y, cm	p, N/cm ²
5.3442	5.930
5.5247	5.888
5.5875	5.856
5.6321	5.824
5.7978	5.803
5.8931	5.771
6.0118	5.749
6.1732	5.800
6.3430	5.851
6.4176	5.902
6.5121	5.973
6.5991	6.014
6.6648	6.034
6.6981	6.013
6.7416	6.044
6.7985	6.075
6.9316	6.064
7.0243	6.042
7.0677	5.990
7.0802	5.886
7.0906	5.741
7.0988	5.616
7.1083	5.491
7.1206	5.315
7.1354	4.846
7.1485	4.143
7.1699	3.603
7.1985	2.898
7.2357	2.462
7.2430	2.338
7.2814	2.234
7.3794	2.213
7.4243	2.212
7.4598	2.211
7.4824	2.169
7.4901	2.189
7.5311	2.178
7.6251	2.188
7.7191	2.187
7.7373	2.165
7.7549	2.164
7.7694	2.153

TABLE 5.- Continued

(p) Pitot profiles: Case 15; station 3; test 11; run 65;
 $P_{t,1} = 5309.0$ kPa; $T_t = 305.6$ K

y, cm	p, N/cm ²
.8200	.774
.8949	.911
.9491	1.069
1.0193	1.279
1.0769	1.552
1.1607	1.752
1.2429	2.066
1.2983	2.359
1.3563	2.651
1.4303	2.913
1.5023	3.259
1.5328	3.541
1.5922	3.751
1.6527	4.044
1.7427	4.317
1.8040	4.516
1.8791	4.685
1.9970	4.865
2.0613	5.023
2.1929	5.120
2.3105	5.290
2.3912	5.366
2.4443	5.431
2.5487	5.465
2.6785	5.500
2.8014	5.556
2.9240	5.570
3.0563	5.605
3.1878	5.671
3.2951	5.685
3.3707	5.708
3.5372	5.734
3.6878	5.781
3.8655	5.797
4.0517	5.823
4.1753	5.796
4.3677	5.791
4.5203	5.807
4.6863	5.812
4.8678	5.818
5.0472	5.823
5.2025	5.808
5.3879	5.803
5.5492	5.819
5.7634	5.793
5.8968	5.808
6.0492	5.802
6.1811	5.827
6.2852	5.851
6.3589	5.844
6.4275	5.888
6.5176	5.954
6.6476	5.999
6.7788	6.107
6.9674	6.122

TABLE 5.- Continued

(p) Concluded

y, cm	p, N/cm ²
7.0897	6.117
7.2805	6.132
7.4197	6.127
7.6133	6.143
7.9516	6.101
8.0492	6.052
8.1207	6.085
8.2323	6.109
8.3583	6.040
8.4395	6.064
8.5485	6.067
8.6150	6.058
8.6585	5.935
8.6909	5.478
8.6953	5.717
8.6961	5.156
8.7171	4.886
8.7407	4.450
8.7563	4.004
8.7803	3.547
8.8024	3.204
8.8082	2.851
8.8295	2.560
8.8578	2.353
8.9355	2.272
9.0717	2.267
9.1613	2.251
9.6247	2.267

TABLE 5.- Continued

(q) Pitot profiles: Case 16; station 4; test 15; run 8;
 $P_{t,1} = 5584.8$ kPa; $T_t = 305.6$ K

y , cm	p , N/cm ²
.3665	.075
.4135	.157
.4714	.249
.5464	.331
.6528	.443
.7789	.525
.9462	.627
.9945	.688
1.0821	.852
1.1962	.944
1.3481	1.088
1.5180	1.241
1.5991	1.385
1.7309	1.549
1.8460	1.775
1.9810	1.940
2.1177	2.156
2.1697	2.238
2.2698	2.330
2.3632	2.412
2.4262	2.535
2.4966	2.710
2.6290	3.030
2.7146	3.195
2.7836	3.411
2.8290	3.618
2.8741	3.731
2.9501	3.812
3.0080	3.915
3.0552	4.111
3.0856	4.276
3.1722	4.399
3.2742	4.626
3.3757	4.832
3.4455	5.028
3.5120	5.079
3.5423	5.172
3.5837	5.285
3.6504	5.439
3.7263	5.510
3.8430	5.561
3.8986	5.706
3.9659	5.850
4.0404	5.973
4.1049	6.014
4.1465	6.044
4.1992	6.074

TABLE 5.- Continued

(q) Concluded

$y, \text{ cm}$	$p, \text{ N/cm}^2$
4.2540	6.064
4.3320	6.125
4.4642	6.207
4.6405	6.257
4.7651	6.328
4.8221	6.368
4.8664	6.367
5.0099	6.366
5.1732	6.365
5.3091	6.364

TABLE 5.- Continued

(r) Pitot profiles: Case 17; station 1; test 11; run 4;
 $P_{t,1} = 2757.9$ kPa; $T_t = 305.6$ K

y , cm	p , N/cm ²
.1022	.025
.1787	.028
.3133	.045
.4169	.049
.5031	.063
.6401	.101
.7234	.126
.7913	.183
.8758	.230
.9497	.342
1.0104	.485
1.0934	.618
1.1450	.772
1.2005	.938
1.2147	1.167
1.2545	1.309
1.3033	1.463
1.3167	1.594
1.3532	1.780
1.4066	1.956
1.4670	2.110
1.5243	2.242
1.5980	2.364
1.6465	2.486
1.6992	2.576
1.7868	2.666
1.8745	2.745
2.0051	2.814
2.1259	2.895
2.2068	2.953
2.3505	2.991
2.4596	3.007
2.5508	3.055
2.6569	3.082
2.7739	3.119
2.9129	3.167
3.0230	3.204
3.1537	3.186
3.4240	3.208
3.6549	3.217
3.8969	3.194
4.1538	3.280
4.4101	3.289
4.5543	3.233
4.7958	3.222
4.9252	3.220
5.0996	3.273
5.2693	3.293
5.3811	3.325

TABLE 5.- Continued

(s) Pitot profiles: Case 18; station 2; test 11; run 41;
 $P_{t,1} = 2551.1$ kPa; $T_t = 305.6$ K

y, cm	p, N/cm ²
.2919	.046
.4141	.051
.5190	.053
.6001	.074
.6754	.092
.8192	.134
.9398	.169
1.0479	.215
1.1354	.253
1.1721	.299
1.2023	.349
1.2326	.399
1.2692	.449
1.2918	.503
1.3141	.569
1.3484	.636
1.4057	.740
1.4276	.823
1.4493	.914
1.4944	1.026
1.5211	1.154
1.5481	1.274
1.5577	1.369
1.6155	1.452
1.6363	1.609
1.6720	1.746
1.7089	1.837
1.7651	1.945
1.8155	2.024
1.8454	2.132
1.8961	2.199
1.9335	2.273
1.9828	2.340
2.0634	2.452
2.1502	2.540
2.2544	2.624
2.4026	2.692
2.5549	2.743
2.6831	2.798
2.7940	2.837
2.8946	2.867
3.0620	2.902
3.2707	2.954
3.4870	2.989
3.6288	3.020
3.8064	3.059
3.9383	3.086
4.0673	3.104
4.1998	3.109
4.3318	3.131
4.4148	3.157
4.5118	3.182
4.5885	3.183
4.6463	3.172
4.6981	3.189

TABLE 5.- Continued

(s) Concluded

y , cm	p , N/cm ²
4.7736	3.198
4.8856	3.212
5.0253	3.218
5.2535	3.229
5.4236	3.235
5.5837	3.224
5.7174	3.222
5.8408	3.215
5.9268	3.212
6.0058	3.200
6.0553	3.217
6.1926	3.178
6.3325	3.155
6.4735	3.156
6.6123	3.145
6.7477	3.143
6.8239	3.173
6.9801	3.212
7.1180	3.239
7.2305	3.270

TABLE 5.- Continued

(t) Pitot profiles: Case 19; station 3; test 11; run 66;
 $P_{t,1} = 2551.1$ kPa; $T_t = 305.6$ K

y , cm	p , N/cm ²
.0335	.044
.0925	.045
.2276	.063
.3429	.065
.5225	.101
.7875	.171
.9702	.248
1.1458	.366
1.2595	.471
1.3518	.588
1.4479	.701
1.5132	.876
1.5922	1.034
1.6365	1.245
1.7086	1.412
1.7750	1.557
1.8475	1.761
1.9193	1.911
2.0033	2.106
2.1365	2.314
2.2451	2.432
2.3965	2.574
2.5666	2.684
2.7817	2.761
2.9964	2.818
3.1405	2.870
3.3650	2.911
3.5771	2.934
3.7763	2.950
4.0771	2.987
4.2828	3.003
4.4808	3.030
4.7120	3.046
4.9610	3.056
5.1688	3.070
5.3907	3.073
5.5911	3.088
5.7436	3.086
5.9025	3.097
6.0061	3.102
6.1583	3.104
6.2762	3.098
6.3941	3.091
6.5177	3.081
6.6867	3.087
6.8416	3.110
6.9656	3.137
7.0722	3.166
7.1473	3.194
7.2355	3.207
7.3650	3.214
7.5193	3.212
7.6517	3.230
7.7772	3.244
7.9001	3.250

TABLE 5.- Continued

(t) Concluded

y, cm	p, N/cm ²
8.0434	3.256
8.1551	3.253
8.2588	3.250
8.3492	3.252
8.4432	3.254
8.5992	3.248
8.7458	3.253
8.8382	3.242
8.9391	3.243
9.0334	3.244
9.0661	3.237
9.1150	3.234
9.1720	3.231
9.2749	3.220
9.3542	3.222
9.4799	3.223
9.6130	3.188
9.7792	2.792
9.8051	2.355
9.8179	2.008
9.8418	1.836
9.8641	1.680
9.8788	1.709
9.8980	1.764

TABLE 5.- Continued

(u) Pitot profiles: Case 20; station 4; test 15; run 7;
 $P_{t,1} = 2895.8$ kPa; $T_t = 305.6$ K

y, cm	p, N/cm ²
.3871	.034
.5933	.149
.7134	.211
.8572	.284
.9809	.326
1.1242	.389
1.2820	.451
1.4062	.524
1.5038	.555
1.6388	.608
1.7072	.691
1.8172	.743
1.9585	.867
2.0141	.940
2.0495	.940
2.0848	.940
2.1394	.992
2.1874	1.034
2.3161	1.128
2.4201	1.221
2.5506	1.315
2.6537	1.440
2.7031	1.533
2.7230	1.533
2.7485	1.502
2.7684	1.554
2.7798	1.637
2.8025	1.668
2.8252	1.627
2.8536	1.648
2.9748	1.752
3.1370	1.887
3.2497	2.012
3.3446	2.126
3.4079	2.147
3.4450	2.189
3.4873	2.241
3.5707	2.324
3.6634	2.407
3.8400	2.532
3.9449	2.636
4.0174	2.709
4.0826	2.750
4.1846	2.813
4.3963	2.896
4.5715	2.959

TABLE 5.- Continued

(u) Concluded

y , cm	p , N/cm ²
4.6378	3.021
4.6802	2.987
4.7683	3.042
4.8598	3.063
5.0772	3.063
5.2837	3.095
5.3734	3.105
5.4547	3.095
5.5301	3.106
5.8999	3.127
5.9085	3.127
6.0729	3.116
6.1506	3.127
6.2164	3.106
6.2802	3.096
6.5938	3.065

TABLE 5.- Continued

(v) Pitot profiles: Case 21; station 1; test 42; run 13;
 $P_{t,1} = 13\ 720.7$ kPa; $T_t = 303.9$ K; $T_w/T_t = 0.952$

y , cm	p , N/cm ²
1.584	12.784
1.582	12.775
1.581	12.753
1.581	12.730
1.581	12.712
1.565	12.703
1.520	12.630
1.458	12.530
1.405	12.466
1.368	12.420
1.350	12.370
1.343	12.334
1.341	12.306
1.341	12.284
1.342	12.297
1.340	12.334
1.314	12.338
1.263	12.297
1.194	12.234
1.133	12.174
1.090	12.133
1.068	12.097
1.059	12.051
1.057	12.042
1.056	12.033
1.057	12.033
1.057	12.020
1.050	12.006
1.014	11.929
.954	11.787
.891	11.614
.845	11.492
.815	11.364
.798	11.282
.788	11.237
.786	11.205
.784	11.159
.781	11.173
.778	11.159
.756	10.950
.708	10.253
.646	9.056
.595	7.872
.559	6.861
.537	6.024
.521	5.304
.512	4.767
.506	4.448

TABLE 5.- Continued

(v) Continued

$y, \text{ cm}$	$p, \text{ N/cm}^2$
.502	4.198
.499	4.121
.483	3.770
.440	2.909
.378	1.926
.320	1.111
.276	.606
.247	.333
.229	.214
.218	.178
.210	.169

TABLE 5.- Continued

(w) Pitot profiles: Case 22; station 2; test 39; run 12;
 $P_{t,1} = 13\ 617.2$ kPa; $T_t = 311.1$ K; $T_w/T_t = 0.959$

y , cm	p , N/cm ²
<u>2.554</u>	<u>13.610</u>
<u>2.401</u>	<u>13.430</u>
<u>2.212</u>	<u>13.240</u>
<u>1.986</u>	<u>13.089</u>
<u>1.756</u>	<u>12.698</u>
<u>1.525</u>	<u>12.372</u>
<u>1.475</u>	<u>12.292</u>
<u>1.343</u>	<u>11.922</u>
<u>1.313</u>	<u>11.913</u>
<u>1.237</u>	<u>11.690</u>
<u>1.148</u>	<u>11.375</u>
<u>1.108</u>	<u>11.052</u>
<u>1.057</u>	<u>10.714</u>
<u>.928</u>	<u>9.449</u>
<u>.899</u>	<u>9.086</u>
<u>.820</u>	<u>7.243</u>
<u>.674</u>	<u>3.006</u>
<u>.672</u>	<u>2.516</u>
<u>.445</u>	<u>.558</u>
<u>.243</u>	<u>.163</u>
<u>.220</u>	<u>.152</u>
<u>.125</u>	<u>.130</u>
<u>.033</u>	<u>.118</u>

(x) Pitot profiles: Case 23; station 3; test 39; run 31;
 $P_{t,1} = 13\ 720.7$ kPa; $T_t = 309.4$ K; $T_w/T_t = 0.943$

y , cm	p , N/cm ²
<u>1.918</u>	<u>12.868</u>
<u>1.685</u>	<u>12.827</u>
<u>1.449</u>	<u>12.819</u>
<u>1.298</u>	<u>12.527</u>
<u>1.200</u>	<u>12.166</u>
<u>1.144</u>	<u>11.898</u>
<u>.949</u>	<u>9.650</u>
<u>.865</u>	<u>8.645</u>
<u>.694</u>	<u>4.360</u>
<u>.626</u>	<u>3.775</u>
<u>.433</u>	<u>1.667</u>
<u>.345</u>	<u>1.442</u>
<u>.191</u>	<u>.793</u>
<u>.132</u>	<u>.717</u>

TABLE 5.- Continued

(y) Pitot profiles: Case 24; station 4; test 42; run 10;
 $P_{t,1} = 13\ 720.7$ kPa; $T_t = 308.9$ K; $T_w/T_t = 0.944$

y, cm	p, N/cm ²
3.910	13.514
3.865	13.551
3.831	13.560
3.810	13.564
3.799	13.573
3.790	13.601
3.786	13.614
3.773	13.555
3.745	13.523
3.698	13.592
3.648	13.646
3.609	13.674
3.584	13.701
3.568	13.728
3.558	13.737
3.554	13.737
3.542	13.755
3.517	13.783
3.474	13.769
3.421	13.737
3.376	13.724
3.344	13.701
3.322	13.696
3.311	13.715
3.305	13.719
3.296	13.719
3.274	13.742
3.233	13.742
3.180	13.733
3.124	13.756
3.084	13.737
3.054	13.733
3.038	13.715
3.030	13.742
3.021	13.751
3.003	13.742
2.967	13.696
2.914	13.692
2.855	13.660
2.805	13.646
2.770	13.660
2.748	13.678
2.735	13.687
2.725	13.715
2.709	13.687
2.678	13.633
2.628	13.596
2.567	13.614
2.510	13.596
2.467	13.578
2.440	13.546
2.424	13.523
2.415	13.560
2.402	13.592
2.379	13.583

TABLE 5.- Continued

(y) Continued

y, cm	p, N/cm ²
2.333	13.532
2.275	13.409
2.216	13.277
2.168	13.205
2.137	13.196
2.119	13.205
2.108	13.223
2.097	13.214
2.078	13.182
2.039	13.141
1.983	13.027
1.921	12.813
1.870	12.636
1.831	12.517
1.810	12.426
1.797	12.358
1.789	12.280
1.773	12.148
1.742	11.971
1.692	11.657
1.633	11.106
1.576	10.550
1.536	10.091
1.510	9.854
1.497	9.781
1.489	9.663
1.476	9.508
1.452	9.207
1.411	8.597
1.350	7.855
1.290	7.122
1.242	6.639
1.212	6.312
1.195	6.075
1.186	5.957
1.178	5.820
1.159	5.633
1.123	5.274
1.069	4.777
1.008	4.254
.956	3.844
.920	3.553
.900	3.389
.889	3.330
.882	3.325
.868	3.325
.840	3.220
.789	2.961
.731	2.606
.673	2.287
.633	2.050
.609	1.909
.597	1.854
.589	1.836
.580	1.823
.556	1.768
.513	1.631

TABLE 5.- Continued

(y) Concluded

y, cm	p, N/cm ²
.456	1.458
.397	1.272
.349	1.112
.320	1.017
.304	.980
.296	.976
.288	.948
.272	.903
.237	.816
.182	.680
.118	.525
.059	.429
.019	.398

TABLE 5.- Continued

(z) Pitot profiles: Case 25; station 5; test 42; run 7;
 $P_{t,1} = 13\ 789.6$ kPa; $T_t = 322.2$ K; $T_w/T_t = 0.899$

y, cm	p, N/cm ²
3.216	13.642
3.168	13.678
3.134	13.714
3.114	13.742
3.103	13.719
3.098	13.723
3.093	13.755
3.082	13.760
3.053	13.742
3.007	13.705
2.955	13.678
2.918	13.669
2.892	13.660
2.878	13.669
2.871	13.669
2.868	13.656
2.858	13.628
2.834	13.628
2.792	13.610
2.736	13.560
2.686	13.488
2.652	13.438
2.631	13.438
2.621	13.415
2.616	13.388
2.608	13.347
2.586	13.289
2.546	13.207
2.489	13.044
2.431	12.822
2.389	12.682
2.363	12.618
2.349	12.564
2.344	12.541
2.337	12.546
2.320	12.473
2.284	12.283
2.230	11.948
2.173	11.544
2.122	11.214
2.086	11.055
2.068	10.983
2.059	10.924
2.052	10.919
2.040	10.874
2.011	10.729
1.962	10.367
1.900	9.837
1.843	9.293
1.803	8.840
1.778	8.591
1.766	8.532
1.760	8.437
1.751	8.287
1.729	8.065
1.688	7.689

TABLE 5.- Continued

(z) Concluded

y, cm	p, N/cm ²
1.629	7.155
1.571	6.593
1.529	6.267
1.504	6.095
1.493	6.047
1.488	5.959
1.481	5.841
1.464	5.714
1.427	5.519
1.372	5.171
1.310	4.718
1.262	4.351
1.231	4.097
1.215	3.970
1.207	3.925
1.202	3.884
1.190	3.807
1.162	3.694
1.112	3.454
1.049	3.150
.991	2.874
.952	2.656
.930	2.529
.921	2.484
.917	2.462
.909	2.452
.888	2.398
.847	2.280
.790	2.086
.729	1.891
.686	1.732
.661	1.623
.648	1.574
.644	1.555
.638	1.537
.623	1.524
.587	1.424
.533	1.297
.470	1.152
.421	1.044
.377	.958
.369	.926
.366	.917
.355	.921
.328	.894
.280	.844
.280	.763
.216	.654
.158	.514
.122	.400
.102	.319
.095	.292
.092	.273
.085	.264
.063	.246
.013	.251

TABLE 5.- Continued

(aa) Pitot profiles: Case 26; station 6; test 39; run 36;
 $P_{t,1} = 13\ 734.5$ kPa; $T_t = 309.7$ K; $T_w/T_t = 0.966$

y , cm	p , N/cm ²
<u>2.299</u>	<u>10.748</u>
<u>2.204</u>	<u>9.855</u>
<u>2.033</u>	<u>8.274</u>
<u>1.846</u>	<u>6.539</u>
<u>1.618</u>	<u>4.827</u>
<u>1.360</u>	<u>3.405</u>
<u>1.088</u>	<u>2.348</u>
<u>.847</u>	<u>1.559</u>
<u>.615</u>	<u>1.035</u>
<u>.348</u>	<u>.592</u>
<u>.102</u>	<u>.119</u>
<u>.045</u>	<u>.101</u>

(bb) Pitot profiles: Case 26; station 6; test 39; run 40;
 $P_{t,1} = 13\ 734.5$ kPa; $T_t = 309.7$ K; $T_w/T_t = 0.966$

y , cm	p , N/cm ²
<u>4.575</u>	<u>14.110</u>
<u>4.478</u>	<u>14.034</u>
<u>4.361</u>	<u>14.011</u>
<u>4.245</u>	<u>14.165</u>
<u>4.150</u>	<u>14.116</u>
<u>3.963</u>	<u>14.071</u>
<u>3.841</u>	<u>13.957</u>
<u>3.697</u>	<u>13.921</u>
<u>3.526</u>	<u>13.818</u>
<u>3.467</u>	<u>13.805</u>
<u>3.367</u>	<u>13.765</u>
<u>3.239</u>	<u>13.686</u>
<u>3.181</u>	<u>13.622</u>
<u>3.113</u>	<u>13.572</u>
<u>3.081</u>	<u>13.613</u>
<u>2.918</u>	<u>13.492</u>
<u>2.794</u>	<u>13.222</u>
<u>2.702</u>	<u>13.063</u>
<u>2.538</u>	<u>12.463</u>
<u>2.413</u>	<u>11.786</u>
<u>2.321</u>	<u>11.190</u>
<u>1.966</u>	<u>8.121</u>
<u>1.596</u>	<u>4.814</u>
<u>1.235</u>	<u>2.912</u>

TABLE 5.- Continued

(cc) Pitot profiles: Case 27; station 7; test 42; run 3;
 $P_{t,1} = 13\ 672.4$ kPa; $T_t = 318.3$ K; $T_w/T_t = 0.916$

y , cm	p , N/cm ²
4.946	13.997
4.926	14.025
4.912	14.029
4.893	14.025
4.860	14.038
4.811	14.048
4.749	14.006
4.686	13.970
4.631	13.947
4.594	13.947
4.570	13.947
4.556	13.943
4.537	13.970
4.506	13.884
4.459	13.984
4.396	13.947
4.329	13.915
4.266	13.888
4.216	13.860
4.183	13.837
4.160	13.806
4.144	13.769
4.119	13.760
4.080	13.774
4.024	13.742
3.956	13.705
3.886	13.646
3.827	13.577
3.786	13.554
3.759	13.532
3.741	13.509
3.719	13.458
3.684	13.417
3.632	13.385
3.565	13.289
3.494	13.057
3.431	12.892
3.385	12.778
3.355	12.746
3.336	12.723
3.317	12.700
3.288	12.673
3.241	12.477
3.179	12.257
3.107	11.870
3.039	11.673
2.985	11.399
2.950	11.207
2.929	11.111
2.914	10.951
2.892	10.814
2.852	10.631
2.794	10.170
2.725	9.718
2.654	9.193

TABLE 5.- Continued

(cc) Continued

y, cm	p, N/cm ²
2.597	8.750
2.557	8.367
2.532	8.179
2.515	8.202
2.495	8.179
2.459	8.006
2.408	7.627
2.343	7.129
2.271	6.563
2.208	6.083
2.161	5.786
2.132	5.613
2.114	5.517
2.098	5.385
2.071	5.202
2.024	5.042
1.962	4.750
1.890	4.321
1.824	3.937
1.772	3.672
1.738	3.489
1.718	3.425
1.704	3.357
1.681	3.275
1.644	3.120
1.588	2.937
1.516	2.709
1.448	2.476
1.389	2.293
1.350	2.174
1.326	2.097
1.312	2.055
1.293	2.042
1.258	1.969
1.205	1.841
1.138	1.699
1.063	1.526
1.000	1.416
.955	1.334
.927	1.284
.912	1.247
.897	1.229
.870	1.202
.826	1.147
.762	1.060
.690	.964
.619	.873
.567	.795
.534	.740
.517	.722
.504	.713

TABLE 5.- Continued

(cc) Concluded

y , cm	p , N/cm ²
.481	.704
.441	.667
.386	.617
.314	.539
.245	.448
.185	.348
.148	.274
.125	.220
.112	.192
.096	.179

TABLE 5.- Continued

(dd) Pitot profiles: Case 27; station 7; test 42; run 4;
 $P_{t,1} = 13\ 672.4$ kPa; $T_t = 318.3$ K; $T_w/T_t = 0.916$

y, cm	p, N/cm ²
2.586	8.174
2.557	7.973
2.535	7.836
2.521	7.795
2.512	7.868
2.506	7.845
2.505	7.836
2.503	7.772
2.490	7.671
2.459	7.465
2.424	7.150
2.393	6.889
2.374	6.775
2.363	6.656
2.357	6.519
2.354	6.524
2.353	6.606
2.344	6.565
2.319	6.428
2.281	6.181
2.245	5.825
2.220	5.779
2.205	5.623
2.198	5.532
2.195	5.504
2.194	5.509
2.189	5.545
2.170	5.477
2.137	5.276
2.106	5.052
2.085	4.864
2.070	4.782
2.062	4.768
2.058	4.768
2.057	4.741
2.053	4.745
2.036	4.718
2.004	4.572
1.963	4.371
1.928	4.206
1.906	4.074
1.894	4.037
1.886	4.019
1.882	4.010
1.879	3.982
1.866	3.886
1.836	3.694
1.793	3.461
1.752	3.237
1.722	3.132
1.702	3.050
1.692	2.999
1.687	2.872
1.683	2.967
1.672	2.940

TABLE 5.- Continued

(dd) Continued

y, cm	p, N/cm ²
1.645	2.062
1.600	2.725
1.555	2.579
1.515	2.432
1.489	2.364
1.475	2.327
1.468	2.309
1.464	2.286
1.456	2.259
1.434	2.208
1.392	2.108
1.344	1.980
1.301	1.866
1.269	1.806
1.251	1.779
1.242	1.760
1.238	1.742
1.231	1.696
1.215	1.664
1.181	1.600
1.131	1.518
1.084	1.440
1.050	1.372
1.029	1.335
1.018	1.312
1.014	1.294
1.009	1.308
.994	1.299
.964	1.267
.917	1.198
.866	1.125
.826	1.052
.799	1.011
.783	.979
.776	.970
.772	.947
.762	.942
.741	.906
.699	.869
.648	.796
.603	.746
.570	.700
.551	.686
.542	.672
.538	.682
.532	.672
.514	.668
.478	.627
.425	.581
.375	.517
.340	.467

TABLE 5.- Continued

(dd) Concluded

y, cm	p, N/cm ²
.318	.426
.308	.407
.303	.394
.300	.394
.285	.375
.254	.343
.198	.293
.142	.275
.101	.266
.077	.275

TABLE 5.- Continued

(ee) Pitot profiles: Case 28; station 8; test 39; run 48;
 $p_{t,1} = 13\ 651.7$ kPa; $T_t = 302.5$ K; $T_w/T_t = 0.985$

y , cm	p , N/cm ²
<u>2.214</u>	<u>5.037</u>
<u>2.050</u>	<u>4.223</u>
<u>1.856</u>	<u>3.455</u>
<u>1.664</u>	<u>2.748</u>
<u>1.452</u>	<u>2.201</u>
<u>1.239</u>	<u>1.686</u>
<u>.977</u>	<u>1.268</u>
<u>.709</u>	<u>.922</u>
<u>.445</u>	<u>.630</u>
<u>.186</u>	<u>.399</u>
<u>.112</u>	<u>.335</u>

(ff) Pitot profiles: Case 28; station 8; test 39; run 49;
 $p_{t,1} = 13\ 651.7$ kPa; $T_t = 302.5$ K; $T_w/T_t = 0.985$

y , cm	p , N/cm ²
<u>4.866</u>	<u>14.059</u>
<u>4.614</u>	<u>14.055</u>
<u>4.409</u>	<u>13.863</u>
<u>4.161</u>	<u>13.748</u>
<u>3.861</u>	<u>13.439</u>
<u>3.638</u>	<u>13.137</u>
<u>3.301</u>	<u>11.819</u>
<u>3.075</u>	<u>10.738</u>
<u>2.826</u>	<u>8.990</u>
<u>2.551</u>	<u>7.036</u>
<u>2.168</u>	<u>4.690</u>
<u>2.049</u>	<u>4.136</u>
<u>1.527</u>	<u>2.304</u>
<u>1.280</u>	<u>1.747</u>
<u>1.024</u>	<u>1.265</u>
<u>.767</u>	<u>.948</u>
<u>.516</u>	<u>.662</u>
<u>.327</u>	<u>.525</u>

TABLE 5.- Continued

(gg) Pitot profiles: Case 29; station 1; test 42; run 15;
 $P_{t,1} = 13\ 824.1$ kPa; $T_t = 303.5$ K; $T_w/T_t = 0.495$

Y, cm	p, N/cm ²
1.708	12.653
1.679	12.649
1.661	12.667
1.654	12.685
1.649	12.694
1.649	12.703
1.649	12.716
1.649	12.721
1.641	12.712
1.606	12.649
1.554	12.518
1.500	12.382
1.467	12.328
1.445	12.310
1.434	12.301
1.431	12.287
1.429	12.278
1.430	12.228
1.429	12.206
1.410	12.174
1.368	12.115
1.309	12.061
1.248	12.030
1.203	12.025
1.175	12.066
1.155	12.084
1.144	12.079
1.137	12.066
1.132	12.048
1.129	12.057
1.123	12.057
1.098	12.021
1.050	11.948
.994	11.867
.944	11.772
.909	11.700
.884	11.636
.869	11.623
.860	11.627
.852	11.641
.849	11.650
.845	11.654
.829	11.609
.792	11.501
.741	11.252
.689	10.999
.648	10.719
.620	10.466
.601	10.222
.589	10.132
.582	10.091
.578	9.996
.576	9.946
.565	9.770
.535	9.133

TABLE 5.- Continued

(gg) Concluded

y, cm	p, N/cm ²
.483	7.836
.427	5.911
.379	4.185
.345	2.838
.324	1.984
.312	1.550
.306	1.315
.299	1.221
.296	1.202
.282	1.139
.248	.949
.192	.692
.134	.470
.084	.294
.048	.195
.024	.136
.007	.109

TABLE 5.- Continued

(hh) Pitot profiles: Case 30; station 2; test 39; run 27;
 $p_{t,1} = 13\ 720.7$ kPa; $T_t = 307.8$ K; $T_w/T_t = 0.542$

y, cm	p, N/cm ²
2.013	12.811
1.780	12.531
1.646	12.504
1.517	12.274
1.427	12.207
1.284	12.058
1.166	11.920
1.041	11.471
.902	11.124
.828	10.464
.661	9.071
.599	6.952
.347	.814
.131	.120
.075	.105

(ii) Pitot profiles: Case 31; station 3; test 39; run 33;
 $p_{t,1} = 13\ 706.9$ kPa; $T_t = 302.2$ K; $T_w/T_t = 0.524$

y, cm	p, N/cm ²
2.035	13.565
1.798	13.558
1.596	13.306
1.381	12.934
1.169	11.836
.949	9.139
.753	5.150
.565	2.613
.378	1.461
.170	.602

TABLE 5:- Continued

(jj) Pitot profiles: Case 32; station 4; test 42; run 12;
 $P_{t,1} = 13\ 762.0$ kPa; $T_t = 303\ 3$ K; $T_w/T_t = 0\ 465$

y , cm	p , N/cm ²
2.438	13.483
2.431	13.493
2.429	13.529
2.426	13.552
2.410	13.556
2.377	13.556
2.327	13.565
2.281	13.552
2.250	13.524
2.232	13.497
2.223	13.497
2.218	13.465
2.215	13.461
2.200	13.465
2.168	13.470
2.119	13.470
2.066	13.434
2.023	13.379
1.994	13.306
1.978	13.261
1.970	13.234
1.965	13.220
1.952	13.243
1.922	13.229
1.872	13.207
1.810	13.138
1.756	13.039
1.720	12.952
1.698	12.907
1.687	12.866
1.680	12.812
1.672	12.739
1.648	12.680
1.603	12.530
1.543	12.271
1.484	11.917
1.439	11.609
1.411	11.286
1.396	11.114
1.389	11.046
1.384	10.982
1.369	10.855
1.336	10.615
1.285	10.138
1.225	9.448
1.176	8.835
1.144	8.268
1.127	7.828
1.120	7.564
1.116	7.383
1.106	7.251
1.080	6.983
1.031	6.611
.975	6.057
.922	5.467

TABLE 5.- Continued

(jj) Concluded

y, cm	p, N/cm ²
.885	4.972
.864	4.632
.853	4.441
.848	4.346
.841	4.287
.823	4.223
.787	4.024
.734	3.711
.680	3.343
.640	3.007
.614	2.780
.601	2.676
.596	2.603
.592	2.567
.582	2.526
.556	2.426
.512	2.263
.459	2.058
.415	1.863
.386	1.727
.372	1.632
.366	1.582
.363	1.550
.354	1.523
.335	1.468
.295	1.386
.245	1.259
.195	1.100
.159	.960
.139	.860
.129	.787
.125	.751
.121	.719
.106	.692
.071	.692
.024	.737

TABLE 5i.- Continued

(kk) Pitot profiles: Case 33; station 5; test 42; run 9;
 $P_{t,1} = 13\ 789.6$ kPa; $T_t = 312.2$ K; $T_w/T_t = 0.488$

y, cm	p, N/cm ²
3.333	13.791
3.307	13.787
3.263	13.801
3.207	13.796
3.157	13.782
3.124	13.778
3.104	13.778
3.095	13.773
3.089	13.773
3.081	13.787
3.061	13.801
3.021	13.859
2.966	13.846
2.912	13.819
2.873	13.819
2.848	13.819
2.833	13.801
2.827	13.791
2.822	13.796
2.805	13.801
2.770	13.814
2.716	13.791
2.655	13.778
2.601	13.764
2.568	13.719
2.549	13.683
2.538	13.678
2.531	13.674
2.517	13.665
2.486	13.628
2.434	13.583
2.368	13.497
2.309	13.393
2.264	13.311
2.238	13.252
2.225	13.257
2.217	13.212
2.207	13.157
2.180	13.085
2.137	12.885
2.074	12.564
2.010	12.188
1.962	11.934
1.931	11.762
1.915	11.662
1.907	11.640
1.900	11.667
1.880	11.599
1.843	11.318
1.785	10.874
1.717	10.235
1.658	9.569
1.619	9.044
1.596	8.754
1.582	8.772

TABLE 5.- Continued

(kk) Concluded

y, cm	p, N/cm ²
1.576	8.731
1.563	8.650
1.532	8.328
1.482	7.789
1.417	7.132
1.360	6.534
1.319	6.167
1.296	5.991
1.282	5.923
1.277	5.877
1.267	5.796
1.242	5.592
1.199	5.211
1.138	4.754
1.076	4.292
1.031	3.920
1.004	3.712
.989	3.599
.983	3.553
.975	3.553
.958	3.490
.919	3.327
.863	3.041
.799	2.706
.748	2.462
.715	2.308
.698	2.212
.689	2.181
.684	2.167
.671	2.131
.639	2.045
.587	1.886
.521	1.682
.460	1.483
.419	1.361
.396	1.275
.386	1.252
.381	1.257
.372	1.243
.351	1.193
.309	1.098
.248	.976
.189	.844
.148	.740
.121	.668
.107	.640
.102	.631
.097	.613
.077	.577
.032	.505

TABLE 5b- Continued

(11) Pitot profiles: Case 34; station 6; test 39; run 45;
 $p_{t,1} = 13\ 686.2\ \text{kPa}$; $T_t = 306.4\ \text{K}$; $T_w/T_t = 0.558$

$y, \text{ cm}$	$p, \text{ N/cm}^2$
<u>1.930</u>	<u>9.545</u>
<u>1.721</u>	<u>7.884</u>
<u>1.490</u>	<u>5.727</u>
<u>1.240</u>	<u>4.050</u>
<u>.973</u>	<u>2.703</u>
<u>.705</u>	<u>1.684</u>
<u>.447</u>	<u>1.047</u>
<u>.175</u>	<u>.552</u>
<u>.111</u>	<u>.483</u>

(mm) Pitot profiles: Case 34; station 6; test 39; run 46;
 $p_{t,1} = 13\ 686.2\ \text{kPa}$; $T_t = 306.4\ \text{K}$; $T_w/T_t = 0.558$

$y, \text{ cm}$	$p, \text{ N/cm}^2$
<u>4.245</u>	<u>14.052</u>
<u>3.930</u>	<u>13.994</u>
<u>3.744</u>	<u>13.965</u>
<u>3.474</u>	<u>13.874</u>
<u>3.202</u>	<u>13.766</u>
<u>3.008</u>	<u>13.648</u>
<u>2.671</u>	<u>13.525</u>
<u>2.145</u>	<u>12.213</u>
<u>1.624</u>	<u>7.732</u>
<u>1.123</u>	<u>3.665</u>
<u>.625</u>	<u>1.541</u>
<u>.139</u>	<u>.513</u>
<u>.113</u>	<u>.476</u>

TABLE 5.- Continued

(nn) Pitot profiles: Case 35; station 7; test 42; run 6;
 $P_{t,1} = 13\ 706.9$ kPa; $T_t = 311.1$ K; $T_w/T_t = 0.459$

Y, cm	p, N/cm ²
4.909	13.880
4.885	13.907
4.870	13.948
4.855	13.985
4.833	13.976
4.794	13.958
4.740	13.944
4.674	13.948
4.612	13.871
4.566	13.990
4.533	14.012
4.511	14.031
4.495	14.012
4.473	13.880
4.438	13.971
4.386	13.948
4.323	13.967
4.256	13.967
4.202	13.948
4.162	13.967
4.138	13.962
4.122	13.953
4.105	13.962
4.075	13.839
4.030	13.889
3.969	13.830
3.900	13.816
3.840	13.794
3.797	13.771
3.769	13.734
3.752	13.739
3.737	13.743
3.712	13.789
3.673	13.766
3.616	13.707
3.550	13.666
3.487	13.602
3.436	13.552
3.403	13.516
3.385	13.497
3.369	13.502
3.349	13.497
3.315	13.452
3.263	13.265
3.198	13.224
3.132	13.078
3.077	12.937
3.038	12.805
3.016	12.805
3.001	12.846
2.983	12.855
2.954	12.750
2.908	12.558
2.846	12.253
2.778	11.888
2.716	11.519

TABLE 5.- Continued

(mm) Continued

y, cm	p, N/cm ²
2.673	11.269
2.647	11.123
2.633	11.091
2.619	11.082
2.597	10.886
2.558	10.617
2.502	10.198
2.433	9.655
2.367	9.181
2.317	8.799
2.286	8.548
2.268	8.384
2.257	8.270
2.239	8.338
2.206	8.106
2.156	7.645
2.093	7.099
2.024	6.565
1.969	6.064
1.930	5.754
1.910	5.581
1.897	5.531
1.883	5.472
1.857	5.262
1.813	4.966
1.752	4.665
1.685	4.300
1.625	3.927
1.581	3.676
1.555	3.539
1.543	3.484
1.532	3.475
1.510	3.412
1.471	3.257
1.415	3.033
1.347	2.783
1.282	2.546
1.233	2.377
1.203	2.268
1.186	2.236
1.177	2.217
1.161	2.163
1.130	2.076
1.079	1.958
1.013	1.821
.945	1.643
.890	1.502
.854	1.415
.835	1.379
.826	1.379
.813	1.365
.787	1.333
.742	1.260
.681	1.146
.613	1.028
.551	.909
.509	.859

TABLE 5.- Continued

(nn) Concluded

y, cm	p, N/cm ²
.486	.823
.473	.805
.463	.805
.444	.786
.406	.741
.350	.672
.282	.581
.207	.508
.149	.486

TABLE 5.- Continued

(oo) Pitot profiles: Case 36; station 8; test 39; run 56;
 $P_{t,1} = 13\ 582.8$ kPa; $T_t = 309.5$ K; $T_w/T_t = 0.501$

y , cm	p , N/cm ²
<u>2.070</u>	<u>5.856</u>
<u>1.904</u>	<u>4.862</u>
<u>1.739</u>	<u>4.044</u>
<u>1.582</u>	<u>3.409</u>
<u>1.371</u>	<u>2.628</u>
<u>1.156</u>	<u>2.029</u>
<u>.931</u>	<u>1.559</u>
<u>.663</u>	<u>1.118</u>
<u>.418</u>	<u>.827</u>
<u>.147</u>	<u>.531</u>
<u>.112</u>	<u>.493</u>

(pp) Pitot profiles: Case 36; station 8; test 39; run 60;
 $P_{t,1} = 13\ 582.8$ kPa; $T_t = 309.5$ K; $T_w/T_t = 0.501$

y , cm	p , N/cm ²
<u>4.400</u>	<u>14.777</u>
<u>4.353</u>	<u>14.777</u>
<u>4.017</u>	<u>14.679</u>
<u>3.973</u>	<u>14.675</u>
<u>3.894</u>	<u>14.650</u>
<u>3.719</u>	<u>14.588</u>
<u>3.542</u>	<u>14.440</u>
<u>3.463</u>	<u>14.420</u>
<u>3.384</u>	<u>14.327</u>
<u>3.203</u>	<u>14.302</u>
<u>3.080</u>	<u>13.610</u>
<u>2.962</u>	<u>13.132</u>
<u>2.754</u>	<u>12.047</u>
<u>2.472</u>	<u>9.548</u>
<u>1.991</u>	<u>5.783</u>
<u>1.521</u>	<u>3.431</u>
<u>1.210</u>	<u>3.216</u>
<u>1.039</u>	<u>1.811</u>
<u>.575</u>	<u>.990</u>
<u>.347</u>	<u>.700</u>

TABLE 5.- Continued

(qq) Pitot profiles: Case 37; station 1; test 42; run 14;
 $P_{t,1} = 13\ 824.1$ kPa; $T_t = 308.3$ K; $T_w/T_t = 0.331$

y, cm	p, N/cm ²
2.237	13.060
2.238	13.110
2.236	13.141
2.223	13.123
2.175	13.060
2.107	12.960
2.044	12.879
2.002	12.861
1.978	12.856
1.968	12.879
1.964	12.897
1.964	12.915
1.963	12.924
1.964	12.929
1.963	12.929
1.948	12.920
1.907	12.893
1.857	12.843
1.815	12.802
1.792	12.802
1.779	12.780
1.776	12.757
1.773	12.730
1.774	12.730
1.774	12.716
1.775	12.685
1.765	12.653
1.733	12.622
1.683	12.572
1.638	12.540
1.608	12.509
1.591	12.509
1.585	12.531
1.584	12.576
1.584	12.576
1.584	12.603
1.584	12.622
1.580	12.608
1.547	12.518
1.494	12.418
1.438	12.346
1.398	12.287
1.369	12.206
1.357	12.165
1.351	12.138
1.350	12.133
1.350	12.133
1.350	12.115
1.339	12.075
1.300	12.034
1.243	12.025
1.180	12.030
1.126	12.030
1.087	12.039
1.058	12.016
1.039	11.971

TABLE 5.- Continued

(qq) Concluded

y, cm	p, N/cm ²
1.026	11.921
1.017	11.903
1.011	11.889
1.005	11.885
.983	11.853
.939	11.804
.882	11.704
.836	11.573
.797	11.433
.771	11.338
.752	11.284
.739	11.243
.727	11.221
.720	11.225
.714	11.216
.697	11.108
.657	10.733
.603	10.001
.552	9.137
.512	8.292
.483	7.475
.462	6.648
.446	5.825
.435	5.116
.425	4.457
.419	4.036
.403	3.489
.368	2.635
.313	1.745
.256	1.035
.210	.583
.179	.330
.159	.208
.143	.163
.129	.141

TABLE 5.- Continued

(rr) Pitot profiles: Case 38; station 2; test 39; run 26;
 $P_{t,1} = 13\ 755.1\ \text{kPa}$; $T_t = 306.7\ \text{K}$; $T_w/T_t = 0.362$

y, cm	$p, \text{N/cm}^2$
2.058	13.010
1.833	12.793
1.564	12.450
1.340	12.303
1.064	11.823
.965	11.691
.835	11.250
.697	10.238
.587	8.740
.541	8.013
.491	6.707
.436	5.004
.397	3.489
.371	2.518
.357	1.780
.168	.552
.103	.166

(ss) Pitot profiles: Case 39; station 3; test 39; run 32;
 $P_{t,1} = 13\ 741.3\ \text{kPa}$; $T_t = 308.3\ \text{K}$; $T_w/T_t = 0.306$

y, cm	$p, \text{N/cm}^2$
1.886	13.300
1.665	13.291
1.646	13.179
1.397	12.929
1.167	12.129
1.147	11.886
1.068	11.251
.897	7.703
.767	6.288
.630	3.180
.405	1.492
.146	.582

TABLE 5.- Continued

(tt) Pitot profiles: Case 40; station 4; test 42; run 11;
 $P_{t,1} = 13\ 603.4$ kPa; $T_t = 305.8$ K; $T_w/T_t = 0.376$

y , cm	p , N/cm ²
3.244	13.673
3.211	13.701
3.191	13.687
3.180	13.719
3.172	13.728
3.151	13.728
3.121	13.714
3.067	13.747
2.999	13.769
2.934	13.806
2.886	13.825
2.857	13.820
2.838	13.797
2.828	13.774
2.814	13.756
2.789	13.769
2.743	13.774
2.681	13.774
2.615	13.792
2.563	13.806
2.526	13.825
2.505	13.811
2.493	13.797
2.482	13.769
2.457	13.751
2.415	13.751
2.354	13.751
2.285	13.733
2.225	13.696
2.183	13.687
2.157	13.650
2.144	13.623
2.133	13.604
2.117	13.590
2.085	13.577
2.034	13.577
1.969	13.549
1.907	13.508
1.858	13.434
1.827	13.402
1.810	13.379
1.802	13.352
1.789	13.310
1.764	13.237
1.717	13.173
1.662	13.145
1.596	13.094
1.542	12.989
1.507	12.888
1.487	12.810
1.478	12.736
1.470	12.690
1.451	12.598
1.415	12.401
1.360	12.015

TABLE 5.- Continued

(tt) Concluded

y, cm	p, N/cm ²
1.295	11.510
1.238	10.968
1.199	10.481
1.176	10.091
1.165	9.825
1.158	9.682
1.145	9.581
1.115	9.246
1.068	8.663
1.007	7.887
.949	7.028
.904	6.307
.876	5.894
.861	5.637
.854	5.444
.844	5.269
.825	5.104
.788	4.865
.736	4.475
.676	3.997
.626	3.575
.592	3.258
.573	3.042
.563	2.918
.556	2.854
.543	2.776
.516	2.647
.470	2.450
.415	2.183
.362	1.931
.324	1.742
.302	1.614
.291	1.531
.286	1.476
.276	1.435
.252	1.403
.213	1.283
.155	1.132
.092	1.022
.040	.966
.008	.948

TABLE 5.- Continued

(uu) Pitot profiles: Case 41; station 5; test 42; run 8;
 $P_{t,1} = 13\,789.6$ kPa; $T_t = 310.6$ K; $T_w/T_t = 0.364$

y , cm	p , N/cm ²
3.259	14.045
3.231	14.072
3.185	14.054
3.124	14.036
3.072	13.999
3.037	13.945
3.017	13.950
3.008	13.990
3.004	13.995
2.998	14.018
2.983	14.036
2.949	14.036
2.899	13.995
2.845	13.954
2.808	13.936
2.786	13.954
2.773	13.963
2.767	13.945
2.765	13.936
2.754	13.900
2.729	13.877
2.683	13.864
2.626	13.845
2.576	13.791
2.543	13.746
2.523	13.755
2.511	13.814
2.505	13.836
2.491	13.855
2.458	13.855
2.405	13.832
2.337	13.773
2.274	13.728
2.227	13.696
2.199	13.682
2.184	13.673
2.177	13.642
2.166	13.610
2.145	13.574
2.105	13.474
2.046	13.324
1.984	13.093
1.934	12.858
1.903	12.668
1.885	12.577
1.876	12.604
1.869	12.631
1.851	12.595
1.814	12.414
1.759	12.006
1.694	11.476
1.636	10.964
1.597	10.602
1.574	10.403
1.563	10.326

TABLE 5.- Continued

(uu) Concluded

y, cm	p, N/cm ²
1.557	10.276
1.543	10.126
1.511	9.832
1.458	9.392
1.393	8.758
1.332	8.051
1.287	7.490
1.262	7.100
1.247	6.896
1.242	6.815
1.233	6.810
1.210	6.620
1.164	6.194
1.103	5.592
1.039	4.994
.990	4.568
.961	4.282
.947	4.115
.940	4.060
.935	4.065
.919	4.056
.884	3.902
.831	3.562
.774	3.177
.725	2.873
.691	2.715
.675	2.602
.667	2.593
.664	2.570
.655	2.520
.631	2.420
.587	2.239
.527	1.995
.470	1.741
.427	1.569
.403	1.478
.392	1.442
.387	1.442
.381	1.433
.365	1.392
.328	1.311
.274	1.166
.212	1.002
.163	.871
.132	.776
.116	.726
.109	.708
.104	.713
.093	.685
.064	.631
.009	.586

TABLE 5.- Continued

(vv) Pitot profiles: Case 42; station 6; test 39; run 43;
 $P_{t,1} = 13\ 651.7$ kPa; $T_t = 314.7$ K; $T_w/T_t = 0.358$

y , cm	p , N/cm ²
<u>2.023</u>	<u>11.203</u>
<u>1.817</u>	<u>9.509</u>
<u>1.584</u>	<u>7.244</u>
<u>1.324</u>	<u>4.939</u>
<u>1.084</u>	<u>3.358</u>
<u>.835</u>	<u>2.223</u>
<u>.612</u>	<u>1.497</u>
<u>.405</u>	<u>.984</u>
<u>.191</u>	<u>.647</u>
<u>.047</u>	<u>.421</u>

(ww) Pitot profiles: Case 42; station 6; test 39; run 44;
 $P_{t,1} = 13\ 651.7$ kPa; $T_t = 314.7$ K; $T_w/T_t = 0.358$

y , cm	p , N/cm ²
<u>4.535</u>	<u>13.760</u>
<u>4.355</u>	<u>13.787</u>
<u>3.979</u>	<u>13.852</u>
<u>3.696</u>	<u>13.744</u>
<u>3.350</u>	<u>13.671</u>
<u>3.093</u>	<u>13.555</u>
<u>2.764</u>	<u>13.470</u>
<u>2.362</u>	<u>13.042</u>
<u>2.196</u>	<u>12.852</u>
<u>1.613</u>	<u>9.067</u>
<u>1.032</u>	<u>3.723</u>
<u>.453</u>	<u>1.333</u>
<u>.098</u>	<u>.669</u>

TABLE 5,- Continued

(xx) Pitot profiles: Case 43; station 7; test 42; run 5;
 $P_{t,1} = 13\ 693.1$ kPa; $T_t = 311.1$ K; $T_w/T_t = 0.330$

y, cm	p, N/cm ²
5.061	13.780
5.010	13.839
4.952	13.880
4.903	13.876
4.869	13.867
4.848	13.862
4.835	13.876
4.827	13.885
4.810	13.894
4.778	13.894
4.730	13.871
4.669	13.858
4.610	13.862
4.563	13.876
4.530	13.912
4.508	13.949
4.495	13.944
4.478	13.953
4.449	13.985
4.400	14.017
4.339	14.008
4.269	13.985
4.210	13.990
4.168	14.026
4.141	14.063
4.123	14.049
4.105	14.035
4.075	14.045
4.028	14.058
3.967	14.040
3.897	14.031
3.831	14.017
3.781	14.013
3.750	14.022
3.730	14.026
3.713	14.022
3.689	14.022
3.647	14.022
3.591	13.990
3.521	13.935
3.452	13.876
3.397	13.835
3.360	13.839
3.336	13.871
3.322	13.903
3.301	13.899
3.267	13.826
3.215	13.757
3.150	13.666
3.077	13.588
3.018	13.552
2.975	13.502
2.949	13.470
2.933	13.465
2.915	13.456
2.885	13.424

TABLE 5.- Continued

(xx) Continued

y, cm	p, N/cm ²
2.841	13.833
2.778	13.187
2.707	12.991
2.640	12.808
2.590	12.653
2.558	12.521
2.540	12.462
2.524	12.434
2.503	12.352
2.463	12.147
2.407	11.786
2.334	11.344
2.264	10.865
2.208	10.377
2.171	10.135
2.153	9.943
2.139	9.775
2.120	9.601
2.088	9.305
2.036	8.885
1.970	8.224
1.898	7.717
1.837	7.233
1.795	6.800
1.772	6.663
1.757	6.595
1.745	6.508
1.716	6.275
1.671	5.997
1.610	5.587
1.539	5.089
1.471	4.624
1.423	4.268
1.394	4.076
1.379	3.899
1.366	3.926
1.346	3.830
1.306	3.670
1.251	3.420
1.181	3.114
1.112	2.804
1.058	2.585
1.024	2.461
1.004	2.402
.993	2.370
.973	2.347
.940	2.252
.890	2.101
.826	1.909
.753	1.732
.692	1.599
.651	1.508
.630	1.449
.618	1.408
.605	1.380
.579	1.357
.538	1.275

TABLE 5.- Continued

(xx) Concluded

y, cm	p, N/cm ²
.475	1.180
.406	1.065
.340	.956
.293	.869
.265	.824
.251	.801
.240	.792
.221	.769
.185	.723
.126	.655
.046	.614

TABLE 5.- Concluded

(yy) Pitot profiles: Case 44; station 8; test 39; run 54;
 $P_{t,1} = 13\ 669.0$ kPa; $T_t = 308.1$ K; $T_w/T_t = 0.334$

y , cm	p , N/cm ²
<u>2.206</u>	<u>8.205</u>
<u>1.978</u>	<u>6.574</u>
<u>1.749</u>	<u>5.172</u>
<u>1.509</u>	<u>3.829</u>
<u>1.256</u>	<u>2.770</u>
<u>.987</u>	<u>1.982</u>
<u>.717</u>	<u>1.447</u>
<u>.434</u>	<u>1.008</u>
<u>.172</u>	<u>.671</u>
<u>.112</u>	<u>.615</u>

(zz) Pitot profiles: Case 44; station 8; test 39; run 55;
 $P_{t,1} = 13\ 669.0$ kPa; $T_t = 308.1$ K; $T_w/T_t = 0.334$

y , cm	p , N/cm ²
<u>4.494</u>	<u>13.924</u>
<u>4.189</u>	<u>13.793</u>
<u>3.960</u>	<u>13.804</u>
<u>3.647</u>	<u>13.749</u>
<u>3.350</u>	<u>13.655</u>
<u>3.199</u>	<u>13.580</u>
<u>2.904</u>	<u>13.225</u>
<u>2.715</u>	<u>12.765</u>
<u>2.348</u>	<u>10.501</u>
<u>2.093</u>	<u>8.111</u>
<u>1.868</u>	<u>6.357</u>
<u>1.472</u>	<u>3.981</u>
<u>.845</u>	<u>1.850</u>
<u>.233</u>	<u>.818</u>
<u>.112</u>	<u>.676</u>

TABLE 6.- TOTAL TEMPERATURE SURVEY DATA

(a) Data summary

Case	Station	Run	Pt,1, kPa	Tt, K (a)	Tw/Tt
Model 1, test 11					
1	4	83	13 238.0	312.8	
2	↓	84	10 755.9	324.7	
3		85	7 929.0	325.8	
4		86	5 377.9	329.7	
Model 2, test 40					
5	1	100	13 720.7	323.3	0.898
6	2	59	13 582.8	321.1	.924
7	3	73	13 562.1	342.2	.875
8	4	96	13 513.8	321.7	.911
9	5	95	13 582.8	320.0	.918
10	6	76	13 410.4	326.1	.908
11	7	90	13 479.3	317.2	.938
12	8	82	13 224.2	323.3	.912
13	1	102	13 424.2	305.6	.504
14	2	63	13 569.0	310.3	.547
15	3	70	13 617.2	315.0	.575
16	4	98	13 575.9	302.8	.476
17	5	94	13 637.9	315.6	.505
18	6	81	13 479.3	312.2	.489
19	7	92	13 341.4	319.4	.469
20	8	87	13 513.8	330.6	.449
21	2	62	13 651.8	338.3	.393
22	3	69	13 631.0	323.3	.502
23	4	97	13 631.0	312.2	.368
24	5	93	13 651.7	327.8	.386
25	6	80	13 341.4	322.2	.375
26	7	91	13 341.4	327.2	.383
27	8	86	13 444.9	332.2	.333

^aMeasured in free stream. No real gas correction required.

TABLE 6.- Continued

(b) Total-temperature profiles: Case 1; station 4; run 83;
 $P_{t,1} = 13\ 238.0$ kPa; $T_t = 312.8$ K

Y, cm	$T_t/T_{t,e}$	
0.2195	0.8270	
0.2606	0.8440	
0.3200	0.8610	
0.4069	0.8760	
0.6218	0.8880	
0.7178	0.8910	
0.7910	0.8940	
0.9235	0.8990	
1.0150	0.9020	
1.1384	0.9040	
1.2893	0.9060	
1.3853	0.9070	
<u>1.4493</u>	<u>0.9080</u>	↑ Increasing wall pressure
1.5179	0.9090	
1.5911	0.9100	
1.7145	0.9100	
1.8562	0.9120	
1.9385	0.9120	
1.9980	0.9120	
2.0620	0.9110	
2.1168	0.9120	
2.2037	0.9150	
2.3271	0.9210	
2.3683	0.9240	
2.4826	0.9310	
2.5466	0.9340	
2.5832	0.9370	
2.6380	0.9400	
2.6883	0.9450	
2.7615	0.9510	
2.9032	0.9650	
2.9947	0.9730	
3.0998	0.9810	
3.1913	0.9880	
3.3193	0.9950	
3.5387	0.9980	
3.6805	0.9980	
3.9228	0.9990	
4.1697	0.9990	
4.3205	0.9990	
4.6863	1.0010	

TABLE 6.- Continued

(c) Total-temperature profiles: Case 2; station 4; run 84;
 $P_{t,1} = 10\,755.9$ kPa; $T_t = 324.7$ K

y , cm	$T_t/T_{t,e}$	
0.2560	0.8600	
0.3109	0.8740	
0.3566	0.8850	
0.4801	0.8920	
0.6447	0.8980	
0.7269	0.9010	
0.8412	0.9030	
0.9510	0.9050	
1.0150	0.9070	
1.1521	0.9060	
1.2847	0.9050	
<u>1.4310</u>	<u>0.9030</u>	
1.4996	0.9030	
1.5636	0.9030	
1.6231	0.9020	
1.7648	0.9010	
1.9294	0.8980	
2.0483	0.8980	
2.1306	0.9000	
2.1763	0.9010	
2.2311	0.9020	
2.3546	0.9060	
2.4597	0.9130	
2.5786	0.9210	
2.6609	0.9260	
2.7341	0.9300	
2.7981	0.9350	
2.8438	0.9390	
2.8804	0.9430	
2.9764	0.9530	
3.0678	0.9620	
3.1455	0.9690	
3.2324	0.9750	
3.3238	0.9820	
3.4244	0.9870	
3.5250	0.9910	
3.6165	0.9950	
3.7902	0.9980	
3.8222	0.9990	
3.8771	0.9990	
3.9411	0.9990	
4.0737	0.9990	
4.3343	1.0000	
4.3983	1.0000	
4.4714	1.0000	
4.6634	1.0000	
4.9378	1.0000	

↑ Increasing wall pressure

TABLE 6.- Continued

(d) Total-temperature profiles: Case 3; station 4; run 85;
 $P_{t,1} = 7929.0$ kPa; $T_t = 3254.8$ K

Y , cm	$T_t/T_{t,e}$	
0.1920	0.8180	
0.2332	0.8270	
0.2880	0.8500	
0.3978	0.8640	
0.5349	0.8760	
0.6447	0.8870	
0.7315	0.8920	
0.8641	0.8980	
1.0104	0.9020	
1.0790	0.9050	
1.1384	0.9050	
1.1979	0.9060	↑ Increasing wall pressure
1.3076	0.9060	
1.4082	0.9060	
1.5133	0.9050	
1.6048	0.9040	
1.6368	0.9040	
1.7328	0.9030	
1.8379	0.9010	
1.9477	0.9010	
2.0163	0.9000	
2.0985	0.9010	
2.1717	0.9020	
2.2357	0.9020	
2.2906	0.9030	
2.3592	0.9040	
2.4780	0.9090	
2.6060	0.9150	
2.6700	0.9190	
2.7341	0.9240	
2.8026	0.9280	
2.8484	0.9310	
2.9078	0.9340	
2.9398	0.9370	
3.0221	0.9440	
3.1272	0.9510	
3.2278	0.9560	
3.2736	0.9590	
3.3376	0.9630	
3.3879	0.9670	
3.4381	0.9700	
3.4701	0.9720	
3.5342	0.9790	
3.5982	0.9840	
3.7262	0.9910	
3.7125	0.9950	
3.9091	0.9970	
3.9456	0.9990	
4.0096	1.0000	
4.0599	1.0000	
4.1971	1.0000	
4.4531	1.0000	

TABLE 6.- Continued

(e) Total-temperature profiles: Case 4; station 4; run 86;
 $P_{t,1} = 5377.9$ kPa; $T_t = 329.7$ K

y , cm	$T_t/T_{t,e}$
0.3658	0.6690
0.4166	0.8110
0.4724	0.8520
0.5486	0.8690
0.6553	0.8830
0.7823	0.8890
0.9500	0.8930
0.9957	0.8960
1.0820	0.8990
1.1989	0.8990
1.3513	0.8970
1.5189	0.8960
<u>1.6002</u>	<u>0.8960</u>
1.7323	0.8950
1.8491	0.8950
1.9812	0.8940
2.1184	0.8950
2.1692	0.8960
2.2708	0.8980
2.3622	0.9000
2.4282	0.9020
2.4994	0.9040
2.6314	0.9110
2.7178	0.9150
2.7838	0.9180
2.8296	0.9210
2.8753	0.9230
2.9515	0.9290
3.0074	0.9320
3.0582	0.9350
3.0886	0.9370
3.1750	0.9420
3.2766	0.9500
3.3782	0.9580
3.4493	0.9630
3.5154	0.9680
3.5458	0.9700
3.5865	0.9730
3.6525	0.9780
3.7287	0.9820
3.8456	0.9870
3.9014	0.9890
3.9675	0.9920
4.0437	0.9940
4.1046	0.9960
4.1453	0.9970
4.2012	0.9970
4.2570	0.9970
4.3332	0.9980
4.4653	0.9990
4.6431	1.0000
4.7650	1.0000
4.8209	1.0000

↑ Increasing wall pressure

TABLE 6.- Continued

(f) Total temperature profiles: Case 5; station 1; test 40; run 100;
 $P_{t,1} = 13\ 720.7$ kPa; $T_t = 323.3$ K; $T_w/T_t = 0.898$

y, cm	$T_t/T_{t,e}$	F_T
3.6679555	1.008881	1.089655
3.6207822	1.007300	1.075136
3.5715277	1.006842	1.071645
3.5326791	1.005408	1.057520
3.5090925	1.006206	1.067095
3.4959117	1.005024	1.054976
3.4924431	1.005370	1.059101
3.4903619	1.004961	1.054400
3.4910557	1.003954	1.043187
3.4917494	1.002370	1.025908
3.4924431	1.001911	1.021004
3.4931368	1.002959	1.033158
3.4806498	1.002836	1.032442
3.4494322	1.004713	1.054878
3.4001777	1.004247	1.050434
3.3446797	1.004706	1.057112
3.3058311	1.003316	1.041015
3.2822445	1.003164	1.039743
3.2697574	1.001602	1.020382
3.2655951	1.001747	1.022438
3.2655951	1.002162	1.028071
3.2635139	1.001757	1.023089
3.2655951	1.002350	1.031209
3.2662888	1.002303	1.030889
3.2649014	1.002275	1.030684
3.2524143	1.001020	1.013867
3.2191155	1.000085	1.001176
3.1677799	1.001239	1.017363
3.1143631	.999641	.994919
3.0727396	.999459	.992300
3.0491530	.999626	.994637
3.0387471	.998508	.978440
3.0318098	.998656	.980484
3.0297287	.999200	.988255
3.0311161	1.000287	1.004250
3.0304224	1.000910	1.013576
3.0318098	1.000715	1.010785
3.0262600	1.000479	1.007289
3.0054483	1.000446	1.006866
2.9624374	.999981	.999699
2.9034707	.998793	.980906
2.8410355	.999887	.998205
2.7924748	.999558	.992863

TABLE 6.- Continued

(f) Continued

y, cm	$T_t/T_{t,e}$	F_T
2.7584823	.999384	.989920
2.7425266	1.000051	1.000843
2.7328144	1.000721	1.012062
2.7286521	.999133	.985438
2.7272646	1.000315	1.005294
2.7272646	1.000518	1.008748
2.7251835	1.000553	1.009392
2.7237960	.999704	.994947
2.7057592	1.000976	1.016739
2.6662169	1.000701	1.012058
2.6051691	1.001356	1.023444
2.5392652	1.000028	1.000488
2.4872359	1.000359	1.006371
2.4539371	.999363	.988600
2.4338191	1.000588	1.010570
2.4234132	1.000182	1.003282
2.4185571	1.000719	1.013072
2.4157822	1.000158	1.002884
2.4150885	1.000213	1.003923
2.4150885	1.000491	1.009082
2.4109261	.999986	.999736
2.3901144	1.001056	1.019835
2.3457160	1.000450	1.008547
2.2909118	1.000825	1.015847
2.2257016	1.000596	1.011547
2.1764472	.998884	.978345
2.1445358	1.000480	1.009323
2.1271927	1.000081	1.001602
2.1181743	.999741	.994854
2.1147057	1.001141	1.023168
2.1133182	1.001268	1.025915
2.1133182	1.000411	1.008397
2.1126245	.999999	.999979
2.1105433	.999422	.988265
2.0973625	.999348	.986618
2.0668386	.998824	.975514
2.0134218	1.000035	1.000734
1.9544552	.999671	.993008
1.9024259	.998164	.960581
1.8684333	.999124	.980787
1.8490091	.999544	.989815
1.8399906	.999177	.981396
1.8344408	1.000398	1.009045
1.8323597	.997997	.954233

TABLE 6.- Continued

(f) Continued

y, cm	$T_t/T_{t,e}$	F_T
1.8309722	.998680	.969575
1.8309722	.998711	.969979
1.8295848	.999297	.983544
1.8191789	.996573	.919253
1.7886550	.997221	.934657
1.7387068	.997284	.934721
1.6769653	.997531	.939704
1.6263234	.997233	.931242
1.5923309	.998748	.968301
1.5715191	.998098	.951107
1.5611133	.998005	.948563
1.5569509	.998269	.954735
1.5548697	.998524	.960933
1.5548697	.998366	.955996
1.5548697	.999745	.992977
1.5541760	.998510	.958533
1.5423827	.998190	.949143
1.5118588	.999907	.997332
1.4612169	.998123	.946045
1.4015566	.997393	.924390
1.3509146	.997935	.939693
1.3183096	.996563	.897566
1.3002727	.996370	.890300
1.2919480	.996755	.899461
1.2884794	.998596	.955497
1.2891731	.997159	.907083
1.2898669	.997618	.922202
1.2898669	.997738	.924224
1.2863982	.996861	.892684
1.2746049	.997023	.895303
1.2440810	.997096	.895974
1.1927454	.996491	.871329
1.1344725	.996542	.873585
1.0852180	.995452	.831324
1.0519193	.995573	.833176
1.0366573	.994976	.807520
1.0297201	.996986	.880394
1.0283326	.995297	.808739
1.0283326	.995547	.813683
1.0297201	.994998	.785539
1.0276389	.995249	.792105
1.0269452	.995201	.786290
1.0151518	.996317	.833105
.9839342	.995272	.783557
.9305174	.994142	.732870

TABLE 6.- Continued

(f) Concluded

y , cm	$T_t/T_{t,e}$	F_T
.8729383	.995672	.798623
.8222963	.993889	.709804
.7903850	.994289	.723635
.7730419	.995811	.793924
.7667984	.995278	.767056
.7640235	.995671	.779802
.7640235	.995170	.747428
.7640235	.996286	.800366
.7647172	.996274	.790756
.7619423	.996311	.791311
.7522301	.996398	.791427
.7196251	.995314	.730720
.6689832	.997728	.866774
.6058542	.999464	.968344
.5579872	.998726	.922738
.5267696	.999955	.997265
.5115076	1.000038	1.002413
.5052641	.997665	.852732
.5038767	.999616	.974912
.5038767	1.000959	1.065332
.5038767	1.000333	1.022984
.5031829	1.000372	1.025907
.5004080	1.000644	1.046046
.4851461	.998617	.899906

TABLE 6.- Continued

(g) Total temperature profiles: Case 6; station 2; test 40; run 59;
 $P_{t,1} = 13\ 582.8\ \text{kPa}$; $T_t = 321.1\ \text{K}$; $T_w/T_t = 0.924$

$y, \text{ cm}$	$T_t/T_{t,e}$	F_T
1.2557709	.999234	.989386
1.2474473	.997931	.971146
1.2446711	.998276	.975902
1.2432843	.998724	.982143
1.2432843	.999543	.993590
1.2335739	.999353	.990937
1.2051309	1.000661	1.009290
1.1537950	.998804	.983199
1.0969092	.996993	.957762
1.0511231	.999316	.990319
1.0233736	.999197	.988552
1.0081133	.997590	.965522
1.0011740	.998782	.982458
.9970135	.999115	.987156
.9963201	.998440	.977173
.9956241	.999279	.989328
.9914636	.999417	.991328
.9713443	.997506	.962736
.9290279	.996992	.954795
.8728354	.997422	.961108
.8201127	.996430	.945921
.7840396	.994457	.915968
.7646137	.996044	.939727
.7542098	.996277	.942900
.7500468	.995682	.933438
.7486599	.995542	.930459
.7486599	.996802	.949821
.7431100	.993993	.904826
.7222973	.992527	.880494
.6778981	.989275	.826932
.6196254	.985030	.755648
.5675960	.977337	.630557
.5336032	.974634	.586188
.5127930	.973353	.554626
.5037734	.972727	.553452
.5003063	.972864	.552043
.4996129	.975458	.593672
.4989170	.972848	.549163
.4954499	.971749	.528520
.4822698	.972339	.532075
.4489704	.972035	.521456
.3962476	.970879	.498623
.3393618	.972198	.515952

TABLE 6.- Continued

(g) Concluded

$y, \text{ cm}$	$T_t/T_{t,e}$	F_T
<u>.2977388</u>	.972237	.513629
<u>.2734564</u>	.972915	.522660
<u>.2609698</u>	.973541	.530202
<u>.2561133</u>	.976055	.574461
<u>.2540330</u>	.972330	.507417
<u>.2547264</u>	.972463	.508662
<u>.2519528</u>	.971044	.478180
<u>.2422398</u>	.969254	.442992
<u>.2089404</u>	.967298	.404582
<u>.1576045</u>	.964215	.341222
<u>.1014146</u>	.960007	.254113
<u>.0611784</u>	.955854	.168543
<u>.0355092</u>	.953340	.104347
<u>.0244094</u>	.953895	.108242
<u>.0188595</u>	.950717	.037606
<u>.0181661</u>	.951532	.047087
<u>.0174727</u>	.952347	.056715
<u>.0167792</u>	.952163	.049986

TABLE 6.- Continued

(h) Total temperature profiles: Case 7; station 3; test 40; run 73;
 $P_{t,1} = 13\ 562.1$ kPa; $T_t = 342.2$ K; $T_w/T_t = 0.875$

y , cm	$T_t/T_{t,e}$	F_T
1.8692266	1.001287	1.016753
1.8088737	.999495	.993360
1.7672482	1.001172	1.015548
1.7422749	1.000408	1.005446
1.7290948	.998888	.984990
1.7242384	.999949	.999303
1.7221581	1.001041	1.014283
1.7193819	.999353	.991051
1.7055084	.999402	.991715
1.6722090	.999777	.996883
1.6160166	1.000208	1.002902
1.5473375	.999451	.992274
1.4814347	1.000156	1.002199
1.4342618	1.000444	1.006275
1.4058189	1.000869	1.012427
1.3912494	.999961	.999438
1.3843127	1.000624	1.009056
1.3815390	1.000800	1.011687
1.3801496	.999745	.996240
1.3704392	.999812	.997224
1.3419963	1.001347	1.020094
1.2899669	1.000208	1.003116
1.2212879	.999391	.990876
1.1553850	.998764	.981460
1.1061294	.999441	.991600
1.0783799	.997824	.967205
1.0638130	.998700	.980307
1.0575696	.998921	.983514
1.0547934	.999462	.991716
1.0541000	.998170	.971737
1.0450805	.998340	.974013
1.0180269	.997324	.957788
.9687712	.992982	.888796
.9007856	.989209	.827970
.8341893	.984787	.756178
.7856296	.979937	.677653
.7578801	.977067	.632878
.7433107	.975308	.604251
.7384542	.976471	.622198
.7356805	.974881	.594465
.7356805	.976800	.623383
.7294372	.976094	.610755
.7079310	.976355	.609704

TABLE 6.- Continued

(h) Concluded

$y, \text{ cm}$	$T_t/T_{t,e}$	F_T
<u>.6635318</u>	<u>.971859</u>	<u>.534930</u>
<u>.6010986</u>	<u>.968948</u>	<u>.480969</u>
<u>.5303368</u>	<u>.966945</u>	<u>.444318</u>
<u>.4762271</u>	<u>.965165</u>	<u>.406087</u>
<u>.4422343</u>	<u>.963874</u>	<u>.380455</u>
<u>.4248912</u>	<u>.964288</u>	<u>.382733</u>
<u>.4165676</u>	<u>.962922</u>	<u>.360788</u>
<u>.4151782</u>	<u>.962427</u>	<u>.353557</u>

TABLE 6.- Continued

(i) Total temperature profiles: Case 8; station 4; test 40; run 96;
 $P_{t,1} = 13\ 513.8$ kPa; $T_t = 321.7$ K; $T_w/T_t = 0.911$

y , cm	$T_t/T_{t,e}$	F_T
2.3674296	.999882	.998760
2.3382931	1.000679	1.007159
2.3216437	.999354	.993183
2.3112378	.999765	.997503
2.3063818	1.000402	1.004283
2.3049943	.998873	.987929
2.3022194	1.000240	1.002583
2.2918136	1.000322	1.003463
2.2668395	.998868	.987731
2.2210536	.999370	.993173
2.1648619	1.000122	1.001332
2.1142200	1.000910	1.009973
2.0774526	1.000038	1.000422
2.0538659	1.001494	1.016534
2.0399914	1.000642	1.007155
2.0330542	.999930	.999218
2.0302793	1.000507	1.005717
2.0254232	1.000621	1.007058
2.0150174	.999540	.994754
1.9886558	.999953	.999456
1.9442574	1.000722	1.008336
1.8832096	1.000851	1.009838
1.8325677	1.000770	1.008955
1.7944129	1.002863	1.033491
1.7722137	1.001599	1.018867
1.7583392	1.002668	1.031654
1.7541768	1.001826	1.021772
1.7507082	1.003236	1.038804
1.7486270	1.000885	1.010667
1.7375274	1.001733	1.020918
1.7104722	1.003662	1.044597
1.6612177	1.002904	1.035499
1.6001699	1.002934	1.036031
1.5356535	1.003791	1.046706
1.4850116	1.005079	1.062981
1.4510191	1.004153	1.051831
1.4329822	1.003657	1.045129
1.4232701	1.001480	1.017973
1.4191078	.998889	.986537
1.4170266	.998795	.985443
1.4100893	.998288	.979251
1.3878901	.999051	.988438

TABLE 6.- Continued

(i) Concluded

y , cm	$T_t/T_{t,e}$	F_T
1.3462666	.996815	.960973
1.2886875	.998135	.976959
1.2338832	.993293	.916786
1.1915660	.992915	.911445
1.1672857	.992238	.902442
1.1527174	.992956	.910619
1.1457802	.990382	.876633
1.1423116	.990846	.881056
1.1395367	.991117	.883604
1.1332931	.988862	.853117
1.1110939	.989420	.859577
1.0666956	.985762	.809284
1.0049540	.981997	.755151
.9355816	.977791	.698763
.8793899	.975339	.665697
.8405413	.972840	.631814
.8197295	.970980	.605290
.8072425	.971414	.607736
.8030801	.971468	.604482
.7996115	.970979	.593358
.7968366	.972099	.607668
.7822684	.971727	.597130
.7510508	.969912	.566682
.6990214	.968234	.538451
.6428297	.966177	.509039
.5970439	.964736	.477935
.5679074	.962914	.448582
.5512580	.963106	.447365
.5443208	.960828	.413991
.5422396	.959679	.398988
.5422396	.958994	.391421
.5394647	.958863	.388350
.5311400	.958156	.373217
.5054722	.958869	.377352

TABLE 6.- Continued

(j) Total temperature profiles: Case 9; station 5; test 40; run 95;
 $P_{t,1} = 13\ 582.8\ \text{kPa}$; $T_t = 320.0\ \text{K}$; $T_w/T_t = 0.918$

$y, \text{ cm}$	$T_t/T_{t,e}$	F_T
2.9383106	.997757	.976425
2.8952997	1.000624	1.006586
2.8342519	.998798	.987235
2.7732041	.997627	.974694
2.7281120	.998322	.982018
2.6996693	1.000179	1.001934
2.6857948	.999471	.994279
2.6781638	1.000454	1.004953
2.6753889	1.000685	1.007463
2.6733077	.998974	.988809
2.6677579	.999611	.995749
2.6448650	.999355	.992897
2.6025478	.999373	.993041
2.5408063	1.000440	1.004931
2.4776773	.999991	.999899
2.4256480	1.000334	1.003777
2.3916555	1.001325	1.015005
2.3722312	1.001812	1.020549
2.3618253	.999774	.997435
2.3548881	.999310	.992130
2.3528069	1.000082	1.000944
2.3444822	1.001568	1.018187
2.3181206	1.001767	1.020584
2.2667850	1.002458	1.028839
2.2022686	1.002776	1.032612
2.1273463	1.002316	1.027231
2.0662985	1.004087	1.048224
2.0225939	1.003666	1.043233
1.9962323	1.004361	1.051504
1.9830516	1.003379	1.039961
1.9775018	1.003294	1.038914
1.9740331	1.003722	1.044101
1.9698708	1.004210	1.049953
1.9532214	1.004222	1.050307
1.9157603	1.002708	1.032256
1.8567936	1.002002	1.023902
1.7881149	1.001812	1.021758
1.7208236	1.001685	1.020380
1.6729566	1.000993	1.012092
1.6445139	1.002322	1.028597
1.6292519	1.001921	1.023795
1.6223147	1.002383	1.029566

TABLE 6.- Continued

(j) Continued

y , cm	$T_t/T_{t,e}$	F_T
<u>1.6181523</u>	<u>1.001527</u>	<u>1.018844</u>
<u>1.6098276</u>	<u>1.000968</u>	<u>1.011894</u>
<u>1.5945657</u>	<u>1.000329</u>	<u>1.004036</u>
<u>1.5577983</u>	<u>.998251</u>	<u>.978440</u>
<u>1.4995254</u>	<u>.997042</u>	<u>.963413</u>
<u>1.4287654</u>	<u>.994468</u>	<u>.931364</u>
<u>1.3607804</u>	<u>.992580</u>	<u>.908077</u>
<u>1.3115260</u>	<u>.988331</u>	<u>.854862</u>
<u>1.2810021</u>	<u>.986576</u>	<u>.832111</u>
<u>1.2657401</u>	<u>.986516</u>	<u>.829918</u>
<u>1.2588029</u>	<u>.986550</u>	<u>.829143</u>
<u>1.2560280</u>	<u>.987751</u>	<u>.843433</u>
<u>1.2539468</u>	<u>.987037</u>	<u>.834226</u>
<u>1.2421535</u>	<u>.985706</u>	<u>.818049</u>
<u>1.2102421</u>	<u>.981612</u>	<u>.768174</u>
<u>1.1589065</u>	<u>.980801</u>	<u>.759292</u>
<u>1.0902277</u>	<u>.977028</u>	<u>.712268</u>
<u>1.0187741</u>	<u>.975989</u>	<u>.697286</u>
<u>.9632761</u>	<u>.974428</u>	<u>.674150</u>
<u>.9265087</u>	<u>.973555</u>	<u>.660418</u>
<u>.9077781</u>	<u>.973621</u>	<u>.658449</u>
<u>.8994534</u>	<u>.973301</u>	<u>.649379</u>
<u>.8959848</u>	<u>.974669</u>	<u>.663599</u>
<u>.8925162</u>	<u>.971994</u>	<u>.628861</u>
<u>.8828040</u>	<u>.971498</u>	<u>.621283</u>
<u>.8571362</u>	<u>.970695</u>	<u>.608282</u>
<u>.8092692</u>	<u>.970118</u>	<u>.595760</u>
<u>.7433653</u>	<u>.968344</u>	<u>.567958</u>
<u>.6746866</u>	<u>.966955</u>	<u>.543444</u>
<u>.6212698</u>	<u>.965639</u>	<u>.520397</u>
<u>.5886647</u>	<u>.960026</u>	<u>.440143</u>
<u>.5706279</u>	<u>.958945</u>	<u>.427613</u>
<u>.5629969</u>	<u>.956748</u>	<u>.405751</u>
<u>.5595283</u>	<u>.955420</u>	<u>.388521</u>
<u>.5574471</u>	<u>.955439</u>	<u>.386731</u>
<u>.5505098</u>	<u>.955560</u>	<u>.383574</u>
<u>.5283107</u>	<u>.956477</u>	<u>.389026</u>
<u>.4825248</u>	<u>.956614</u>	<u>.382806</u>
<u>.4180084</u>	<u>.954816</u>	<u>.348105</u>
<u>.3444736</u>	<u>.948824</u>	<u>.254094</u>
<u>.2834258</u>	<u>.944365</u>	<u>.183221</u>
<u>.2431898</u>	<u>.942031</u>	<u>.144293</u>
<u>.2209906</u>	<u>.941396</u>	<u>.138621</u>

TABLE 6.- Continued

(j) Concluded

$y, \text{ cm}$	$T_t/T_{t,e}$	F_T
<u>.2105847</u>	<u>.940202</u>	<u>.126375</u>
<u>.2071161</u>	<u>.940768</u>	<u>.130481</u>
<u>.2064223</u>	<u>.940010</u>	<u>.112921</u>
<u>.2043412</u>	<u>.938776</u>	<u>.092434</u>
<u>.1876918</u>	<u>.940692</u>	<u>.113760</u>
<u>.1509244</u>	<u>.939979</u>	<u>.095812</u>

TABLE 6.- Continued

(k) Total temperature profiles: Case 10; station 6; test 40; run 76;
 $P_{t,1} = 13\ 410.4$ kPa; $T_t = 326.1$ K; $T_w/T_t = 0.908$

y , cm	$T_t/T_{t,e}$	F_T
<u>3.1676238</u>	<u>1.000527</u>	<u>1.005094</u>
<u>3.0892318</u>	<u>1.000011</u>	<u>1.000108</u>
<u>3.0219421</u>	<u>1.002023</u>	<u>1.019669</u>
<u>2.9782364</u>	<u>1.001899</u>	<u>1.018529</u>
<u>2.9539565</u>	<u>1.002570</u>	<u>1.025274</u>
<u>2.9421633</u>	<u>1.000689</u>	<u>1.006819</u>
<u>2.9359200</u>	<u>1.001215</u>	<u>1.012078</u>
<u>2.9345331</u>	<u>1.000438</u>	<u>1.004377</u>
<u>2.9338397</u>	<u>1.002047</u>	<u>1.020604</u>
<u>2.9269004</u>	<u>1.002189</u>	<u>1.022177</u>
<u>2.8929076</u>	<u>1.003254</u>	<u>1.033176</u>
<u>2.8318612</u>	<u>1.002797</u>	<u>1.028583</u>
<u>2.7555520</u>	<u>1.004932</u>	<u>1.050366</u>
<u>2.6896466</u>	<u>1.002890</u>	<u>1.029466</u>
<u>2.6473302</u>	<u>1.002132</u>	<u>1.021653</u>
<u>2.6216635</u>	<u>1.002820</u>	<u>1.028582</u>
<u>2.6091744</u>	<u>1.003652</u>	<u>1.037107</u>
<u>2.6036245</u>	<u>1.003421</u>	<u>1.034690</u>
<u>2.6015442</u>	<u>1.003886</u>	<u>1.039503</u>
<u>2.6008508</u>	<u>1.001912</u>	<u>1.019476</u>
<u>2.5918312</u>	<u>1.004219</u>	<u>1.043021</u>
<u>2.5515951</u>	<u>1.003542</u>	<u>1.036265</u>
<u>2.4849988</u>	<u>1.003972</u>	<u>1.040896</u>
<u>2.4038331</u>	<u>1.002707</u>	<u>1.028020</u>
<u>2.3254411</u>	<u>1.003295</u>	<u>1.034360</u>
<u>2.2678619</u>	<u>1.002509</u>	<u>1.026288</u>
<u>2.2317888</u>	<u>1.001266</u>	<u>1.013315</u>
<u>2.2123654</u>	<u>1.000070</u>	<u>1.000741</u>
<u>2.2005722</u>	<u>.999127</u>	<u>.990761</u>
<u>2.1950223</u>	<u>1.000045</u>	<u>1.000480</u>
<u>2.1915526</u>	<u>1.000792</u>	<u>1.008399</u>
<u>2.1846159</u>	<u>1.000112</u>	<u>1.001191</u>
<u>2.1575598</u>	<u>.999995</u>	<u>.999947</u>
<u>2.1020634</u>	<u>.999430</u>	<u>.993965</u>
<u>2.0250582</u>	<u>.997673</u>	<u>.975319</u>
<u>1.9501358</u>	<u>.995496</u>	<u>.952111</u>
<u>1.8925565</u>	<u>.994304</u>	<u>.939050</u>
<u>1.8571769</u>	<u>.993828</u>	<u>.933659</u>
<u>1.8370601</u>	<u>.993075</u>	<u>.925161</u>
<u>1.8266537</u>	<u>.993779</u>	<u>.932402</u>
<u>1.8224906</u>	<u>.991945</u>	<u>.912008</u>
<u>1.8183301</u>	<u>.990890</u>	<u>.899903</u>
<u>1.8093106</u>	<u>.990453</u>	<u>.894772</u>

TABLE 6.- Continued

(k) Concluded

y , cm	$T_t/T_{t,e}$	F_T
1.7746243	.990998	.900384
1.7101083	.989464	.882797
1.6317163	.985849	.842453
1.5484704	.982293	.803346
1.4839544	.981016	.788664
1.4409420	.979587	.772132
1.4159687	.979271	.767575
1.4027887	.978734	.760111
1.3972388	.979249	.764579
1.3944625	.979659	.767242
1.3909954	.980521	.775798
1.3729589	.977739	.742513
1.3250901	.976235	.723495
1.2522505	.973536	.689897
1.1738585	.970356	.650685
1.1086490	.968170	.623957
1.0677195	.967099	.611285
1.0441330	.966409	.605191
1.0316464	.966153	.601664
1.0254005	.966111	.601014
1.0233203	.966233	.601082
1.0184638	.966460	.602580
.9955708	.965777	.591823
.9414612	.964370	.572637
.8651519	.960297	.521074
.7819034	.956536	.472007
.7153072	.954621	.444300
.6716014	.954282	.434309
.6480150	.953793	.423006
.6362217	.953832	.418952

TABLE 6.- Continued

(1) Total temperature profiles: Case 11; station 7; test 40; run 90;
 $P_{t,1} = 13\ 479.3\ \text{kPa}$; $T_t = 317.2\ \text{K}$; $T_w/T_t = 0.938$

$y, \text{ cm}$	$T_t/T_{t,e}$	F_T
3.9546591	.999045	.990139
3.9116482	1.000613	1.006458
3.8533753	.999633	.996063
3.7923275	.999435	.993834
3.7493166	1.001426	1.015823
3.7236487	1.000964	1.010829
3.7104680	.999459	.993886
3.7042244	.999101	.989757
3.7035307	.999164	.990447
3.7056119	1.001053	1.012058
3.7014495	.999661	.996103
3.6757817	1.000506	1.005855
3.6286084	1.000818	1.009517
3.5640920	.999731	.996848
3.4940258	1.000343	1.004035
3.4378341	1.000932	1.011067
3.4038416	1.000641	1.007695
3.3823361	1.002876	1.035060
3.3705428	1.001788	1.021975
3.3649930	1.002046	1.025442
3.3636056	1.001195	1.014965
3.3615244	1.003394	1.043163
3.3476499	1.002581	1.033077
3.3101888	1.002130	1.027577
3.2526096	1.001796	1.023410
3.1832371	1.001475	1.019454
3.1263517	.000895	1.011916
3.0861156	1.003277	1.044111
3.0625290	1.003220	1.043719
3.0493482	1.003442	1.046980
3.0431047	1.003030	1.041630
3.0382486	1.002654	1.036460
3.0333926	1.001648	1.022662
3.0167432	1.004149	1.057422
2.9792820	1.003105	1.043212
2.9196217	1.003912	1.054775
2.8481680	1.002534	1.035692
2.7794893	1.002821	1.040092
2.7281536	1.001590	1.022675
2.6955486	1.003470	1.050027
2.6768180	1.003457	1.050215
2.6671059	1.003490	1.051107
2.6629435	1.001656	1.024362

TABLE 6.- Continued

(1) Continued

y, cm	$T_t/T_{t,e}$	F_T
2.6594749	1.001811	1.026765
2.6490690	1.001792	1.026550
2.6185451	1.002835	1.042098
2.5658220	1.001689	1.025207
2.4964496	1.000606	1.009098
2.4312324	.998337	.974860
2.3799038	.997809	.966757
2.3452176	.995593	.932799
2.3278744	.998021	.969527
2.3181623	.995991	.937952
2.3133062	.996613	.947060
2.2105213	.996487	.944600
2.3022066	.996781	.948841
2.2772325	.996788	.948655
2.2286718	.995744	.931475
2.1620742	.994268	.907659
2.0913143	.994270	.907810
2.0358163	.990554	.847720
1.9983552	.990517	.847131
1.9775434	.988128	.808622
1.9664438	.988180	.808085
1.9608940	.988972	.819147
1.9581191	.989570	.827354
1.9525693	.989320	.821901
1.9303701	.989164	.817429
1.8845843	.984488	.737034
1.8193742	.985203	.748280
1.7451456	.983412	.716443
1.6792418	.982631	.702046
1.6348434	.981202	.677540
1.6077281	.980888	.670770
1.5946073	.979940	.654425
1.5883638	.980969	.669127
1.5862826	.980131	.653076
1.5821203	.981371	.672624
1.5640834	.979720	.641804
1.5231537	.978191	.611412
1.4607184	.976327	.574148
1.3878773	.975945	.561761
1.3247484	.973856	.519745
1.2789625	.974512	.528571
1.2539884	.972129	.482914
1.2394202	.973160	.498594

TABLE 6.- Continued

(1) Concluded

y, cm	$T_t/T_{t,e}$	F_T
1.2338704	.970174	.444523
1.2317893	.971646	.471525
1.2290144	.970154	.440688
1.2130587	.970422	.441801
1.1728226	.968424	.402225
1.1103874	.967391	.376335
1.0354651	.964642	.318319
.9653989	.963921	.295422
.9133696	.962588	.263996
.8814582	.963665	.279885
.8661963	.960370	.212622
.8592590	.960686	.211053
.8564841	.959555	.190342
.8550967	.960388	.199681
.8453845	.959713	.182612
.8120858	.960173	.186436
.7565878	.956481	.106437
.6844404	.955595	.078733
.6185365	.952676	.013016
.5706695	.952459	.004992
.5429205	.950611	-.043762
.5283523	.950736	-.042074
.5214151	.950064	-.056376
.5200276	.950081	-.065445
.5179464	.949732	-.078702
.5054594	.950002	-.082615
.4707732	.950592	-.075729
.4090216	.953153	-.028484
.3354968	.951073	-.083179
.2571059	.947271	-.168484
.1974456	.945188	-.231972
.1585570	.946960	-.198982
.1384790	.948638	-.175758
.1287668	.950581	-.143447
.1252982	.950621	-.151515
.1239108	.951914	-.124717
.1197484	.951420	-.146532
.0961618	.951991	-.136472
.0448261	.949783	-.187660

TABLE 6.- Continued

(m) Total temperature profiles: Case 12; station 8; test 40; run 82;
 $P_{t,1} = 13\ 224.2$ kPa; $T_t = 323.3$ K; $T_w/T_t = 0.912$

y , cm	$T_t/T_{t,e}$	F_T
<u>4.5066280</u>	<u>1.000834</u>	<u>1.008798</u>
<u>4.4761023</u>	<u>1.002112</u>	<u>1.022472</u>
<u>4.4580658</u>	<u>1.001213</u>	<u>1.012987</u>
<u>4.4476619</u>	<u>1.001680</u>	<u>1.018137</u>
<u>4.4428054</u>	<u>1.001599</u>	<u>1.017456</u>
<u>4.4386424</u>	<u>1.001065</u>	<u>1.011745</u>
<u>4.4261557</u>	<u>1.000869</u>	<u>1.009645</u>
<u>4.3997931</u>	<u>1.000895</u>	<u>1.009954</u>
<u>4.3547005</u>	<u>.999644</u>	<u>.996011</u>
<u>4.2957344</u>	<u>1.001492</u>	<u>1.016723</u>
<u>4.2346880</u>	<u>1.000870</u>	<u>1.009749</u>
<u>4.1861257</u>	<u>1.001447</u>	<u>1.016218</u>
<u>4.1528289</u>	<u>1.000829</u>	<u>1.009301</u>
<u>4.1320161</u>	<u>1.001093</u>	<u>1.012273</u>
<u>4.1209163</u>	<u>1.001649</u>	<u>1.018707</u>
<u>4.1132862</u>	<u>1.001455</u>	<u>1.016534</u>
<u>4.1084297</u>	<u>1.001539</u>	<u>1.017615</u>
<u>4.0952496</u>	<u>1.001262</u>	<u>1.014528</u>
<u>4.0651133</u>	<u>1.001187</u>	<u>1.013760</u>
<u>4.0203272</u>	<u>1.002006</u>	<u>1.023472</u>
<u>3.9578915</u>	<u>1.001115</u>	<u>1.013112</u>
<u>3.8878256</u>	<u>1.001834</u>	<u>1.021733</u>
<u>3.8260833</u>	<u>1.001712</u>	<u>1.020303</u>
<u>3.7802972</u>	<u>1.001261</u>	<u>1.014972</u>
<u>3.7518543</u>	<u>1.002115</u>	<u>1.025194</u>
<u>3.7345112</u>	<u>1.002590</u>	<u>1.030817</u>
<u>3.7247982</u>	<u>1.001854</u>	<u>1.022062</u>
<u>3.7192509</u>	<u>1.002912</u>	<u>1.034763</u>
<u>3.7088445</u>	<u>1.002374</u>	<u>1.028350</u>
<u>3.6824818</u>	<u>1.002752</u>	<u>1.032870</u>
<u>3.6380825</u>	<u>1.002631</u>	<u>1.031446</u>
<u>3.5777297</u>	<u>1.001809</u>	<u>1.021567</u>
<u>3.5083572</u>	<u>1.002099</u>	<u>1.025215</u>
<u>3.4445346</u>	<u>1.002906</u>	<u>1.035296</u>
<u>3.3966683</u>	<u>1.003645</u>	<u>1.044554</u>
<u>3.3647558</u>	<u>1.002798</u>	<u>1.034404</u>
<u>3.3467192</u>	<u>1.003343</u>	<u>1.041454</u>
<u>3.3349260</u>	<u>1.003349</u>	<u>1.041728</u>
<u>3.3286827</u>	<u>1.002415</u>	<u>1.030167</u>
<u>3.3203591</u>	<u>1.002539</u>	<u>1.031843</u>
<u>3.2981595</u>	<u>1.002874</u>	<u>1.036019</u>
<u>3.2551472</u>	<u>1.002621</u>	<u>1.032899</u>

TABLE 6.- Continued

(m) Continued

y , cm	$T_t/T_{t,e}$	F_T
3.1954876	1.003375	1.042362
3.1268086	1.001825	1.022908
3.0595164	1.003304	1.041819
3.0081830	1.002667	1.033815
2.9762704	1.000684	1.008715
2.9561536	1.001187	1.015246
2.9457472	1.000900	1.011654
2.9401973	1.000910	1.011871
2.9318712	1.000840	1.010928
2.9110610	1.000633	1.008266
2.8735985	1.001011	1.013268
2.8181021	.999934	.999137
2.7501164	.999139	.988649
2.6793571	.997781	.970737
2.6217778	.996178	.949376
2.5822351	.997532	.967140
2.5586487	.995073	.933699
2.5454661	.994999	.932260
2.5392228	.996102	.946815
2.5329794	.995260	.934889
2.5156363	.995034	.930739
2.4802567	.994396	.922060
2.4268405	.992874	.900305
2.3588548	.991877	.885754
2.2860152	.989472	.851691
2.2263532	.989318	.848877
2.1868105	.987839	.827213
2.1632240	.986999	.814877
2.1507374	.986484	.805753
2.1444941	.985648	.792263
2.1396376	.985935	.793922
2.1271509	.986816	.806500
2.0980145	.986020	.792484
2.0487615	.984294	.766605
1.9842429	.982306	.735094
1.9162598	.981489	.724127
1.8586806	.980692	.708922
1.8184444	.980049	.697667
1.7948580	.979370	.685903
1.7830648	.978497	.672225
1.7782083	.978984	.673521
1.7740452	.978423	.663595
1.7629454	.979057	.671105

TABLE 6.- Continued

(m) Concluded

y , cm	$T_t/T_{t,e}$	F_T
1.7345025	.977931	.654044
1.6873296	.975991	.622715
1.6228136	.975764	.616349
1.5562148	.973089	.572165
1.4979421	.971003	.540968
1.4590954	.971826	.546498
1.4362024	.969733	.515845
1.4251026	.971103	.531337
1.4202461	.970739	.522139
1.4181633	.970820	.519795
1.4112265	.969754	.496759
1.3911097	.968349	.471642
1.3515670	.966980	.444815
1.2919075	.965335	.413640
1.2239219	.964166	.389427
1.1621795	.963076	.367507
1.1153935	.961857	.345298
1.0900334	.961546	.335927
1.0761574	.961594	.333163
1.0699140	.961334	.318452
1.0671404	.960040	.297548
1.0608970	.960493	.299168
1.0428605	.960319	.289136
1.0026244	.959610	.274278
.9436557	.958070	.240211
.8742832	.953314	.143611
.8104607	.951920	.112224
.7639812	.950117	.076187
.7362342	.950255	.066385
.7230516	.949837	.061373
.7175017	.949920	.056502
.7161149	.948331	.021493
.7133412	.948933	.027067
.6994652	.948628	.019676
.6654724	.947234	-.014554
.6120562	.946066	-.044235
.5447640	.944912	-.071543
.4809414	.944847	-.082910
.4330751	.943919	-.106368
.4046322	.943534	-.116602
.3893718	.945249	-.093095

TABLE 6.- Continued

(n) Total temperature profiles: Case 13; station 1; test 40; run 102;
 $P_{t,1} = 13\ 424.2$ kPa; $T_t = 305.6$ K; $T_w/T_t = 0.504$

y , cm	$T_t/T_{t,e}$	F_T
.8791692	.996879	.993368
.8673759	.997160	.993968
.8639072	.997619	.994938
.8611323	.997017	.993660
.8604386	.996555	.992675
.8597449	.996836	.993270
.8569700	.995631	.990710
.8458704	.996833	.993259
.8167340	.996549	.992652
.7660920	.996360	.992247
.7071254	.995483	.990372
.6550961	.997882	.995485
.6204098	.994061	.987340
.6002918	.994700	.988697
.5912734	.993273	.985654
.5878048	.994254	.987746
.5871110	.992231	.983438
.5871110	.994304	.987842
.5871110	.993210	.985497
.5857236	.993426	.985959
.5725428	.992085	.983092
.5392440	.991786	.982450
.4851335	.988239	.974859
.4206171	.979301	.955722
.3630379	.960394	.915247
.3234956	.944261	.880710
.2992153	.928221	.846448
.2860345	.920875	.830733
.2804847	.916515	.821348
.2784035	.912979	.813822
.2777098	.912238	.812075
.2777098	.909875	.806889
.2763223	.906460	.799584
.2645290	.902905	.791919
.2312302	.884769	.752972
.1798946	.860194	.699986
.1132970	.834581	.645094
.0522492	.817508	.608399

TABLE 6.- Continued

(o) Total temperature profiles: Case 14; station 2; test 40; run 63;
 $P_{t,1} = 13\ 569.0$ kPa; $T_t = 310.3$ K; $T_w/T_t = 0.547$

y , cm	$T_t/T_{t,e}$	F_T
1.2696063	.999503	.998900
1.2154967	.998101	.995797
1.1773408	.998536	.996759
1.1544478	.998344	.996332
1.1433505	.999248	.998335
1.1398809	.998781	.997299
1.1391875	.998879	.997516
1.1398809	.998816	.997374
1.1364112	.997673	.994838
1.1156010	.998431	.996518
1.0774451	.999078	.997954
1.0184790	.998711	.997135
.9650628	.997793	.995094
.9303766	.997714	.994917
.9088704	.998247	.996101
.8991575	.997108	.993563
.8949969	.997948	.995431
.8943010	.997209	.993783
.8936076	.998124	.995822
.8915273	.997321	.994030
.8776538	.997309	.994000
.8464347	.997761	.995006
.7937119	.997423	.994248
.7368261	.995078	.989010
.6917334	.994634	.988013
.6646799	.993191	.984784
.6514973	.992837	.983989
.6473368	.992675	.983618
.6459499	.991803	.981659
.6473368	.991594	.981186
.6466434	.992111	.982333
.6362370	.990781	.979348
.6050178	.986882	.970601
.5529885	.979652	.954377
.4981854	.971205	.935443
.4579493	.962458	.915800
.4329760	.958225	.906245
.4225696	.955402	.899833
.4191000	.954296	.897316
.4184066	.953986	.896608
.4177132	.955180	.899225
.4163263	.954134	.896867

TABLE 6.- Continued

(o) Concluded

$y, \text{ cm}$	$T_t/T_{t,e}$	F_T
<u>.4073068</u>	<u>.954452</u>	<u>.897518</u>
<u>.3823335</u>	<u>.946877</u>	<u>.880442</u>
<u>.3386277</u>	<u>.934509</u>	<u>.852542</u>
<u>.2824378</u>	<u>.917994</u>	<u>.815358</u>
<u>.2317953</u>	<u>.901687</u>	<u>.778555</u>
<u>.1991893</u>	<u>.889872</u>	<u>.751752</u>
<u>.1818462</u>	<u>.882048</u>	<u>.734054</u>
<u>.1762963</u>	<u>.876528</u>	<u>.721504</u>
<u>.1749095</u>	<u>.872892</u>	<u>.713284</u>
<u>.1756029</u>	<u>.869370</u>	<u>.705272</u>
<u>.1762963</u>	<u>.868179</u>	<u>.702435</u>
<u>.1721358</u>	<u>.864636</u>	<u>.694367</u>
<u>.1485468</u>	<u>.861118</u>	<u>.686200</u>
<u>.1110869</u>	<u>.854933</u>	<u>.672247</u>
<u>.0819506</u>	<u>.853279</u>	<u>.668401</u>
<u>.0632206</u>	<u>.849970</u>	<u>.660784</u>
<u>.0548945</u>	<u>.847506</u>	<u>.655226</u>

TABLE 6.- Continued

(p) Total temperature profiles: Case 15; station 3; test 40; run 70;
 $P_{t,1} = 13\ 617.2\ \text{kPa}$; $T_t = 315.0\ \text{K}$; $T_w/T_t = 0.575$

$y, \text{ cm}$	$T_t/T_{t,e}$	F_T
<u>2.0278700</u>	<u>1.000992</u>	<u>1.002331</u>
<u>2.0056729</u>	<u>1.000555</u>	<u>1.001304</u>
<u>1.9612737</u>	<u>1.000843</u>	<u>1.001982</u>
<u>1.9030010</u>	<u>1.001069</u>	<u>1.002515</u>
<u>1.8502782</u>	<u>1.001884</u>	<u>1.004433</u>
<u>1.8148986</u>	<u>1.001733</u>	<u>1.004081</u>
<u>1.7940858</u>	<u>1.001049</u>	<u>1.002474</u>
<u>1.7843729</u>	<u>.999166</u>	<u>.998033</u>
<u>1.7795164</u>	<u>1.000063</u>	<u>1.000150</u>
<u>1.7781295</u>	<u>1.001020</u>	<u>1.002409</u>
<u>1.7781295</u>	<u>1.000167</u>	<u>1.000395</u>
<u>1.7746624</u>	<u>1.000534</u>	<u>1.001261</u>
<u>1.7545431</u>	<u>1.000343</u>	<u>1.000810</u>
<u>1.7122267</u>	<u>.999233</u>	<u>.998188</u>
<u>1.6546474</u>	<u>1.000395</u>	<u>1.000933</u>
<u>1.6026181</u>	<u>.999411</u>	<u>.998608</u>
<u>1.5713989</u>	<u>1.000167</u>	<u>1.000395</u>
<u>1.5533624</u>	<u>.998822</u>	<u>.997215</u>
<u>1.5443454</u>	<u>1.001079</u>	<u>1.002552</u>
<u>1.5415692</u>	<u>.999277</u>	<u>.998289</u>
<u>1.5422626</u>	<u>1.000882</u>	<u>1.002088</u>
<u>1.5422626</u>	<u>.999940</u>	<u>.999859</u>
<u>1.5381021</u>	<u>.999132</u>	<u>.997944</u>
<u>1.5214524</u>	<u>.999623</u>	<u>.999107</u>
<u>1.4805228</u>	<u>.999059</u>	<u>.997770</u>
<u>1.4236370</u>	<u>.999922</u>	<u>.999815</u>
<u>1.3653643</u>	<u>1.000122</u>	<u>1.000290</u>
<u>1.3251282</u>	<u>.999872</u>	<u>.999696</u>
<u>1.3029286</u>	<u>.999973</u>	<u>.999937</u>
<u>1.2925222</u>	<u>1.000466</u>	<u>1.001107</u>
<u>1.2869723</u>	<u>.999300</u>	<u>.998336</u>
<u>1.2855854</u>	<u>.999389</u>	<u>.998548</u>
<u>1.2855854</u>	<u>.999740</u>	<u>.999381</u>
<u>1.2841986</u>	<u>1.000283</u>	<u>1.000673</u>
<u>1.2696292</u>	<u>1.000627</u>	<u>1.001491</u>
<u>1.2328627</u>	<u>.998762</u>	<u>.997055</u>
<u>1.1732031</u>	<u>1.000201</u>	<u>1.000479</u>
<u>1.1093806</u>	<u>.999897</u>	<u>.999755</u>
<u>1.0580446</u>	<u>1.001339</u>	<u>1.003190</u>
<u>1.0289083</u>	<u>.999953</u>	<u>.999887</u>
<u>1.0122586</u>	<u>1.000229</u>	<u>1.000546</u>
<u>1.0074021</u>	<u>.999587</u>	<u>.999015</u>

TABLE 6.- Continued

(p) Continued

y, cm	$T_t/T_{t,e}$	F_T
1.0053218	1.000685	1.001635
1.0067087	.999958	.999900
1.0046259	1.000321	1.000766
.9921392	1.000672	1.001604
.9581464	1.000430	1.001026
.9005672	.998669	.996820
.8409076	.997160	.993211
.7902651	.995694	.989699
.7604354	.992547	.982166
.7465619	.992242	.981423
.7403186	.992316	.981583
.7389292	.991940	.980671
.7389292	.992323	.981581
.7396251	.993488	.984372
.7306056	.992191	.981257
.7035495	.988990	.973566
.6522136	.983397	.960115
.5939409	.975856	.941962
.5467680	.971813	.932187
.5176317	.966559	.919491
.5030648	.966769	.920015
.4989017	.965222	.916254
.4975149	.965095	.915892
.4989017	.966497	.919179
.4995951	.965574	.916918
.4926584	.966150	.918284
.4669892	.961224	.906375
.4191229	.954304	.889599
.3608502	.944392	.865581
.3136773	.938442	.851142
.2845410	.933067	.838098
.2713609	.932032	.835593
.2665044	.931346	.833901
.2651150	.930489	.831746
.2658110	.929042	.828152
.2665044	.931008	.832829
.2623414	.931574	.834123
.2429180	.928406	.826397
.1985188	.921246	.808965
.1423264	.912211	.786891
.0896036	.904407	.767823
.0542239	.897484	.750929
.0348005	.893233	.740606

TABLE 6.- Continued

(p) Concluded

Y, cm	$T_t/T_{t,e}$	F_T
<u>.0278613</u>	<u>.890794</u>	<u>.734707</u>
<u>.0264744</u>	<u>.888950</u>	<u>.730246</u>
<u>.0278613</u>	<u>.887646</u>	<u>.726978</u>
<u>.0292506</u>	<u>.887568</u>	<u>.726707</u>
<u>.0264744</u>	<u>.887299</u>	<u>.725917</u>

TABLE 6.- Continued

(q) Total temperature profiles: Case 16; station 4; test 40; run 98;
 $P_{t,1} = 13\ 575.9$ kPa; $T_t = 302.8$ K; $T_w/T_t = 0.476$

y, cm	$T_t/T_{t,e}$	F_T
1.9880048	.999056	.998250
1.9193260	.998587	.997380
1.8548096	.999787	.999605
1.8048614	.999404	.998894
1.7722563	1.000365	1.000678
1.7542195	.999159	.998440
1.7445074	.999692	.999428
1.7389576	.999570	.999201
1.7361827	1.001146	1.002128
1.7195333	.999052	.998238
1.6827658	.999369	.998827
1.6251867	1.000022	1.000041
1.5551205	.999230	.998568
1.4878292	.998519	.997245
1.4385747	1.000994	1.001849
1.4059697	1.000388	1.000722
1.3879328	1.001023	1.001904
1.3782207	1.000232	1.000432
1.3740583	1.002457	1.004575
1.3726709	.999827	.999678
1.3615713	1.002739	1.005103
1.3352097	1.002344	1.004369
1.2880364	1.001643	1.003065
1.2256012	1.001409	1.002628
1.1645534	1.003374	1.006294
1.1180739	1.002290	1.004273
1.0882437	1.003935	1.007344
1.0715943	1.004109	1.007670
1.0639633	1.004479	1.008358
1.0591073	1.001749	1.003264
1.0577198	1.003315	1.006188
1.0542512	1.002664	1.004974
1.0355206	1.003332	1.006223
.9966720	1.001715	1.003204
.9383991	1.002404	1.004491
.8815137	.997966	.996200
.6385028	.995000	.990660
.8093663	.993572	.987992
.7947981	.995014	.990681
.7864734	.992410	.985808
.7830048	.993381	.987613
.7816173	.992671	.986282

TABLE 6.- Continued

(q) Concluded

$y, \text{ cm}$	$T_t/T_{t,e}$	F_T
.7795362	.991263	.983636
.7677428	.990457	.982125
.7365252	.989426	.980185
.6844959	.986188	.974118
.6248355	.979693	.961945
.5734999	.976347	.955679
.5408948	.972900	.949214
.5214705	.970230	.944196
.5110647	.970568	.944804
.5075960	.970899	.945400
.5055149	.970410	.944452
.5034337	.968973	.941727
.4916404	.969501	.942695
.4597290	.967411	.938761
.4083934	.963948	.932227
.3417958	.953547	.912676
.2772794	.946441	.899297
.2267187	.939115	.885492
.1945822	.934863	.877460
.1864015	.932463	.872966
.1794642	.931940	.871999
.1794642	.930619	.869499
.1753019	.931524	.871169
.1628148	.928949	.866261
.1315972	.924617	.858043
.0816490	.916073	.841947
.0157452	.907730	.826132

TABLE 64- Continued

(r) Total temperature profiles: Case 17; station 5; test 40; run 94;
 $P_{t,1} = 13\ 637.9$ kPa; $T_t = 315.6$ K; $T_w/T_t = 0.505$

y , cm	$T_t/T_{t,e}$	F_T
2.7718959	.998892	.997806
2.7441469	.999601	.999211
2.7295787	.998445	.996922
2.7226414	1.000542	1.001072
2.7191728	.997627	.995301
2.7184791	.999551	.999111
2.7073795	.998321	.996672
2.6782431	.998212	.996455
2.6276011	.998604	.997232
2.5603098	.996574	.993204
2.4874687	.998080	.996189
2.4340519	.997665	.995367
2.3993657	.999609	.999223
2.3813288	.997594	.995217
2.3702292	.998546	.997110
2.3674543	.997402	.994840
2.3653732	.998751	.997520
2.3570485	.996643	.993331
2.3286058	.998294	.996607
2.2821262	.999732	.999466
2.2210784	1.000453	1.000902
2.1454624	1.001443	1.002876
2.0830272	1.002312	1.004608
2.0420974	1.000084	1.000168
2.0178170	1.001052	1.002097
2.0067174	1.001855	1.003698
2.0004739	1.000937	1.001869
1.9990865	1.002115	1.004222
1.9907618	1.002492	1.004976
1.9685626	1.002782	1.005559
1.9241642	1.002715	1.005425
1.8610352	1.000941	1.001879
1.7861130	1.000360	1.000719
1.7257589	1.000944	1.001886
1.6848291	1.000489	1.000978
1.6633237	1.000108	1.000217
1.6522241	1.001938	1.003879
1.6494492	1.000169	1.000338
1.6473680	1.000100	1.000199
1.6418182	1.000027	1.000054
1.6210065	1.000230	1.000461
1.5807704	.997756	.995502

TABLE 6.- Continued

(r) Continued

y, cm	$T_t/T_{t,e}$	F_T
1.5197226	.997680	.995348
1.4448004	.994922	.989813
1.3761216	.992303	.984568
1.3261734	.991795	.983542
1.2962432	.989068	.978073
1.2831625	.986704	.973335
1.2776127	.988173	.976275
1.2776127	.985334	.970591
1.2720629	.984393	.968731
1.2561072	.982348	.964661
1.2193398	.980568	.961064
1.1603732	.978729	.957334
1.0882258	.973138	.946102
1.0250969	.971461	.942720
.9793110	.968946	.937631
.9550307	.969505	.938700
.9425436	.969807	.939294
.9397687	.968837	.937264
.9390750	.967873	.935279
.9356064	.967628	.934715
.9203444	.967681	.934766
.8835770	.967310	.933970
.8225292	.963205	.925678
.7517692	.958338	.915878
.6789282	.950590	.900416
.6234302	.944919	.889169
.5894377	.942175	.883695
.5748695	.943293	.885888
.5686259	.939828	.878969
.5686259	.938913	.877035
.5672385	.941113	.881332
.5603012	.938395	.875715
.5332460	.936732	.872224
.4826041	.934208	.866999
.4153128	.927997	.854423
.3466340	.920787	.839665
.2883611	.914640	.827107
.2536749	.911203	.820072
.2363318	.907139	.811810
.2293945	.906523	.810545
.2287008	.905100	.807582
.2293945	.905032	.807381
.2196824	.904251	.805575

TABLE 6.- Continued

(r) Concluded

Y, cm	$T_t/T_{t,e}$	F_T
.1891585	.901454	.799732
.1350479	.897078	.790771
.0656755	.893256	.783021

TABLE 6.- Continued

(s) Total temperature profiles: Case 18; station 6; test 40; run 81;
 $P_{t,1} = 13\,479.3$ kPa; $T_t = 312.2$ K; $T_w/T_t = 0.489$

y , cm	$T_t/T_{t,e}$	F_T
2.6356495	.997545	.995289
2.5617272	.997264	.994747
2.4930481	.998624	.997358
2.4396294	.997737	.995652
2.4070259	.997494	.995187
2.3875000	.998841	.997774
2.3727264	.997977	.996116
2.3744199	.997304	.994823
2.3695635	.998543	.997201
2.3549966	.998032	.996219
2.3203103	.997373	.994949
2.2648113	.998020	.996192
2.1947454	.996822	.993886
2.1323097	.996203	.992693
2.0788935	.995593	.991516
2.0435138	.995553	.991436
2.0240904	.996211	.992702
2.0143775	.996860	.993948
2.0115013	.995117	.990592
2.0060514	.997454	.995095
1.9907910	.995971	.992240
1.9561048	.996066	.992422
1.9019926	.996549	.993350
1.8312333	.994433	.989272
1.7597806	.991896	.984382
1.6952645	.990570	.981809
1.6522522	.988882	.978549
1.6279724	.987882	.976612
1.6175660	.986424	.973792
1.6113227	.986084	.973119
1.6078555	.987178	.975218
1.5981426	.985755	.972464
1.5710865	.984931	.970867
1.5218334	.982768	.966689
1.4593976	.979905	.961147
1.3865555	.976733	.955013
1.3262026	.974219	.950138
1.2838862	.971667	.945186
1.2615866	.970445	.942796
1.2491999	.971018	.943869
1.2436500	.969979	.941824
1.2415672	.970263	.942364

TABLE 6.- Continued

(s) Concluded

y , cm	$T_t/T_{t,e}$	F_T
1.2346305	.968172	.938273
1.2096572	.967151	.936271
1.1631778	.965251	.932547
1.1021289	.961601	.925433
1.0272065	.957724	.917882
.9599168	.953587	.909851
.9134348	.948127	.899277
.8870747	.945979	.895125
.8738946	.944774	.892806
.8669553	.944673	.892561
.8534882	.944387	.891954
.8579383	.942882	.889005
.8378190	.940757	.884782
.7941158	.937600	.878604
.7386168	.932416	.868482
.6671640	.925715	.855392
.6047283	.919330	.842840
.5610250	.915048	.834424
.5360492	.912460	.829307
.5249494	.909194	.822932
.5200929	.907685	.819988
.5166258	.907786	.820187
.5131562	.906087	.816915
.4971999	.902872	.810604
.4597400	.897916	.800899
.4035476	.890328	.786016
.3341751	.880143	.766079
.2648026	.869916	.745969
.2120798	.861740	.729937
.1787804	.855567	.717825
.1635201	.852493	.711716
.1551940	.850176	.707107
.1551940	.849609	.705915
.1517269	.848703	.704096
.1392403	.845488	.697750
.1024712	.840027	.687105
.0435051	.837296	.681899

TABLE 6.- Continued

(t) Total temperature profiles: Case 19; station 7; test 40; run 92;
 $P_{t,1} = 13\,341.4$ kPa; $T_t = 319.4$ K; $T_w/T_t = 0.469$

y , cm	$T_t/T_{t,e}$	F_T
3.9851833	1.002406	1.004403
3.8991614	1.001580	1.002894
3.7874717	1.001751	1.003210
3.7361361	1.001740	1.003191
3.7257302	1.001262	1.002315
3.7208741	1.001478	1.002715
3.6639887	1.000940	1.001728
3.5405057	1.001061	1.001952
3.4343658	1.001809	1.003330
3.3934360	1.000975	1.001794
3.3823364	1.000960	1.001768
3.3670745	1.000615	1.001134
3.2886836	1.001244	1.002296
3.1596508	1.000699	1.001290
3.0819536	1.001415	1.002611
3.0562858	1.000389	1.000718
3.0486548	1.000804	1.001484
3.0091125	.999513	.999101
2.8932605	.999334	.998769
2.7621465	.998837	.997850
2.6969363	1.000086	1.000160
2.6768183	.999888	.999792
2.6664124	.999630	.999314
2.5970400	.999618	.999292
2.4617636	1.000673	1.001247
2.3604798	1.001295	1.002403
2.3209375	1.000669	1.001242
2.3098379	1.000567	1.001054
2.2834764	1.002161	1.004015
2.1829863	1.001319	1.002451
2.0476099	1.000410	1.000763
1.9719939	.999918	.999848
1.9470198	1.000025	1.000047
1.9373077	.998361	.996945
1.8838909	.997763	.995825
1.7562455	.993582	.988013
1.6341499	.991708	.984498
1.5807331	.989593	.980534
1.5675524	.989420	.980197
1.5529841	.988750	.978924
1.4669623	.986275	.974267
1.3302985	.980455	.963330

TABLE 6.- Continued

(t) Concluded

y, cm	$T_t/T_{t,e}$	F_T
<u>1.2435829</u>	<u>.977649</u>	<u>.958036</u>
<u>1.2165276</u>	<u>.975864</u>	<u>.954652</u>
<u>1.2082029</u>	<u>.974678</u>	<u>.952404</u>
<u>1.1596422</u>	<u>.974290</u>	<u>.951645</u>
<u>1.0361592</u>	<u>.967660</u>	<u>.939154</u>
<u>.8994954</u>	<u>.961963</u>	<u>.928400</u>
<u>.8370601</u>	<u>.956903</u>	<u>.918840</u>
<u>.8224919</u>	<u>.956709</u>	<u>.918424</u>
<u>.8106986</u>	<u>.956605</u>	<u>.918222</u>
<u>.7392450</u>	<u>.948792</u>	<u>.903455</u>
<u>.6046623</u>	<u>.936260</u>	<u>.879729</u>
<u>.5054597</u>	<u>.926105</u>	<u>.860483</u>
<u>.4742421</u>	<u>.923438</u>	<u>.855328</u>
<u>.4693860</u>	<u>.923614</u>	<u>.855616</u>
<u>.4409433</u>	<u>.920217</u>	<u>.849183</u>
<u>.3375783</u>	<u>.909849</u>	<u>.829479</u>
<u>.1988333</u>	<u>.895228</u>	<u>.801551</u>
<u>.1280734</u>	<u>.886215</u>	<u>.784555</u>
<u>.1114240</u>	<u>.882747</u>	<u>.777806</u>
<u>.1051805</u>	<u>.881415</u>	<u>.775291</u>

TABLE 6.- Continued

(u) Total temperature profiles: Case 20; station 8; test 40; run 87;
 $P_{t,1} = 13\ 513.8$ kPa; $T_t = 330.6$ K; $T_w/T_t = 0.449$

y , cm	$T_t/T_{t,e}$	F_T
3.8996232	1.000608	1.001087
3.8469001	1.000507	1.000907
3.7789151	1.001115	1.001998
3.7130112	1.001173	1.002104
3.6609819	1.000627	1.001125
3.6311517	.999669	.999405
3.6145023	1.000279	1.000503
3.6075650	.999973	.999951
3.6054839	1.000220	1.000396
3.6054839	.999074	.998329
3.5957717	.999882	.999787
3.5694102	1.000553	1.000999
3.5208494	.998992	.998179
3.4570268	.997540	.995558
3.3862668	.997968	.996328
3.3307689	.999306	.998745
3.2926140	.999680	.999420
3.2718022	1.000423	1.000766
3.2613964	.999466	.999032
3.2565403	.999162	.998481
3.2530717	.999709	.999472
3.2440533	.999921	.999857
3.2183854	.999468	.999033
3.1739870	.999313	.998752
3.1087769	.999464	.999026
3.0331609	1.000681	1.001238
2.9624010	.998266	.996850
2.9117591	.997337	.995161
2.8798477	.999064	.998299
2.8645858	.999360	.998836
2.8562611	.999937	.999886
2.8534862	.999816	.999666
2.8451615	1.000601	1.001094
2.8194937	.999781	.999600
2.7702392	.999195	.998535
2.7036416	.998475	.997222
2.6245570	.996768	.994109
2.5524096	.996057	.992813
2.5010740	.997378	.995220
2.4691627	.994720	.990371
2.4525133	.994284	.989576
2.4434948	.994082	.989204

TABLE 6- Continued

(u) Continued

y, cm	$T_t/T_{t,e}$	F_T
2.4393325	.994850	.990604
2.4358639	.994472	.989911
2.4192145	.995705	.992158
2.3810596	.992658	.986592
2.3207055	.993680	.988457
2.2443958	.990279	.982242
2.1680861	.988046	.978156
2.1112007	.986803	.975880
2.0751270	.986727	.975730
2.0550089	.984108	.970938
2.0452968	.984289	.971261
2.0411344	.982216	.967461
2.0369721	.982000	.967061
2.0203227	.982039	.967121
1.9814741	.982390	.967753
1.9232012	.980242	.963813
1.8455041	.978051	.959792
1.7643383	.974088	.952530
1.6984344	.971852	.948418
1.6561172	.970169	.945317
1.6339180	.969108	.943361
1.6228184	.967456	.940315
1.6186560	.967996	.941284
1.6172686	.969306	.943676
1.6054753	.967674	.940674
1.5756451	.964871	.935516
1.5201471	.962901	.931872
1.4493872	.960451	.927340
1.3716900	.956038	.919218
1.3099485	.953056	.913723
1.2690187	.949751	.907639
1.2482070	.949149	.906512
1.2378011	.949293	.906746
1.2364137	.949012	.906212
1.2343325	.949317	.906731
1.2273953	.948567	.905311
1.2024212	.947794	.903839
1.1538604	.945387	.899368
1.0872628	.939400	.888269
1.0074845	.933426	.877229
.9360308	.929408	.869780
.8874701	.924539	.860757
.8583337	.923899	.859522

TABLE 6.- Continued

(u) Concluded

Y, cm	$T_t/T_{t,e}$	F_T
.8458466	.921721	.855508
.8402968	.922173	.856313
.8389094	.922245	.856436
.8319721	.922803	.857409
.8125478	.919222	.850734
.7667620	.912817	.838811
.7022456	.907072	.828100
.6252421	.900078	.815131
.5530948	.891088	.798436
.5031466	.886414	.789700
.4747039	.883773	.784744
.4587482	.882282	.781961
.4559733	.881088	.779627
.4559733	.881460	.780294
.4552796	.878765	.775214
.4400176	.878522	.774765
.4039439	.874374	.766969
.3428961	.868125	.755309
.2665864	.859580	.739347
.1916641	.848850	.719302
.1354724	.838427	.699862
.1007862	.830506	.685072
.0848305	.824404	.673713
.0771995	.820033	.665484
.0785870	.818674	.662784
.0765058	.816987	.659551
.0619376	.814032	.653884

TABLE 6.- Continued

(v) Total temperature profiles: Case 21; station 2; test 40; run 62;
 $P_{t,1} = 13\ 651.8$ kPa; $T_t = 339.3$ K; $T_w/T_t = 0.393$

y , cm	$T_t/T_{t,e}$	F_T
1.1391849	.998103	.996727
1.1044987	.997929	.996425
1.0524693	.997698	.996024
.9990531	.998042	.996619
.9581236	.998308	.997076
.9317609	.997337	.995396
.9199677	.997691	.996007
.9144178	.997466	.995617
.9137244	.997223	.995194
.9130309	.997256	.995249
.9116441	.996361	.993699
.9005443	.996842	.994532
.8693277	.996701	.994285
.8193786	.996653	.994200
.7687361	.996980	.994766
.7305827	.996866	.994567
.7076897	.996261	.993516
.6958965	.996386	.993730
.6924269	.996256	.993503
.6910400	.995935	.992944
.6910400	.996041	.993126
.6896506	.996040	.993121
.6806336	.996672	.994217
.6535776	.995948	.992958
.6070981	.994370	.990214
.5502123	.991898	.985912
.5044262	.988649	.980254
.4732096	.985669	.975066
.4586427	.985132	.974128
.4510100	.984564	.973128
.4496232	.984272	.972611
.4496232	.985020	.973899
.4496232	.985255	.974306
.4433799	.983488	.971221
.4191000	.980029	.965177
.3726205	.970863	.949176
.3171215	.957120	.925207
.2720289	.943119	.900747
.2408123	.934692	.885984
.2255495	.925440	.869760
.2199996	.921064	.862051
.2179193	.917827	.856393

TABLE 6,- Continued

(v) Concluded

$y, \text{ cm}$	$T_t/T_{t,e}$	F_T
.2199996	.915353	.852002
.2193061	.913891	.849387
.2151431	.911530	.845179
.1929460	.901992	.828474
.1492402	.883105	.795372
.0895807	.862014	.758334

TABLE 6.- Continued

(w) Total temperature profiles: Case 22; station 3; test 40; run 69;
 $P_{t,1} = 13\ 631.0$ kPa; $T_t = 323.3$ K; $T_w/T_t = 0.502$

y, cm	$T_t/T_{t,e}$	F_T
1.7608194	1.000436	1.000884
1.7455566	1.000509	1.001031
1.7407026	1.000863	1.001751
1.7379264	1.000651	1.001322
1.7379264	.999897	.999791
1.7379264	.999997	.999993
1.7316831	.999757	.999505
1.7067098	1.000260	1.000529
1.6636975	1.000668	1.001359
1.6165246	1.000411	1.000837
1.5797581	.999291	.998556
1.5575585	.998898	.997758
1.5457653	1.000345	1.000703
1.5416022	1.000563	1.001147
1.5402154	.999823	.999639
1.5402154	.999771	.999534
1.5409088	.999882	.999759
1.5353589	1.000386	1.000787
1.5152421	1.000202	1.000412
1.4694560	.999180	.998325
1.4125702	.999224	.998413
1.3598474	.998880	.997709
1.3251612	.999955	.999909
1.3064287	.998798	.997538
1.2987985	1.000074	1.000151
1.2967183	.999347	.998663
1.2960248	.999425	.998822
1.2953289	.998301	.996520
1.2918618	.999043	.998039
1.2738252	.998589	.997109
1.2328957	1.000200	1.000410
1.1725402	1.000089	1.000183
1.1163503	1.000127	1.000261
1.0733380	1.000866	1.001780
1.0504449	1.000532	1.001093
1.0393451	1.001725	1.003547
1.0358780	1.001849	1.003803
1.0351821	1.001787	1.003676
1.0358780	1.001241	1.002551
1.0337952	1.002742	1.005641
1.0192283	1.003387	1.006971
.9831527	1.002900	1.005971

TABLE 6.- Continued

(w) Concluded

y, cm	$T_t/T_{t,e}$	F_T
.9227998	1.002382	1.004909
.8638337	1.000077	1.000159
.8138846	.998692	.997302
.7833614	.996834	.993465
.7701813	.996035	.991811
.7639380	.996103	.991948
.7632421	.996708	.993198
.7632421	.996618	.993012
.7611618	.996115	.991968
.7438187	.995960	.991642
.7028891	.989708	.978712
.6425362	.982095	.962962
.5828741	.974074	.946348
.5419446	.967775	.933252
.5183581	.964387	.926186
.5072583	.963812	.924974
.5051781	.964705	.926788
.5030953	.964676	.926678
.5051781	.965296	.927920
.5044846	.966595	.930621
.4968519	.964008	.925230
.4684090	.958806	.914382
.4191559	.952141	.900468
.3608832	.944446	.884401
.3164840	.934510	.863726
.2880411	.929064	.852364
.2748610	.927231	.848460
.2706980	.924882	.843470
.2706980	.926543	.846856
.2713914	.925595	.844814
.2720848	.925458	.844456
.2637612	.923281	.839826
.2367051	.918660	.830070
.1881454	.909399	.810705
.1277925	.895906	.782432
.0757631	.885255	.760058
.0445440	.878585	.745937
.0272009	.874723	.737699

TABLE 6.- Continued

(x) Total temperature profiles: Case 23; station 4; test 40; run 97;
 $P_{t,1} = 13\ 631.0$ kPa; $T_t = 312.2$ K; $T_w/T_t = 0.368$

y , cm	$T_t/T_{t,e}$	F_T
1.7576995	.999230	.998792
1.6938768	.999826	.999727
1.6307479	.998020	.996892
1.5856558	.998870	.998225
1.5551319	.998939	.998333
1.5384825	.998552	.997725
1.5308515	1.000478	1.000752
1.5253017	.999983	.999974
1.5211394	.999027	.998470
1.5142021	.999013	.998449
1.4892280	.999431	.999106
1.4476045	.999151	.998665
1.3879442	.997868	.996648
1.3192654	.999396	.999051
1.2589114	.999144	.998654
1.2172879	.998522	.997675
1.1909263	.999075	.998544
1.1770518	.998634	.997848
1.1701146	.998299	.997321
1.1673397	.997677	.996341
1.1597087	.998987	.998404
1.1354284	.996994	.995266
1.0917237	.993005	.988980
1.0279010	.989350	.983219
.9578348	.984014	.974809
.8995619	.980464	.969204
.8614071	.976082	.962289
.8378204	.975693	.961652
.8246397	.972909	.957250
.8170087	.972628	.956788
.8142338	.973888	.958764
.8100714	.974155	.959172
.7955032	.971906	.955621
.7635919	.969620	.951998
.7080939	.966308	.946750
.6401089	.959514	.935996
.5748987	.952134	.924325
.5270317	.948186	.918066
.4985890	.943391	.910487
.4833270	.940076	.905251
.4770835	.938450	.902652
.4730149	.938042	.901985

TABLE 6.- Continued

(x) Concluded

$y, \text{ cm}$	$T_t/T_{t,e}$	F_T
.4722275	.935031	.897190
.4597404	.935486	.897889
.4319914	.933231	.894316
.3806558	.926163	.883124
.3154456	.911522	.859934
.2516230	.897098	.837041
.2044497	.885131	.818026
.1739258	.875471	.802625
.1579701	.872257	.797436
.1517266	.868580	.791615
.1503391	.866181	.787752
.1475642	.863586	.783634
.1392395	.862236	.781419
.1107968	.858784	.775901

TABLE 6.- Continued

(y) Total temperature profiles: Case 24; station 5; test 40; run 93;
 $P_{t,1} = 13\ 651.7$ kPa; $T_t = 327.8$ K; $T_w/T_t = 0.386$

y , cm	$T_t/T_{t,e}$	F_T
<u>2.4833145</u>	<u>.999322</u>	<u>.998896</u>
<u>2.4285103</u>	<u>.999245</u>	<u>.998769</u>
<u>2.3931303</u>	<u>1.000068</u>	<u>1.000110</u>
<u>2.3737060</u>	<u>.998351</u>	<u>.997311</u>
<u>2.3646876</u>	<u>.999264</u>	<u>.998799</u>
<u>2.3612190</u>	<u>.998022</u>	<u>.996773</u>
<u>2.3591378</u>	<u>.998562</u>	<u>.997652</u>
<u>2.3542817</u>	<u>.999043</u>	<u>.998436</u>
<u>2.3306951</u>	<u>.998867</u>	<u>.998148</u>
<u>2.2876841</u>	<u>.999023</u>	<u>.998402</u>
<u>2.2301050</u>	<u>.999576</u>	<u>.999307</u>
<u>2.1586513</u>	<u>.999419</u>	<u>.999049</u>
<u>2.0982973</u>	<u>1.002373</u>	<u>1.003884</u>
<u>2.0573675</u>	<u>.999598</u>	<u>.999342</u>
<u>2.0330871</u>	<u>.999956</u>	<u>.999929</u>
<u>2.0212938</u>	<u>1.001740</u>	<u>1.002850</u>
<u>2.0178252</u>	<u>1.001709</u>	<u>1.002799</u>
<u>2.0164377</u>	<u>1.000975</u>	<u>1.001596</u>
<u>2.0101942</u>	<u>1.000198</u>	<u>1.000324</u>
<u>1.9886887</u>	<u>1.000235</u>	<u>1.000385</u>
<u>1.9435966</u>	<u>.998007</u>	<u>.996737</u>
<u>1.8825488</u>	<u>.997243</u>	<u>.995485</u>
<u>1.8083203</u>	<u>.995478</u>	<u>.992587</u>
<u>1.7444976</u>	<u>.995189</u>	<u>.992110</u>
<u>1.6987118</u>	<u>.994245</u>	<u>.990560</u>
<u>1.6730439</u>	<u>.993976</u>	<u>.990113</u>
<u>1.6612506</u>	<u>.994052</u>	<u>.990234</u>
<u>1.6570883</u>	<u>.994432</u>	<u>.990856</u>
<u>1.6557008</u>	<u>.995430</u>	<u>.992497</u>
<u>1.6529259</u>	<u>.990903</u>	<u>.985068</u>
<u>1.6348891</u>	<u>.990093</u>	<u>.983739</u>
<u>1.5953468</u>	<u>.989256</u>	<u>.982357</u>
<u>1.5349927</u>	<u>.986928</u>	<u>.978519</u>
<u>1.4649265</u>	<u>.984096</u>	<u>.973850</u>
<u>1.3969415</u>	<u>.981263</u>	<u>.969196</u>
<u>1.3504619</u>	<u>.978731</u>	<u>.965031</u>
<u>1.3227129</u>	<u>.975869</u>	<u>.960315</u>
<u>1.3102259</u>	<u>.976322</u>	<u>.961069</u>
<u>1.3046761</u>	<u>.975163</u>	<u>.959156</u>
<u>1.3032886</u>	<u>.974070</u>	<u>.957342</u>
<u>1.2991263</u>	<u>.974281</u>	<u>.957683</u>
<u>1.2797020</u>	<u>.973270</u>	<u>.956011</u>

TABLE 6.- Continued

(y) Concluded

$y, \text{ cm}$	$T_t/T_{t,e}$	F_T
1.2339152	.970873	.952061
1.1728684	.967225	.946023
1.0951712	.965059	.942427
1.0244113	.957708	.930344
.9730756	.950607	.918646
.9439392	.946053	.911103
.9286772	.944680	.908818
.9252086	.946523	.911811
.9231274	.949734	.917048
.9224337	.948794	.915457
.9106404	.948232	.914508
.8794228	.946517	.911625
.8253122	.941427	.903165
.7587147	.935714	.893719
.6879547	.929739	.883856
.6359254	.922550	.871923
.6026266	.917569	.863674
.5880584	.917079	.862797
.5825086	.913549	.856872
.5825086	.914523	.858396
.5811211	.915014	.859196
.5693278	.913360	.856423
.5353353	.909390	.849823
.4826122	.901620	.836860
.4118523	.895057	.825883
.3383174	.885200	.809485
.2807383	.879604	.800135
.2453583	.875562	.793430
.2287089	.872555	.788383
.2224654	.873348	.789658
.2210779	.871565	.786648
.2224654	.870587	.784968
.2155281	.871178	.785894
.1926352	.867592	.779915
.1482368	.861103	.769054
.0851079	.857787	.763411

TABLE 6.- Continued

(z) Total temperature profiles: Case 25; station 6; test 40; run 80;
 $P_{t,1} = 13\ 341.4\ \text{kPa}$; $T_t = 322.2\ \text{K}$; $T_w/T_t = 0.375$

Y, cm	$T_t/T_{t,e}$	F_T
2.7386153	.997395	.995840
2.7150289	.995996	.993606
2.6685494	.995654	.993061
2.6047268	.997260	.995625
2.5332715	.996807	.994900
2.4694490	.996629	.994614
2.4215827	.997197	.995520
2.3945266	.994991	.991993
2.3799597	.995690	.993110
2.3709401	.995806	.993294
2.3650862	.997028	.995246
2.3619231	.996596	.994553
2.3438866	.996813	.994900
2.3071176	.995718	.993145
2.2488449	.995082	.992127
2.1850223	.995953	.993519
2.1198129	.996219	.993944
2.0684769	.996447	.994307
2.0351775	.995561	.992885
2.0171410	.994509	.991197
2.0095108	.995002	.991985
2.0046544	.995444	.992692
1.9977176	.995509	.992796
1.9775983	.994501	.991175
1.9366687	.994688	.991474
1.8770092	.993476	.989526
1.8027802	.991124	.985747
1.7320209	.991477	.986308
1.6786047	.989617	.983316
1.6432225	.987394	.979734
1.6251860	.986847	.978852
1.6161690	.986272	.977921
1.6113125	.985531	.976725
1.6078429	.986989	.979066
1.5953562	.986950	.978996
1.5648330	.984664	.975312
1.5141905	.981512	.970234
1.4489811	.978306	.965060
1.3768324	.974707	.959254
1.3248030	.971832	.954593
1.2894234	.970753	.952833
1.2720803	.968454	.949117

TABLE 6.- Continued

(z) Concluded

y, cm	$T_t/T_{t,e}$	F_T
1.2623698	.968610	.949356
1.2582068	.967730	.947930
1.2533503	.967700	.947876
1.2429439	.968281	.948793
1.2145010	.967194	.947022
1.1666347	.961654	.938073
1.1021187	.958554	.933042
1.0292766	.953342	.924599
.9640672	.948772	.917187
.9196683	.945749	.912259
.8933078	.944608	.910384
.8801252	.941901	.905976
.8745779	.941577	.905432
.8724951	.942429	.906774
.8641715	.941576	.905363
.8426653	.939599	.902111
.7958793	.935390	.895255
.7406869	.928977	.884828
.6706210	.921624	.872874
.6095746	.916284	.864159
.5665622	.911727	.856706
.5422824	.906064	.847483
.5297957	.905353	.846285
.5256327	.902827	.842165
.5242458	.903420	.843080
.5166157	.903846	.843746
.4978832	.900929	.838931
.4597298	.893739	.827202
.4000678	.886617	.815597
.3334715	.874616	.796073
.2651793	.862408	.776159
.2155393	.853463	.761557
.1870964	.847759	.752191
.1718335	.844001	.746022
.1669771	.842537	.743591
.1662836	.840247	.739786
.1614272	.839719	.738884
.1454709	.837672	.735417
.1093978	.830927	.724307
.0518185	.823828	.712663

TABLE 6.- Continued

(aa) Total temperature profiles: Case 26; station 7; test 40; run 91;
 $P_{t,1} = 13\ 341.4\ \text{kPa}$; $T_t = 327.2\ \text{K}$; $T_w/T_t = 0.383$

$y, \text{ cm}$	$T_t/T_{t,e}$	F_T
<u>3.4960985</u>	<u>.999006</u>	<u>.998407</u>
<u>3.4891612</u>	<u>.999766</u>	<u>.999626</u>
<u>3.4246448</u>	<u>1.000118</u>	<u>1.000190</u>
<u>3.2963057</u>	<u>.999971</u>	<u>.999954</u>
<u>3.1832286</u>	<u>.999817</u>	<u>.999706</u>
<u>3.1381365</u>	<u>.998851</u>	<u>.998154</u>
<u>3.1242620</u>	<u>.999468</u>	<u>.999145</u>
<u>3.1062251</u>	<u>.999461</u>	<u>.999134</u>
<u>3.0208970</u>	<u>1.000309</u>	<u>1.000498</u>
<u>2.8946391</u>	<u>.999213</u>	<u>.998733</u>
<u>2.8190231</u>	<u>1.000102</u>	<u>1.000165</u>
<u>2.7926615</u>	<u>.998852</u>	<u>.998151</u>
<u>2.7843368</u>	<u>.998408</u>	<u>.997434</u>
<u>2.7330012</u>	<u>.999191</u>	<u>.998696</u>
<u>2.6067433</u>	<u>.998909</u>	<u>.998241</u>
<u>2.4749356</u>	<u>.998973</u>	<u>.998344</u>
<u>2.4111129</u>	<u>.999366</u>	<u>.998977</u>
<u>2.3923823</u>	<u>.998931</u>	<u>.998274</u>
<u>2.3771204</u>	<u>.999277</u>	<u>.998831</u>
<u>2.3021981</u>	<u>.999260</u>	<u>.998804</u>
<u>2.1683092</u>	<u>.999194</u>	<u>.998696</u>
<u>2.0781250</u>	<u>.998562</u>	<u>.997675</u>
<u>2.0455199</u>	<u>.998241</u>	<u>.997154</u>
<u>2.0358078</u>	<u>.998051</u>	<u>.996844</u>
<u>2.0038964</u>	<u>.997570</u>	<u>.996062</u>
<u>1.8984503</u>	<u>.995618</u>	<u>.992900</u>
<u>1.7645614</u>	<u>.993539</u>	<u>.989518</u>
<u>1.6951889</u>	<u>.992208</u>	<u>.987351</u>
<u>1.6750709</u>	<u>.991696</u>	<u>.986516</u>
<u>1.6660524</u>	<u>.991910</u>	<u>.986850</u>
<u>1.6063921</u>	<u>.990242</u>	<u>.984134</u>
<u>1.4773593</u>	<u>.984819</u>	<u>.975302</u>
<u>1.3719131</u>	<u>.981667</u>	<u>.970148</u>
<u>1.3316771</u>	<u>.980336</u>	<u>.967963</u>
<u>1.3219649</u>	<u>.980366</u>	<u>.967992</u>
<u>1.2997658</u>	<u>.979111</u>	<u>.965953</u>
<u>1.2061129</u>	<u>.975621</u>	<u>.960245</u>
<u>1.0659805</u>	<u>.969606</u>	<u>.950419</u>
<u>.9834272</u>	<u>.964637</u>	<u>.942277</u>
<u>.9612280</u>	<u>.963619</u>	<u>.940560</u>
<u>.9549845</u>	<u>.962994</u>	<u>.939505</u>
<u>.9078112</u>	<u>.961124</u>	<u>.936385</u>

TABLE 6.- Continued

(aa) Concluded

y, cm	$T_t/T_{t,e}$	F_T
<u>.7836345</u>	<u>.953051</u>	<u>.923132</u>
<u>.6594578</u>	<u>.941090</u>	<u>.903491</u>
<u>.6053472</u>	<u>.935594</u>	<u>.894432</u>
<u>.5942476</u>	<u>.935218</u>	<u>.893757</u>
<u>.5831480</u>	<u>.933270</u>	<u>.890471</u>
<u>.5054509</u>	<u>.926456</u>	<u>.879237</u>
<u>.3701745</u>	<u>.912539</u>	<u>.856264</u>
<u>.2765217</u>	<u>.901686</u>	<u>.838353</u>
<u>.2473852</u>	<u>.897856</u>	<u>.832027</u>
<u>.2425292</u>	<u>.895549</u>	<u>.828156</u>
<u>.2113115</u>	<u>.891658</u>	<u>.821704</u>
<u>.0996218</u>	<u>.879647</u>	<u>.801860</u>

TABLE 6:- Continued

(bb) Total temperature profiles: Case 27; station 8; test 40; run 86;
 $P_{t,1} = 13\,444.9$ kPa; $T_t = 332.2$ K; $T_w/T_t = 0.333$

y , cm	$T_t/T_{t,e}$	F_T
3.6130655	1.003301	1.004896
3.5665859	1.002937	1.004360
3.5409181	1.002592	1.003850
3.5249624	1.002152	1.003199
3.5180252	1.001966	1.002924
3.5124754	1.003005	1.004470
3.5069256	1.002504	1.003726
3.4833389	1.003961	1.005895
3.4382468	1.004235	1.006303
3.3716492	1.001329	1.001979
3.2953395	1.000639	1.000951
3.2204172	1.002194	1.003271
3.1649192	1.001901	1.002837
3.1288456	1.001637	1.002446
3.1108087	1.000172	1.000258
3.0983217	1.000370	1.000554
3.0927719	.999640	.999461
3.0851409	1.001861	1.002786
3.0657166	1.001361	1.002036
3.0240931	1.001774	1.002656
2.9630453	1.000850	1.001272
2.8867356	1.003043	1.004553
2.8083447	1.000869	1.001301
2.7438283	1.000032	1.000048
2.7028985	.999008	.998514
2.6765370	.999996	.999994
2.6668248	.998897	.998346
2.6591939	1.000118	1.000178
2.6529503	.996560	.994835
2.6293637	.998802	.998202
2.5856590	.998348	.997518
2.5197552	.997566	.996344
2.4413643	.996221	.994325
2.3601985	.994903	.992347
2.2991507	.994817	.992218
2.2596084	.992406	.988597
2.2381029	.990245	.985348
2.2256159	.989998	.984969
2.2200661	.989427	.984103
2.2152100	.990508	.985717
2.2041104	.989467	.984143
2.1708116	.987910	.981794

TABLE 6.- Continued

(bb) Continued

y, cm	$T_t/T_{t,e}$	F_T
2.1167011	.987003	.980430
2.0445537	.984983	.977388
1.9661628	.983692	.975449
1.8954029	.981159	.971641
1.8482296	.978860	.968183
1.8197869	.977920	.966765
1.8072998	.979021	.968421
1.8003626	.976082	.963989
1.7962002	.975505	.963106
1.7830194	.975630	.963275
1.7524956	.974468	.961499
1.6990787	.972133	.957956
1.6304000	.968899	.953053
1.5492342	.963313	.944613
1.4770868	.961671	.942137
1.4257512	.959608	.939029
1.3973085	.958457	.937305
1.3827402	.957717	.936202
1.3771904	.956766	.934769
1.3751093	.956252	.933994
1.3695595	.956989	.935096
1.3425042	.952538	.928344
1.2960246	.948934	.922865
1.2273459	.945438	.917526
1.1489550	.940531	.910060
1.0733390	.935376	.902225
1.0192284	.930893	.895429
.9873171	.929185	.892857
.9713614	.928956	.892528
.9637305	.927769	.890752
.9609556	.927097	.889735
.9560995	.927220	.889922
.9373689	.926233	.888421
.8943580	.924062	.885105
.8333102	.917402	.874989
.7549193	.911263	.865622
.6758347	.899800	.848184
.6127057	.894205	.839594
.5745508	.890169	.833393
.5544328	.888305	.830530
.5474956	.885392	.826099
.5433332	.886540	.827867
.5419458	.885029	.825596

TABLE 6.- Concluded

(bb) Concluded

y, cm	$T_t/T_{t,e}$	F_T
.5239089	.883747	.823651
.4815917	.878115	.815116
.4198502	.872321	.806278
.3428468	.863959	.793574
.2623747	.857265	.783324
.1999395	.848825	.770420
.1617846	.844039	.763004
.1444415	.842069	.759876
.1375042	.841080	.758247
.1361168	.839231	.755321
.1340356	.838277	.753827
.1243234	.836140	.750558
.0924121	.832478	.745006

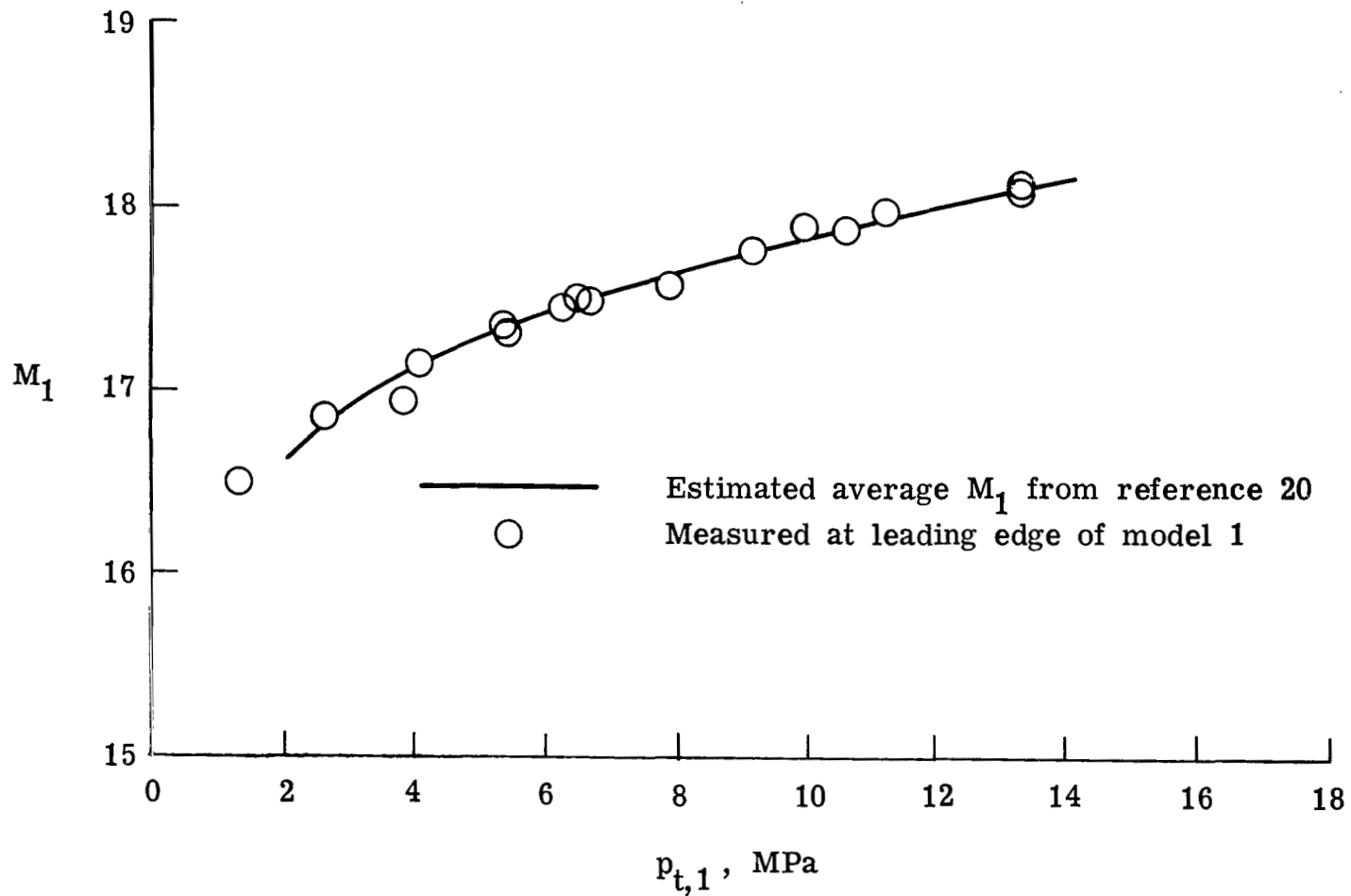
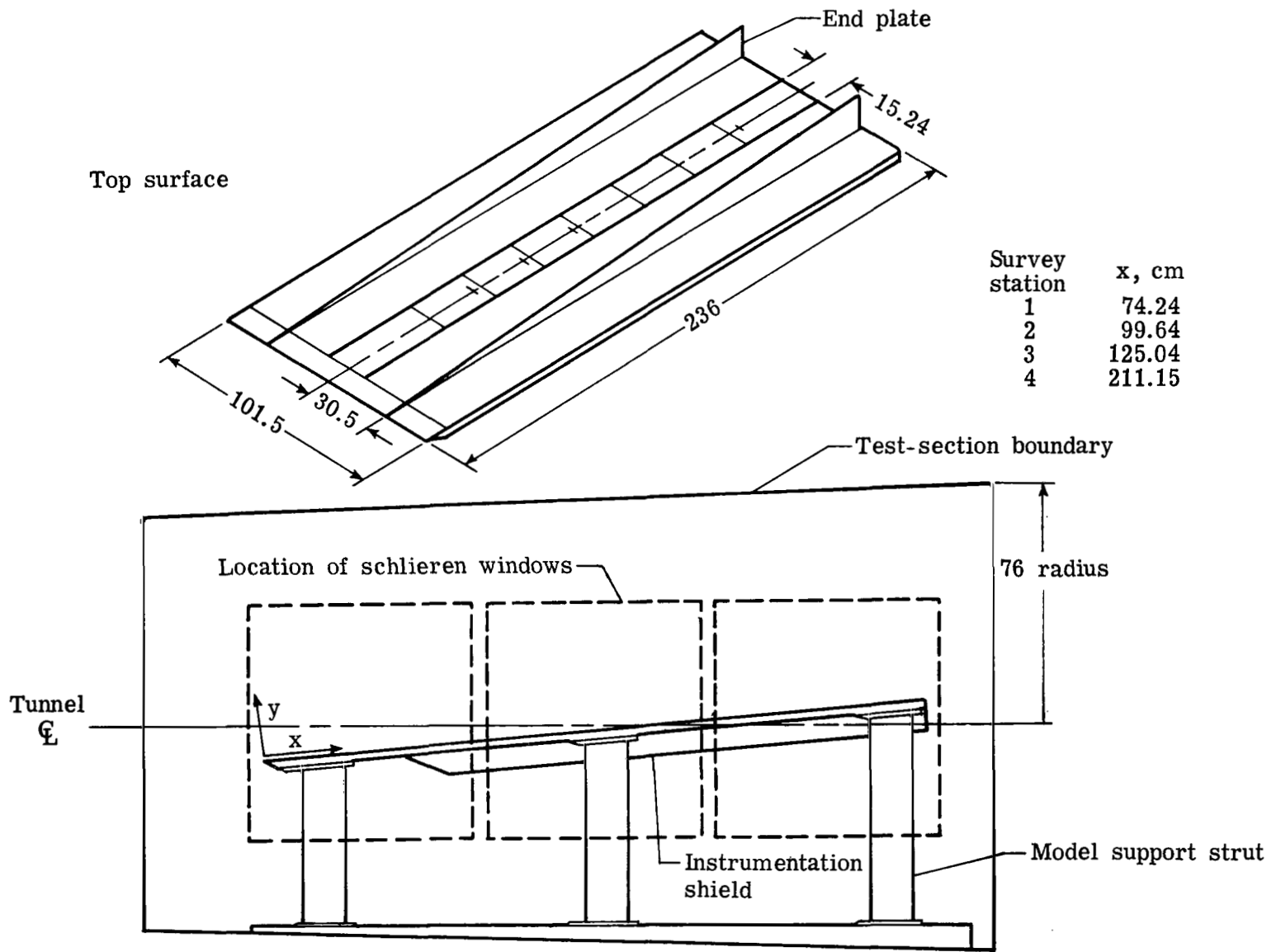
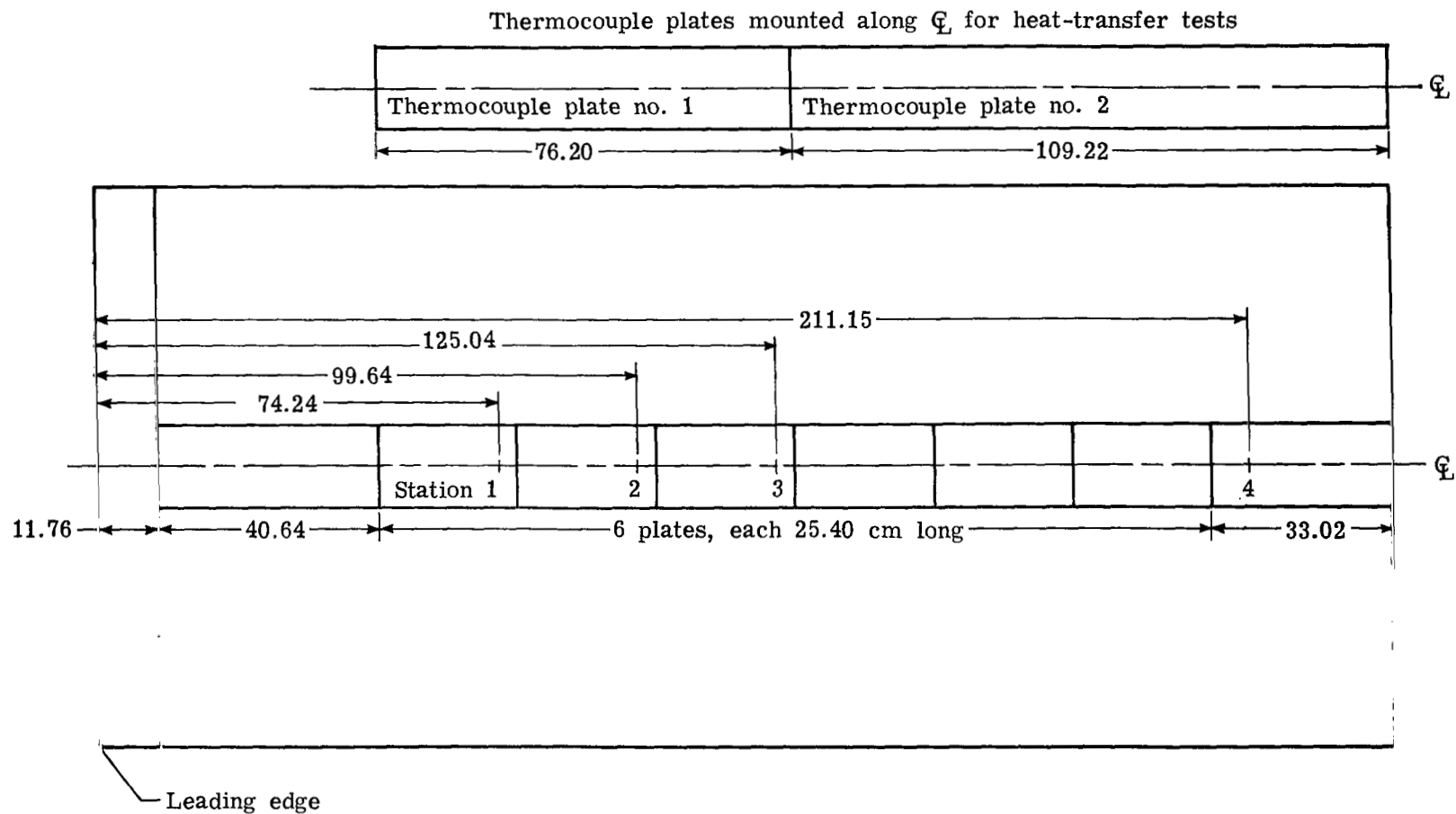


Figure 1.- Free-stream Mach number at leading edge of model 1.



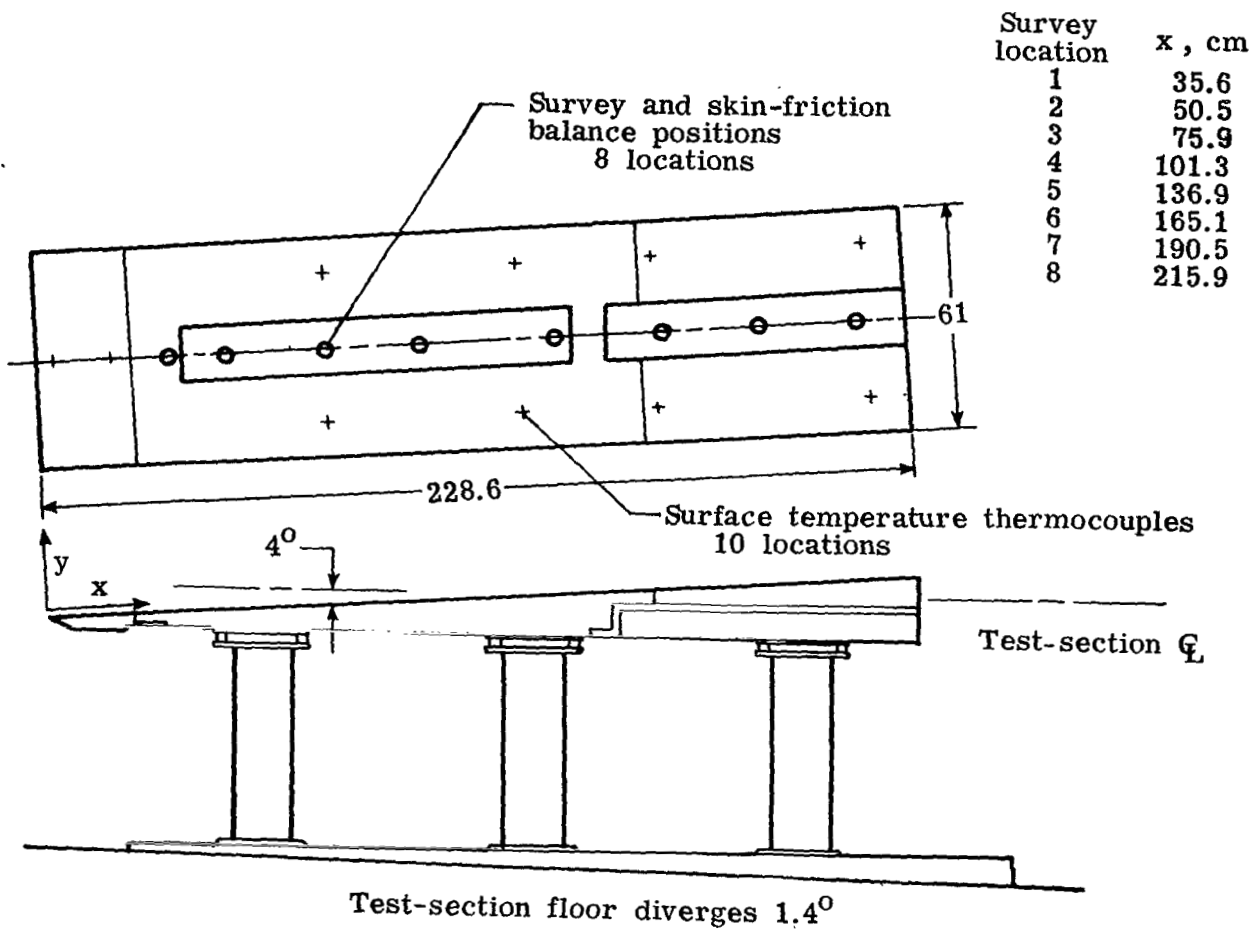
(a) Model 1. Dimensions are in cm.

Figure 2.- Model sketches.



(b) Plan view of model 1 showing instrumentation plates.

Figure 2.- Continued.



(c) Model 2. Dimensions are in cm.

Figure 2.- Concluded.

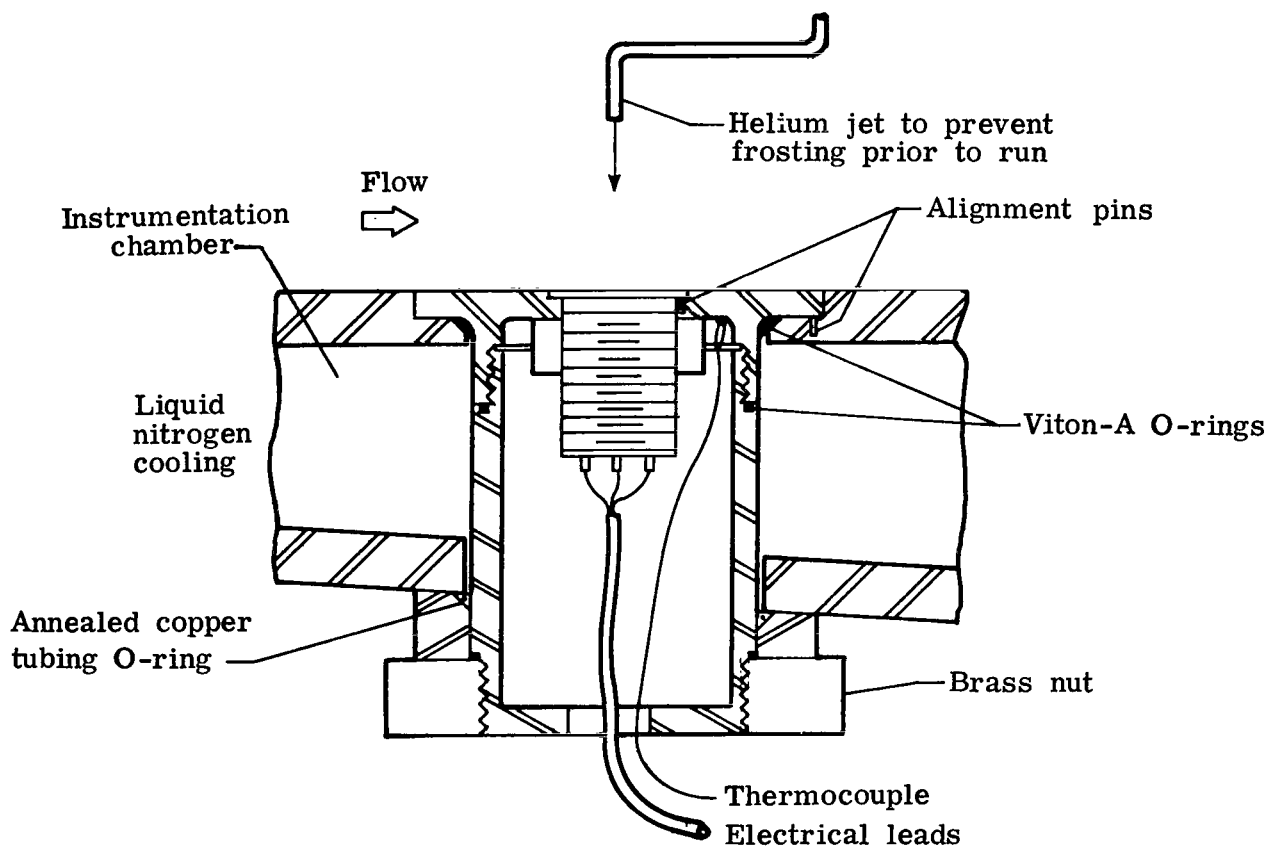


Figure 3.- Skin-friction balance mounting arrangement for model 2.

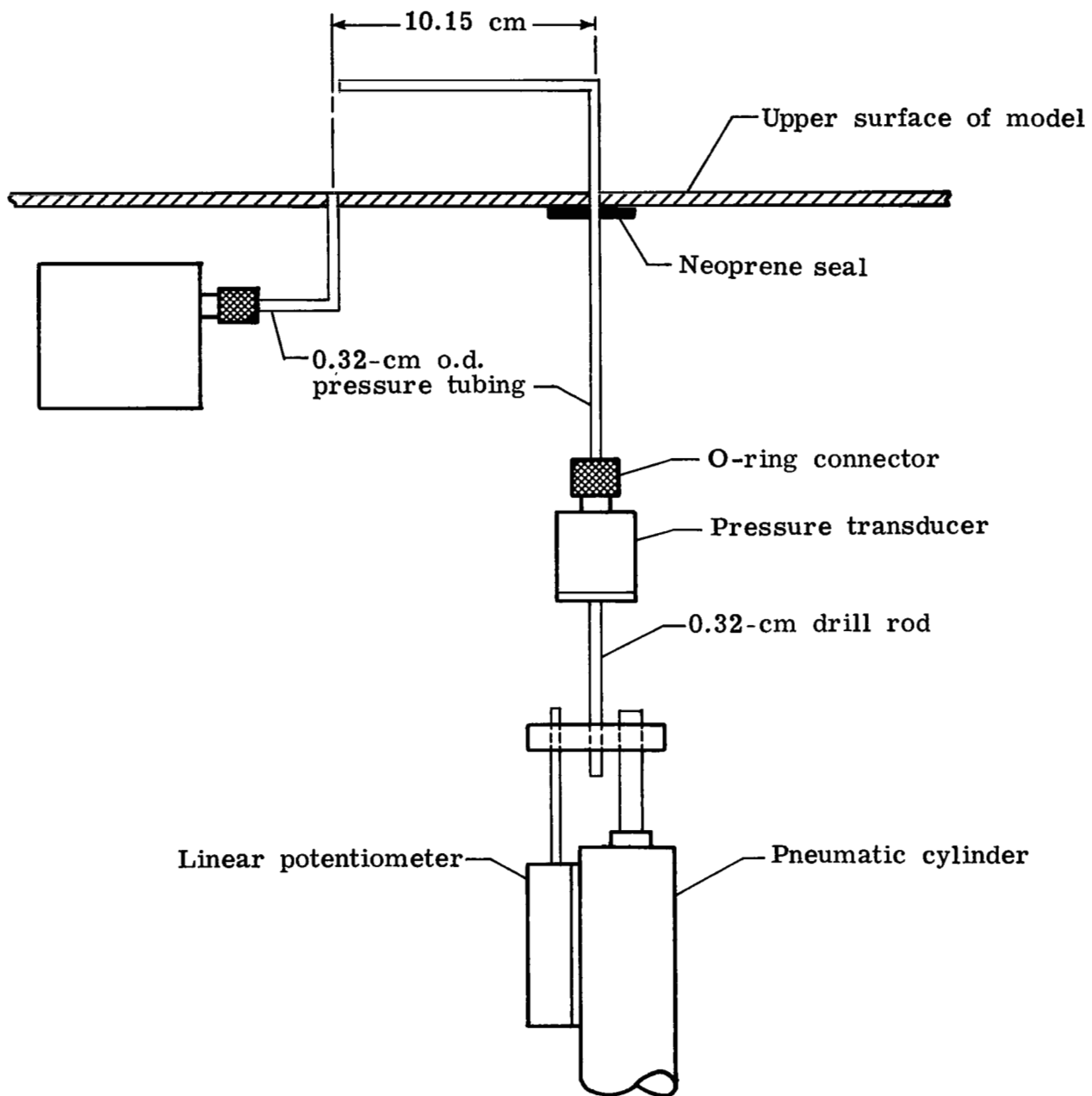
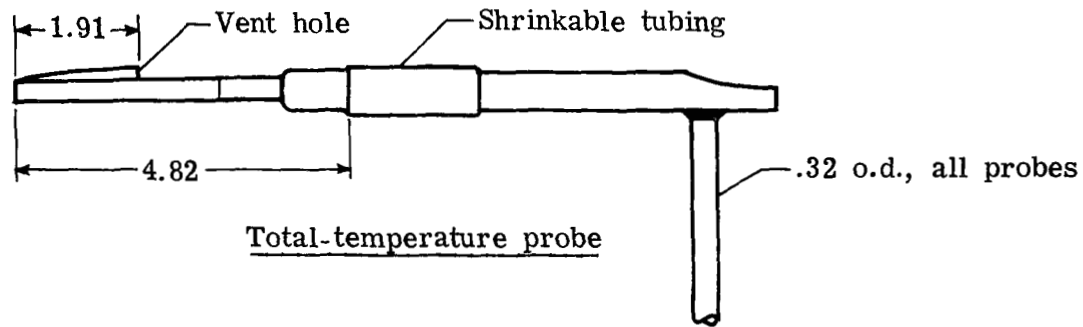
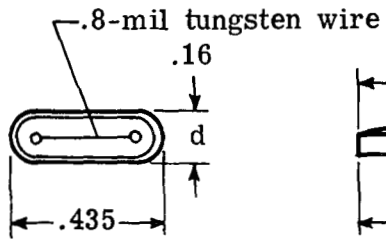
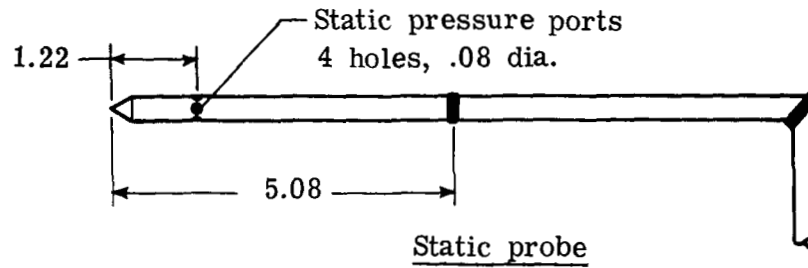
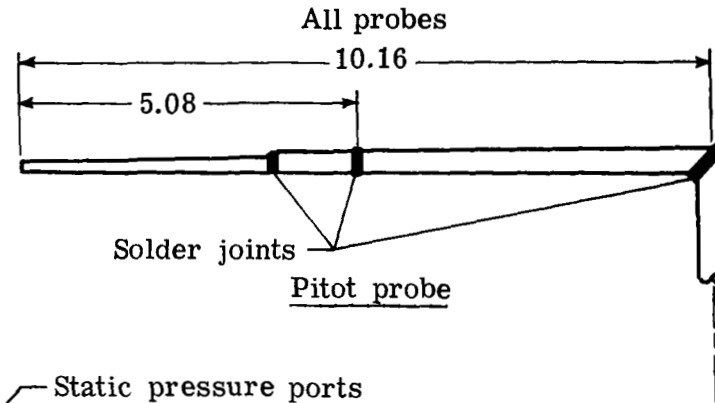
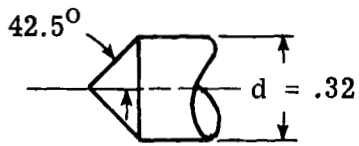
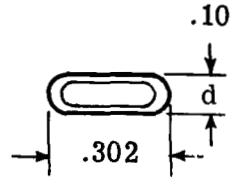


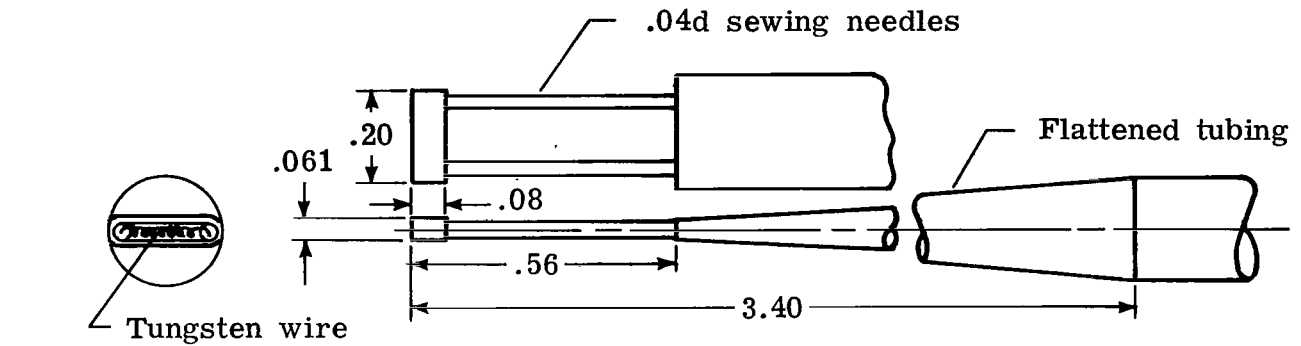
Figure 4.- Survey mechanism for model 1.

Tip details
External dimensions



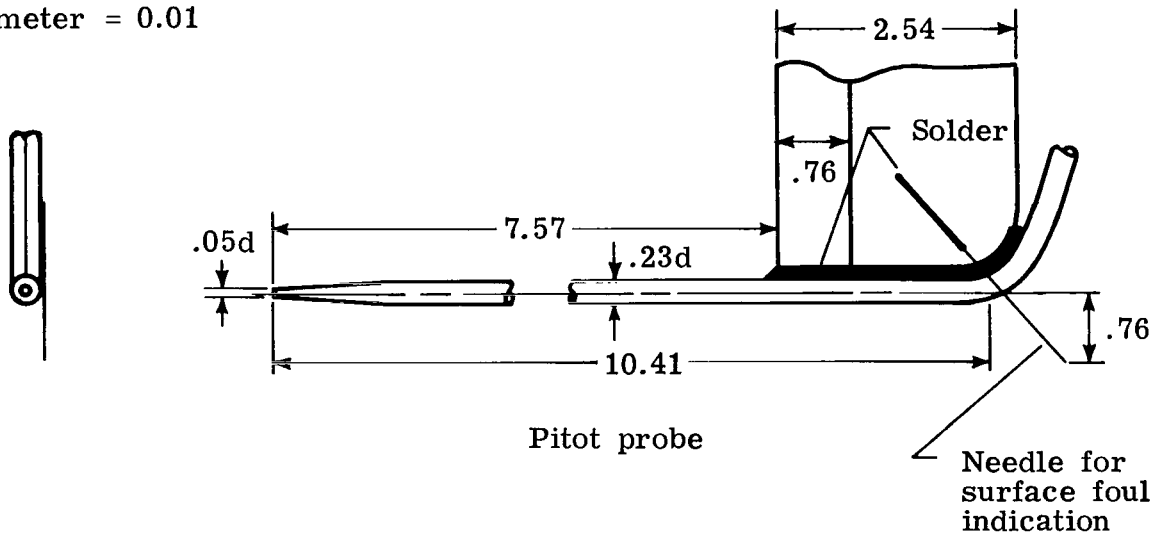
(a) Probes for model 1. Dimensions are in cm.

Figure 5.- Probe details.



Wire diameter = 0.001
 Coil diameter = 0.01

Fine wire probe



Pitot probe

(b) Probes for model 2.

Figure 5.- Concluded.

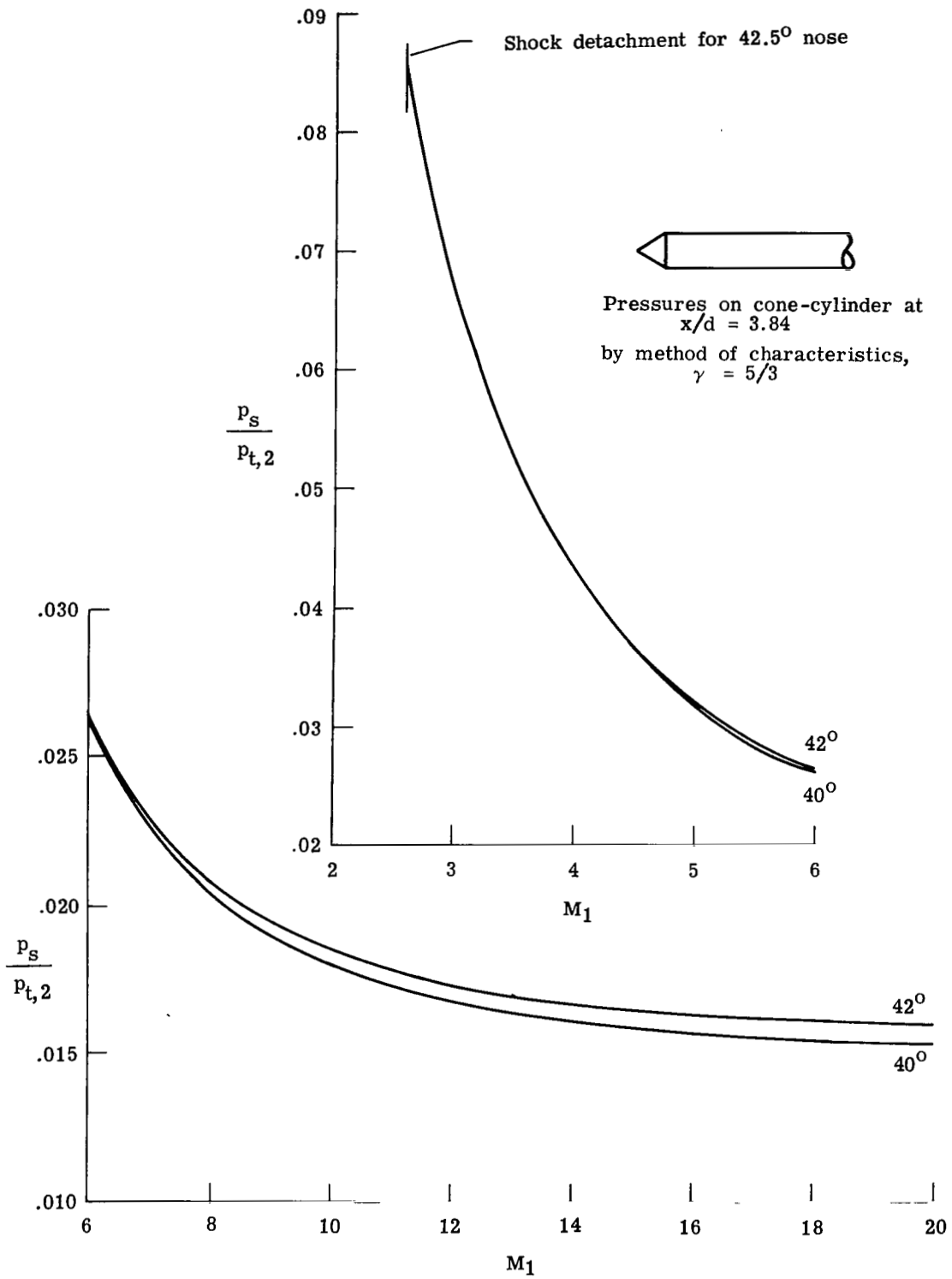


Figure 6.- Static-pressure probe calibration. Inviscid theory.

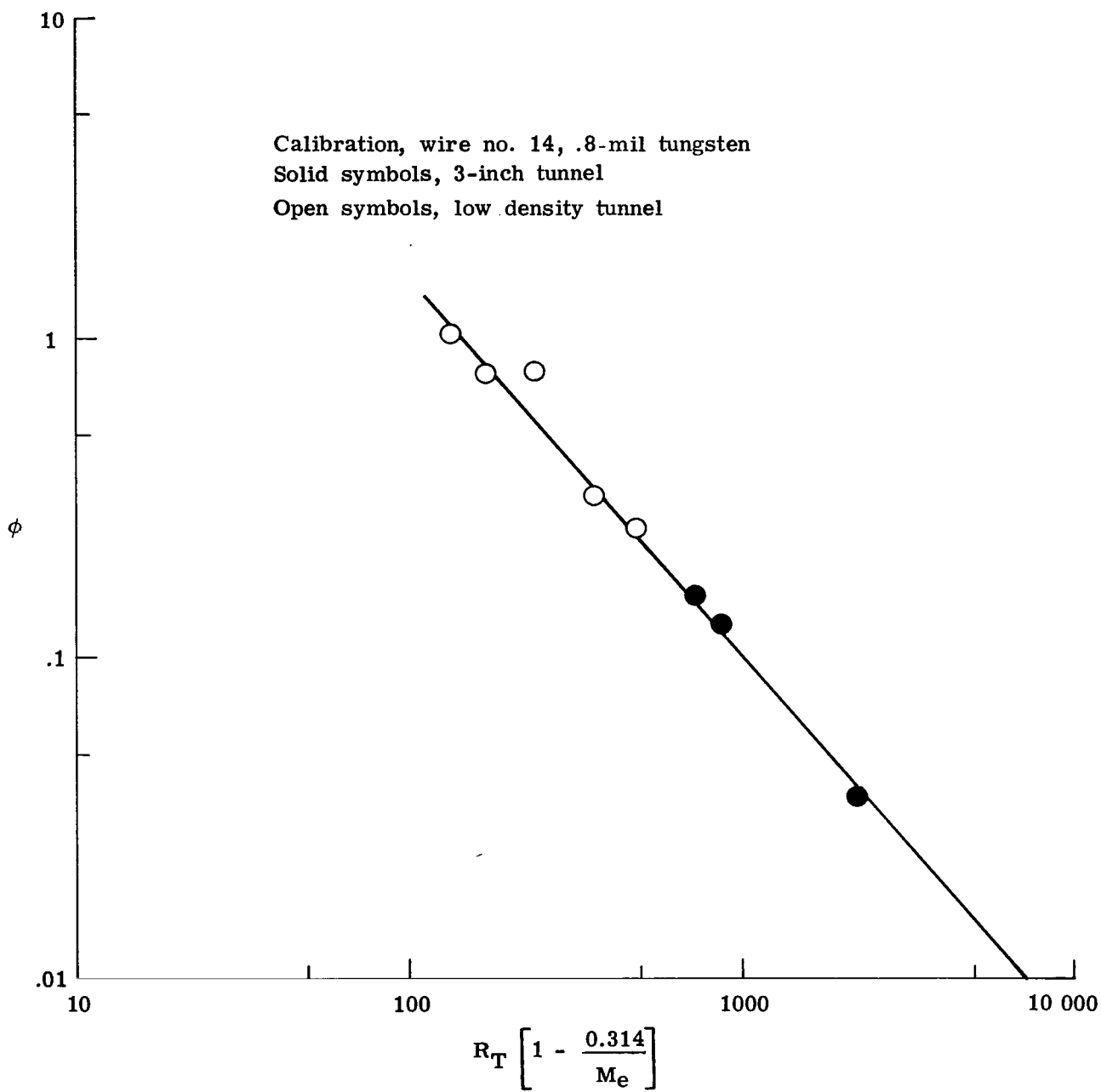


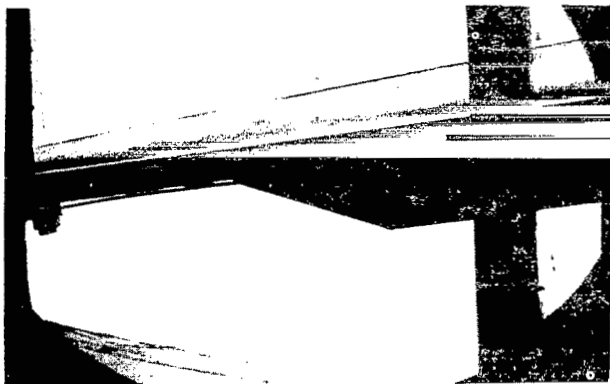
Figure 7.- Calibration of fine-wire total-temperature probe used on model 1.



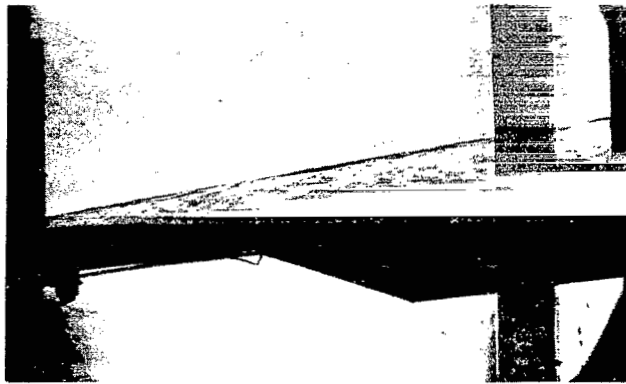
(a) $M_1 = 16.5$; $R_1/m = 5.48 \times 10^6$.



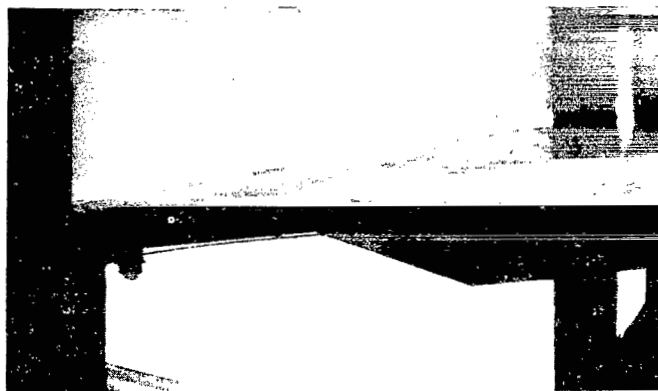
(b) $M_1 = 16.9$; $R_1/m = 14.14 \times 10^6$.



(c) $M_1 = 17.5$; $R_1/m = 25.03 \times 10^6$.



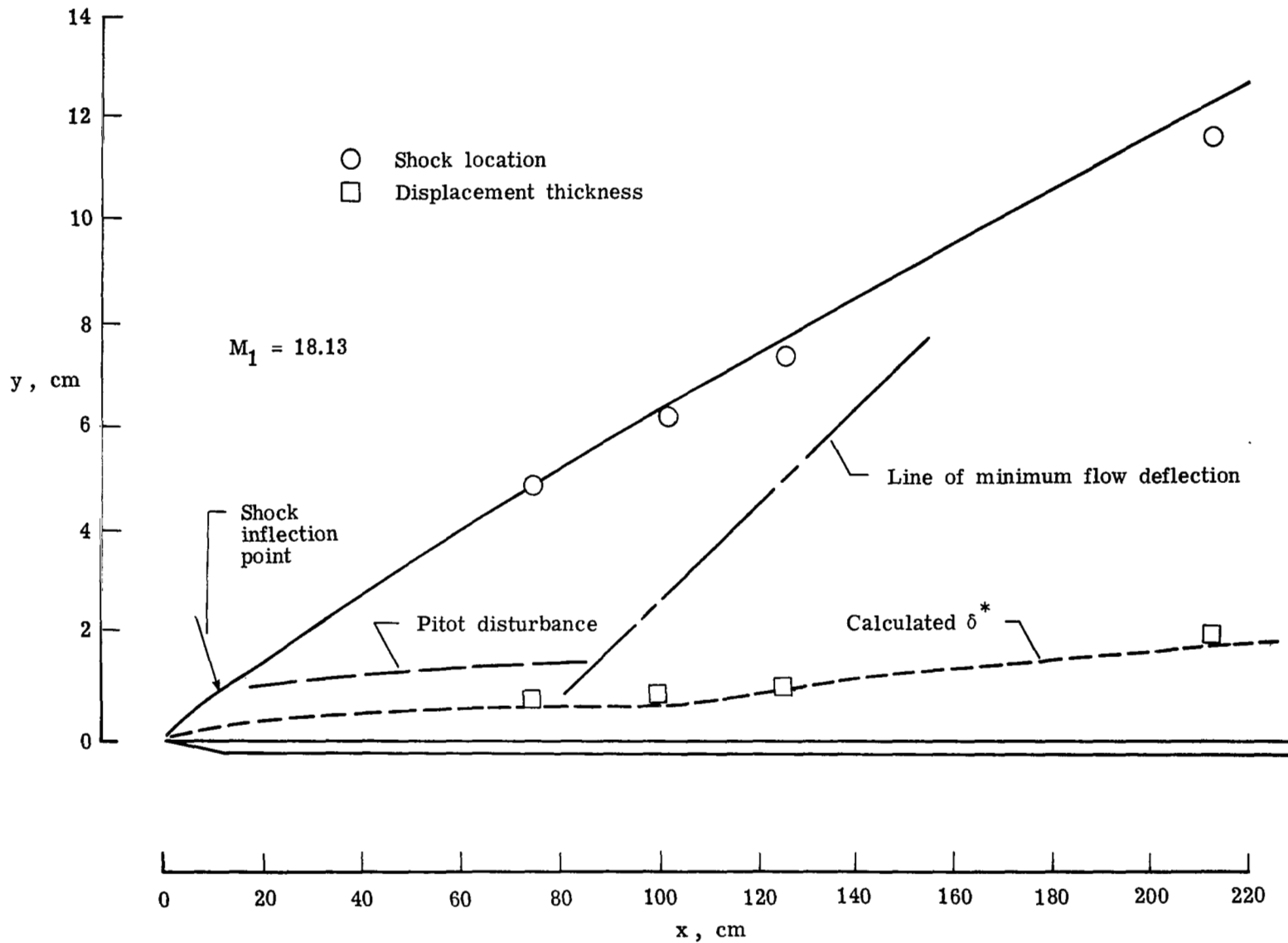
(d) $M_1 = 17.9$; $R_1/m = 37.57 \times 10^6$.



(e) $M_1 = 18.0$; $R_1/m = 42.33 \times 10^6$.

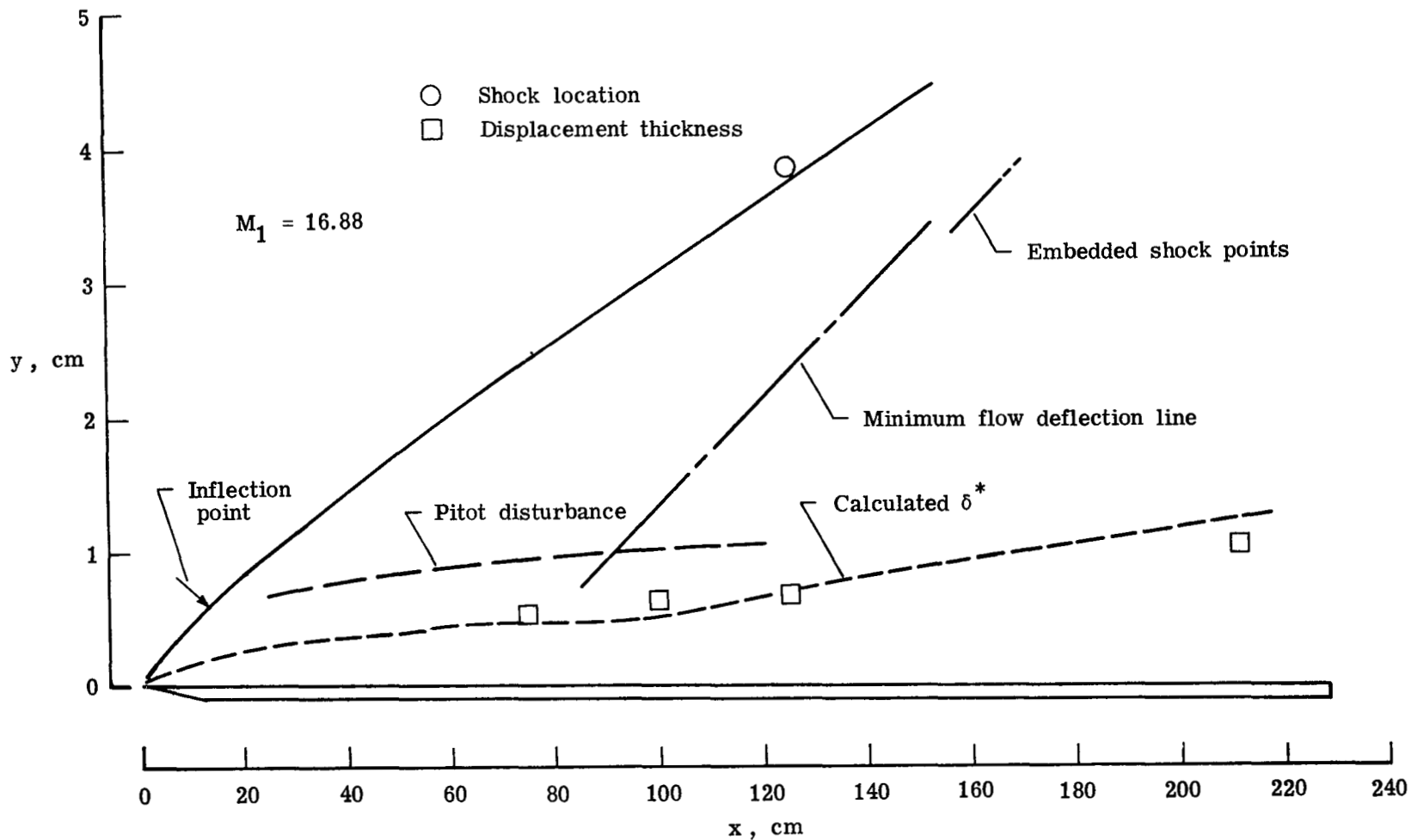
L-78-105

Figure 8.- Schlieren photographs of model 1.



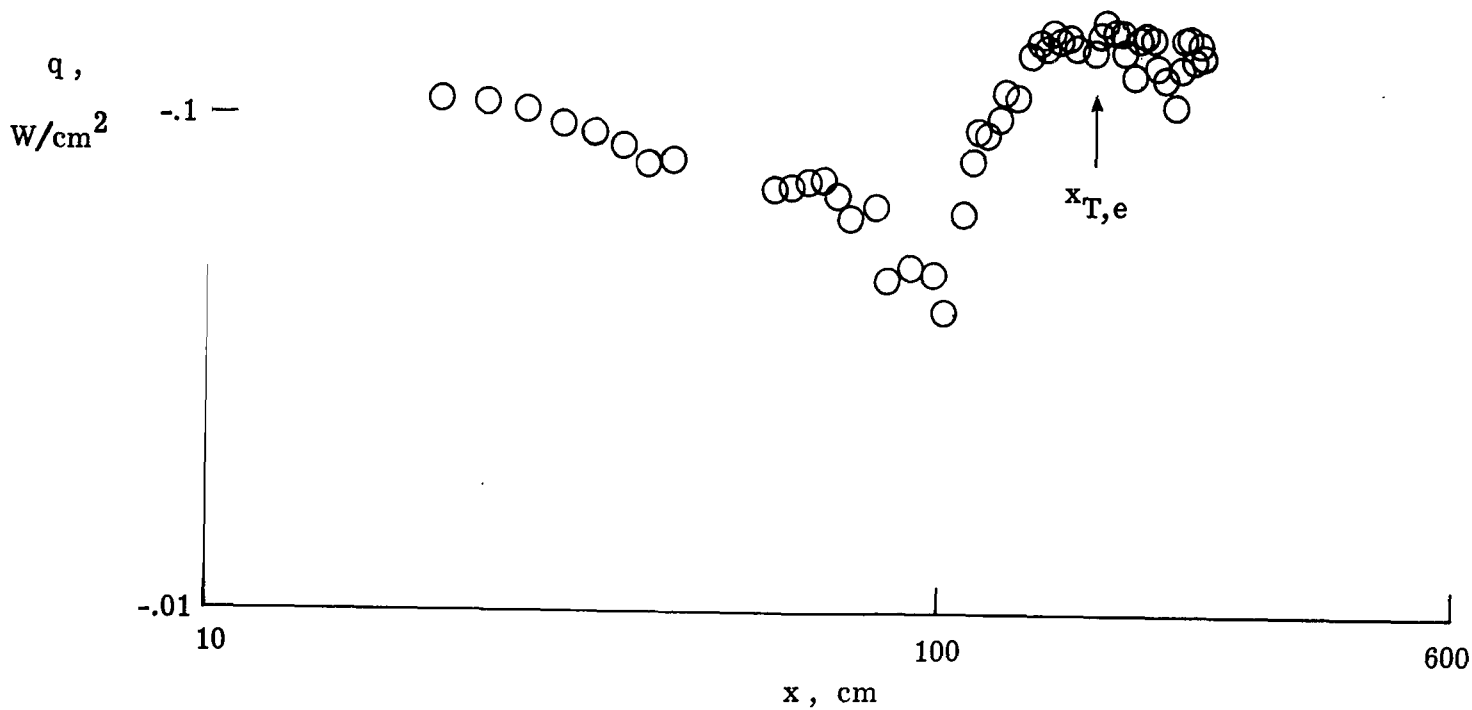
(a) Flow field at $R_1/m = 34.5 \times 10^6$.

Figure 9.- Flow field details for model 1.



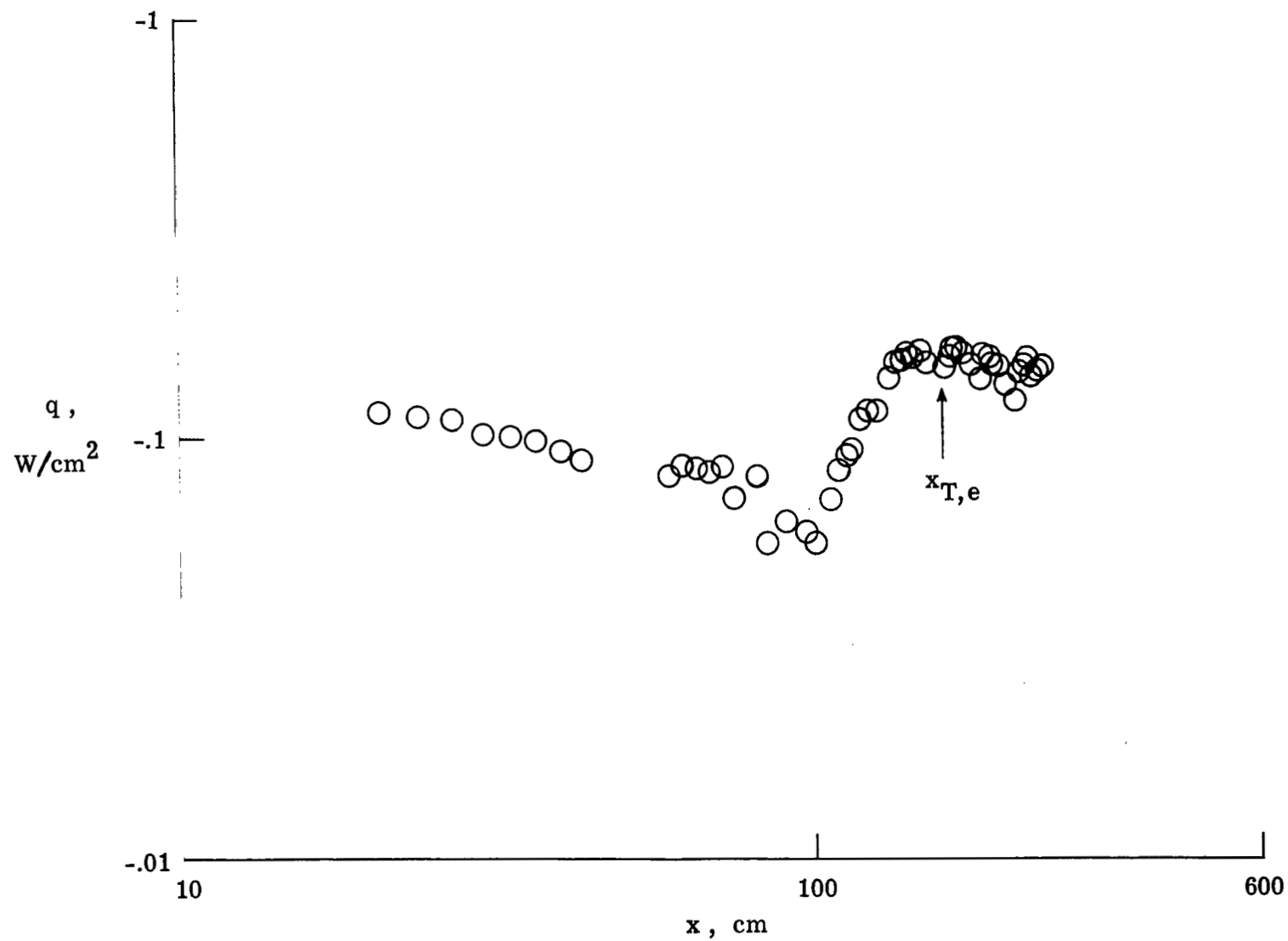
(b) Flow field at $R_1/m = 7.8 \times 10^6$.

Figure 9.- Concluded.



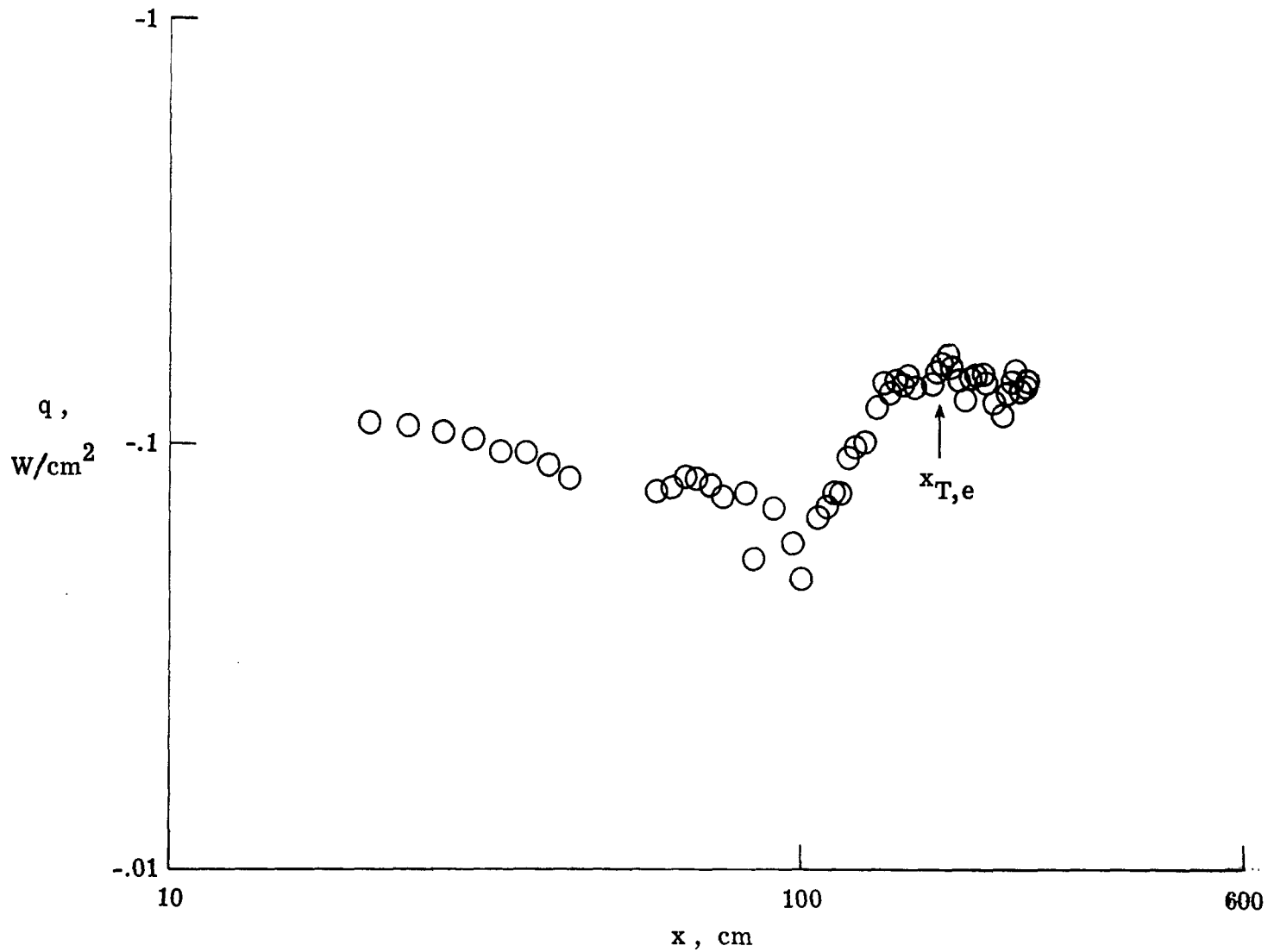
(a) $R_1/m = 43.18 \times 10^6$; $T_w/T_t = 0.92$.

Figure 10.- Heat-transfer data on model 1.



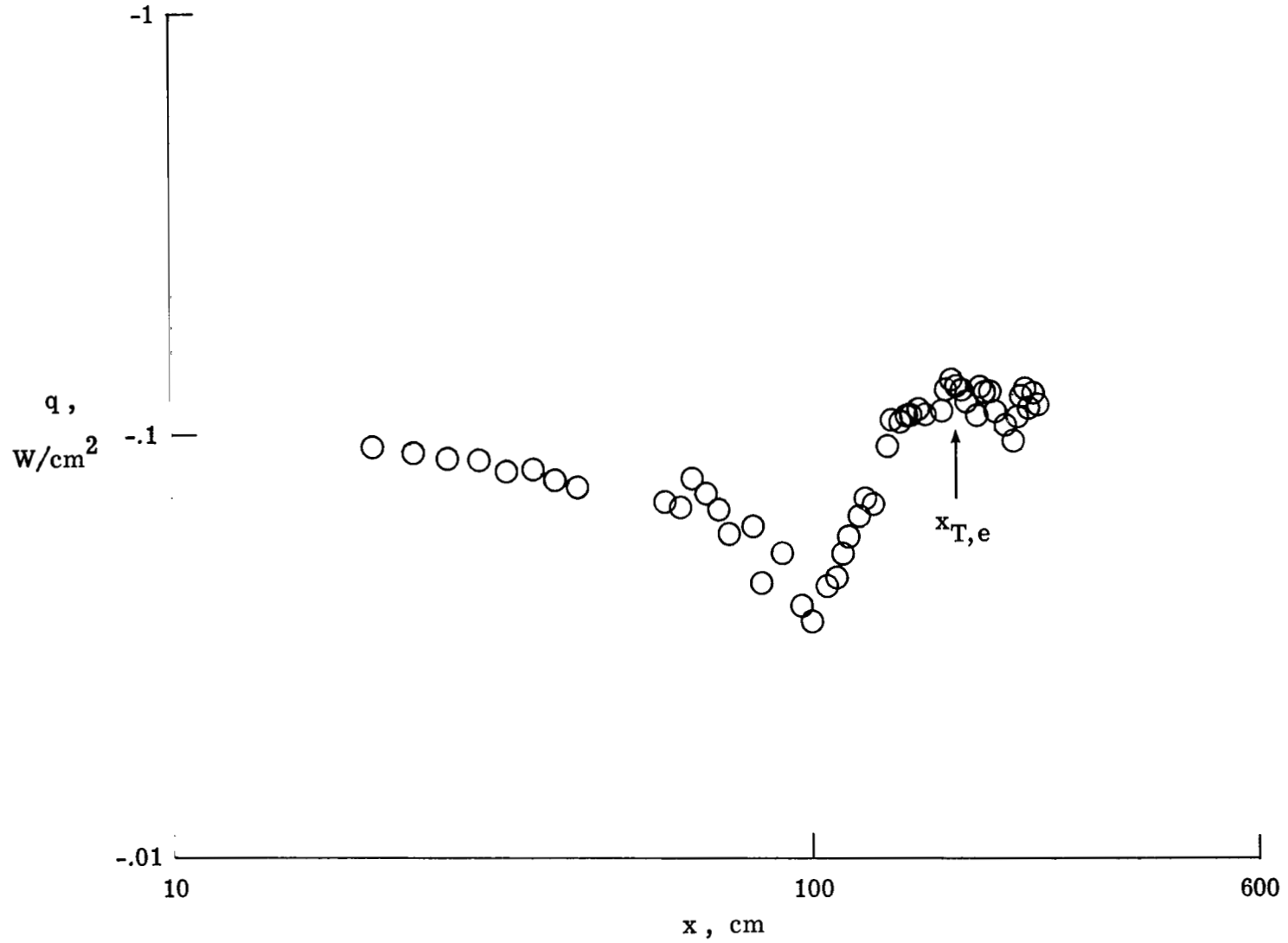
(b) $R_1/m = 39.91 \times 10^6$; $T_w/T_t = 0.94$.

Figure 10.- Continued.



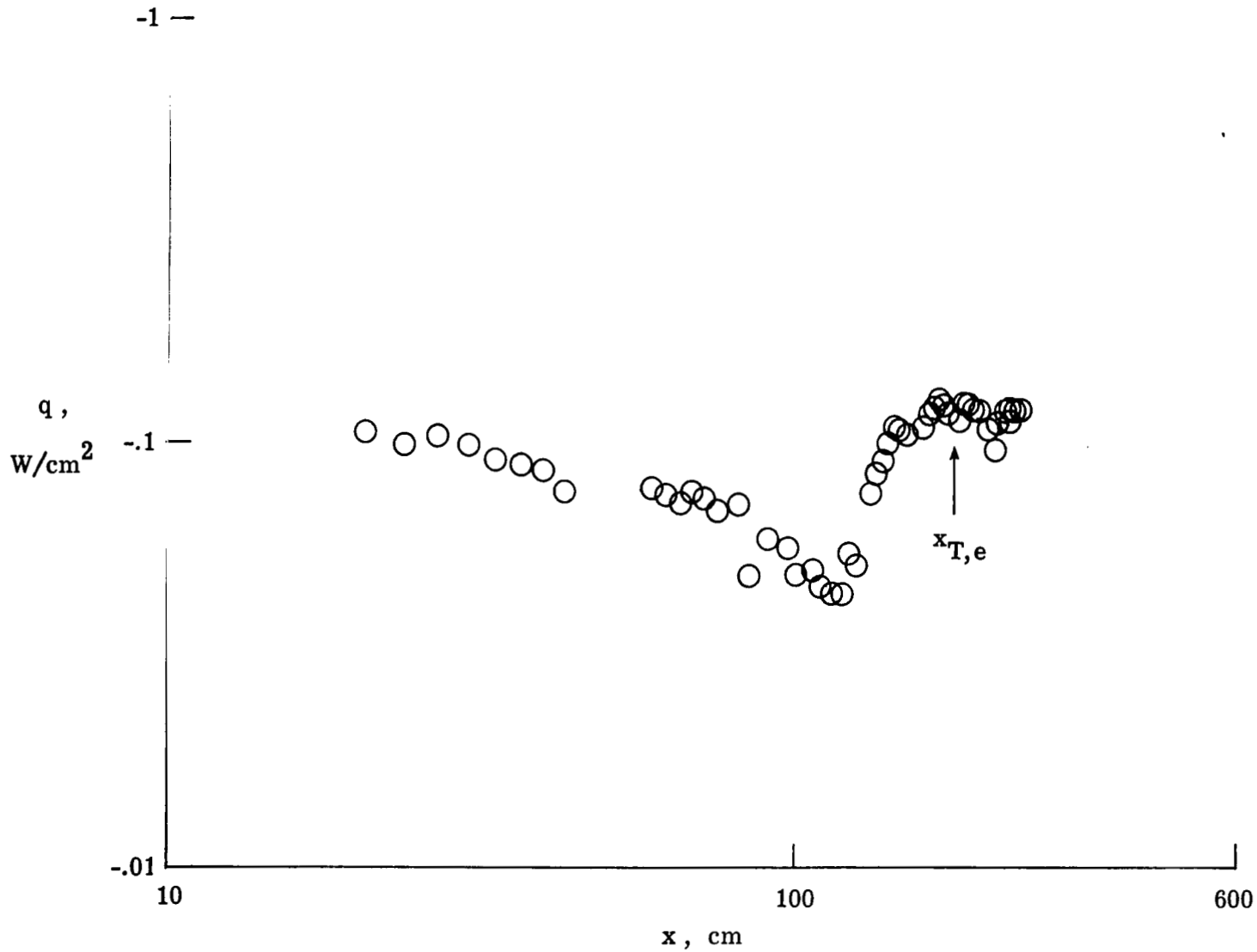
(c) $R_1/m = 36.24 \times 10^6$; $T_w/T_t = 0.94$.

Figure 10.- Continued.



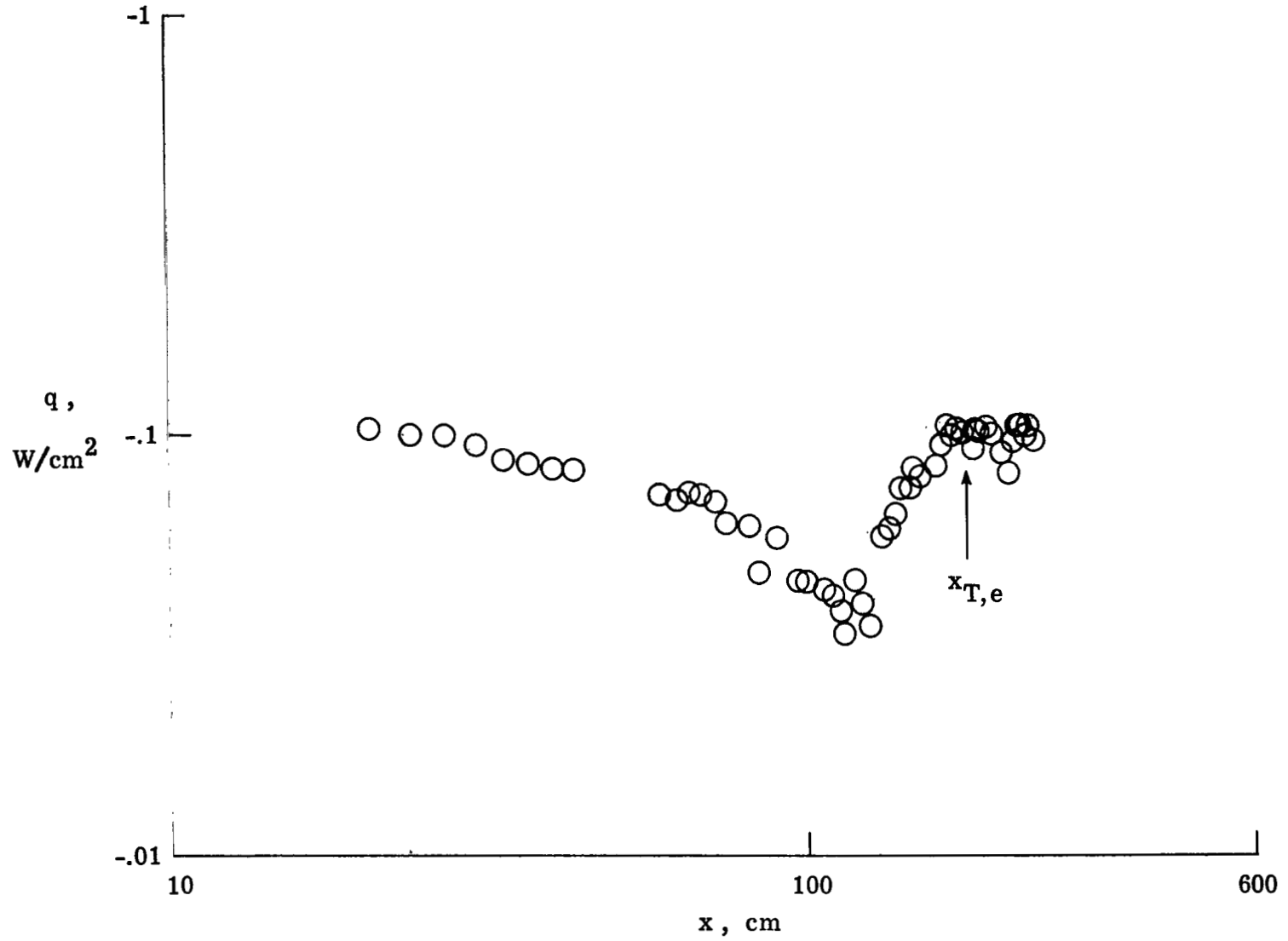
(d) $R_1/m = 31.07 \times 10^6$; $T_w/T_t = 0.94$.

Figure 10.- Continued.



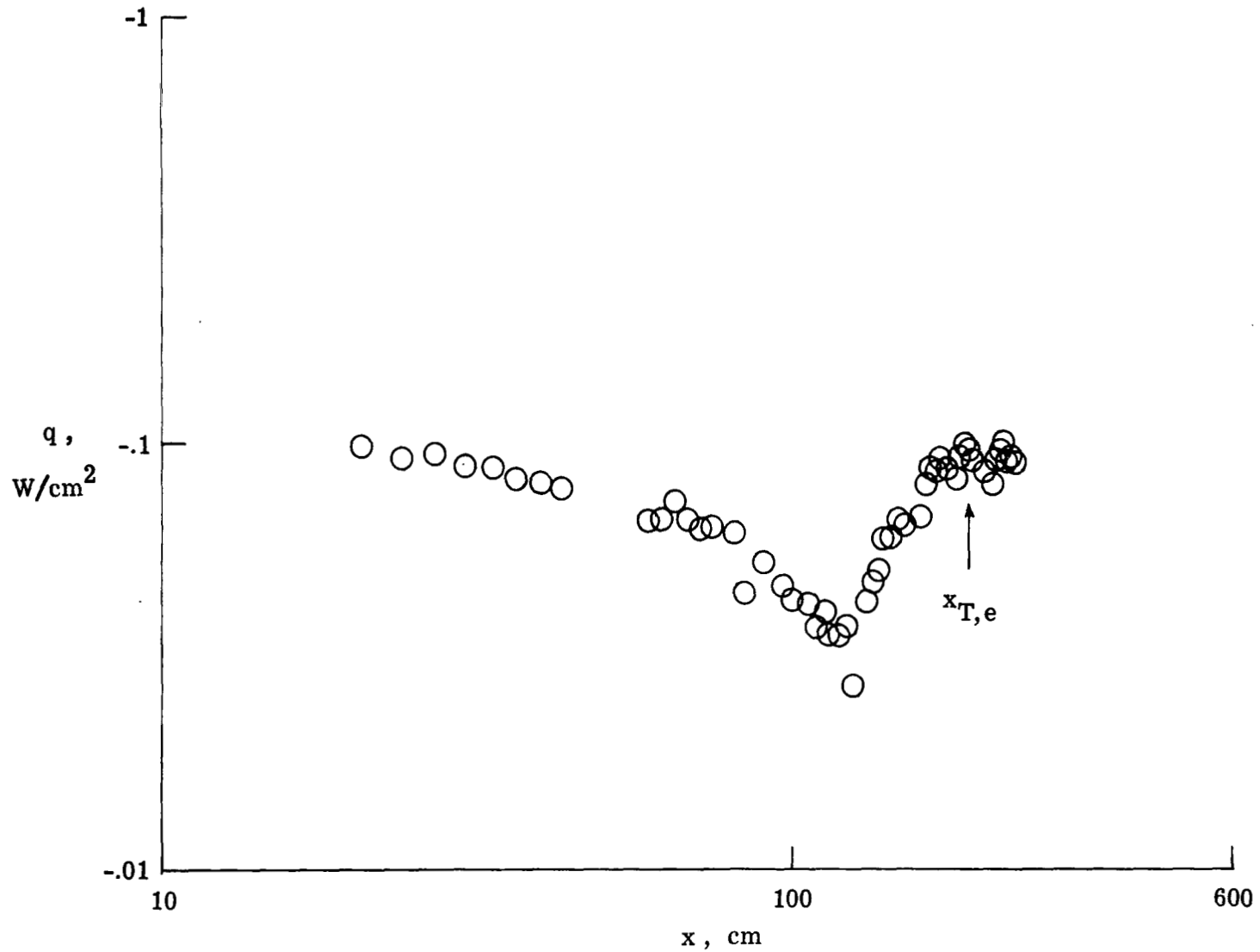
(e) $R_1/m = 27.31 \times 10^6$; $T_w/T_t = 0.95$.

Figure 10.- Continued.



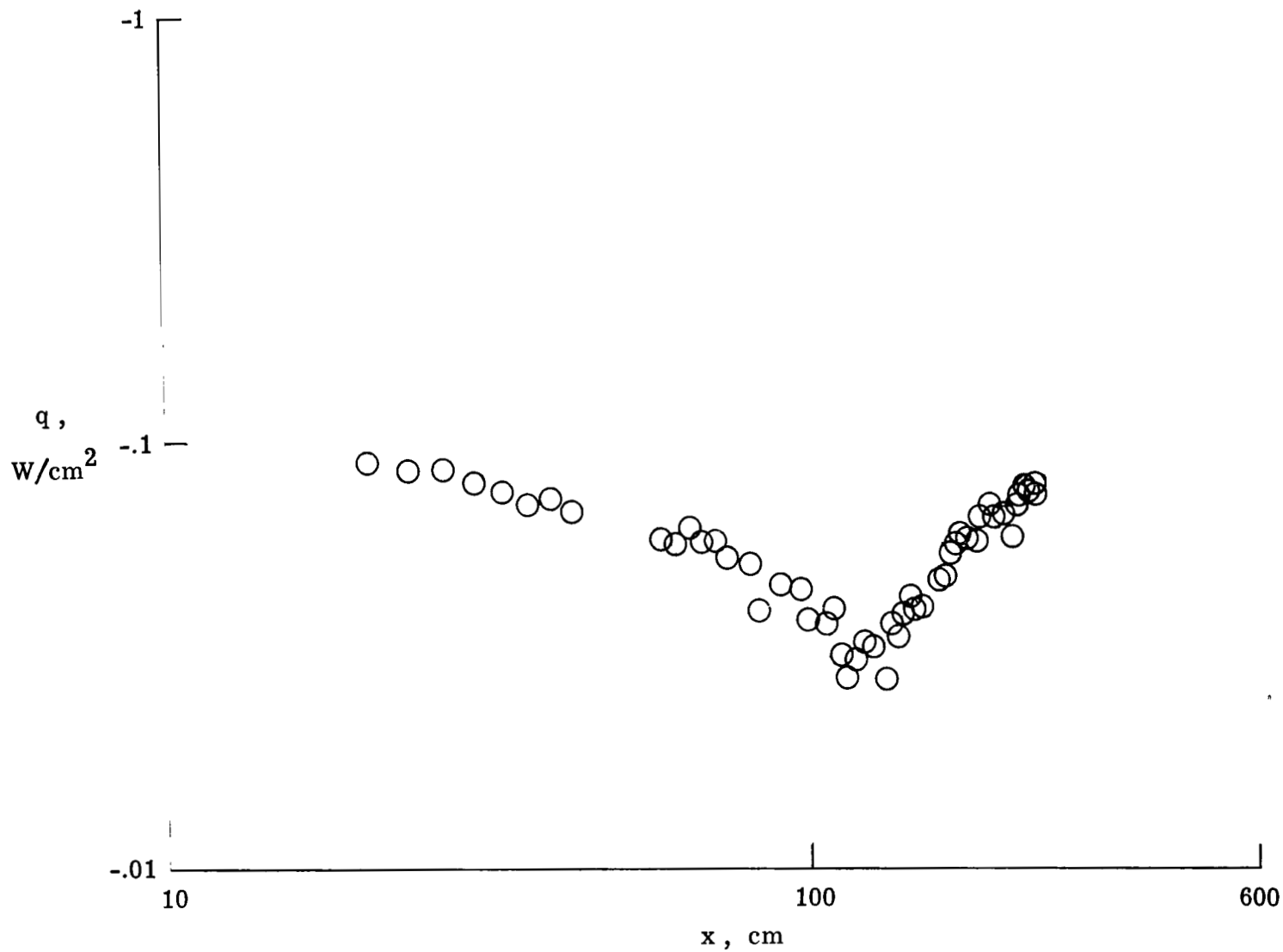
(f) $R_1/m = 22.63 \times 10^6$; $T_w/T_t = 0.95$.

Figure 10.- Continued.



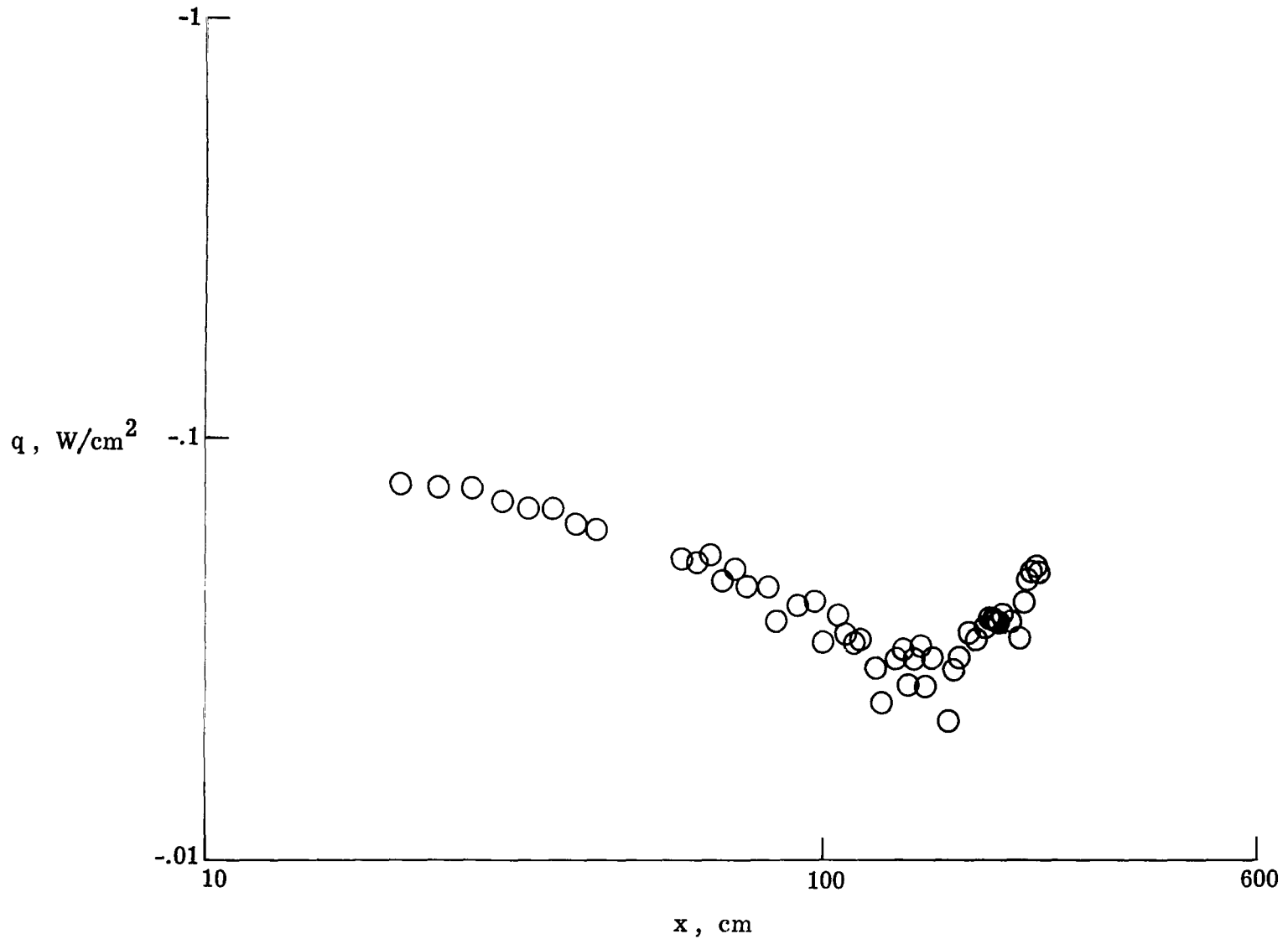
(g) $R_1/m = 19.25 \times 10^6$; $T_w/T_t = 0.96$.

Figure 10.- Continued.



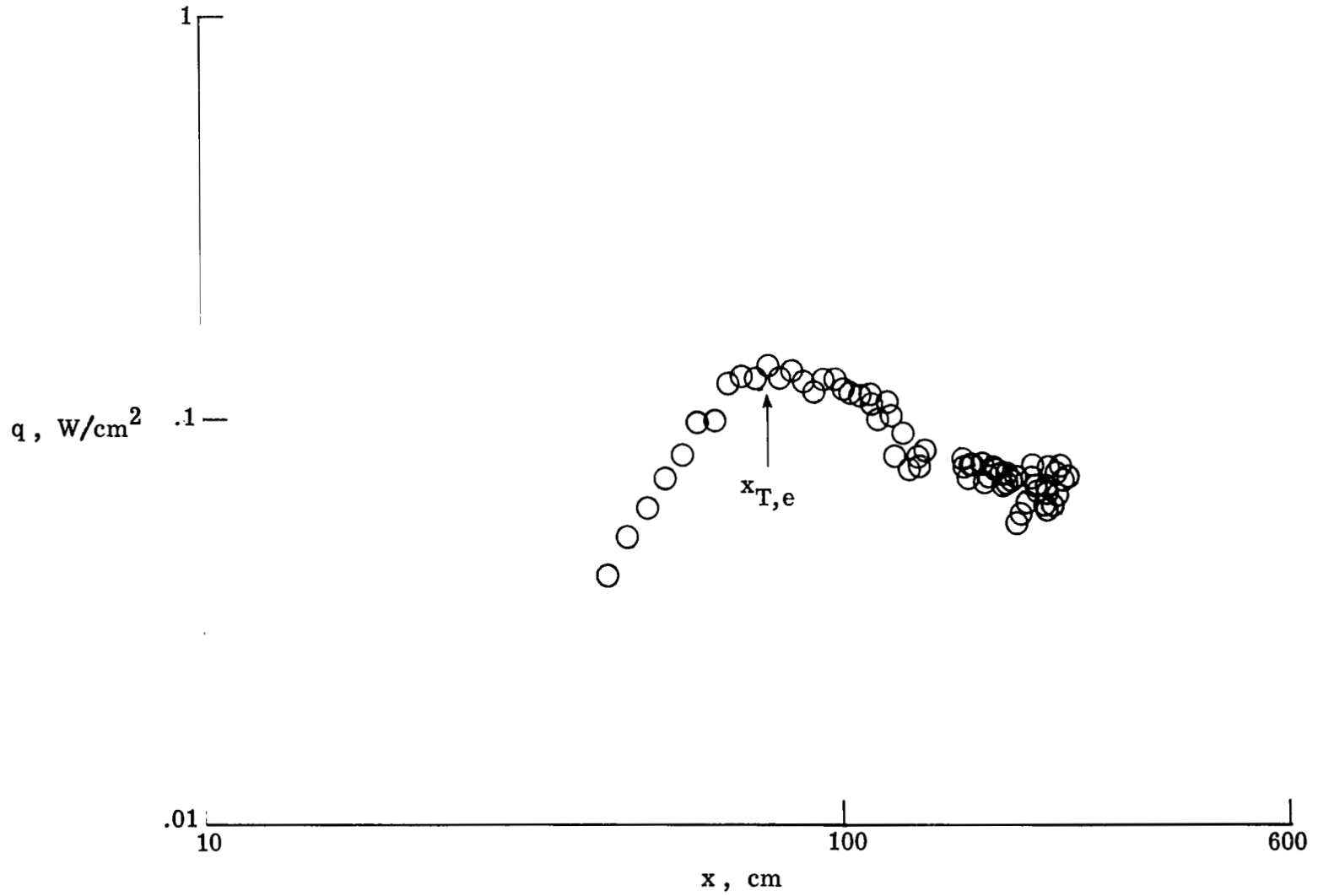
(h) $R_1/m = 14.43 \times 10^6$; $T_w/T_t = 0.96$.

Figure 10.- Continued.



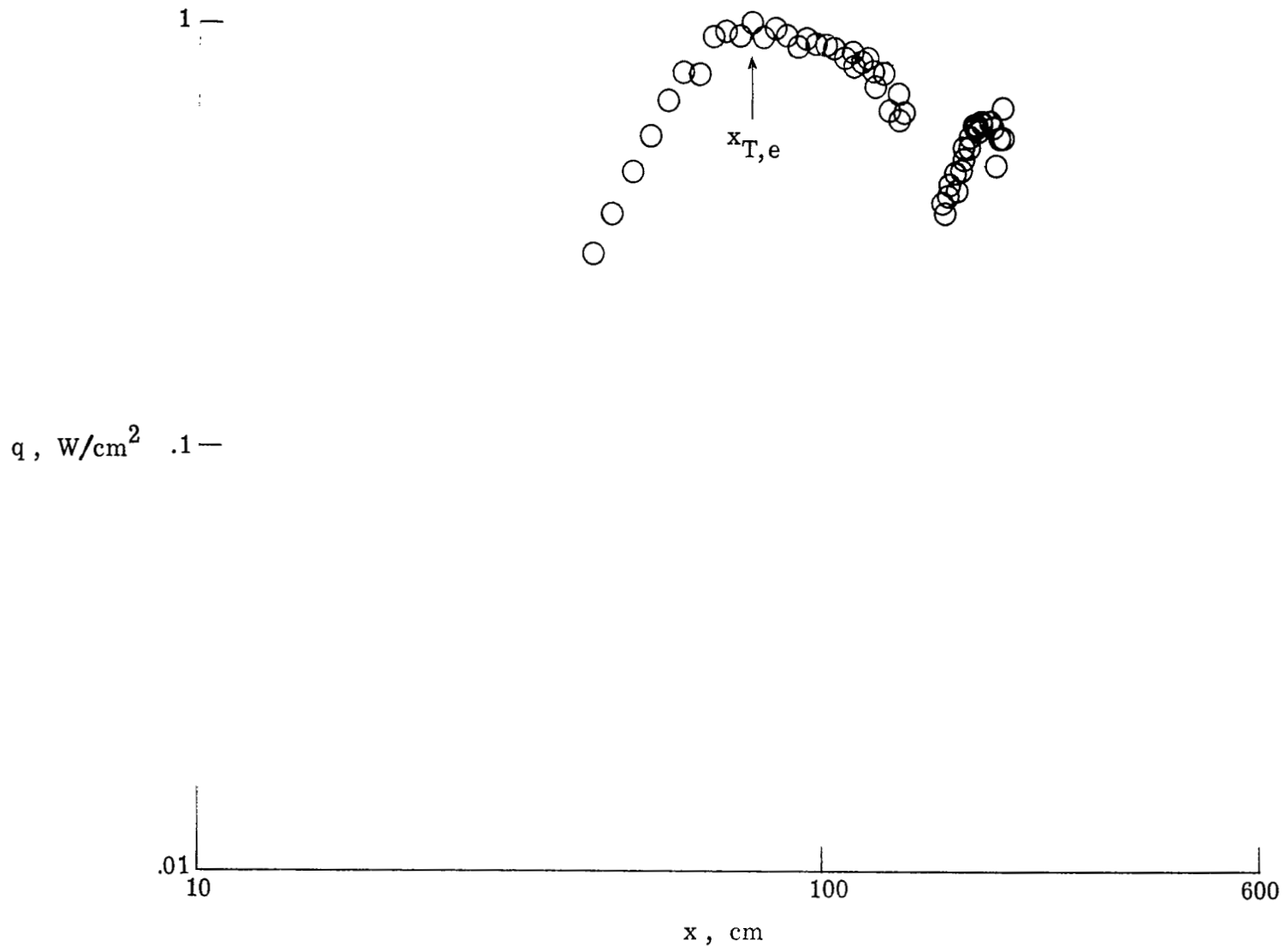
(i) $R_1/m = 9.86 \times 10^6$; $T_w/T_t = 0.97$.

Figure 10.- Concluded.



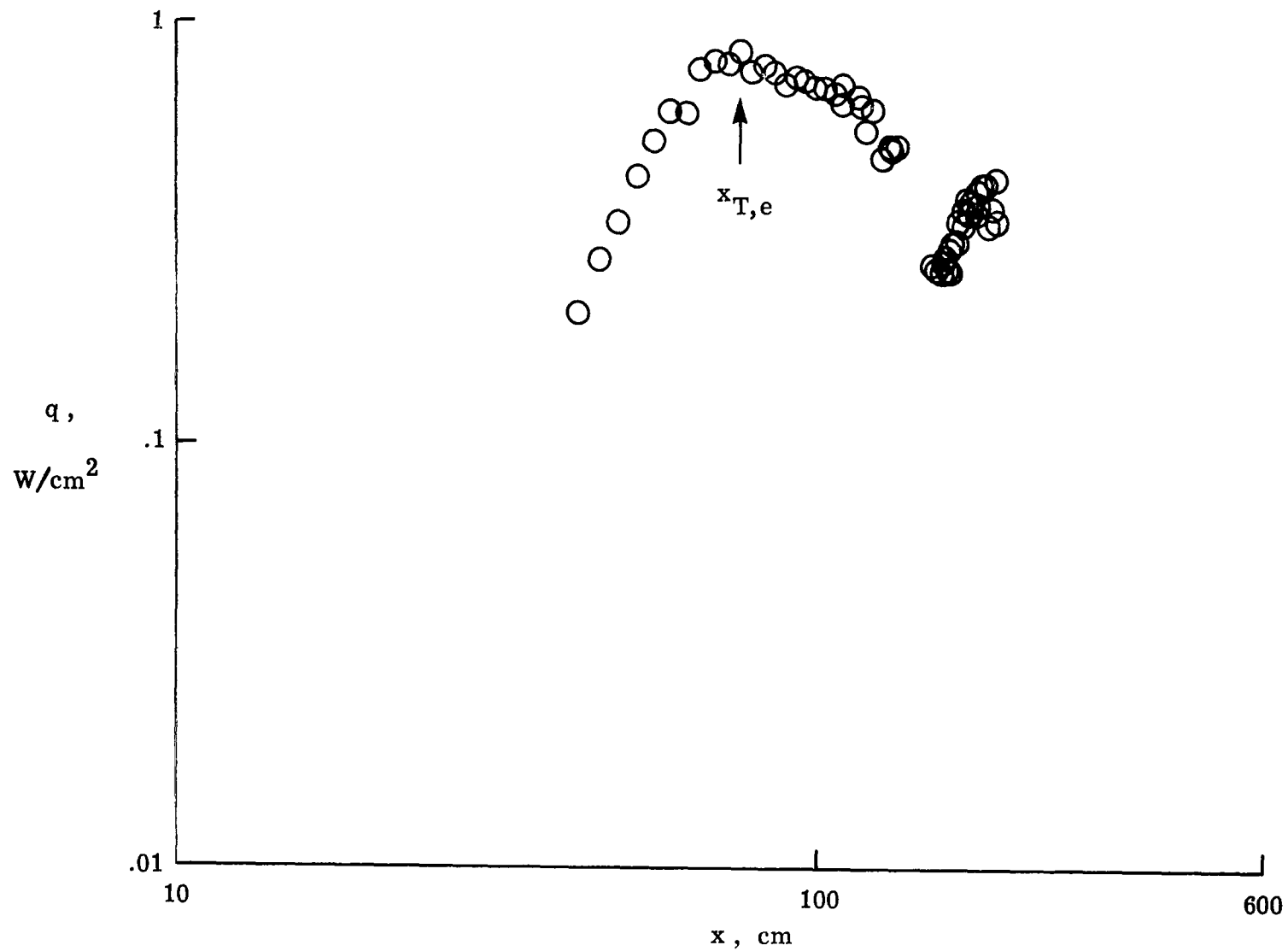
(a) $R_1/m = 41.9 \times 10^6$; $T_w/T_t = 0.43$.

Figure 11.- Heat-transfer data on model 2.



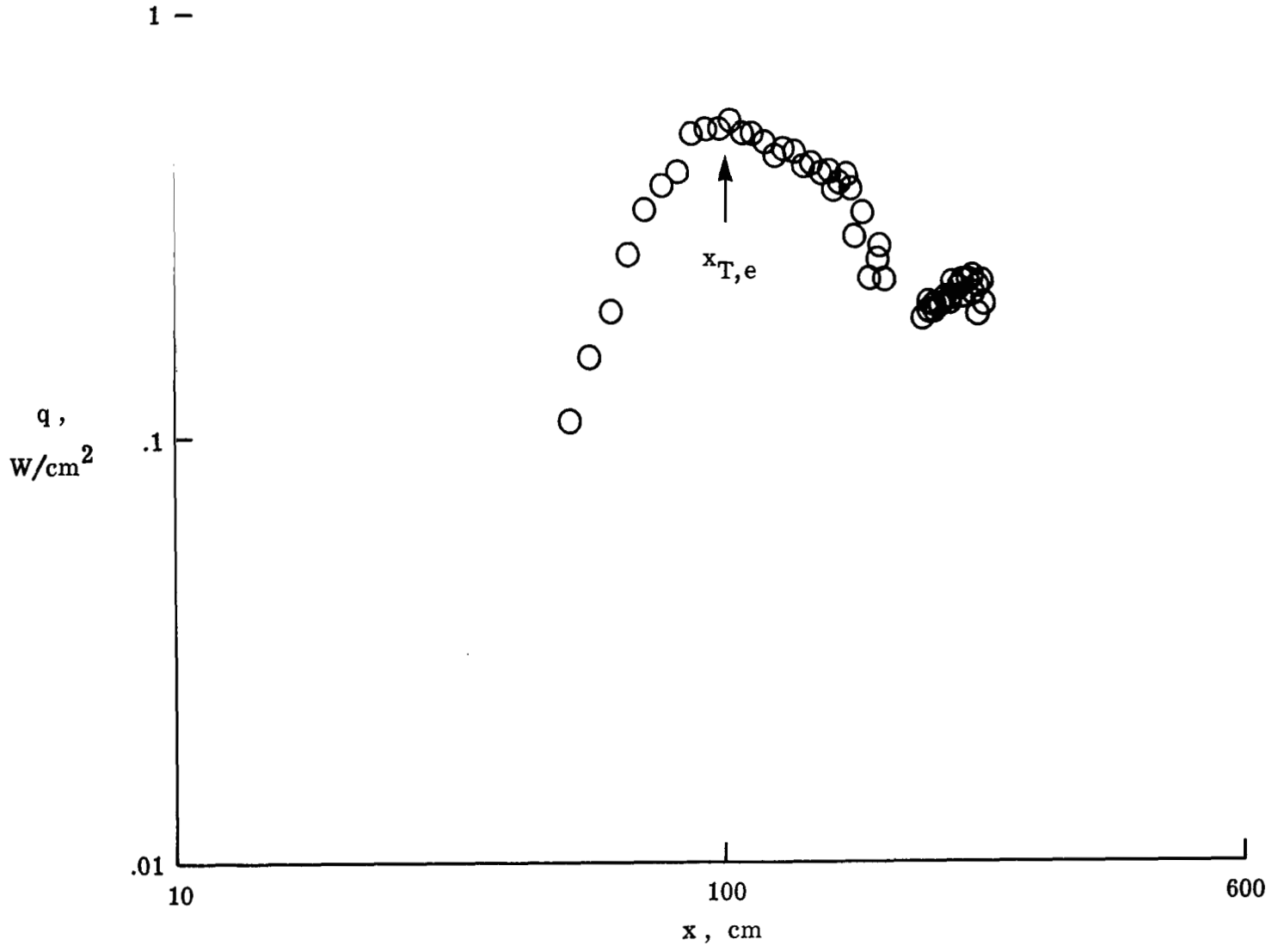
(b) $R_1/m = 39.4 \times 10^6$; $T_w/T_t = 0.50$.

Figure 11.- Continued.



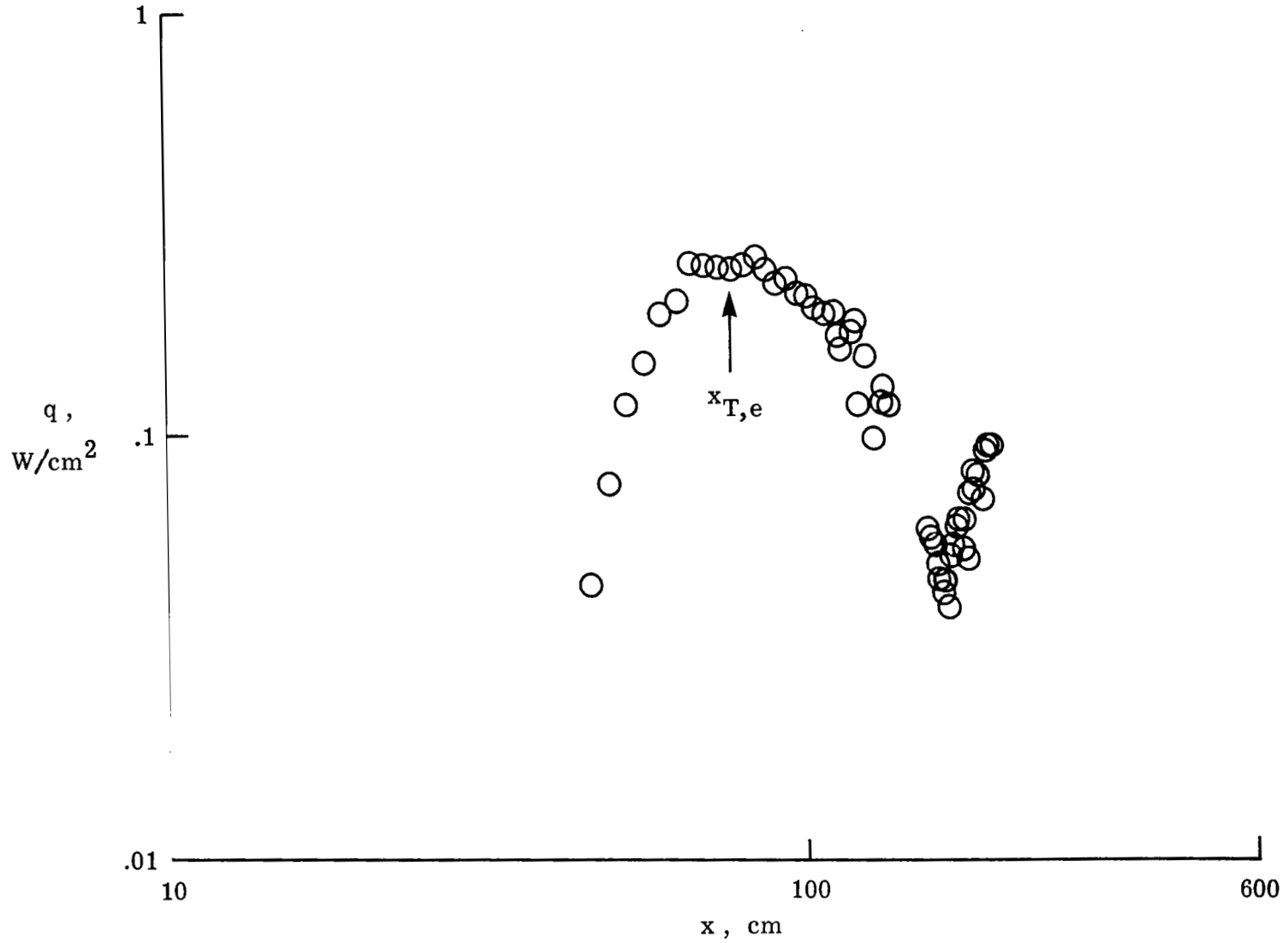
(c) $R_1/m = 38.43 \times 10^6$; $T_w/T_t = 0.58$.

Figure 11.- Continued.



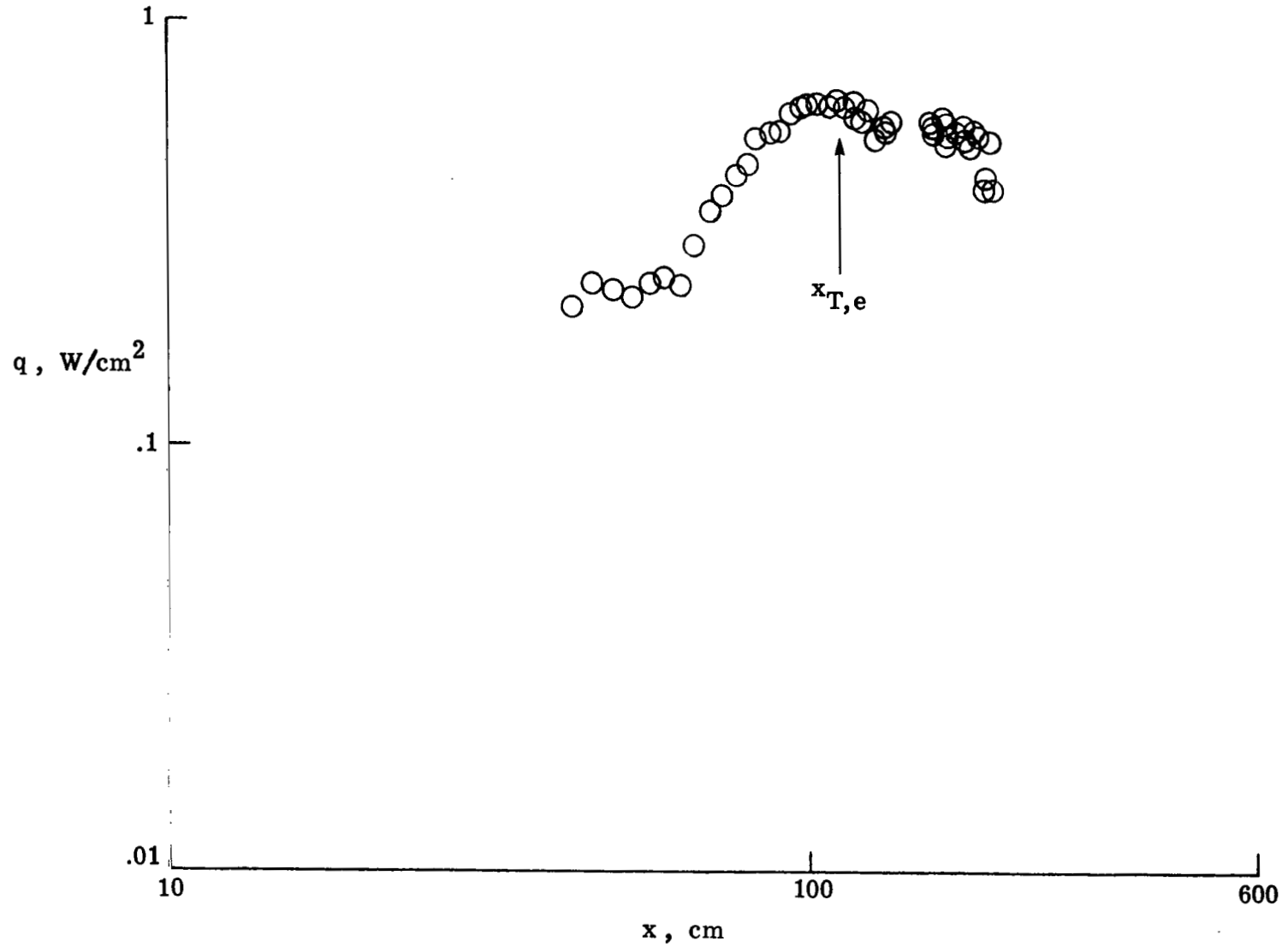
(d) $R_1/m = 38.64 \times 10^6$; $T_w/T_t = 0.68$.

Figure 11.- Continued.



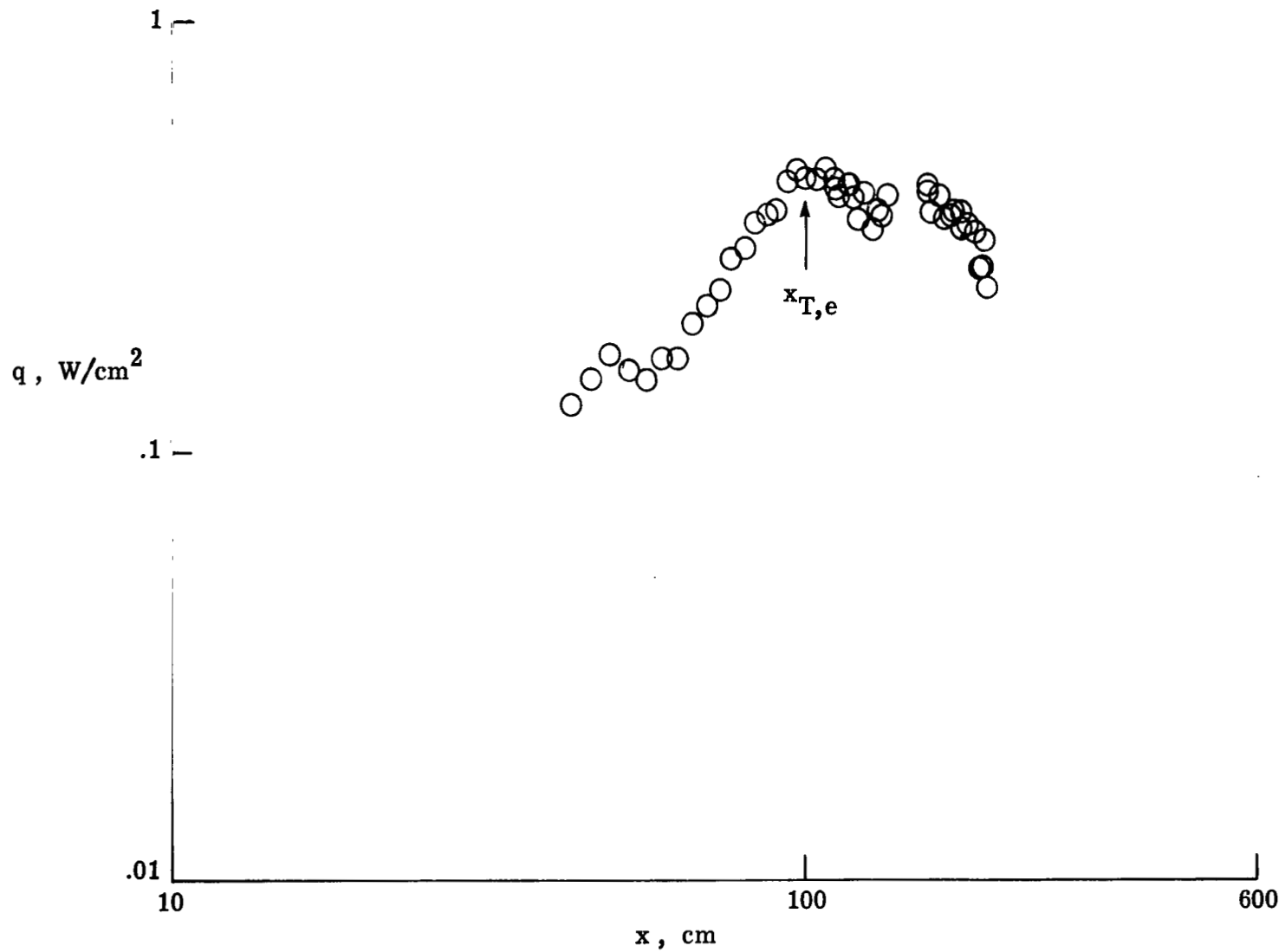
(e) $R_1/m = 40.36 \times 10^6$; $T_w/T_t = 0.79$.

Figure 11.- Continued.



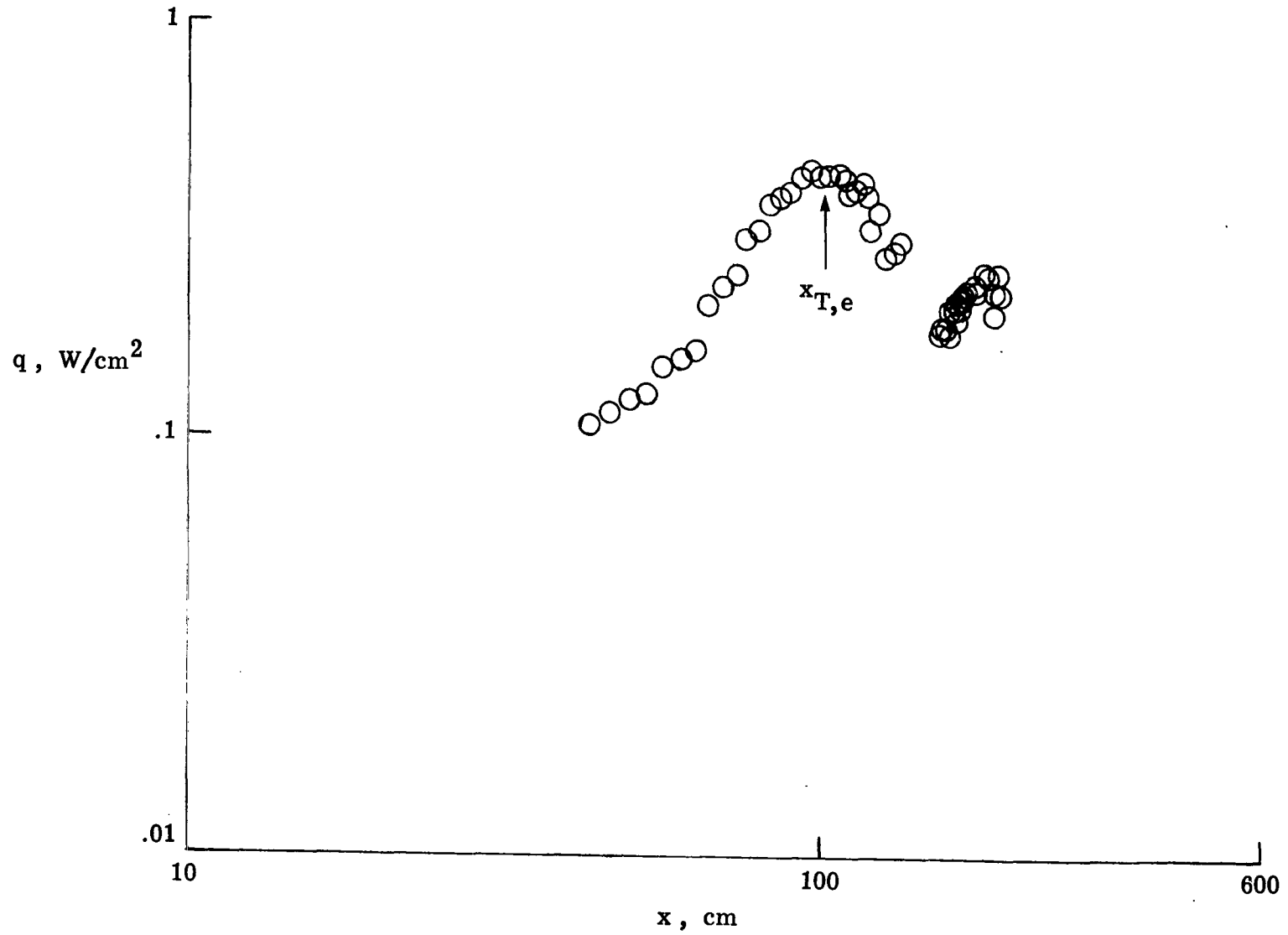
(g) $R_1/m = 20.63 \times 10^6$; $T_w/T_t = 0.38$.

Figure 11.- Continued.



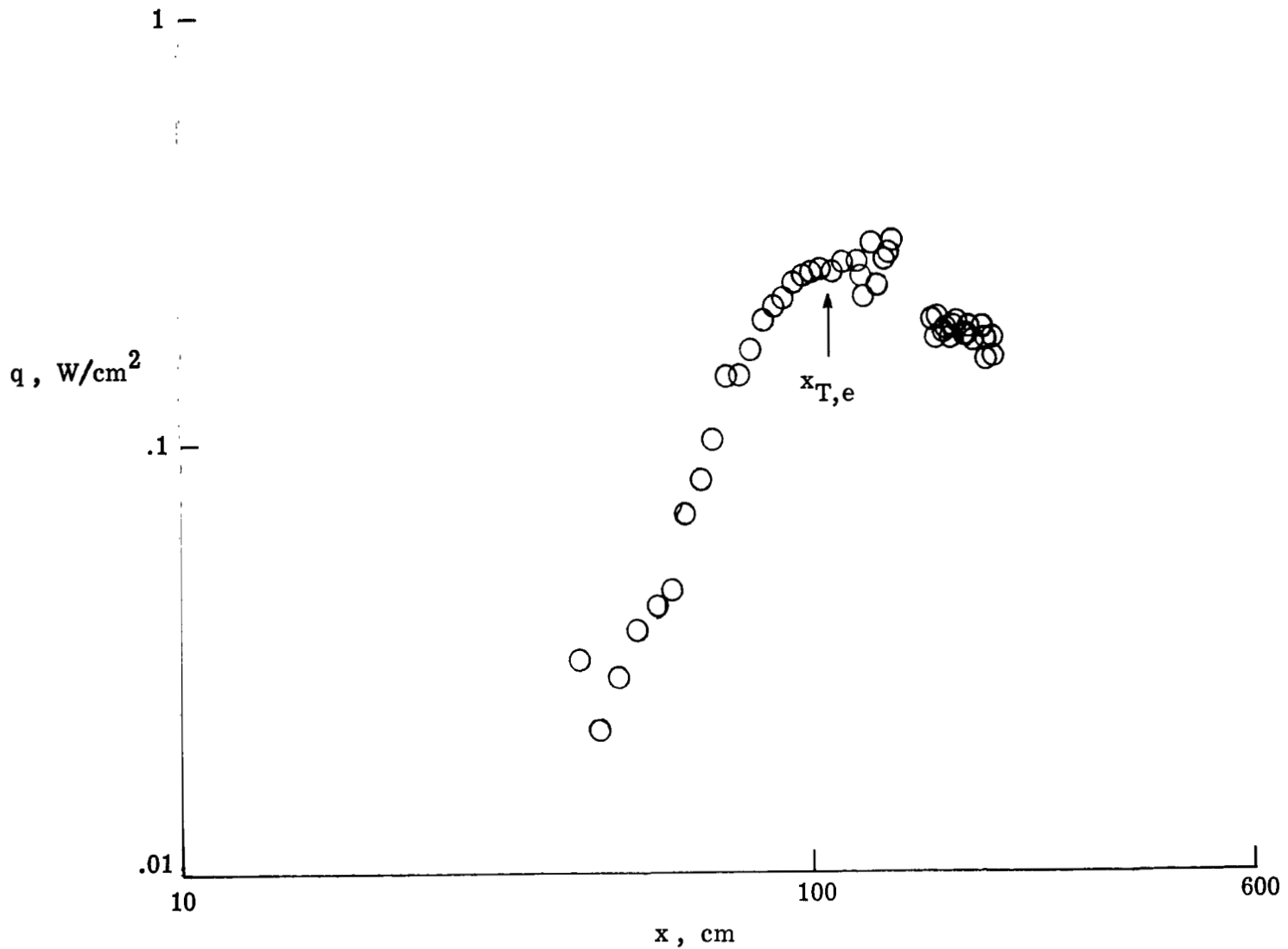
(h) $R_1/m = 19.18 \times 10^6$; $T_w/T_t = 0.57$.

Figure 11.- Continued.



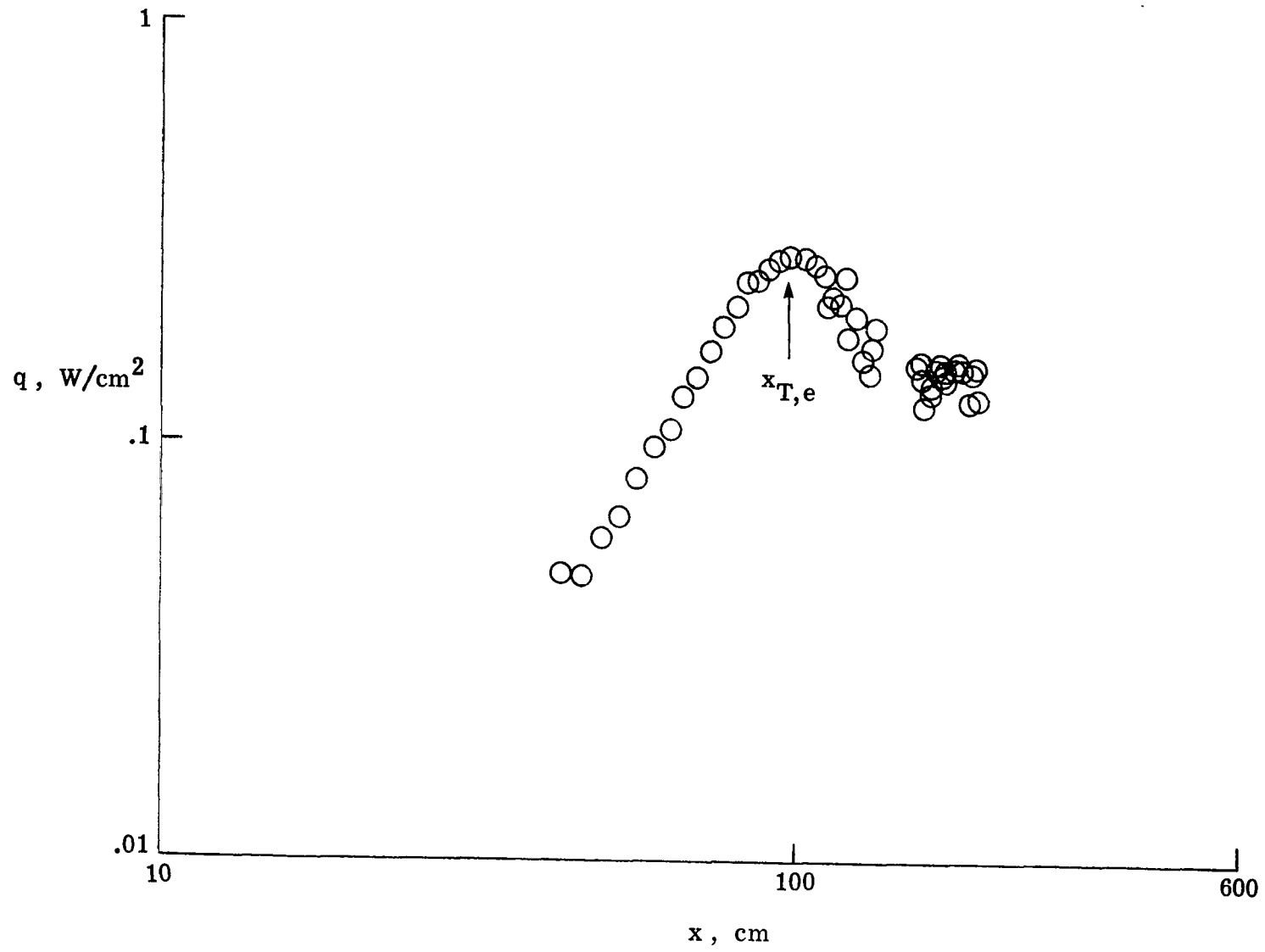
(i) $R_1/m = 20.03 \times 10^6$; $T_w/T_t = 0.61$.

Figure 11.- Continued.



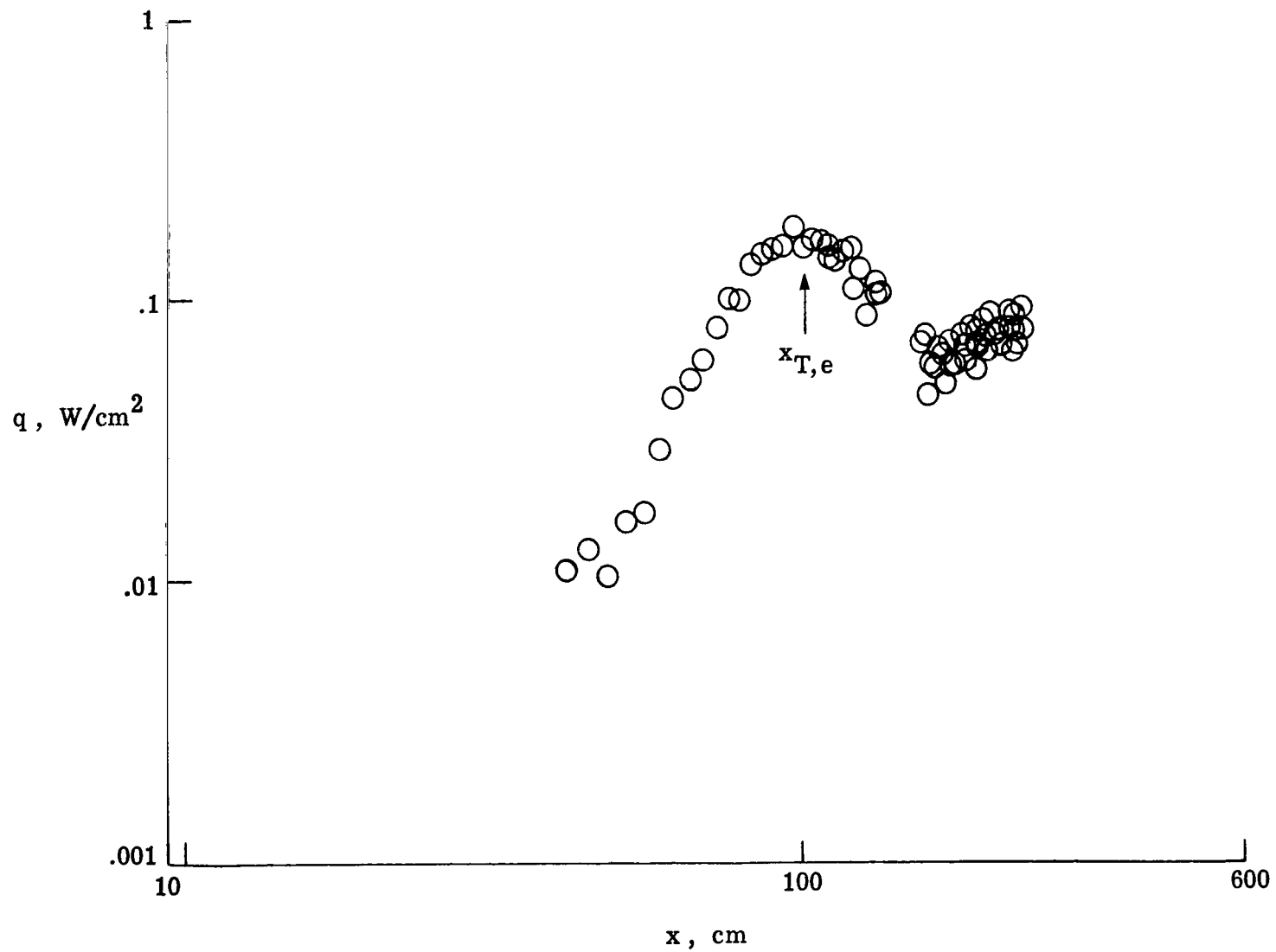
(j) $R_1/m = 19.58 \times 10^6$; $T_w/T_t = 0.68$.

Figure 11.- Continued.



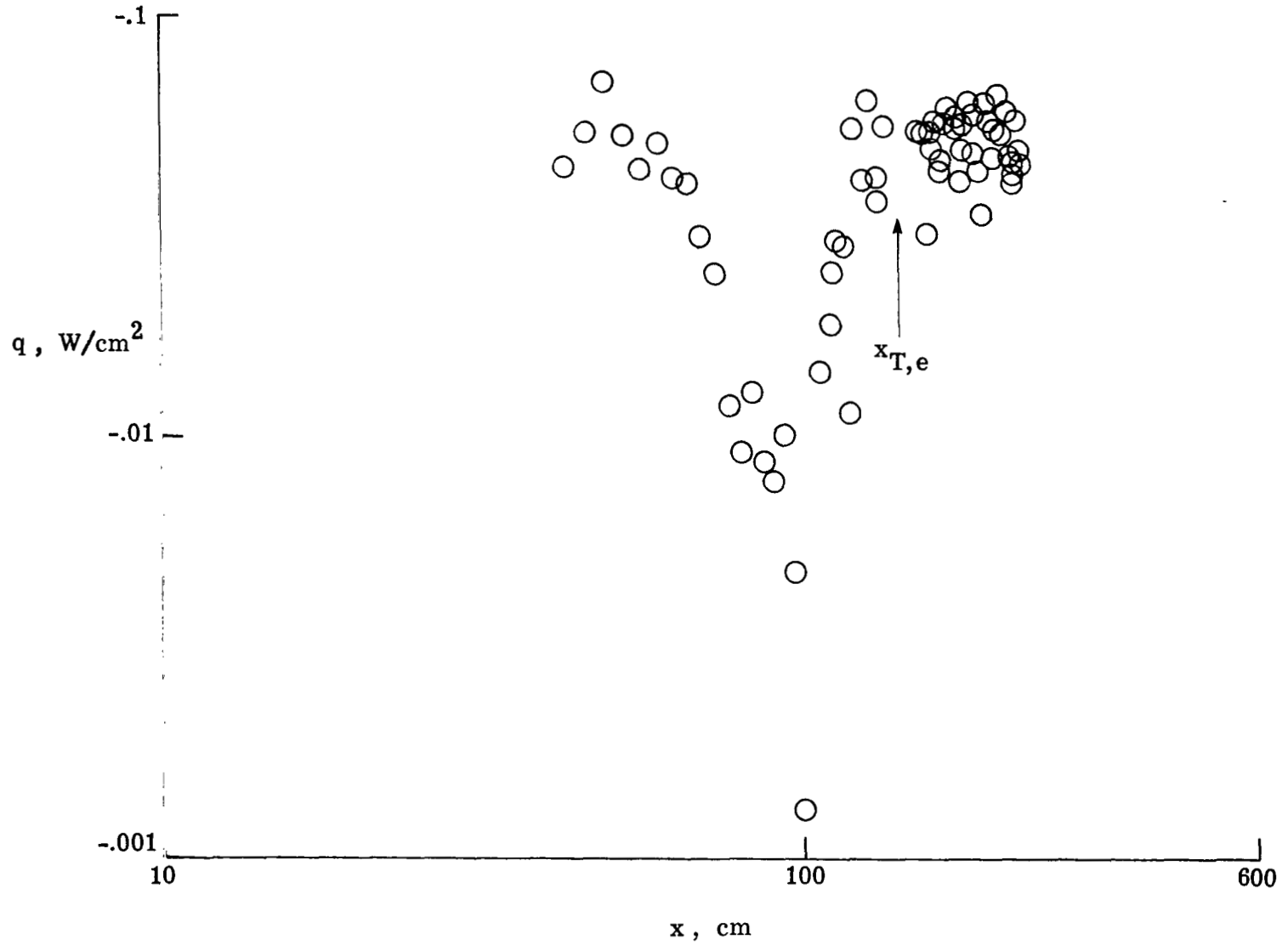
(k) $R_1/m = 19.46 \times 10^6$; $T_w/T_t = 0.70$.

Figure 11.- Continued.



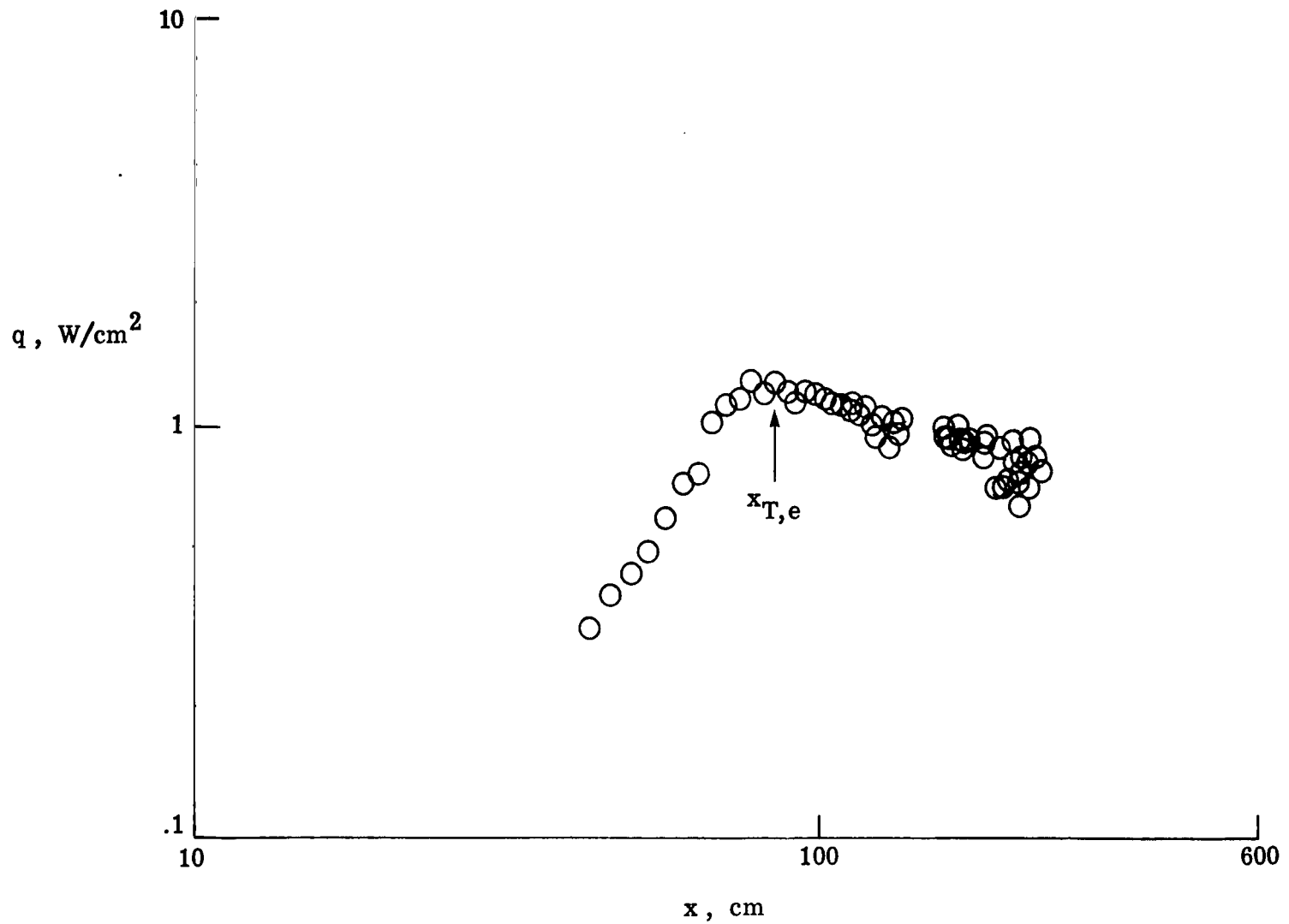
(1) $R_1/m = 19.75 \times 10^6$; $T_w/T_t = 0.79$.

Figure 11.- Continued.



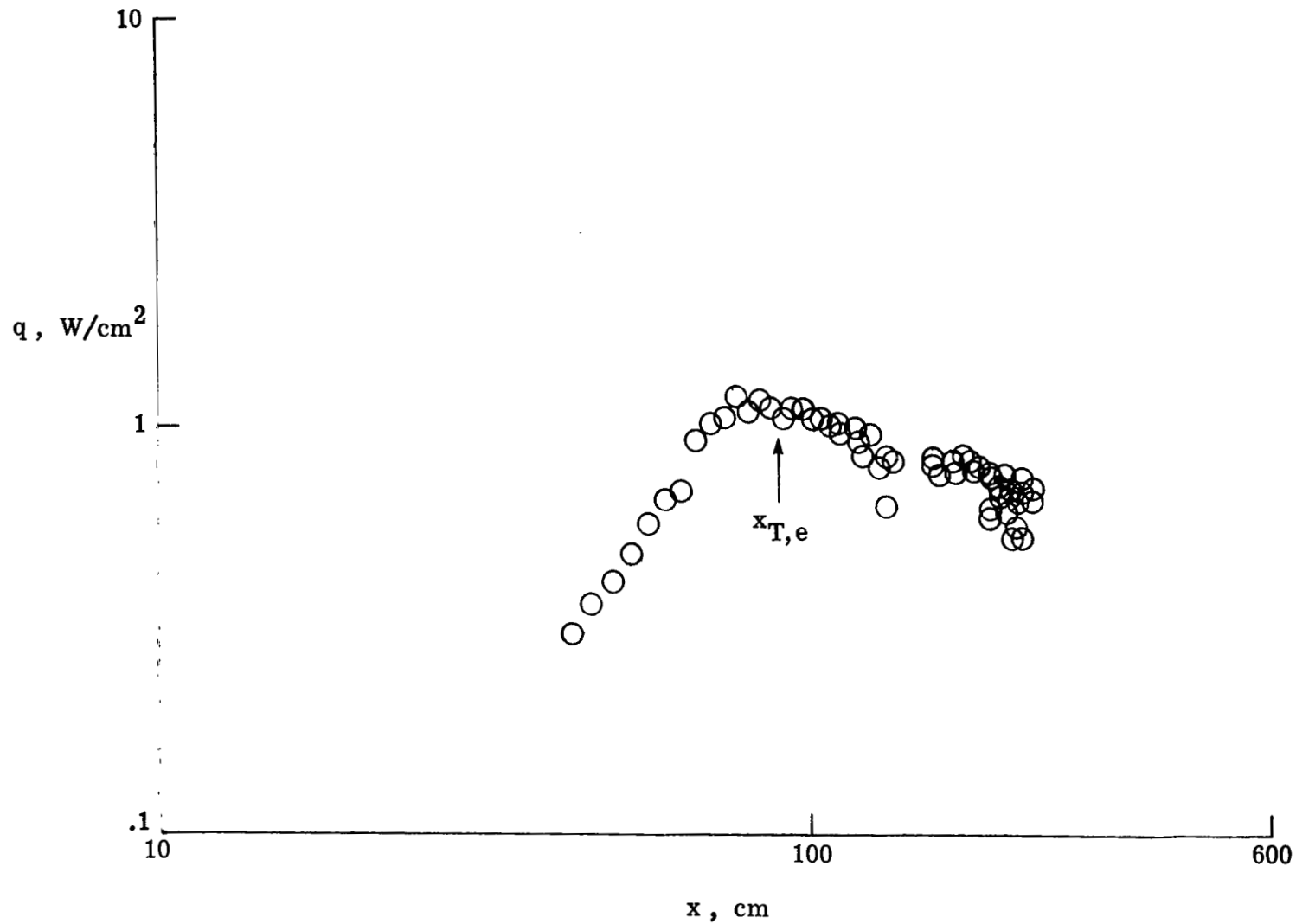
(m) $R_1/m = 19.29 \times 10^6$; $T_w/T_t = 0.92$.

Figure 11.- Continued.



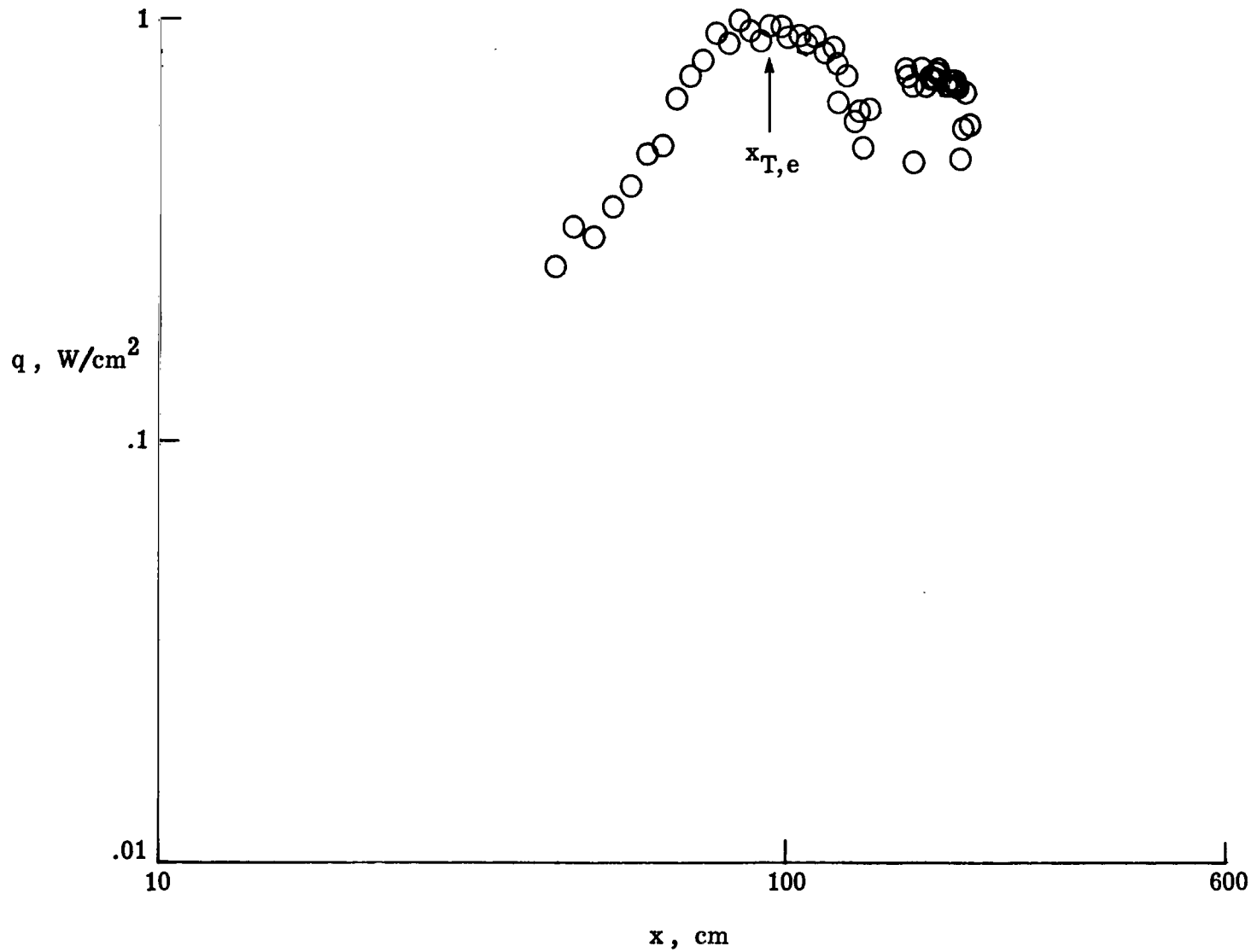
(n) $R_1/m = 35.97 \times 10^6$; $T_w/T_t = 0.37$.

Figure 11.- Continued.



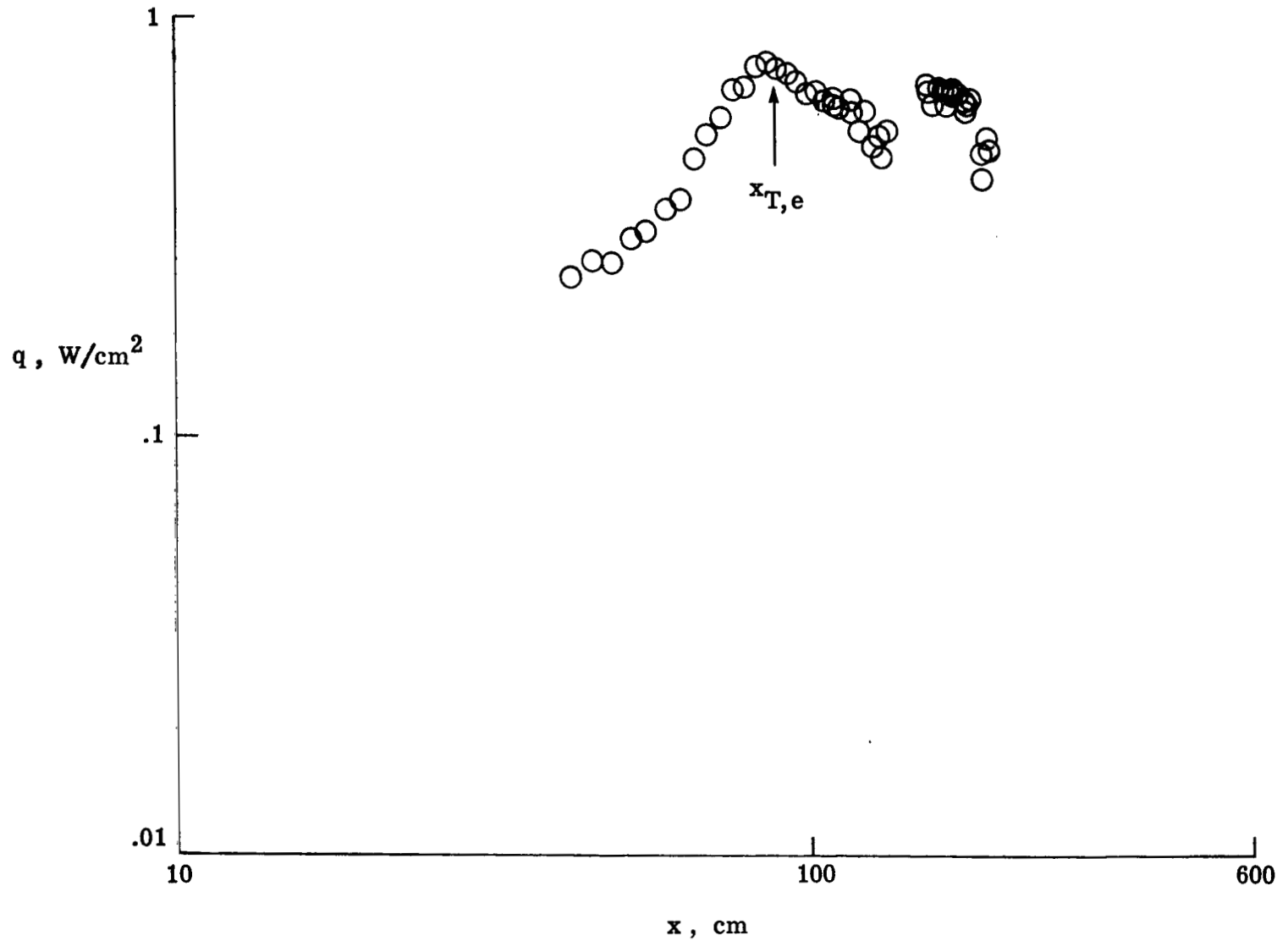
(o) $R_1/m = 32.95 \times 10^6$; $T_w/T_t = 0.38$.

Figure 11.- Continued.



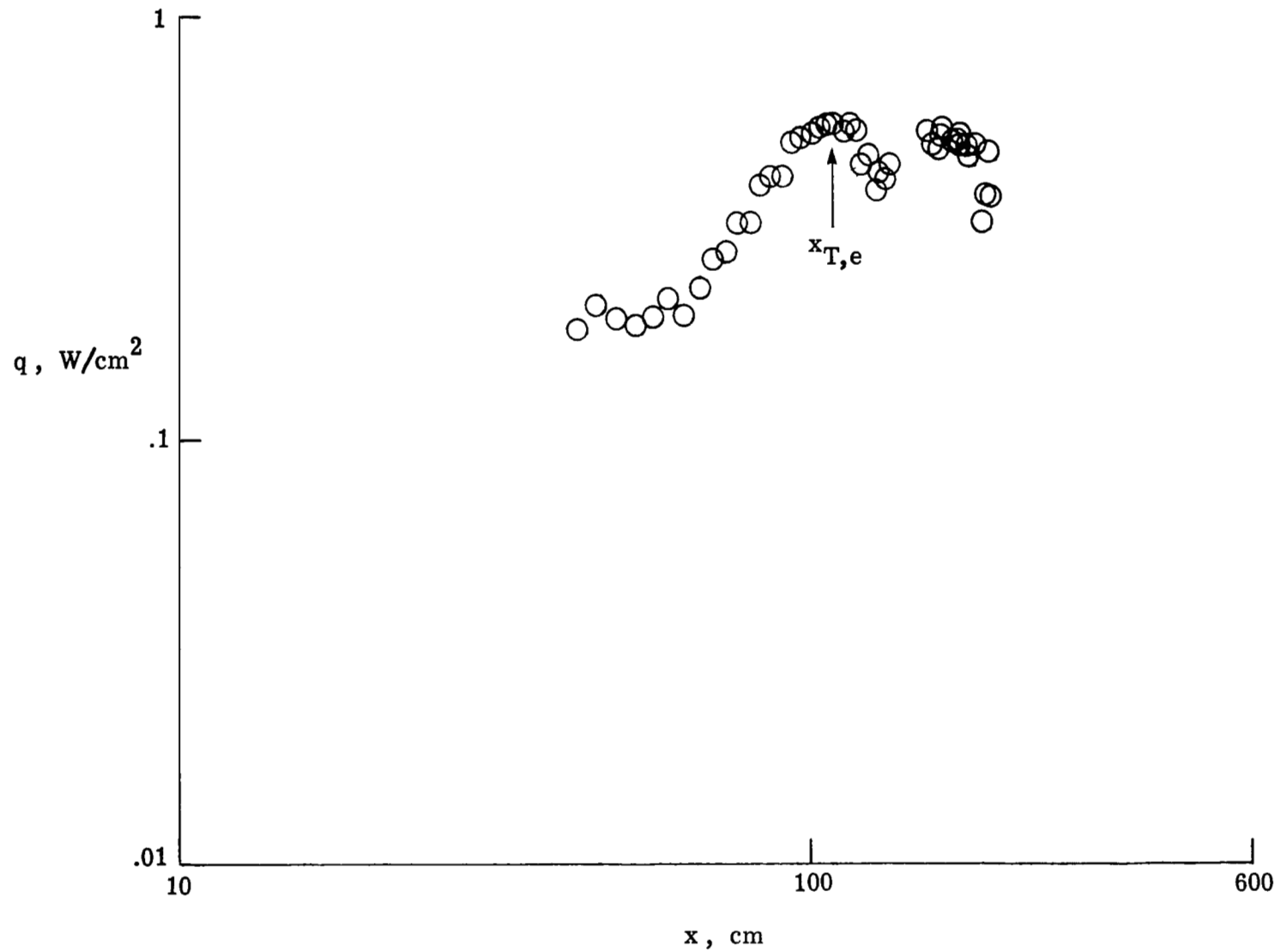
(p) $R_1/m = 29.58 \times 10^6$; $T_w/T_t = 0.41$.

Figure 11.- Continued.



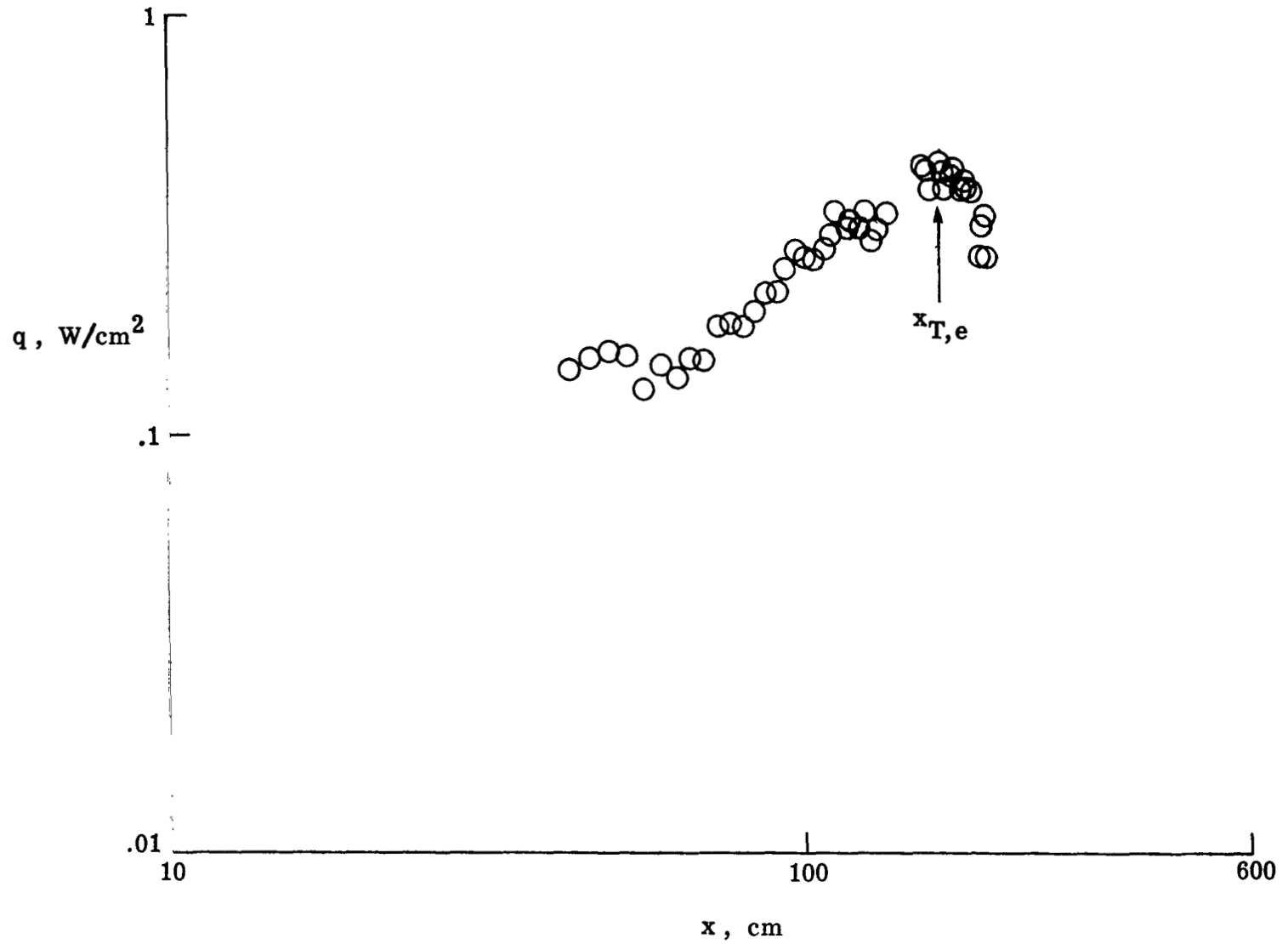
(q) $R_1/m = 20.63 \times 10^6$; $T_w/T_t = 0.38$.

Figure 11.- Continued.



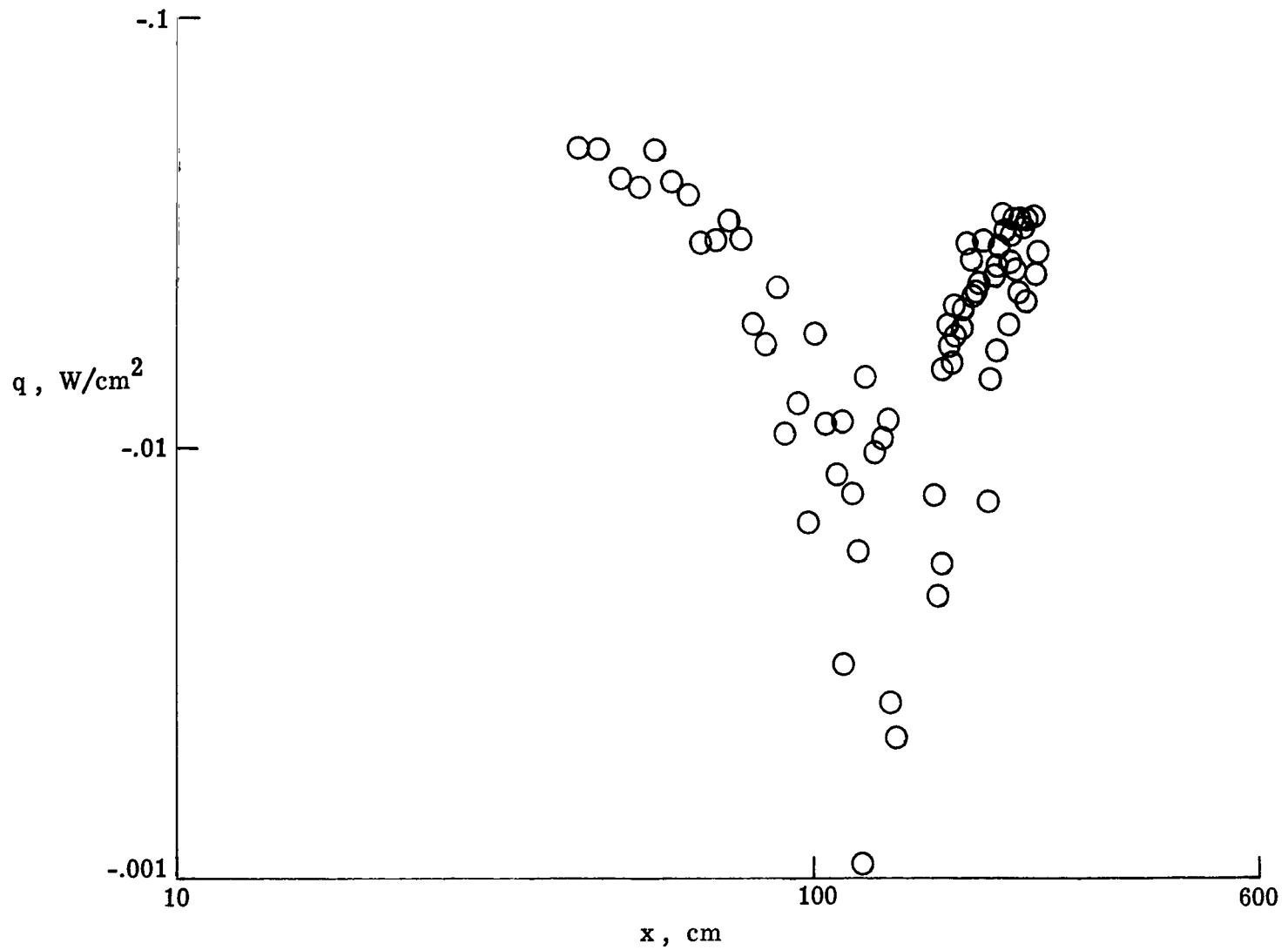
(r) $R_1/m = 18.16 \times 10^6$; $T_w/T_t = 0.41$.

Figure 11.- Continued.



(s) $R_1/m = 13.77 \times 10^6$; $T_w/T_t = 0.44$.

Figure 11.- Continued.



(t) $R_1/m = 12.38 \times 10^6$; $T_w/T_t = 0.93$.

Figure 11.- Concluded.

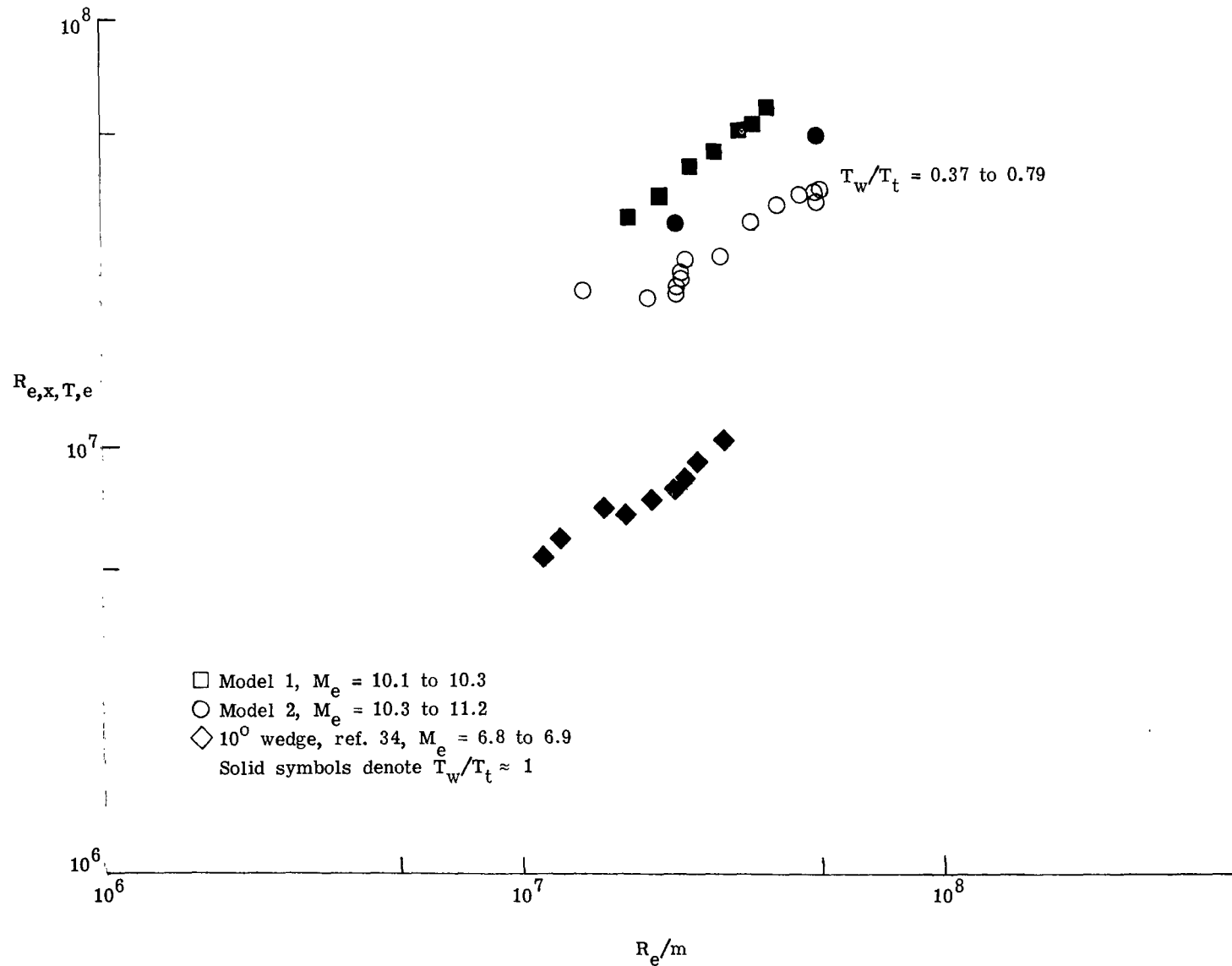


Figure 12.- Variation of peak heating Reynolds number with edge unit Reynolds number.

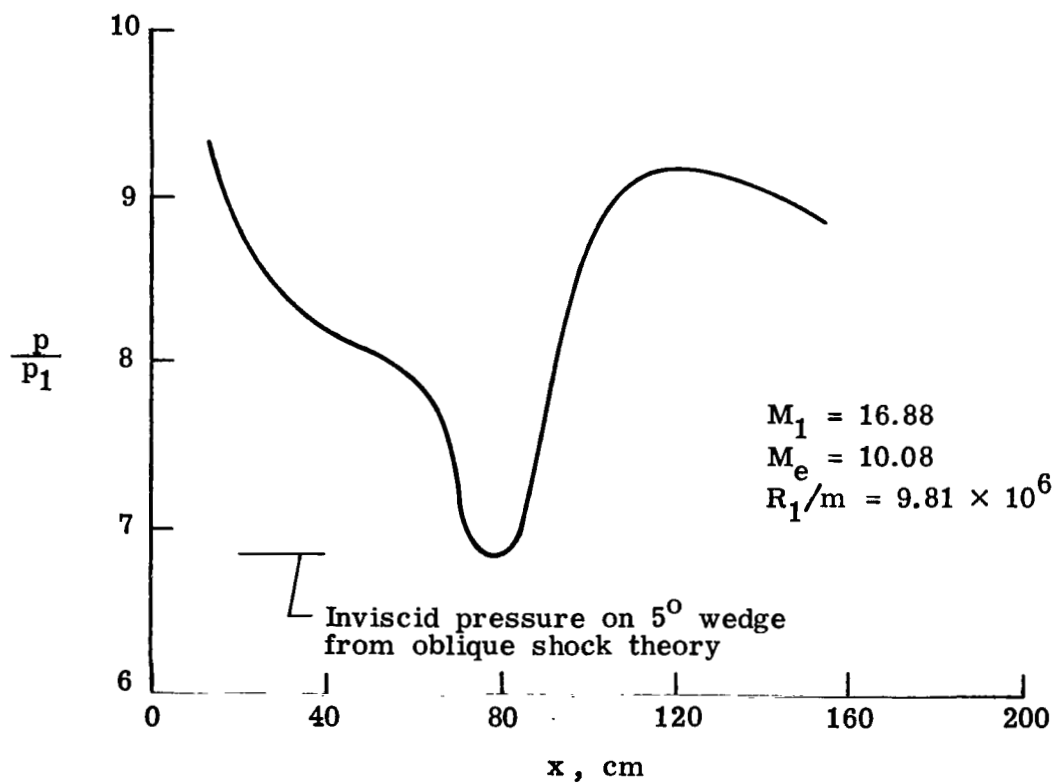
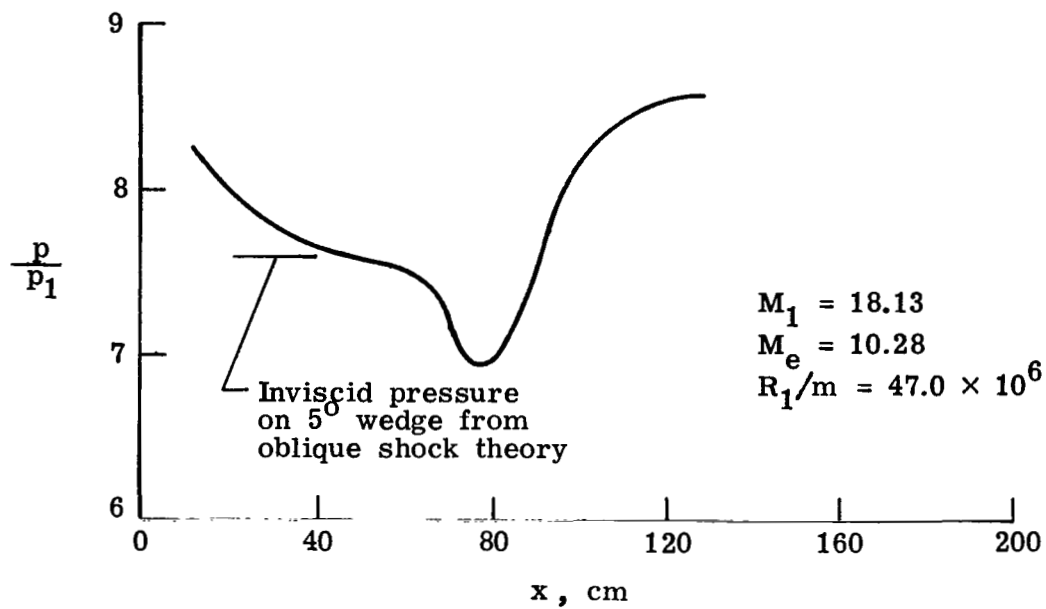
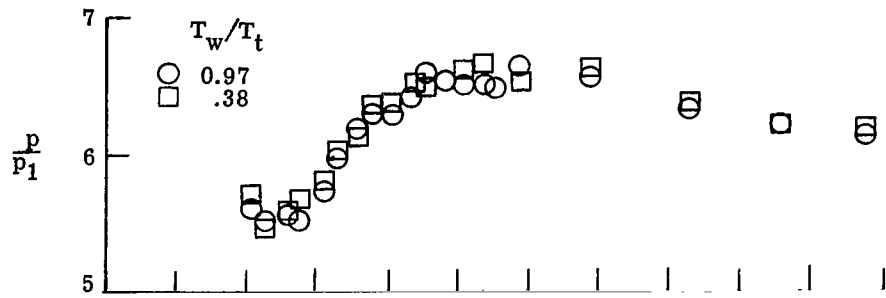
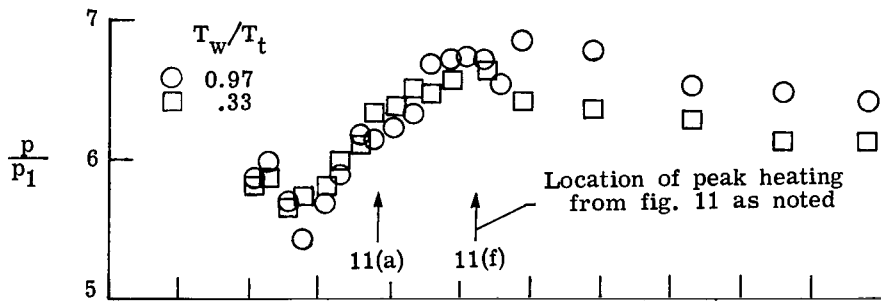


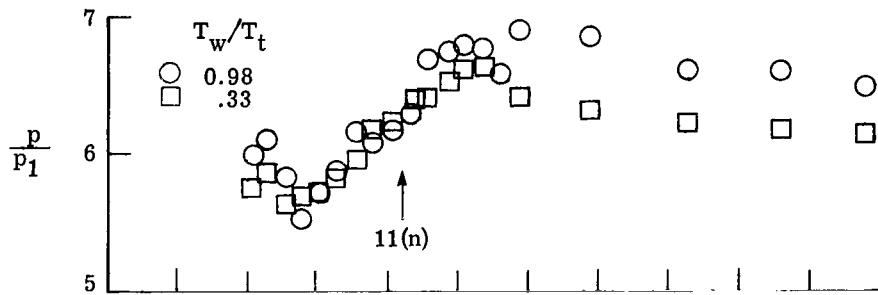
Figure 13.- Calculated surface pressures on model 1.



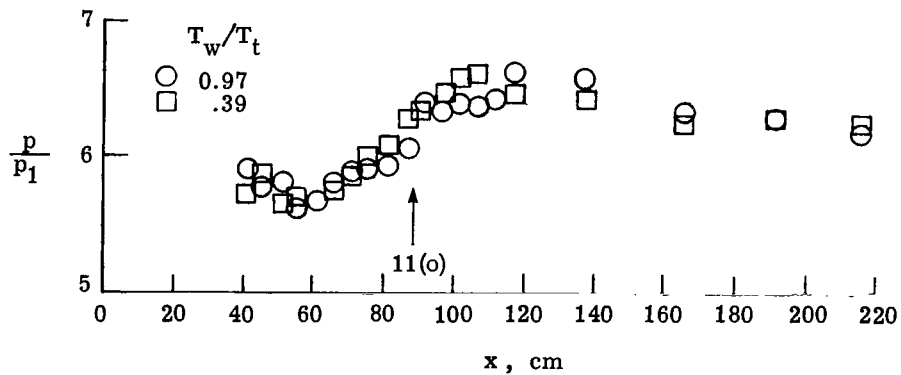
(a) $R_1/m = 46.2 \times 10^6$; $M_1 = 18.05$.



(b) $R_1/m = 41.6 \times 10^6$; $M_1 = 17.96$.

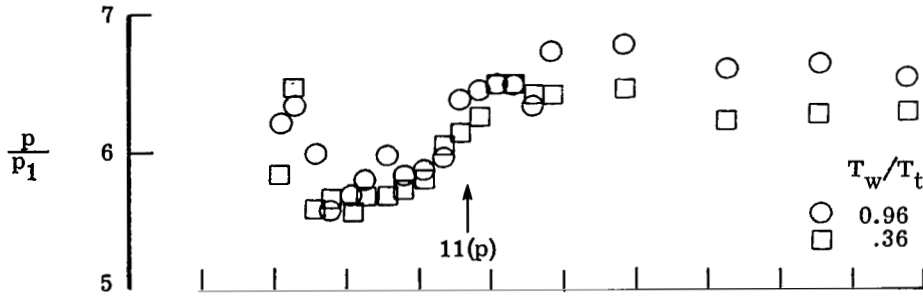


(c) $R_1/m = 37.5 \times 10^6$; $M_1 = 17.90$.

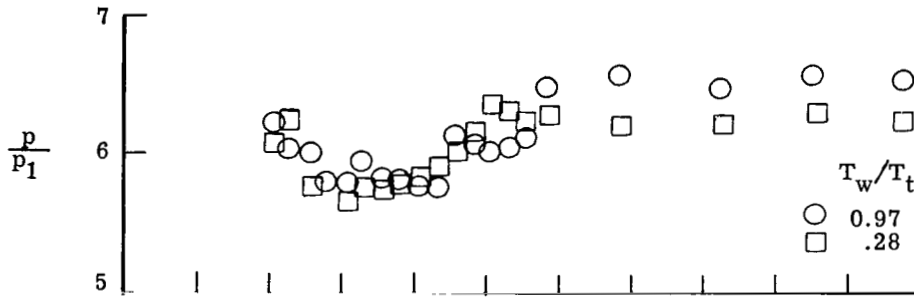


(d) $R_1/m = 32.9 \times 10^6$; $M_1 = 17.8$.

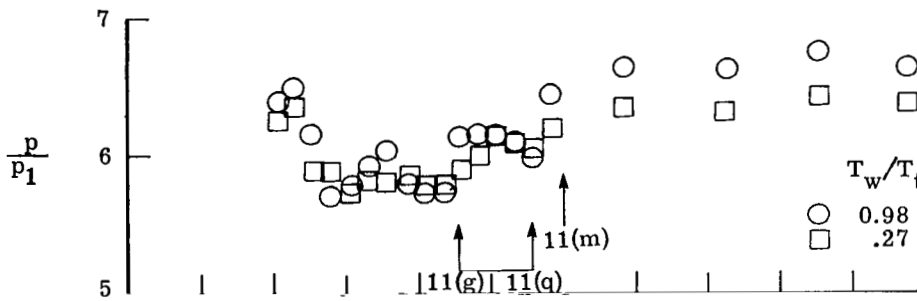
Figure 14.- Surface pressures on model 2.



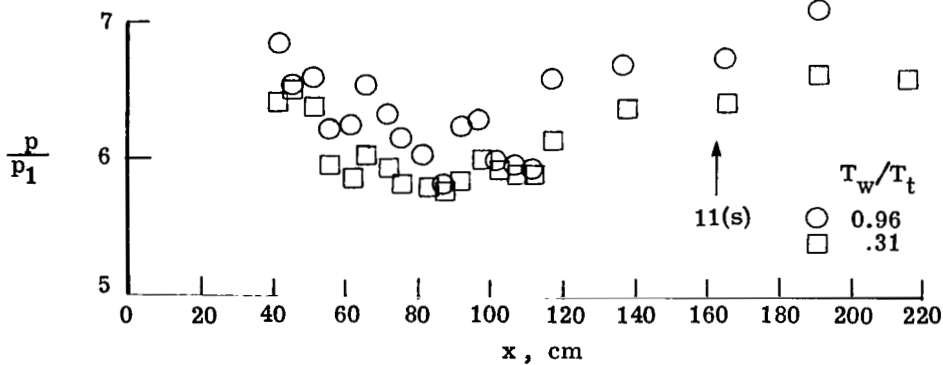
(e) $R_1/m = 27.8 \times 10^6$; $M_1 = 17.70$.



(f) $R_1/m = 23.2 \times 10^6$; $M_1 = 17.58$.

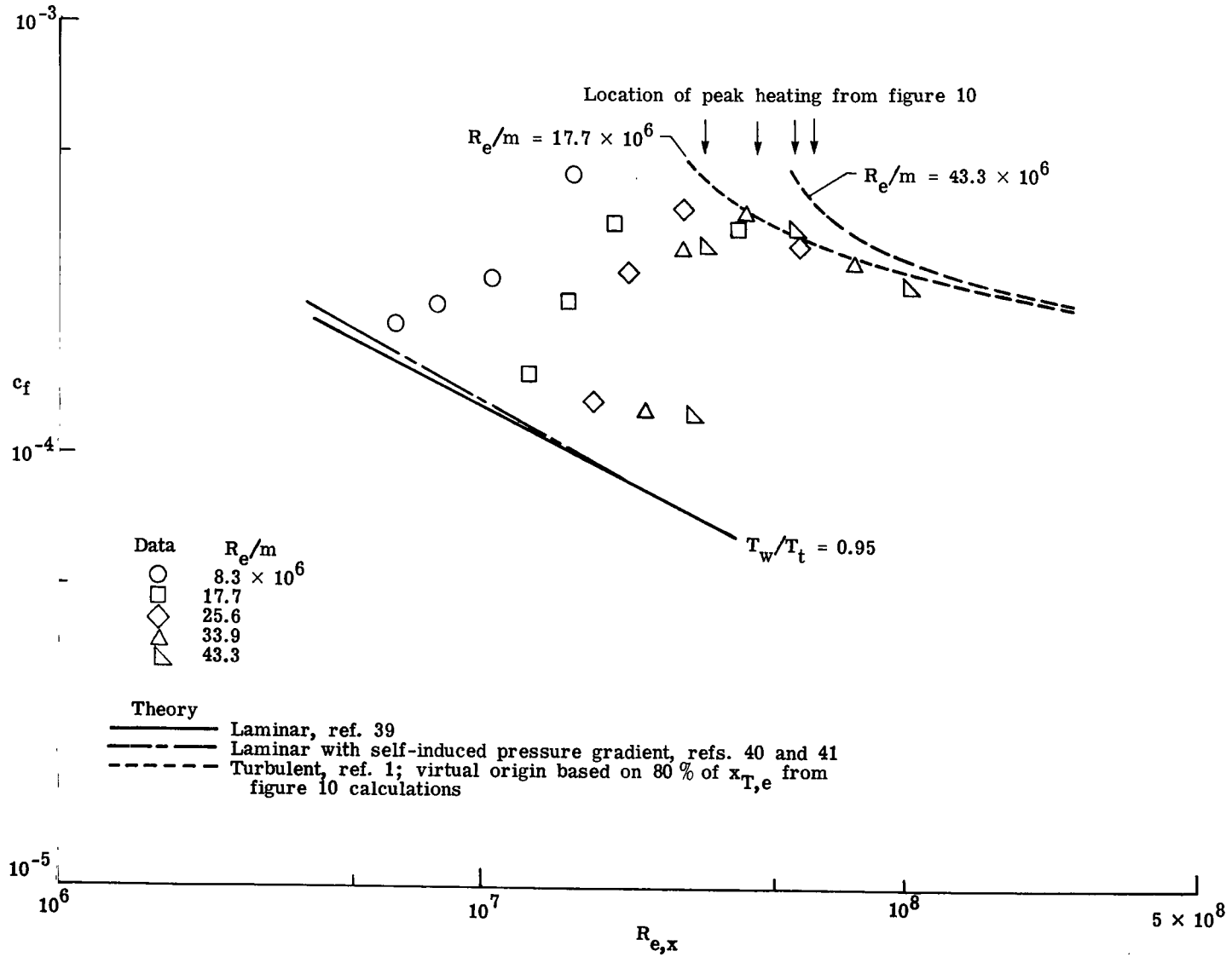


(g) $R_1/m = 20.2 \times 10^6$; $M_1 = 17.50$.



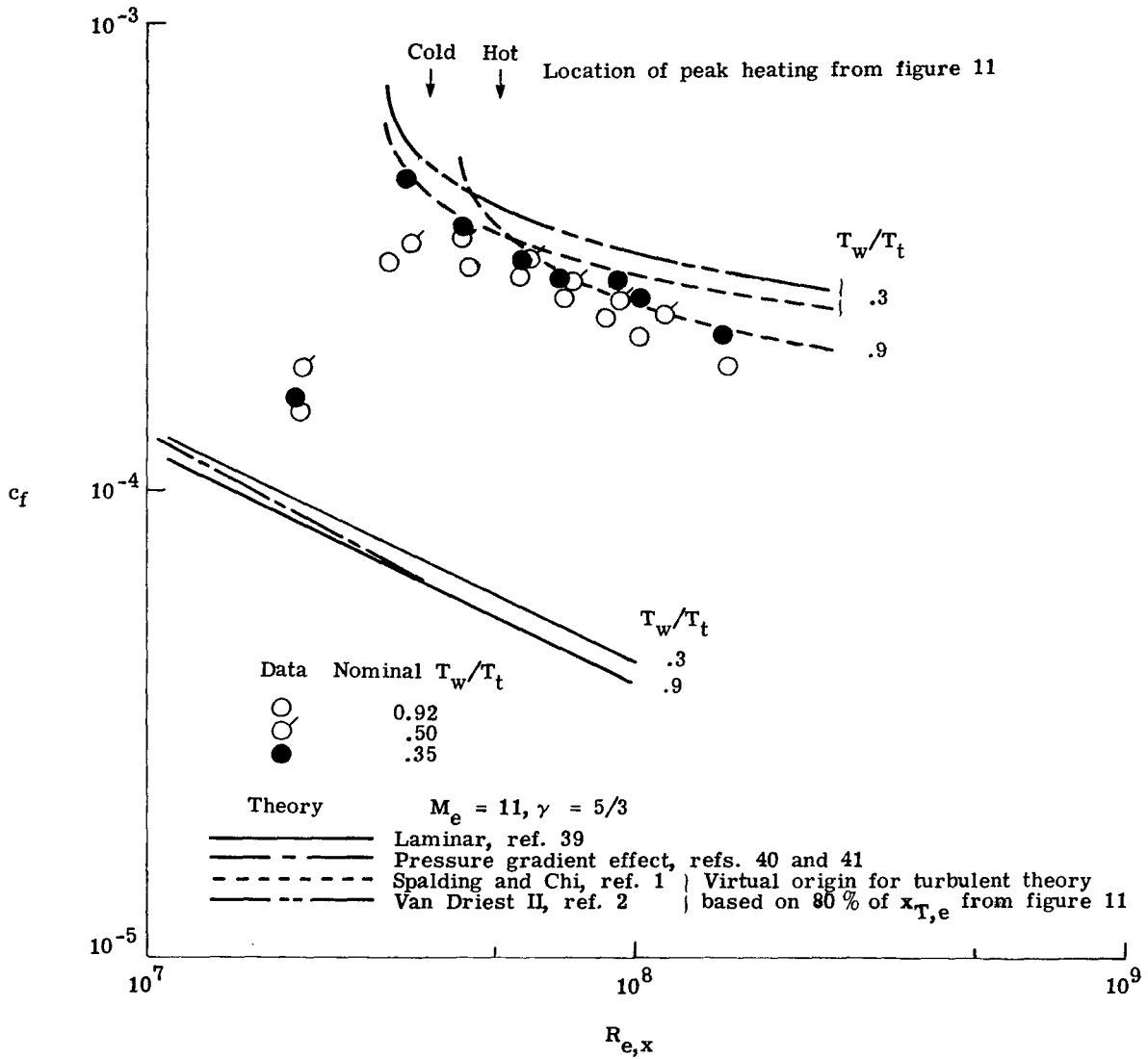
(h) $R_1/m = 14.1 \times 10^6$; $M_1 = 17.28$.

Figure 14.- Concluded.



(a) Data for model 1.

Figure 15.- Measured skin friction.



(b) Data for model 2.

Figure 15.- Concluded.

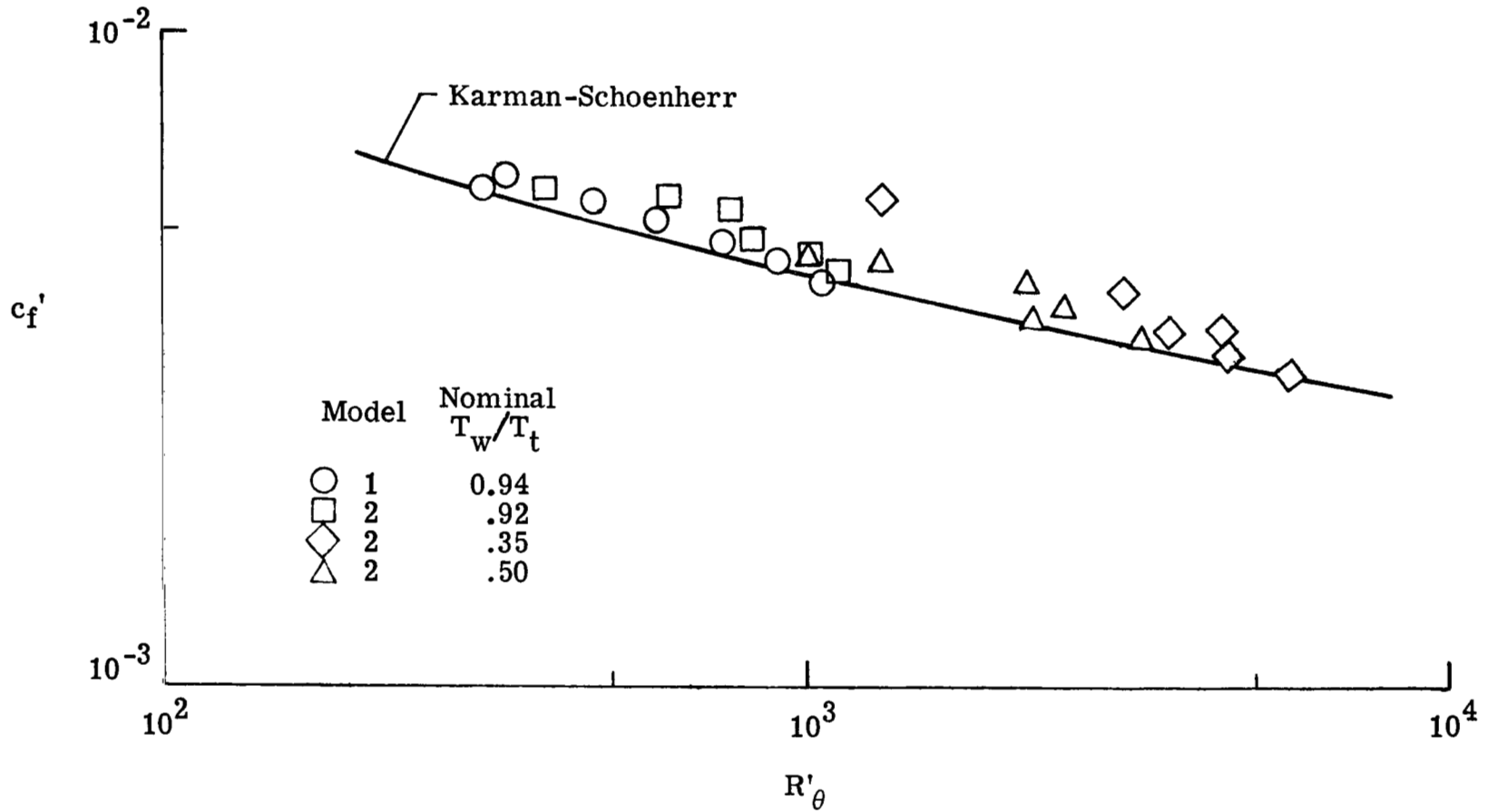
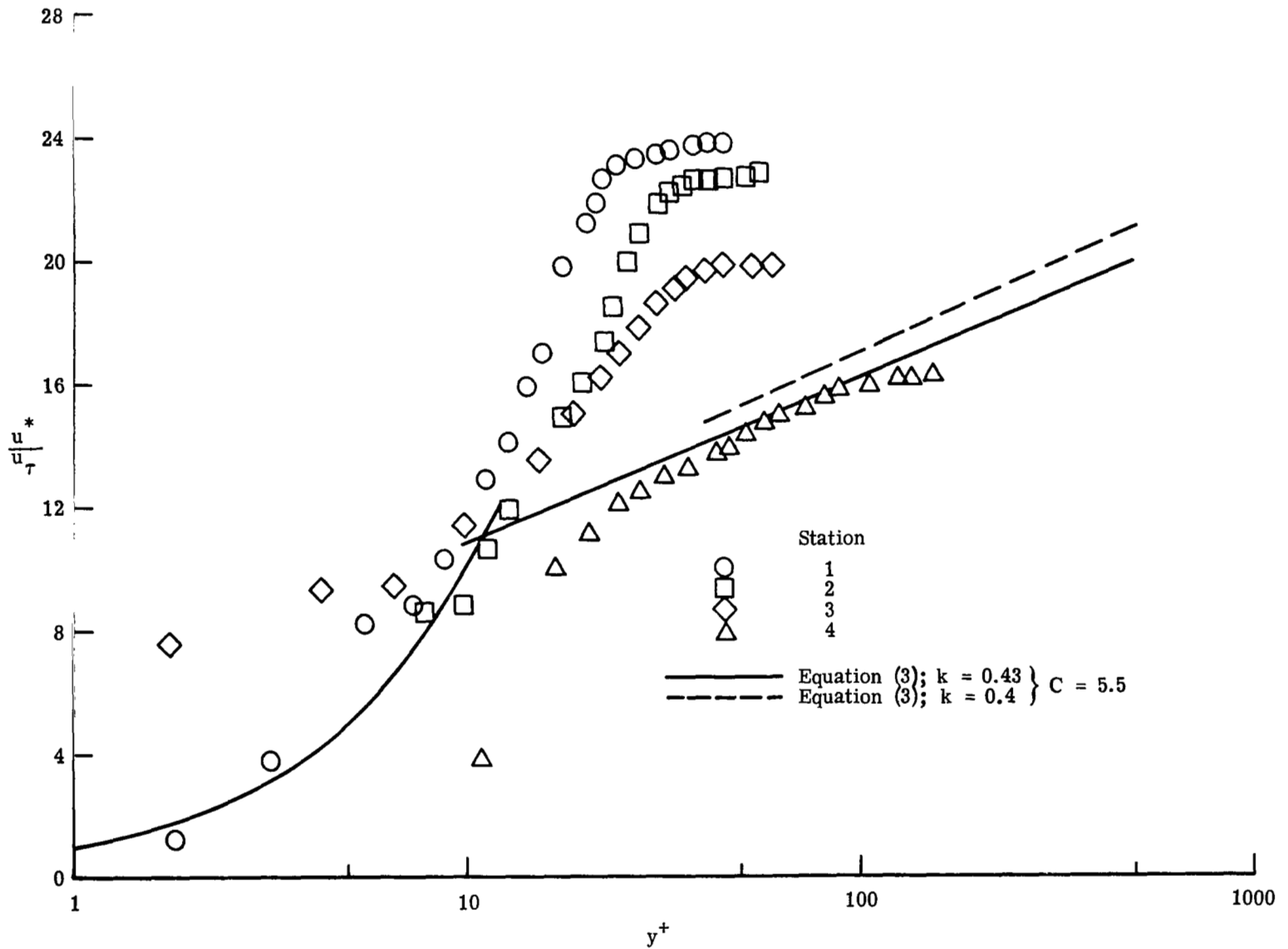
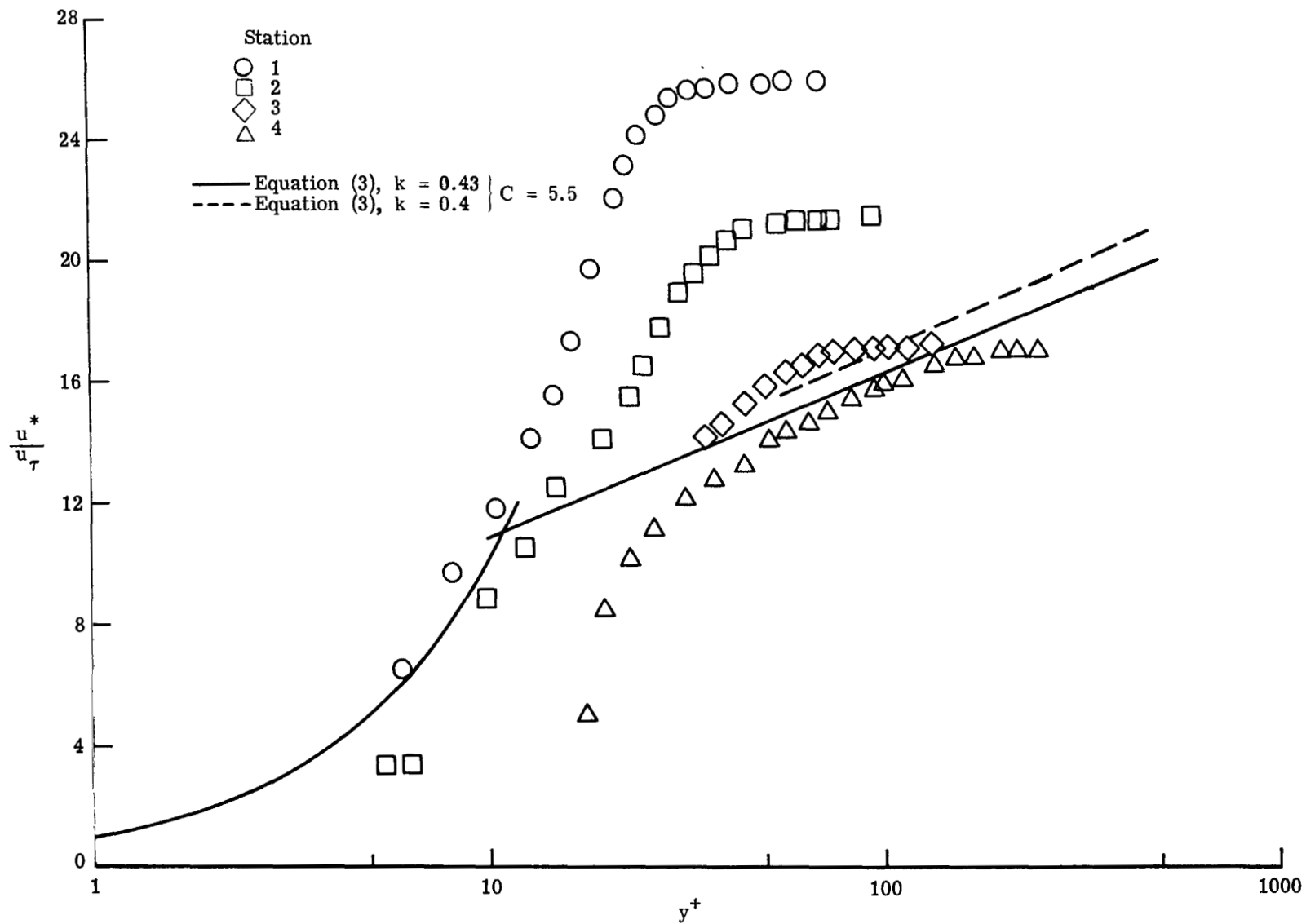


Figure 16.- Turbulent skin friction reduced to incompressible form.



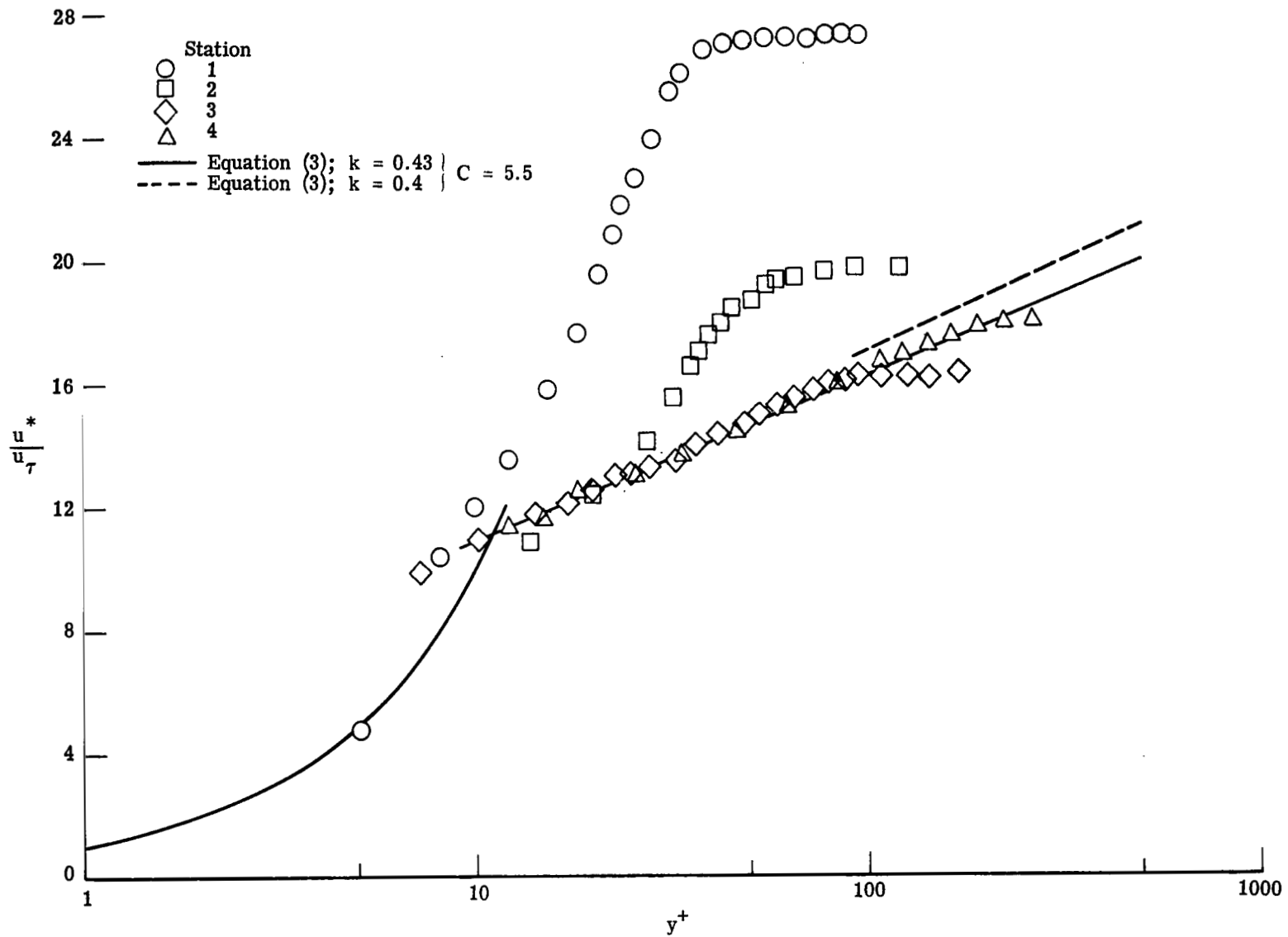
(a) $M_e = 9.5$; $Re/m = 9.62 \times 10^6$.

Figure 17.- Generalized velocity profiles on model 1.



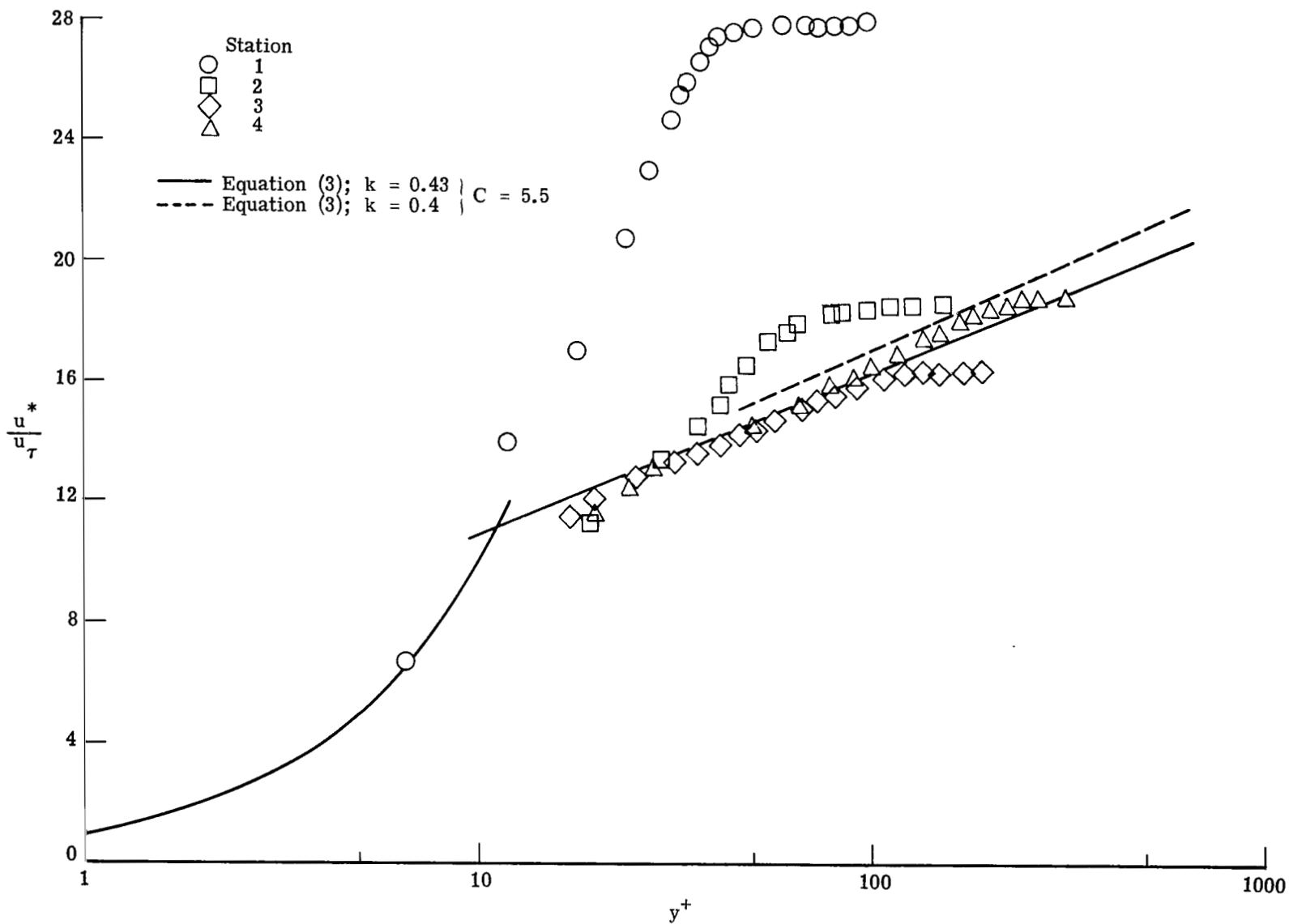
(b) $M_e = 9.7$; $Re/m = 18.75 \times 10^6$.

Figure 17.- Continued.



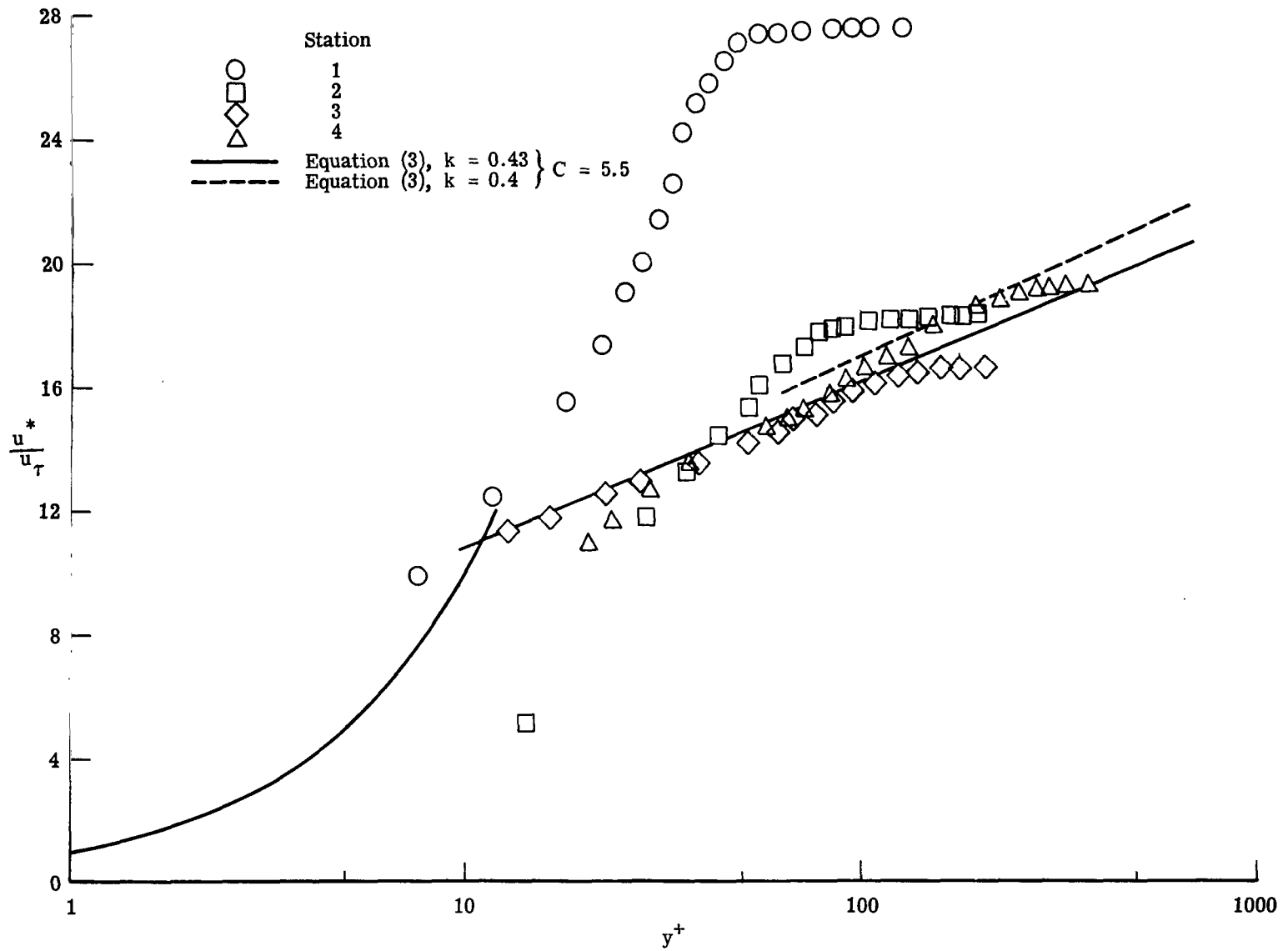
(c) $M_e = 9.7$; $Re/m = 27.50 \times 10^6$.

Figure 17.- Continued.



(d) $M_e = 10.0$; $Re/m = 37.06 \times 10^6$.

Figure 17.- Continued.



(e) $M_e = 10.1$; $R_e/m = 46.57 \times 10^6$.

Figure 17.- Concluded.

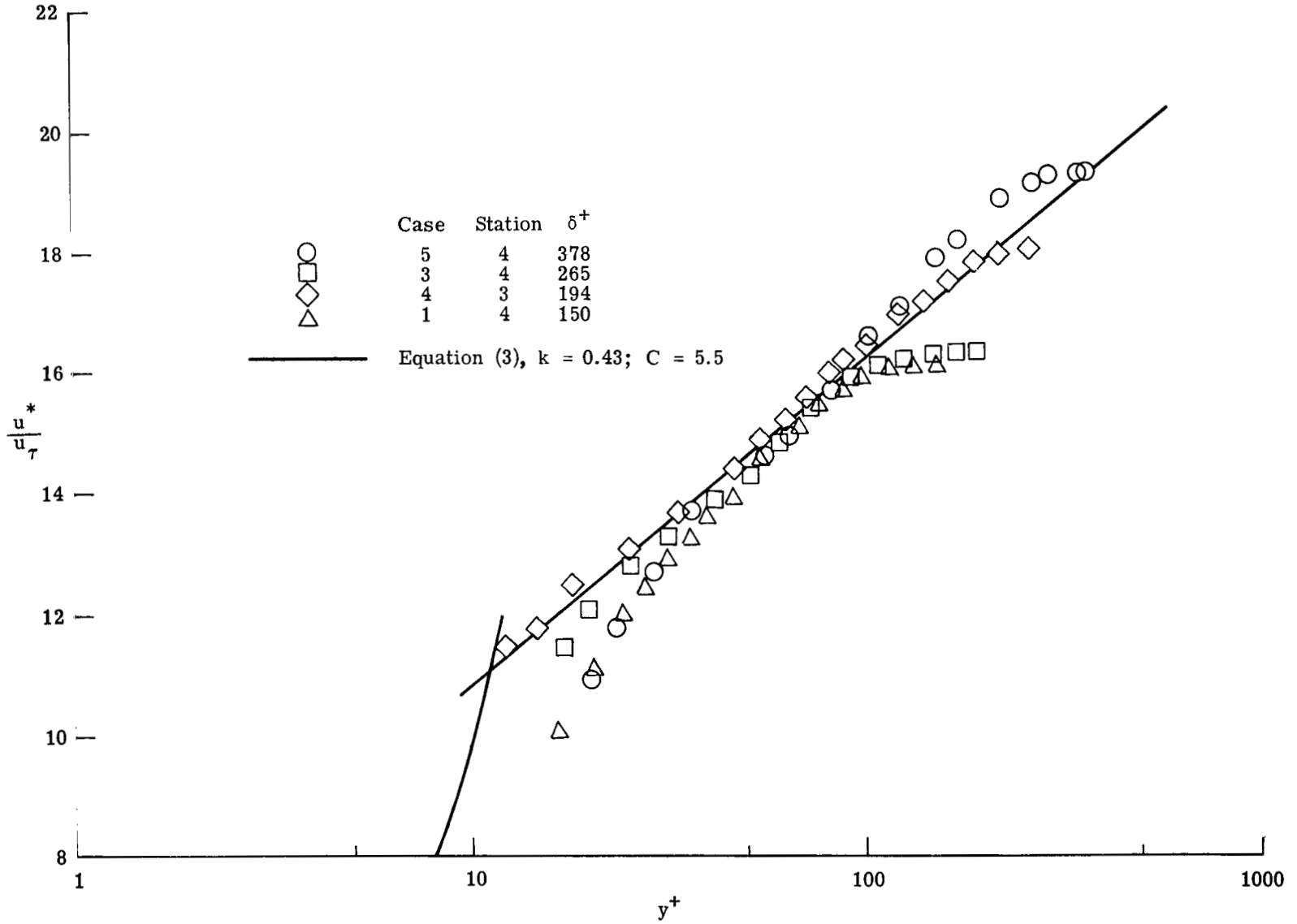
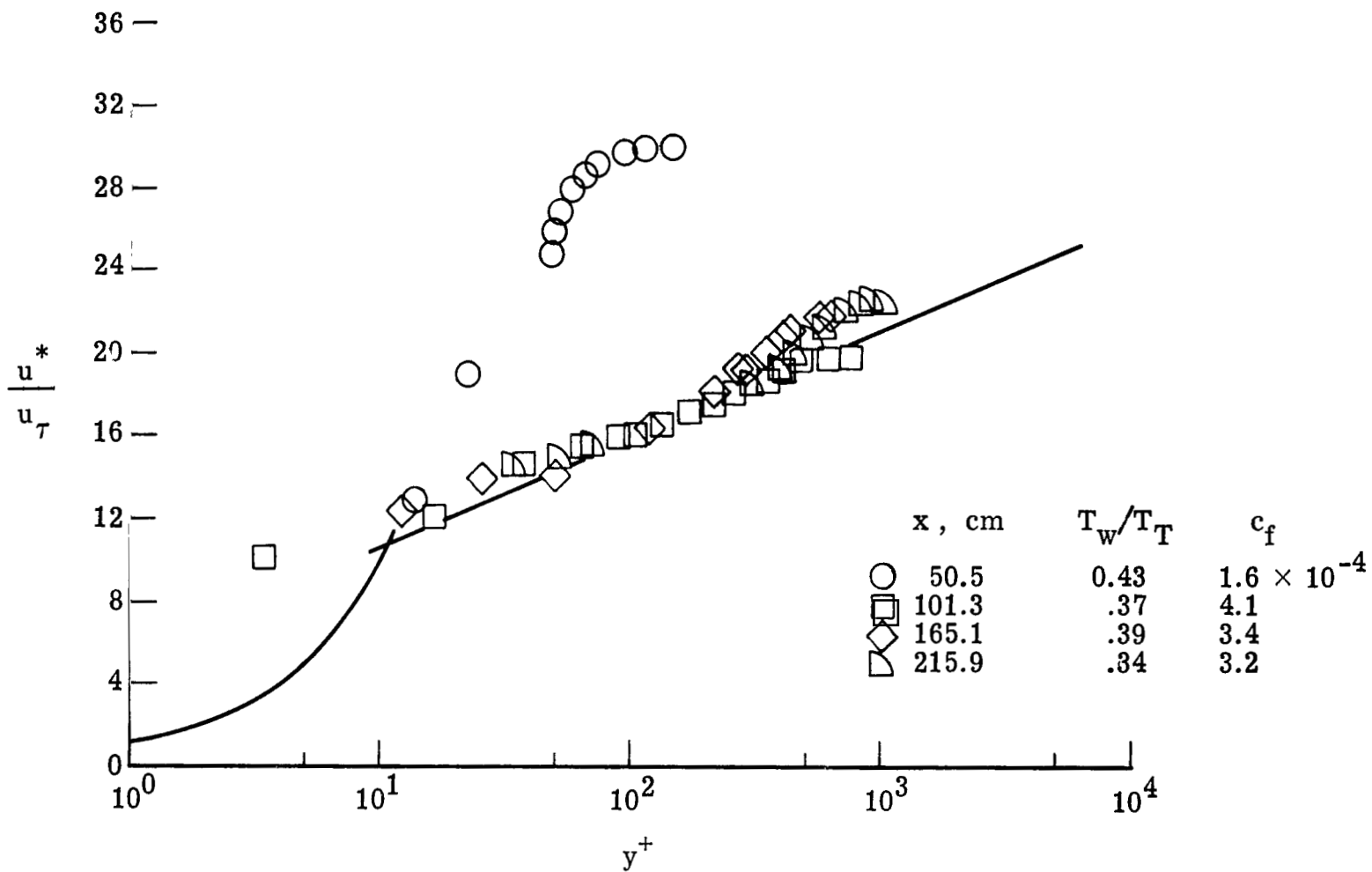
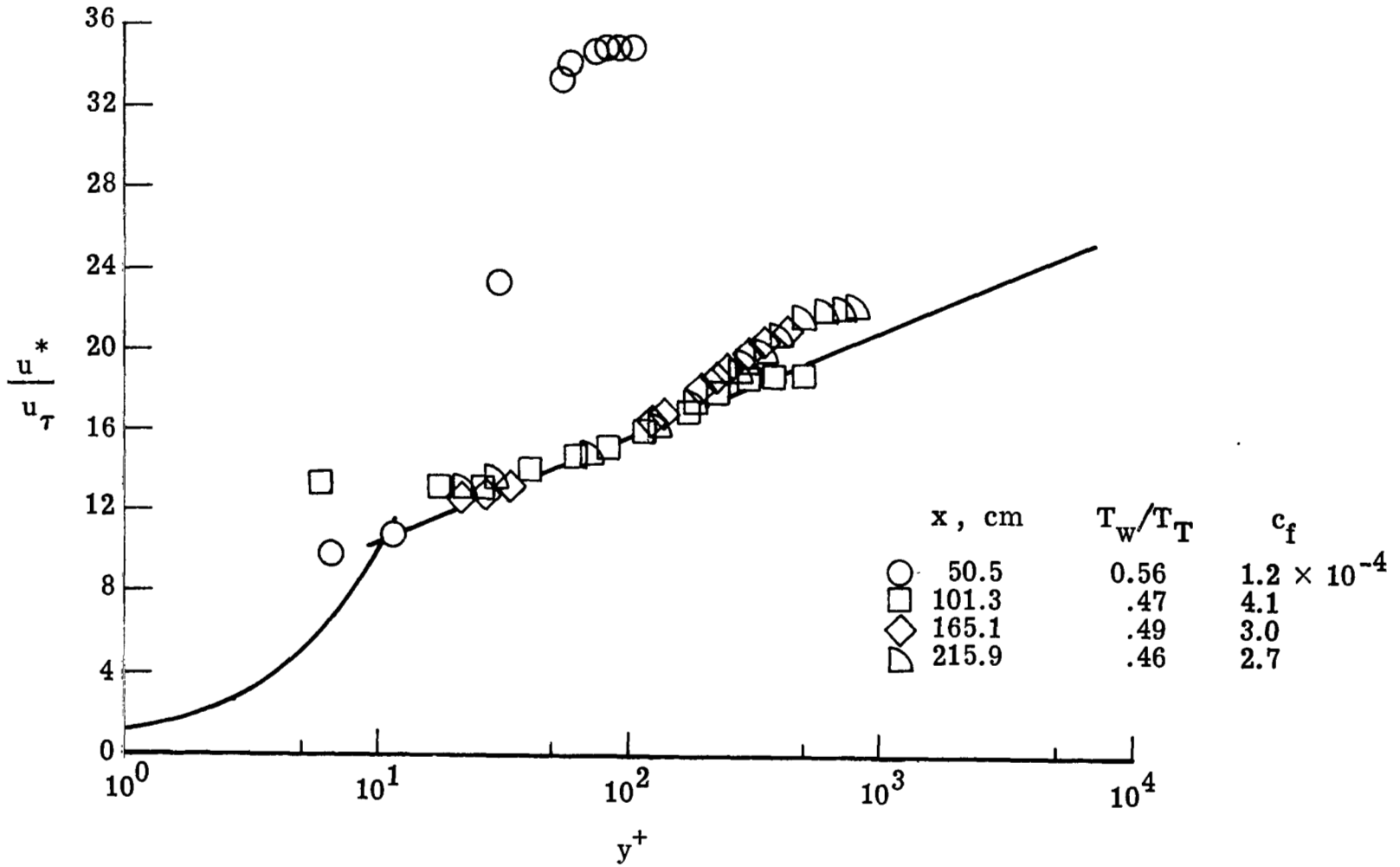


Figure 18.- Turbulent profiles on model 1.



(a) $T_w/T_t \approx 0.4$.

Figure 19.- Generalized velocity profiles on model 2.



(b) $T_w/T_t \approx 0.5$.

Figure 19.- Concluded.

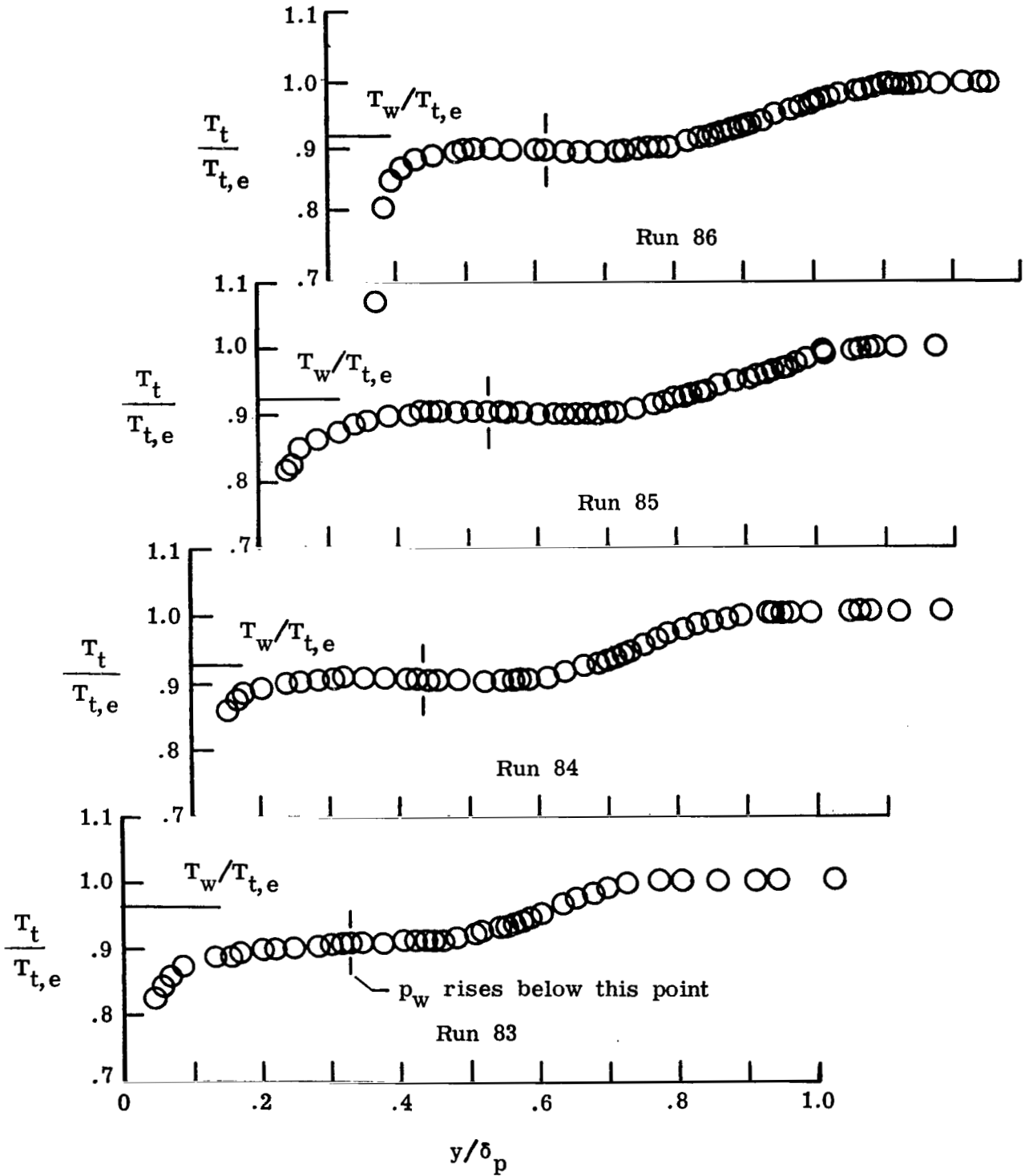


Figure 20.- Total-temperature profile data on model 1.

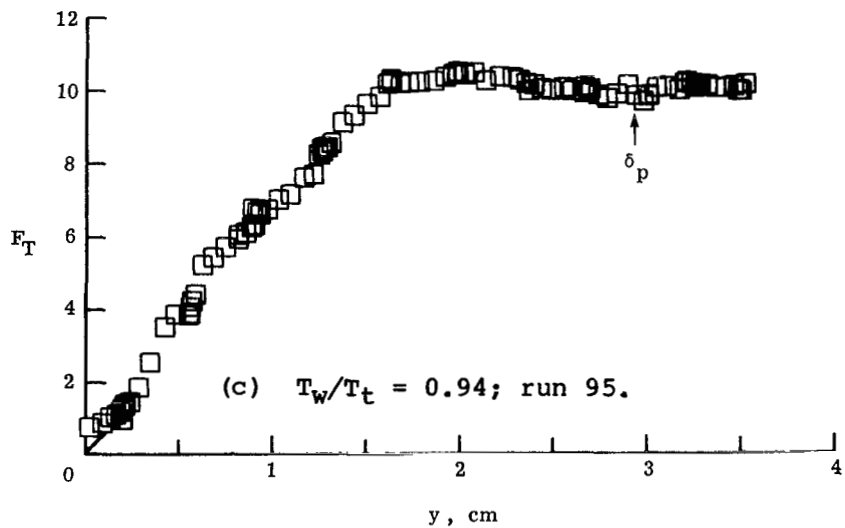
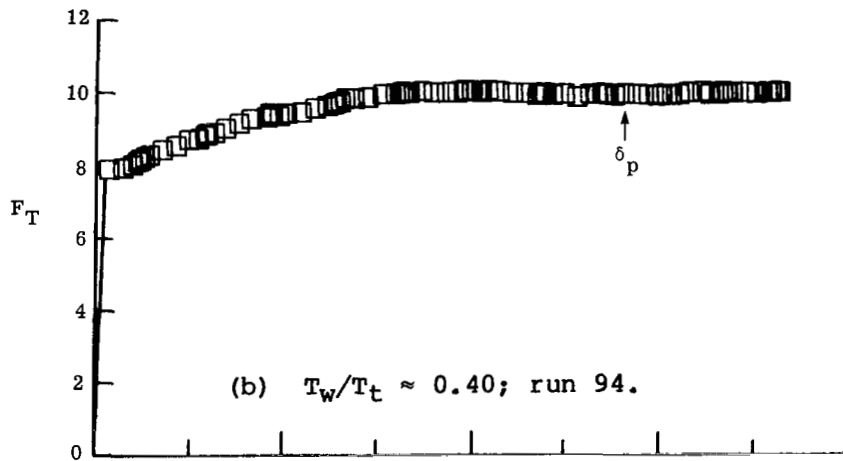
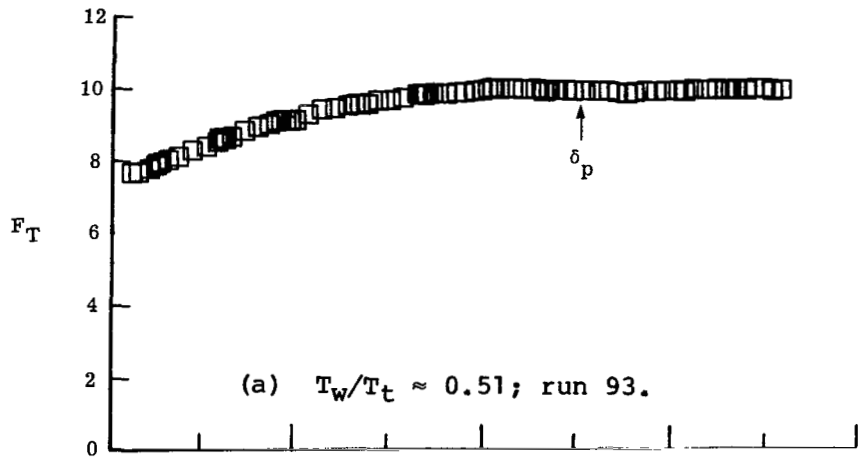
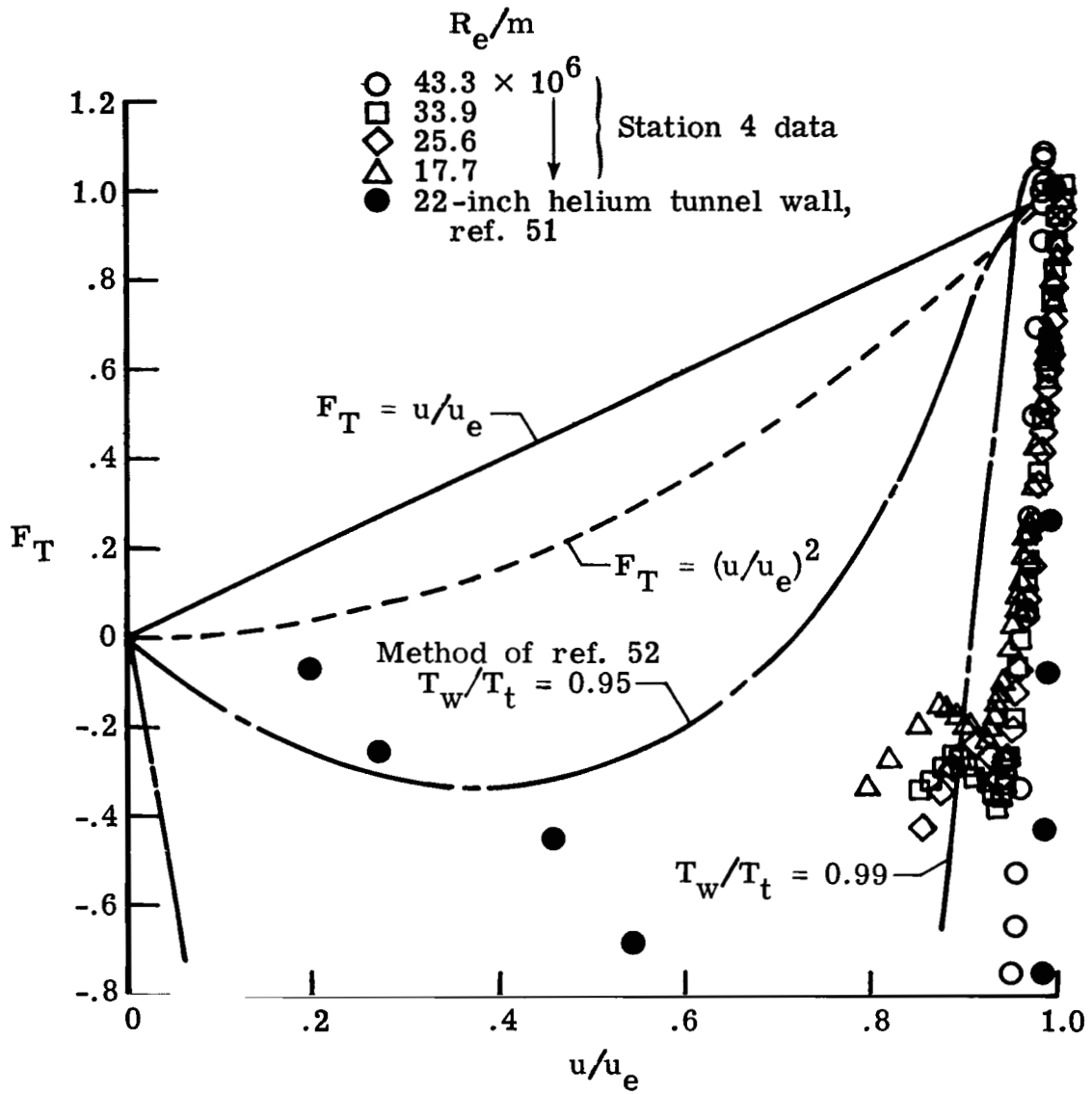
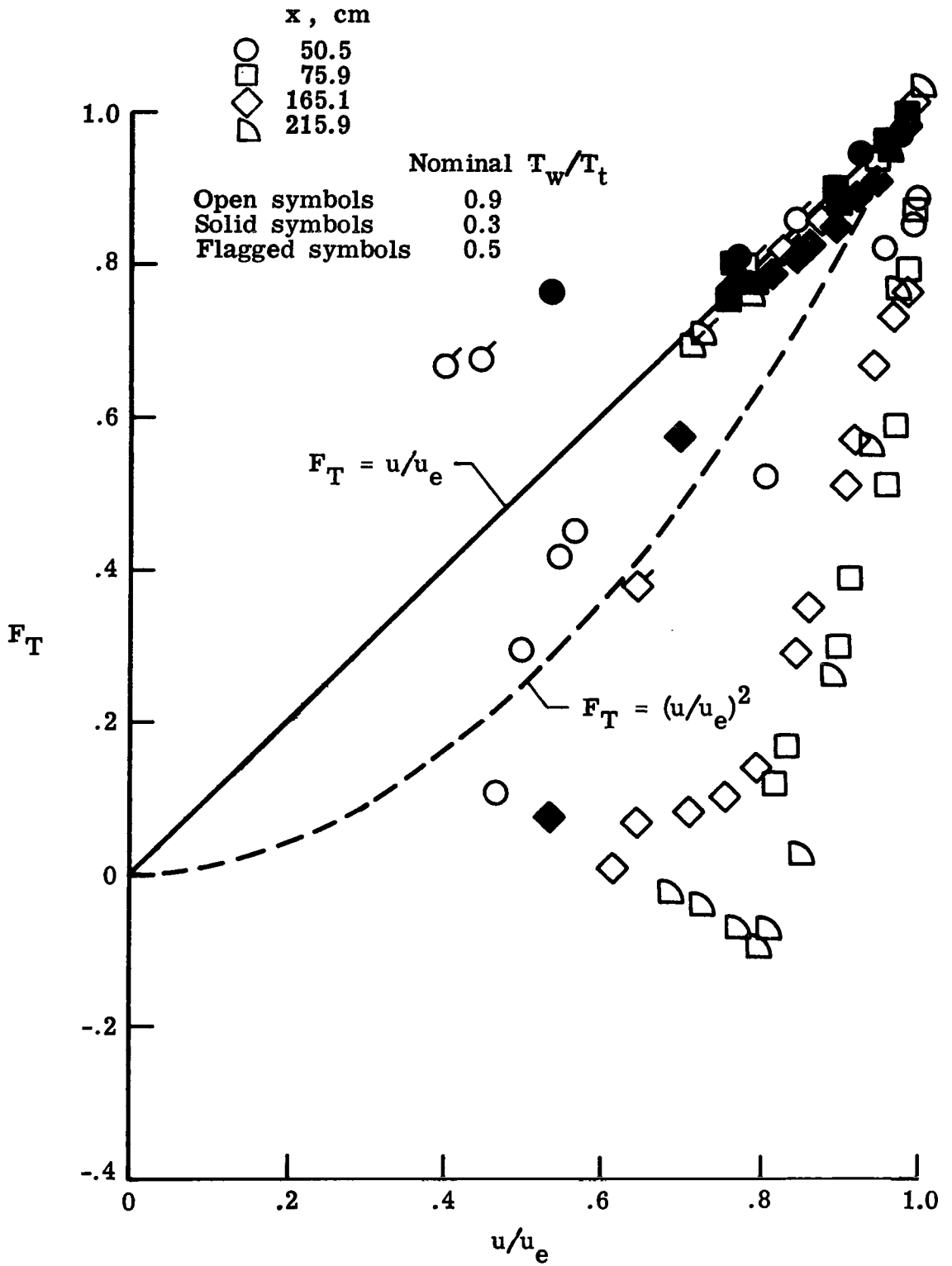


Figure 21.- Representative total temperature profiles on model 2 at station 5.



(a) Data for model 1.

Figure 22.- Total temperature distributions in Crocco form.



(b) Data for model 2.

Figure 22.- Concluded.

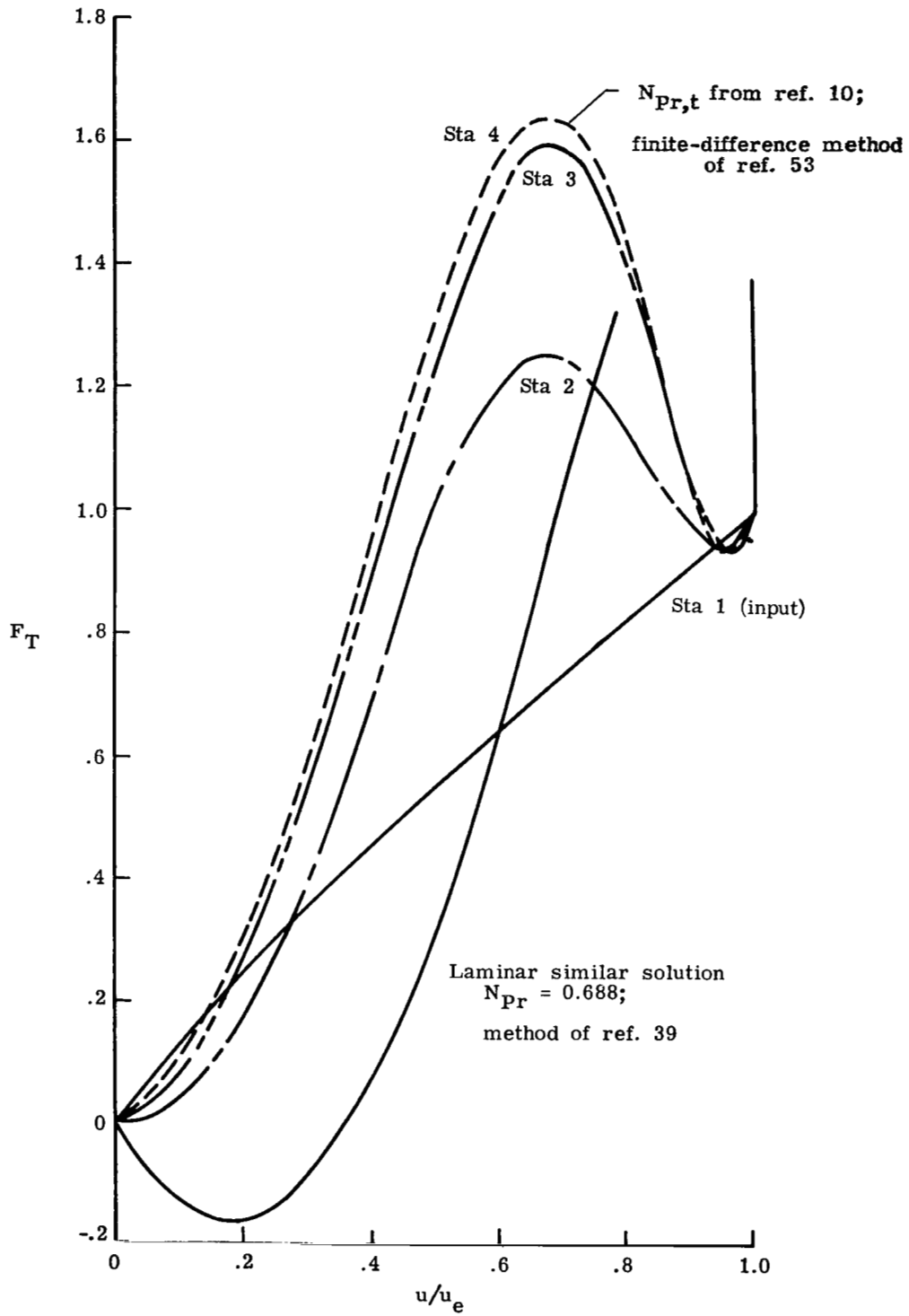


Figure 23.- Calculated total temperature profiles in laminar and turbulent boundary layers.

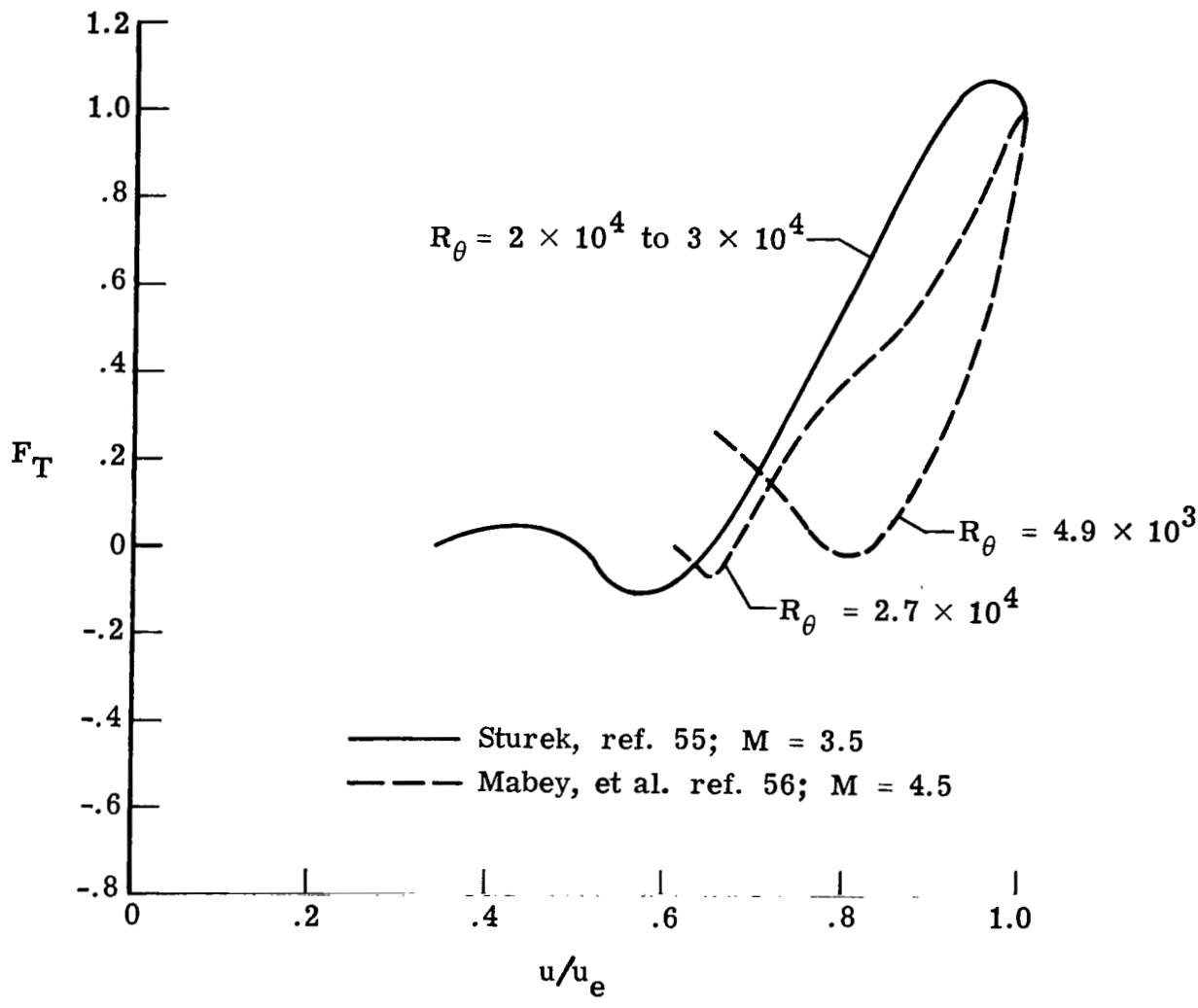


Figure 24.- Near-adiabatic wall total temperature distributions from other sources.

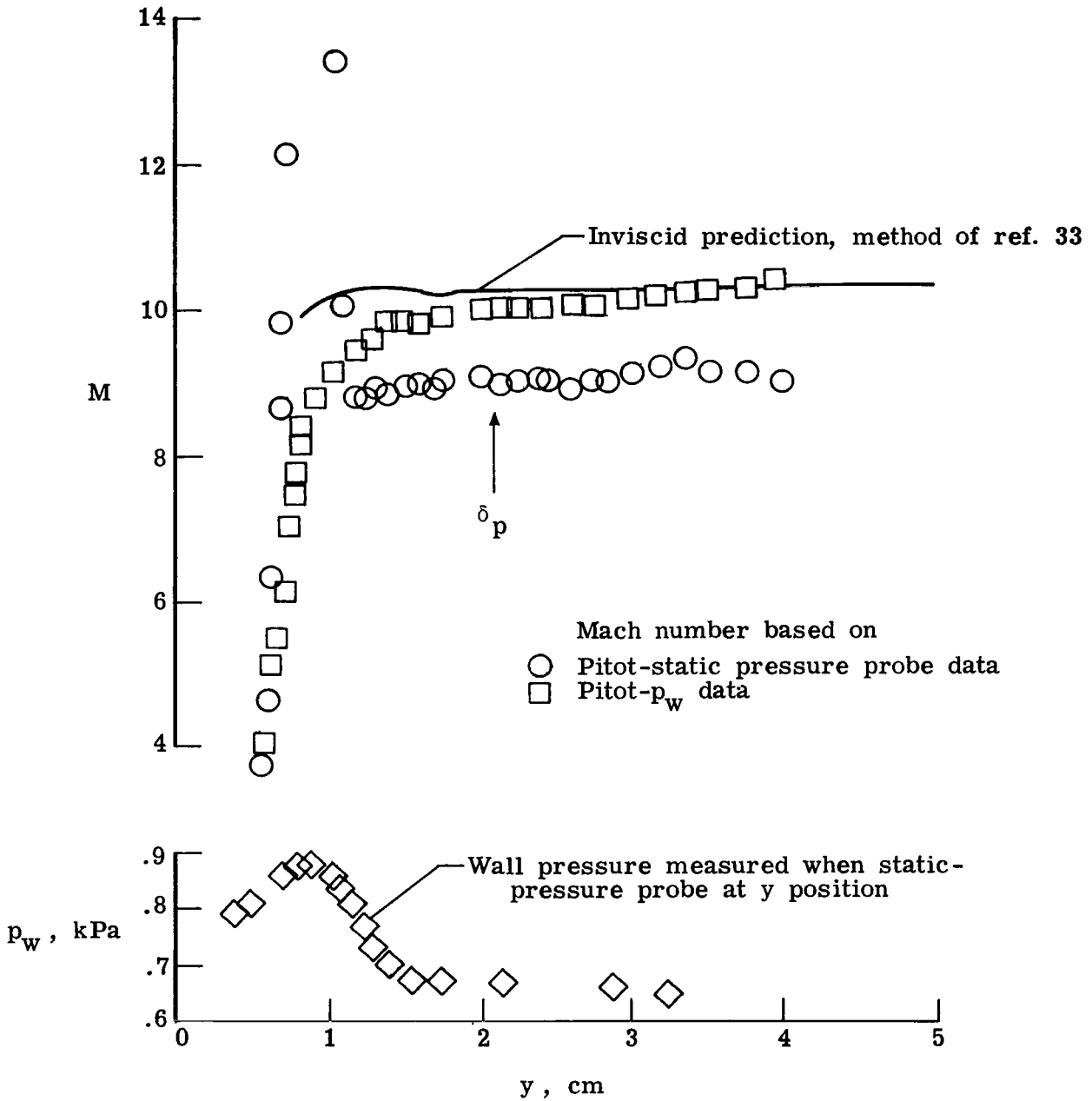


Figure 25.- Effect of probe interference on static pressure probe. Pitot derived Mach number distribution.

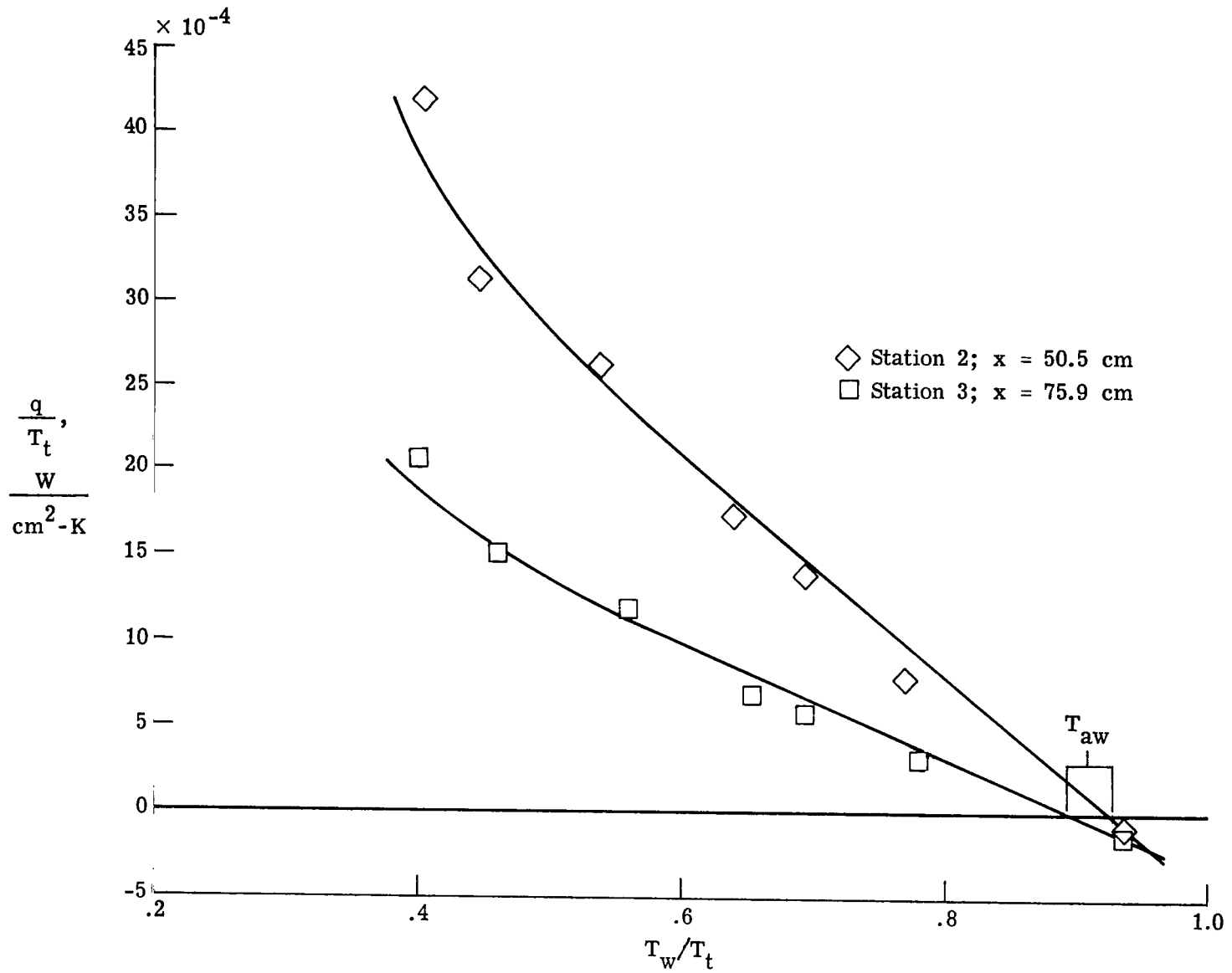


Figure 26.- Method of determining T_{aw} from heat-transfer data of model 2.

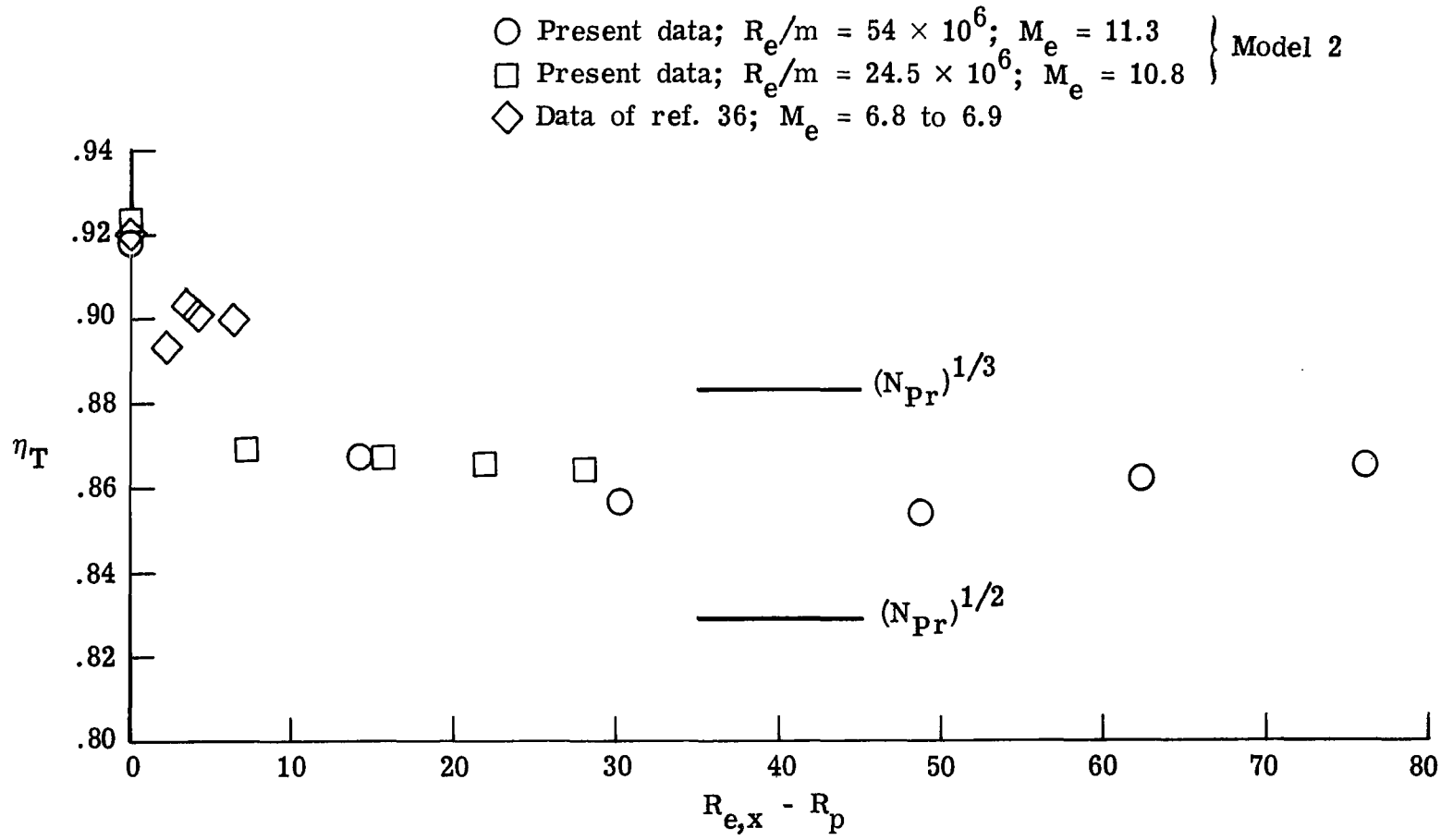


Figure 27.- Turbulent recovery factors in hypersonic helium flow.

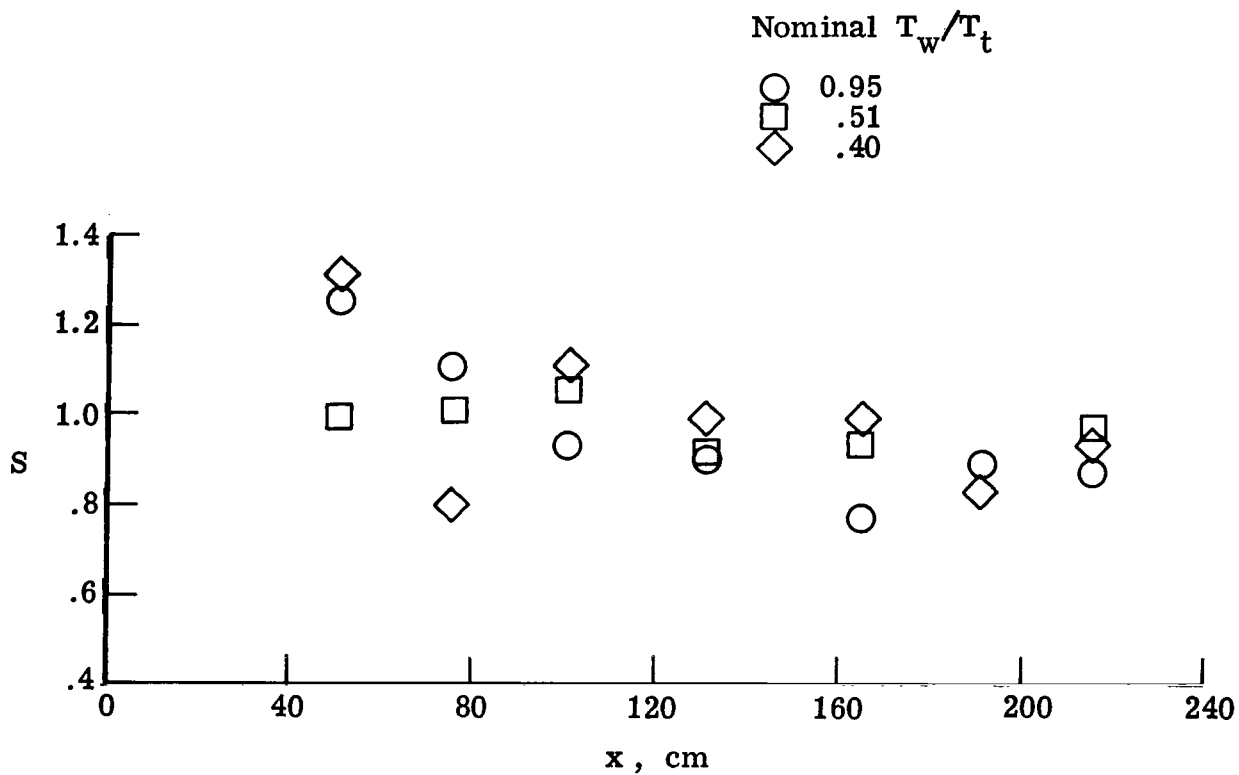


Figure 28.- Reynolds analogy factors on model 2. $M_e = 11.3$; $Re/m = 54 \times 10^6$.

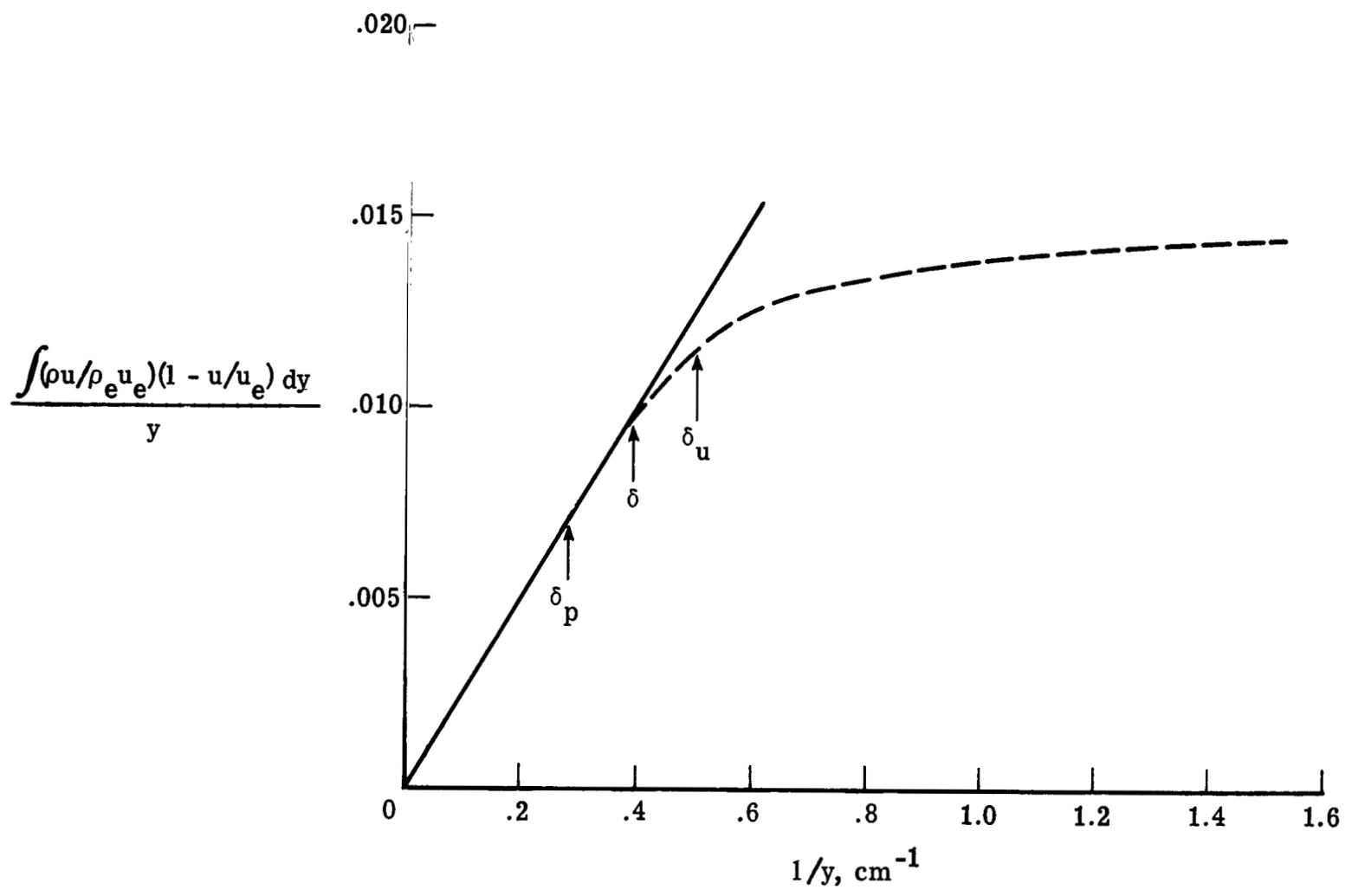
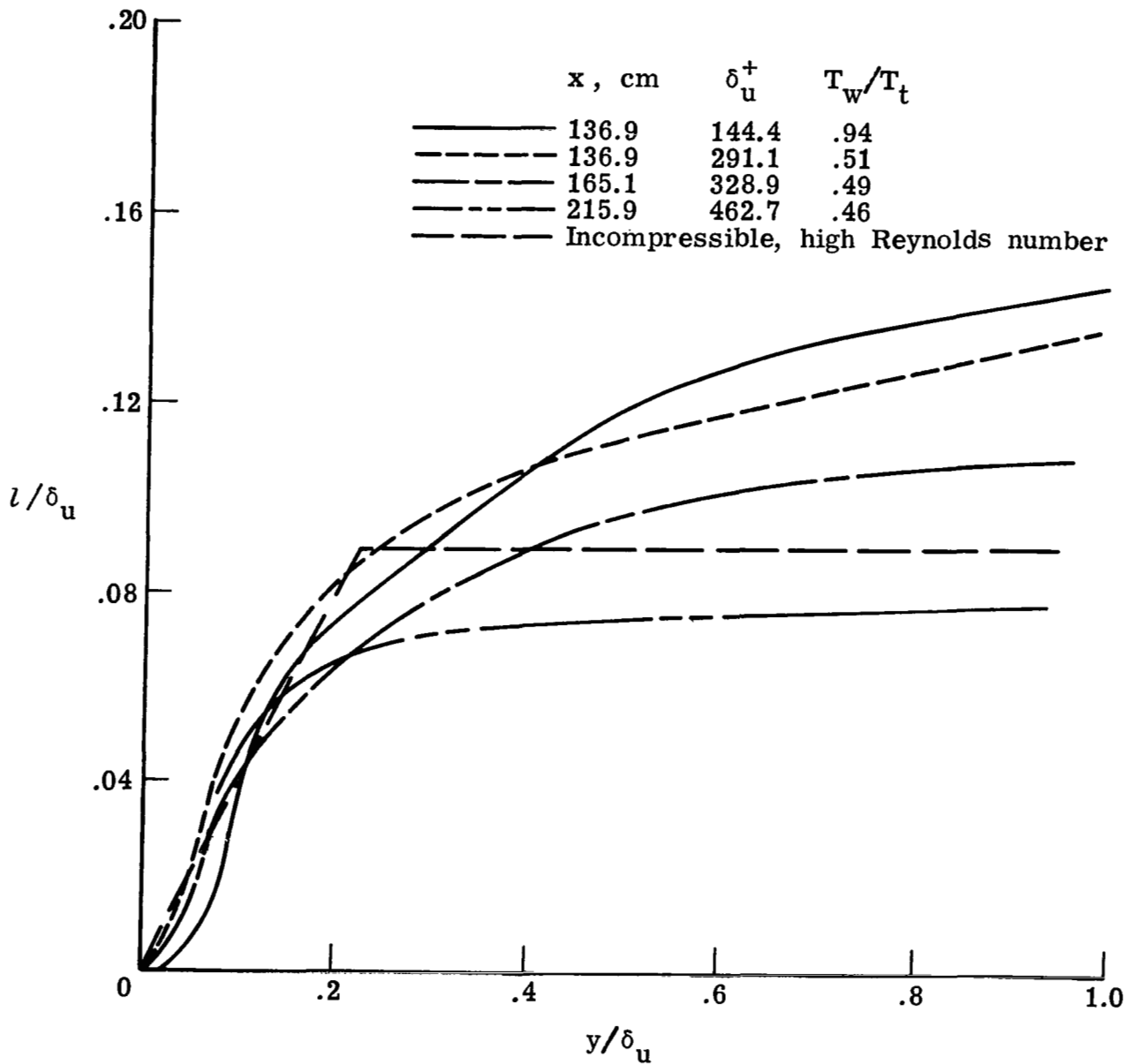
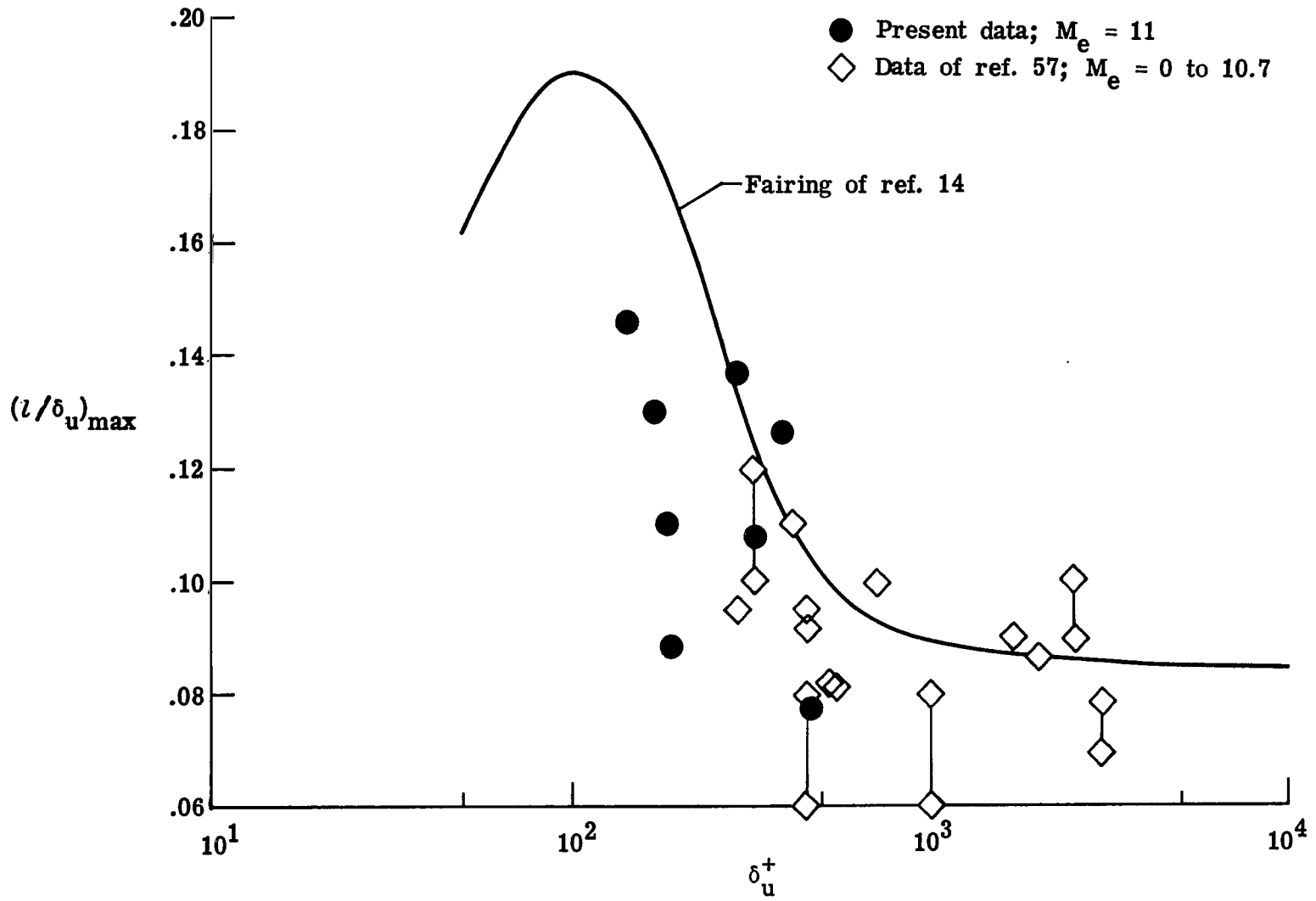


Figure 29.- Method of estimating similarity thickness δ .



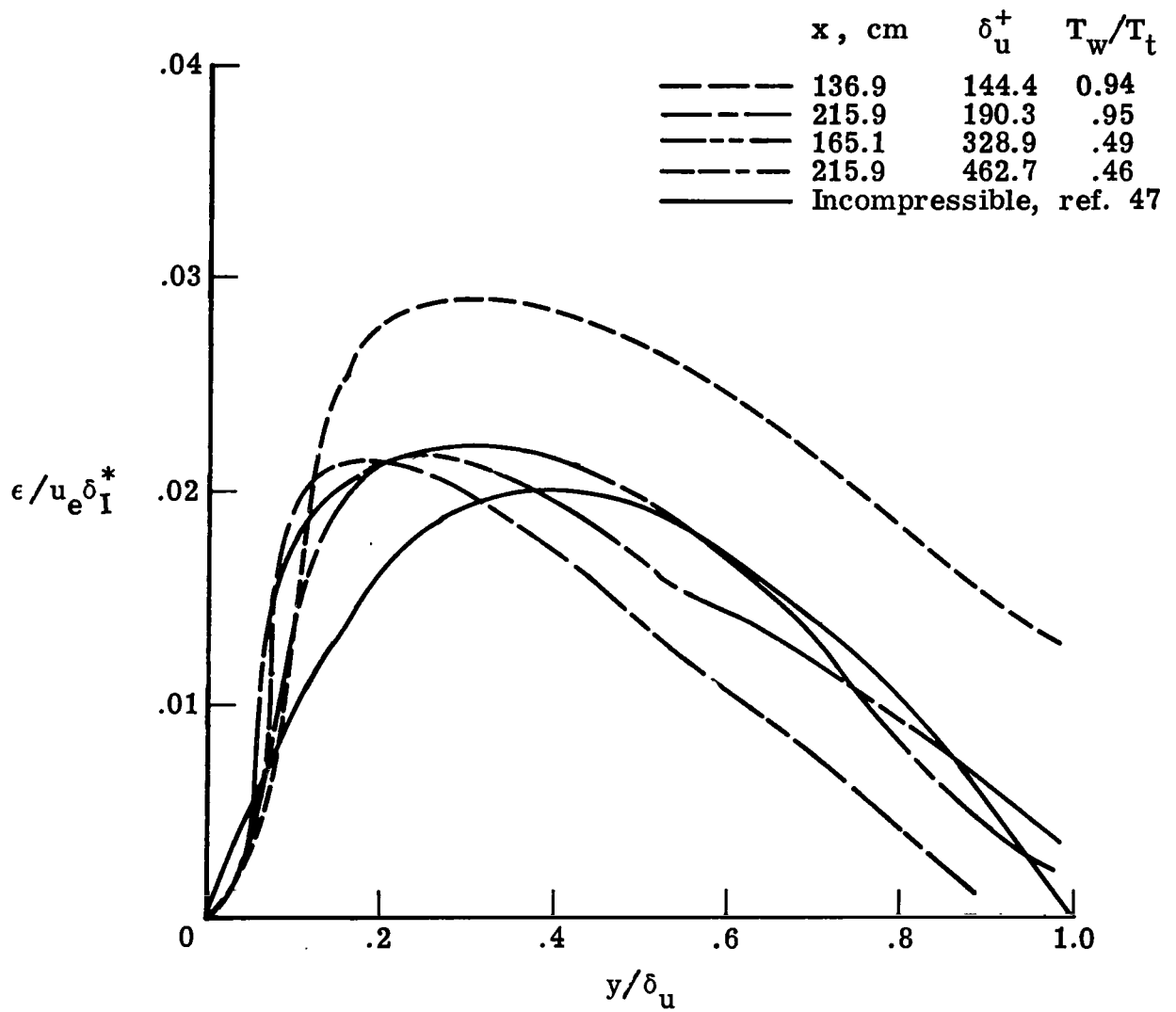
(a) Representative mixing-length distributions through boundary layer.

Figure 30.- Turbulence parameters derived from mean profiles.



(b) Low Reynolds number effect on maximum mixing lengths.

Figure 30.- Continued.



(c) Eddy viscosity distributions.

Figure 30.- Concluded.

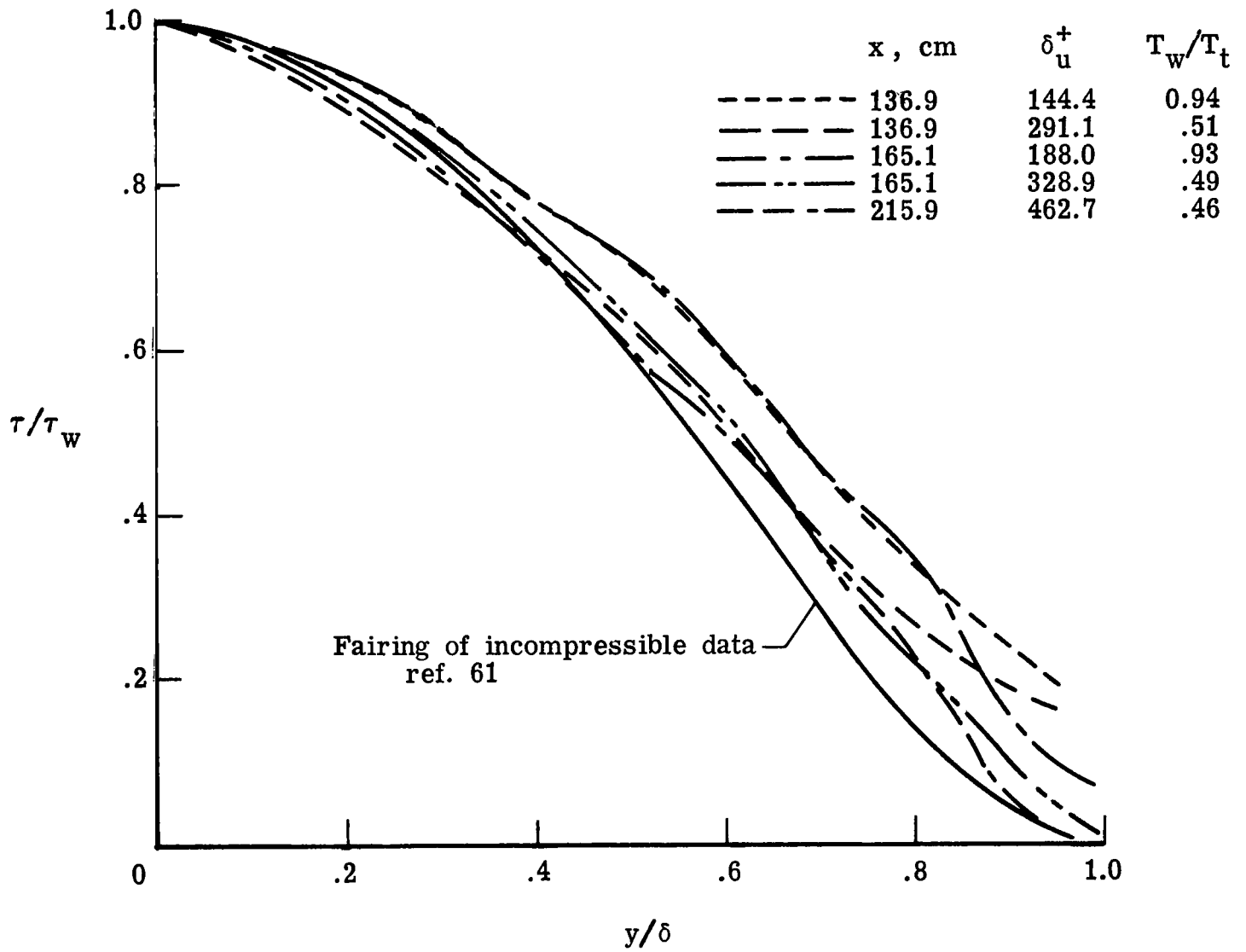


Figure 31.- Total shear stress distributions.

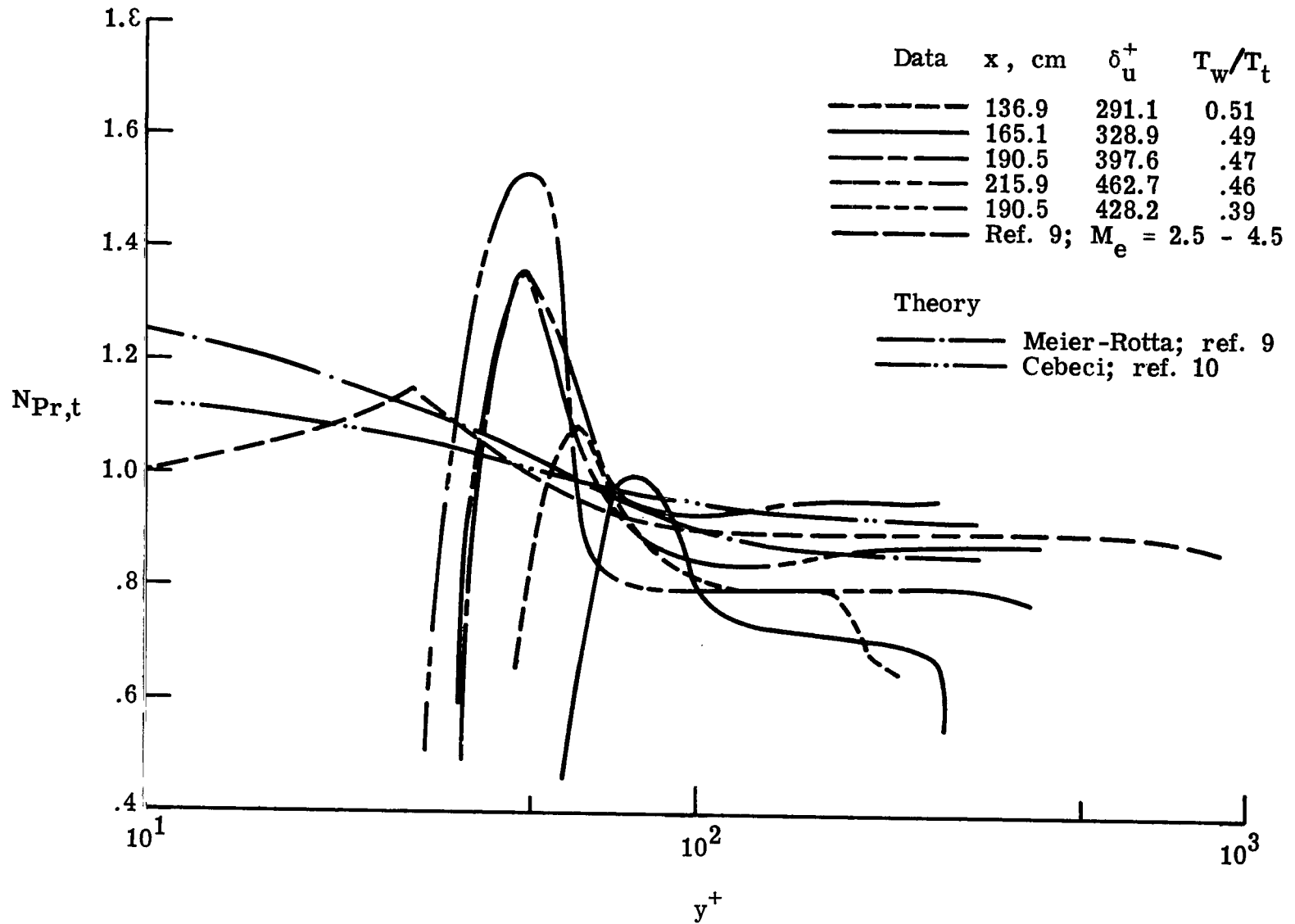


Figure 32.- Turbulent Prandtl number distributions.

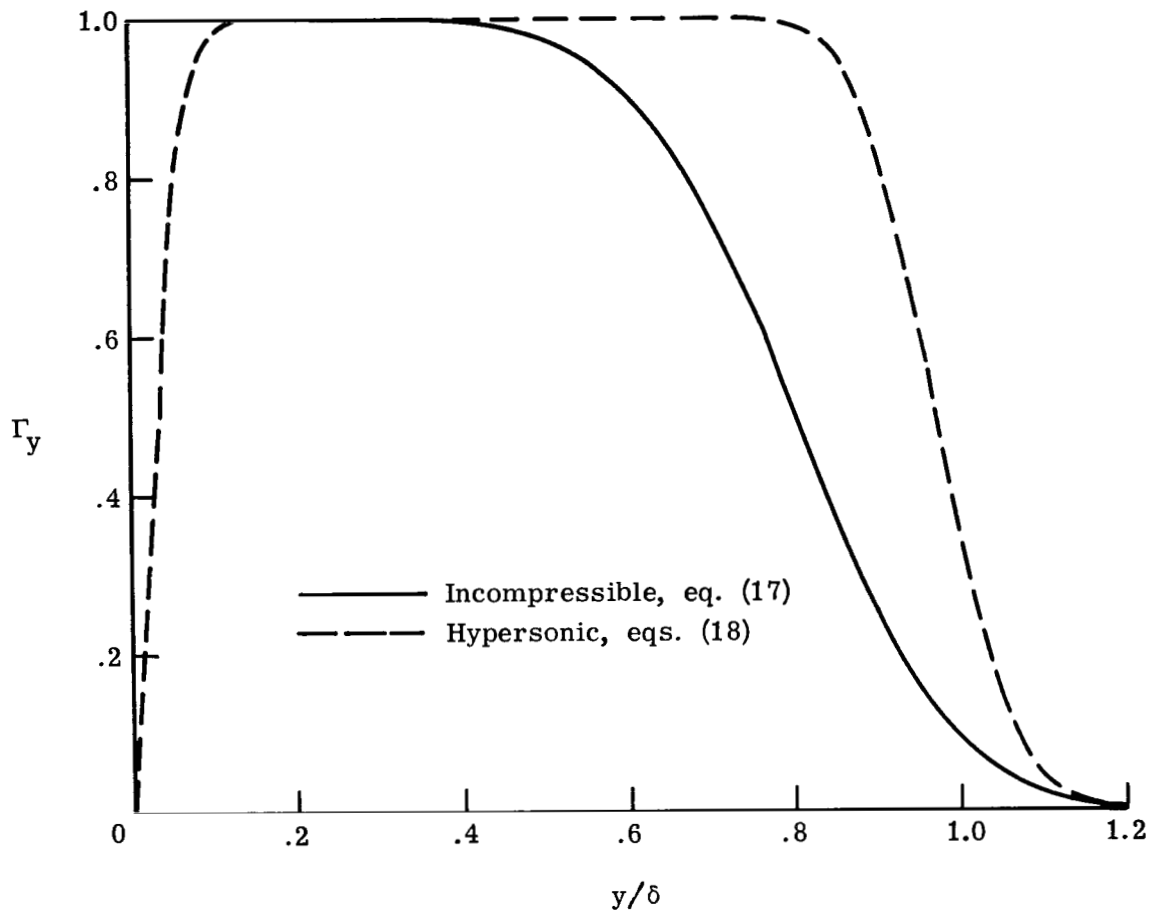


Figure 33.- Intermittency normal to surface.

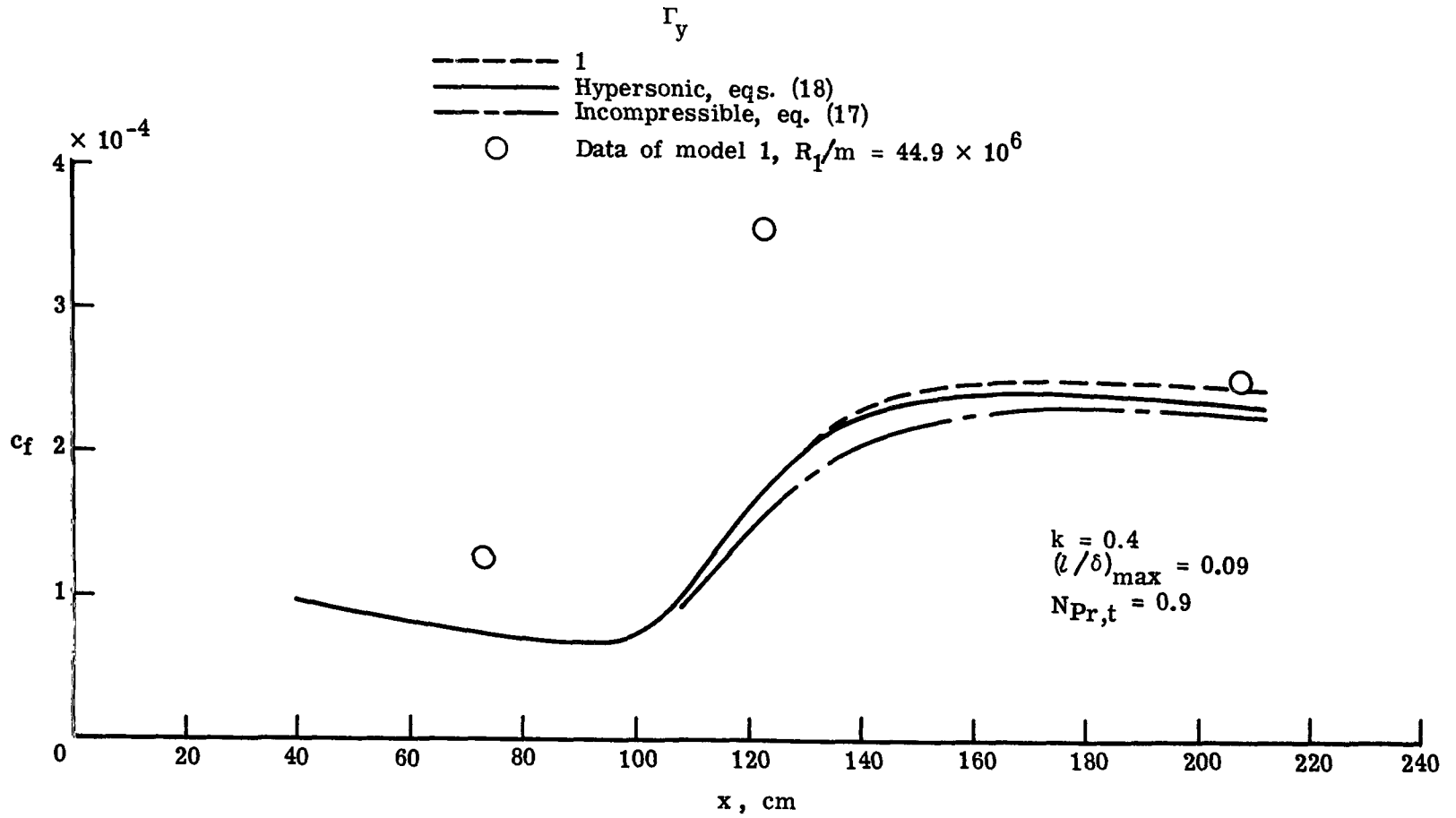


Figure 34.- Effect of Γ_y on calculated skin-friction coefficients.

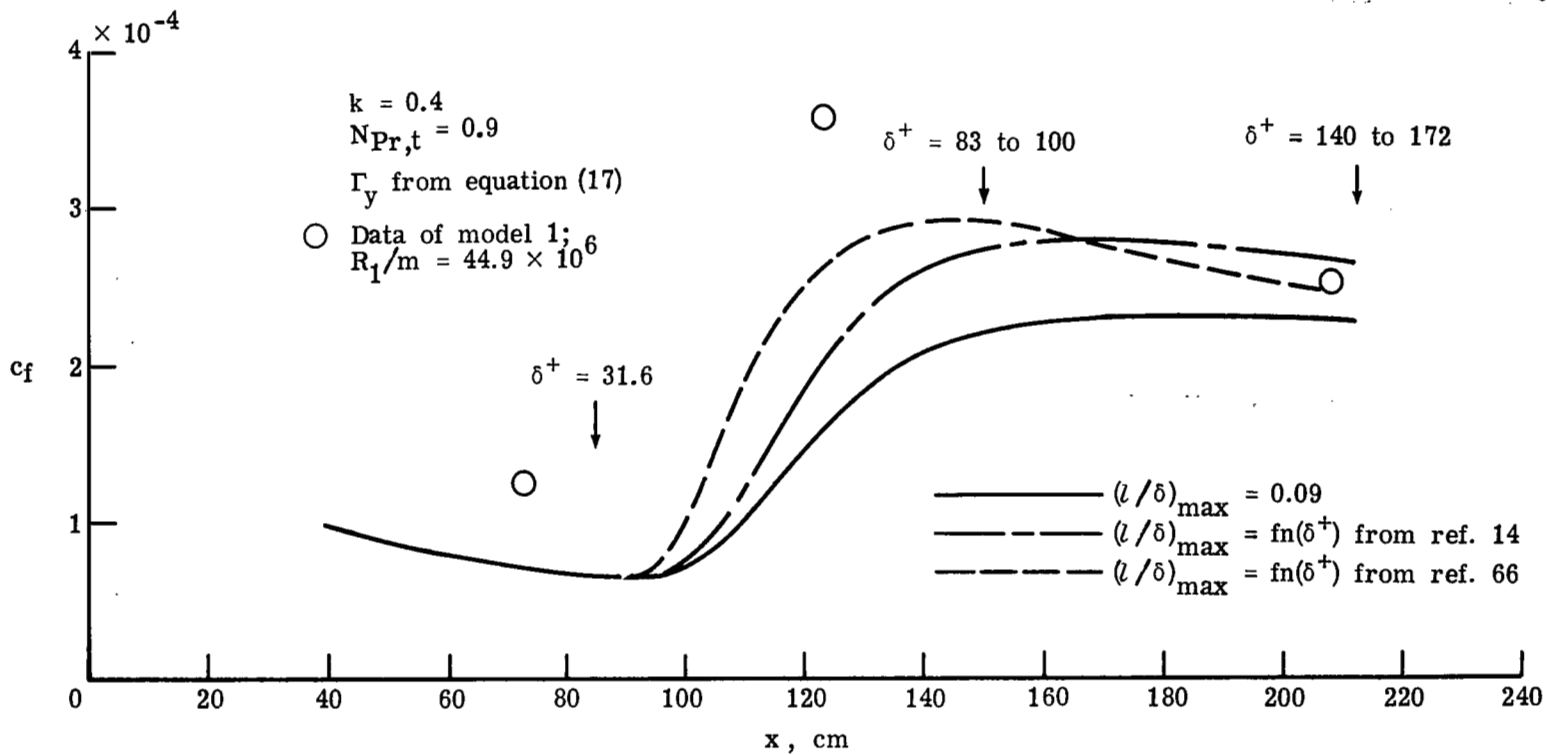


Figure 35.- Low Reynolds number effect on calculated skin-friction coefficients.

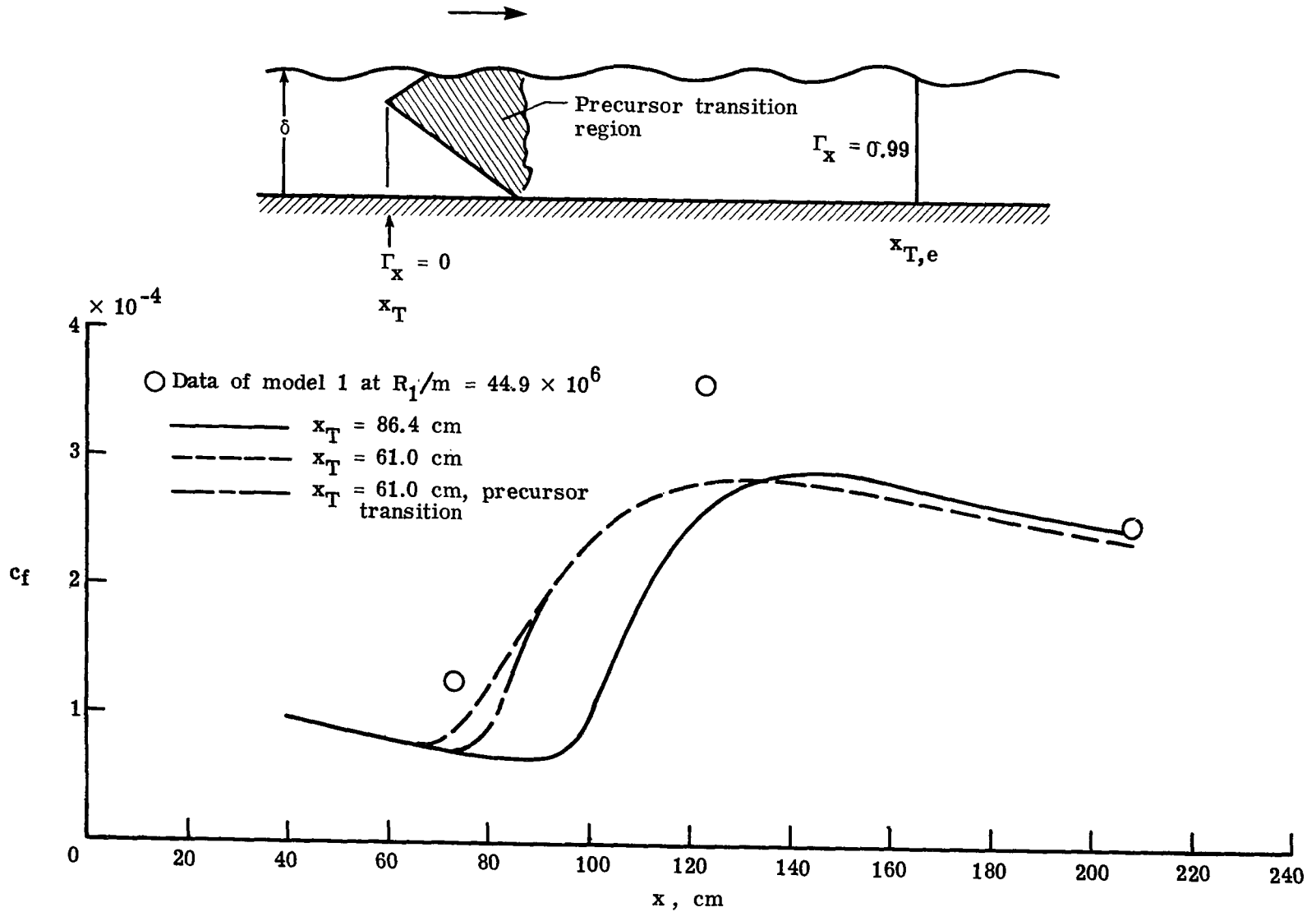
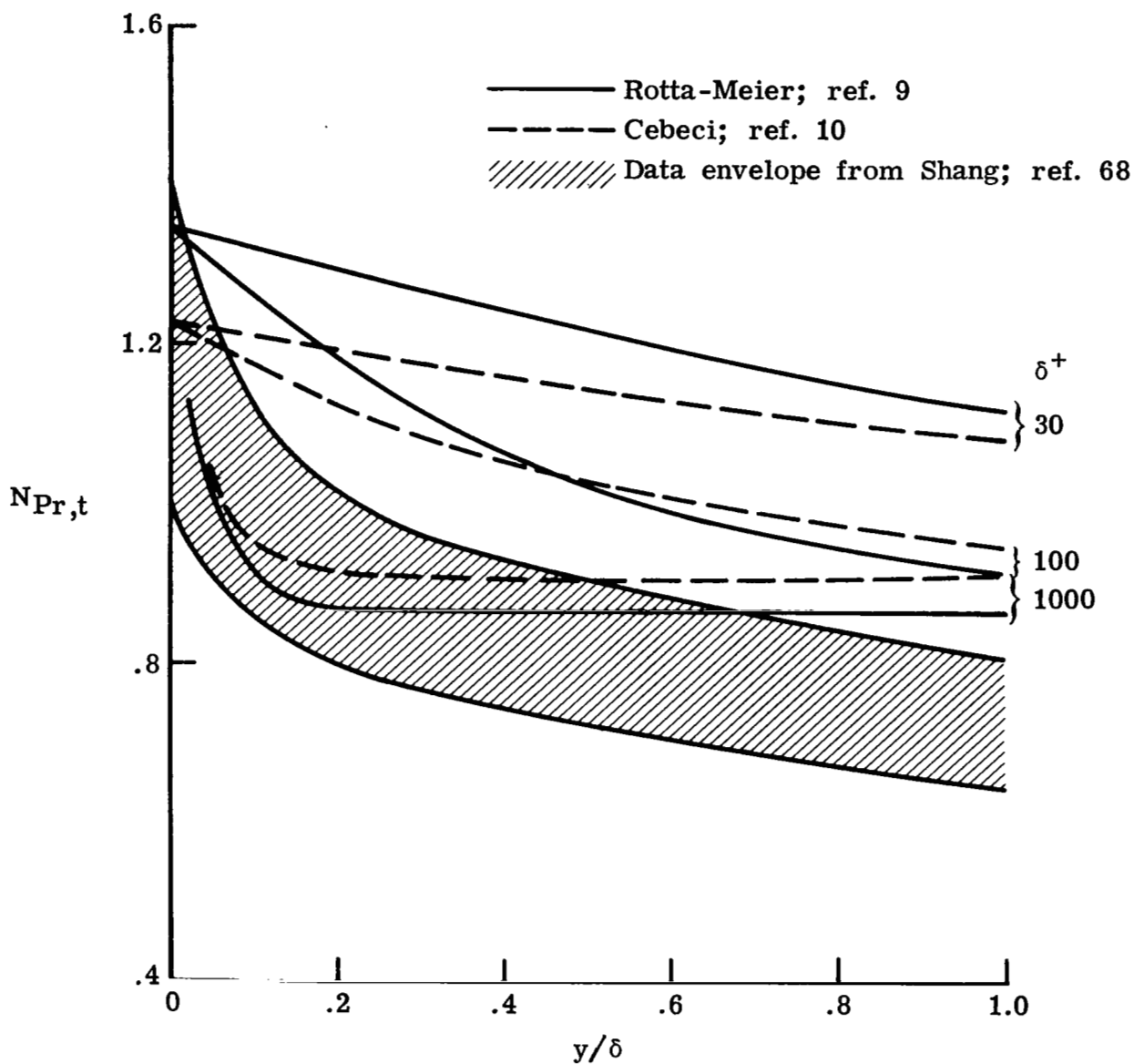
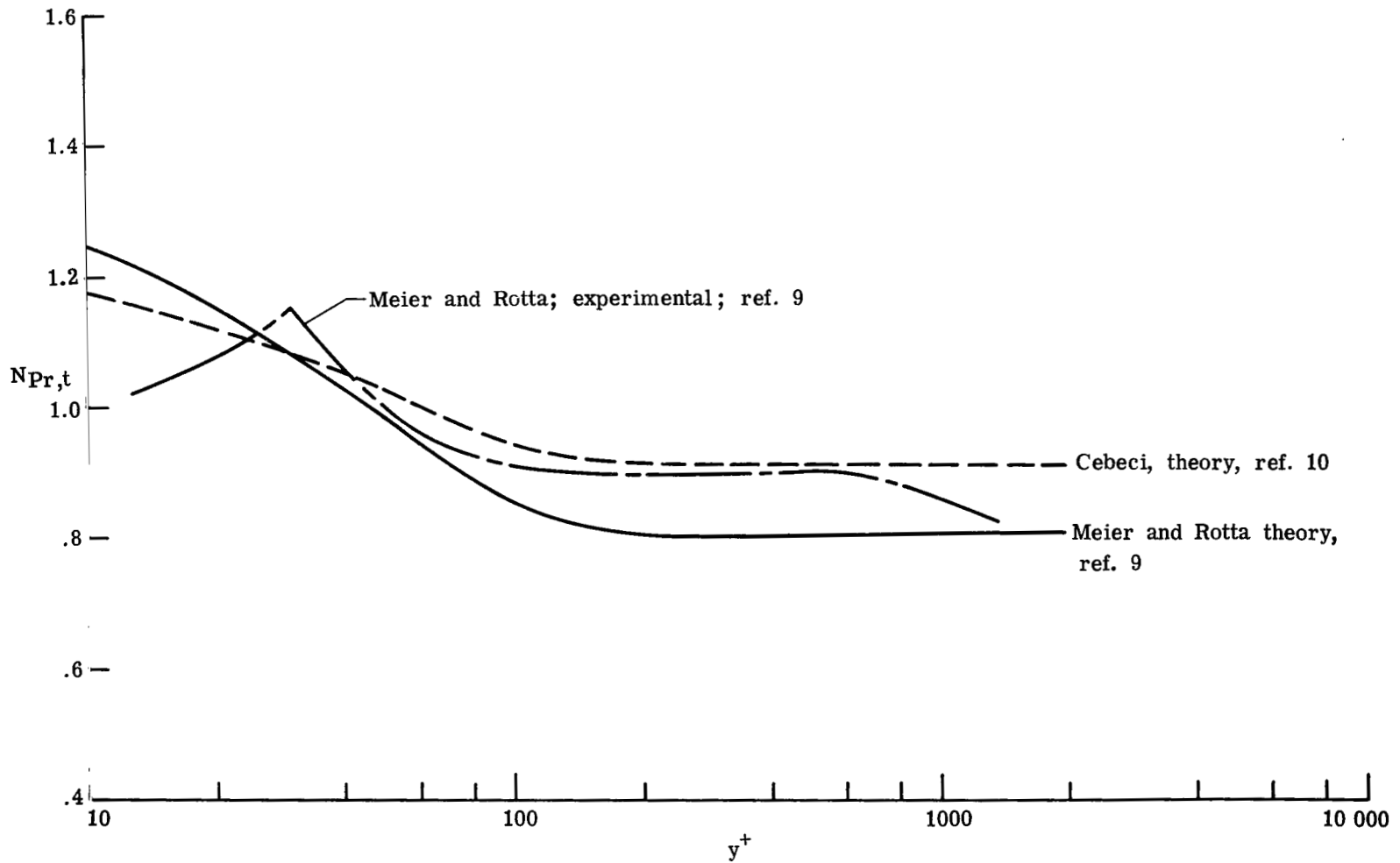


Figure 36.- Effect of precursor transition on calculated skin-friction coefficients.



(a) Theoretical distributions in y/δ .

Figure 37.- Static turbulent Prandtl number distributions through boundary layers.



(b) Theoretical and experimental distributions in law-of-the-wall coordinates.

Figure 37.- Concluded.

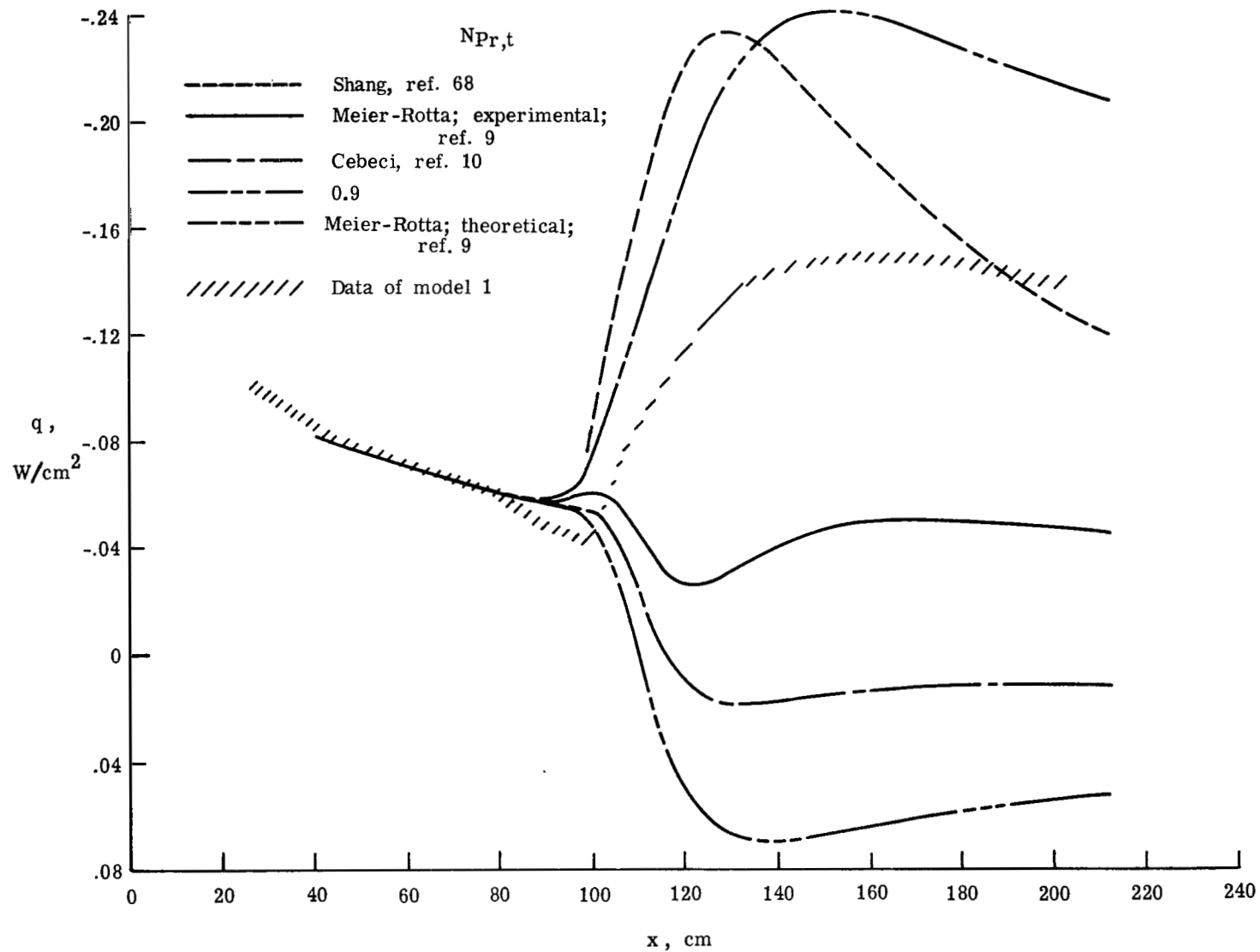


Figure 38.- Effect of $N_{Pr,t}$ on calculated q .

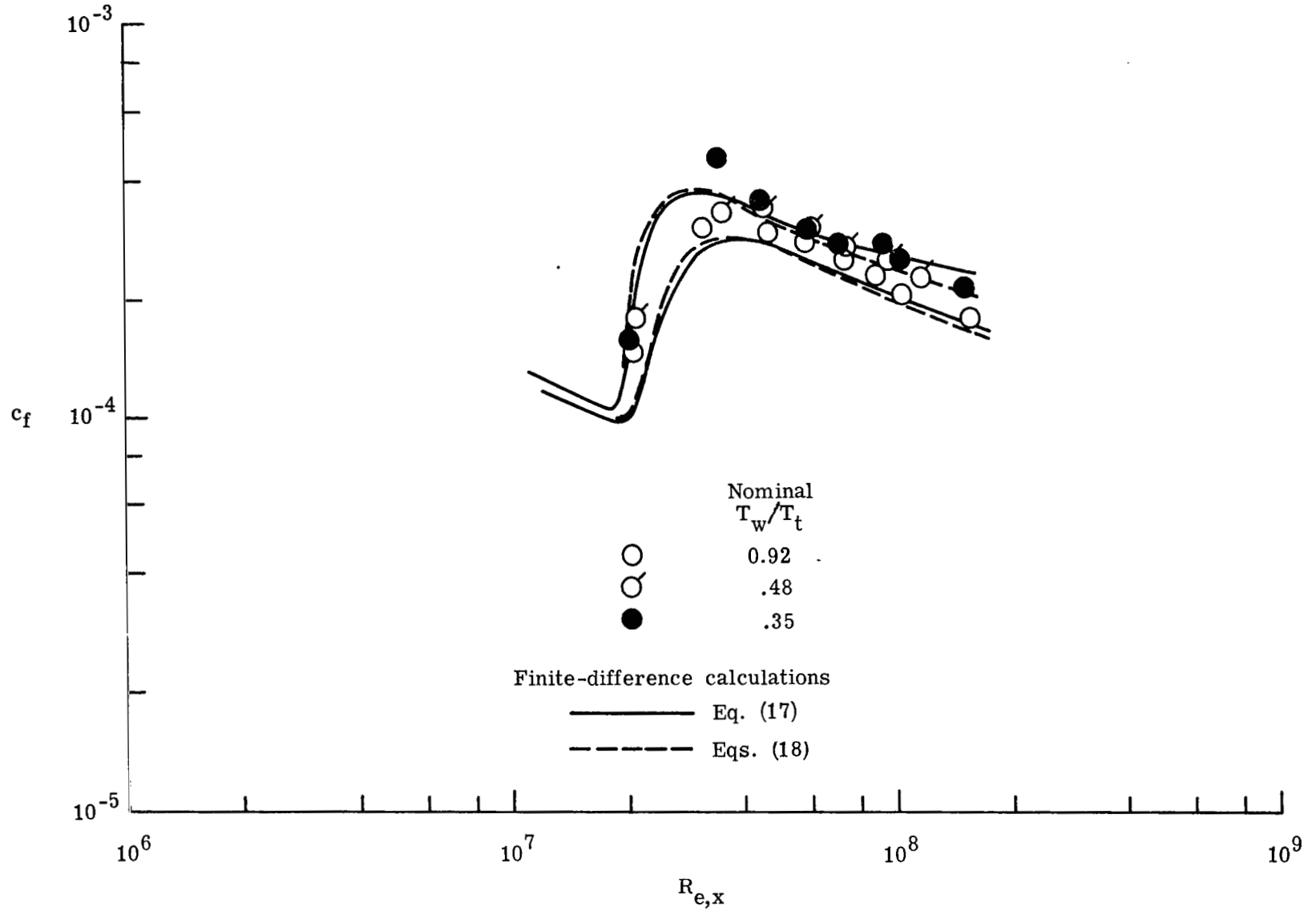
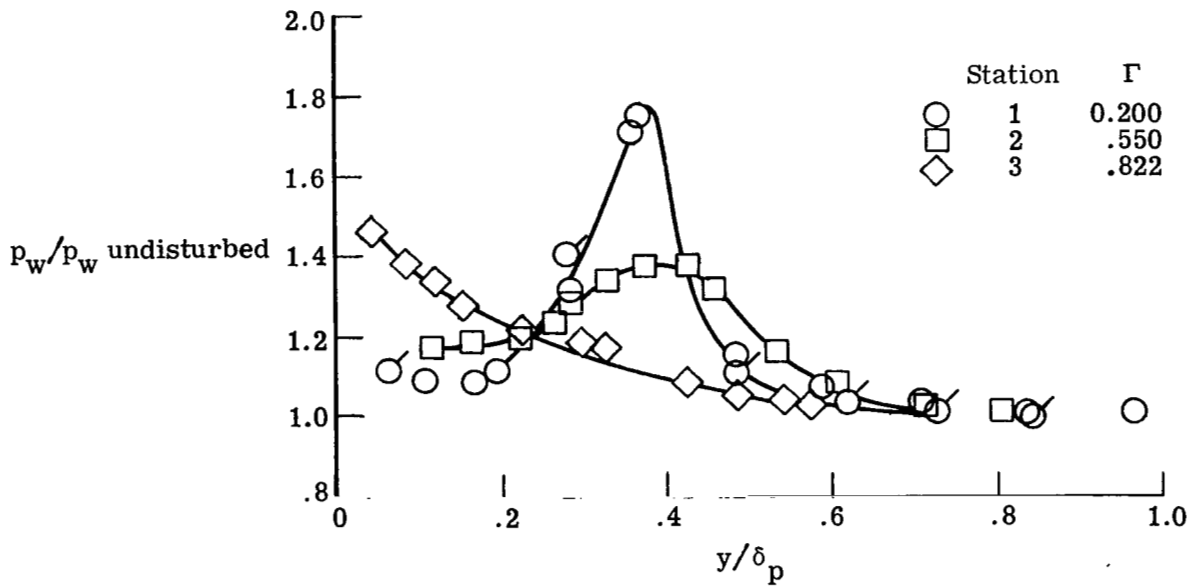
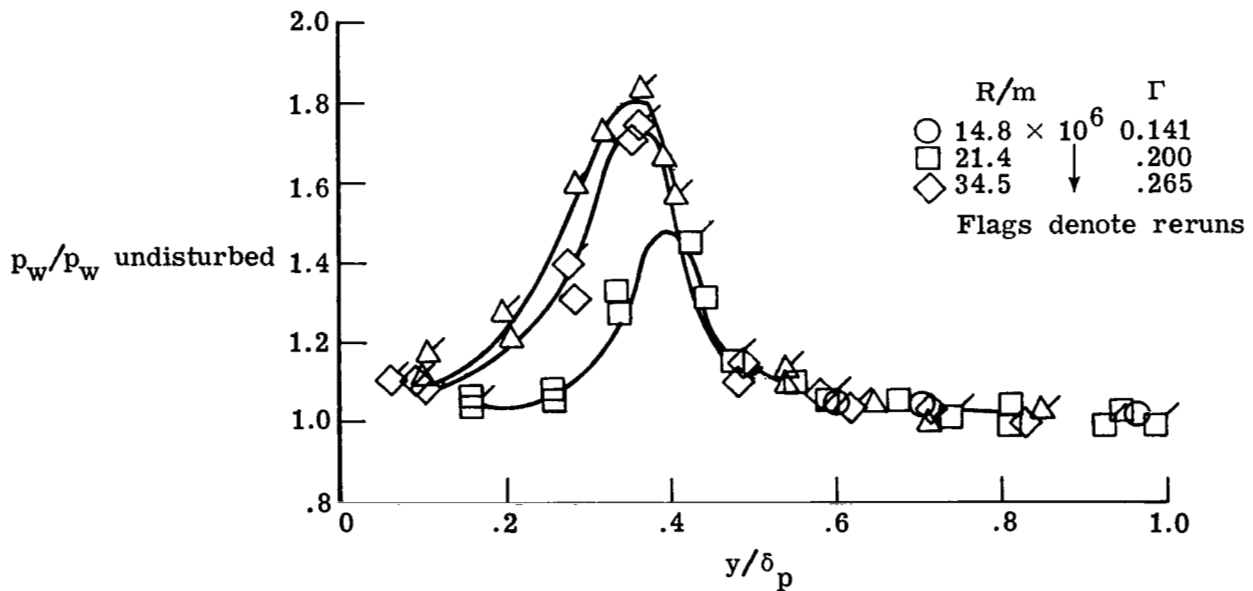


Figure 39.- Comparison of calculated and experimental skin friction on model 2.

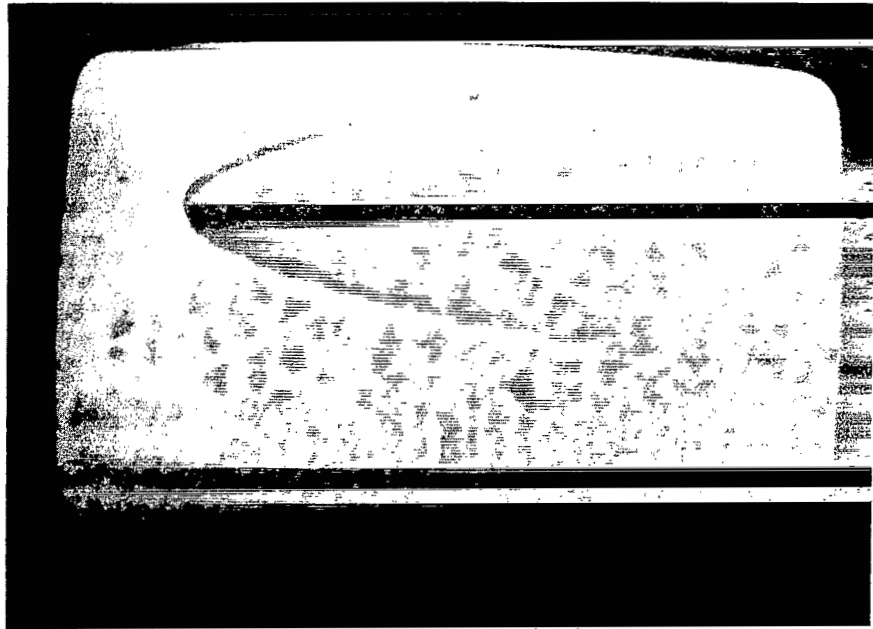


(a) Increasing turbulence at $R_e/m = 28.2 \times 10^6$.

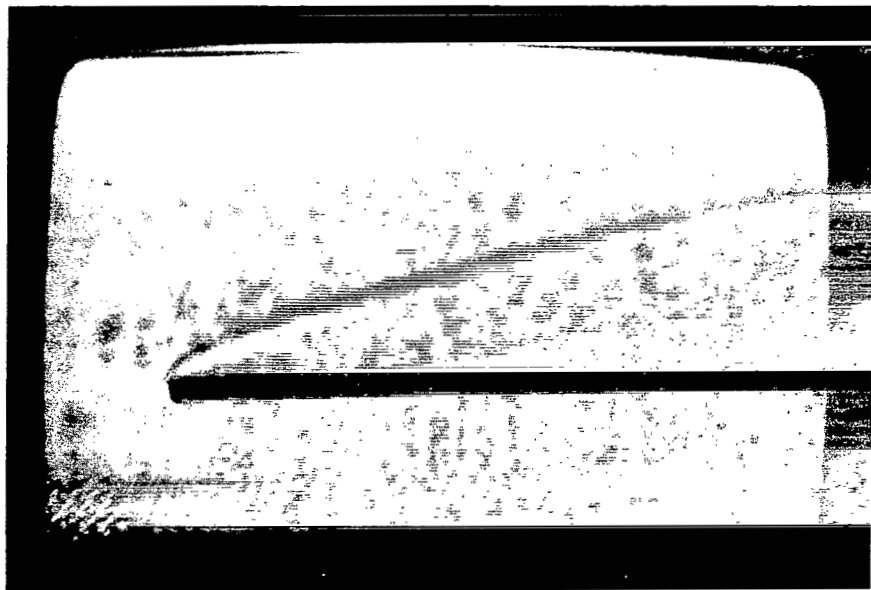


(b) Early transitional flow, increasing unit Reynolds number at station 1.

Figure 40.- Probe interference effects on model 1.



(a) $y = 2.5$ cm; probe outside boundary layer.



(b) $y = 1.23$ cm; probe near outer edge of boundary layer.
L-78-106

Figure 41.- Schlieren photographs of pitot probe traversing the boundary layer on model 2.

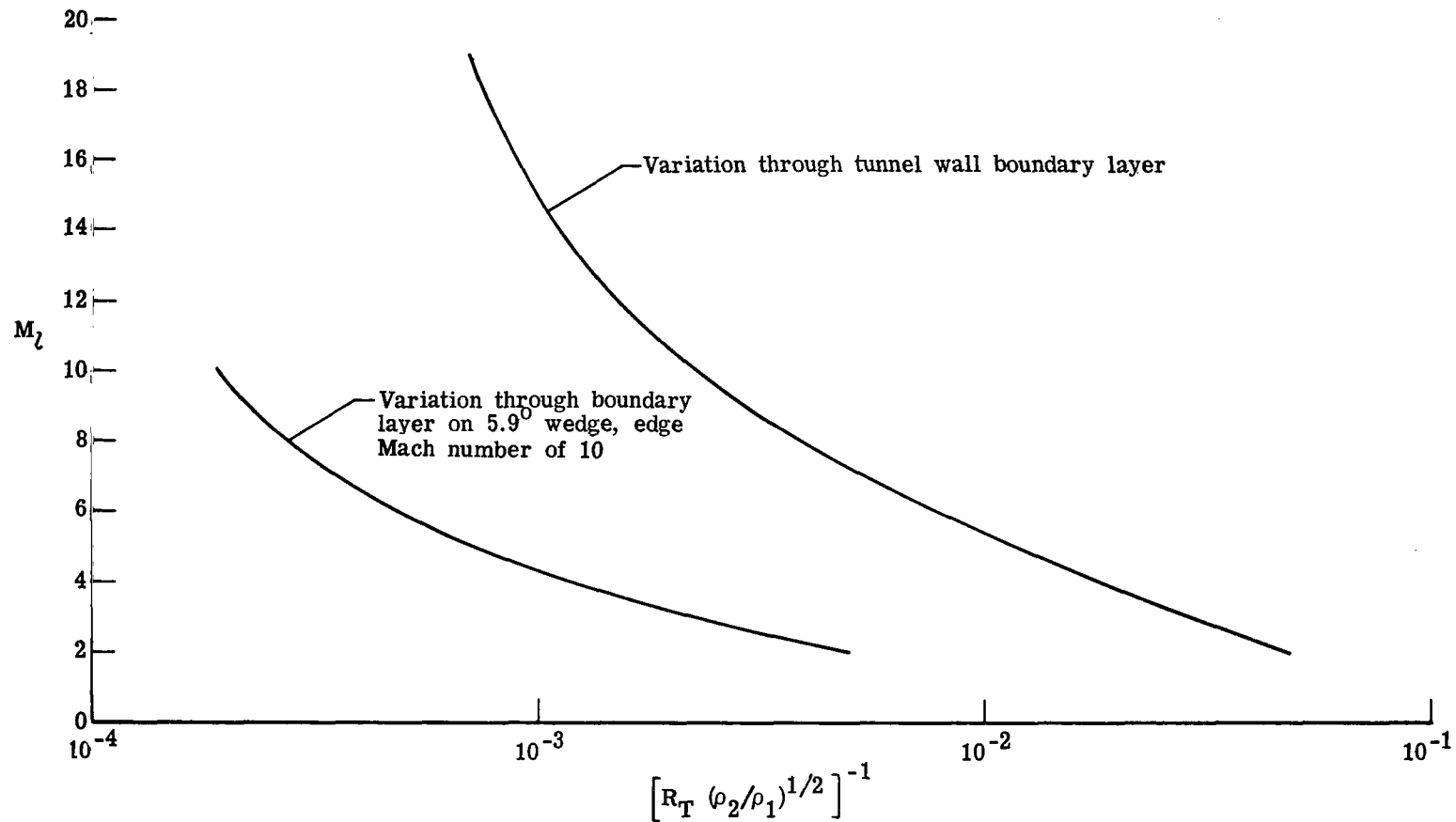


Figure 42.- Variations of pitot correction parameter through boundary layer as a function of local Mach number. $P_{t,1} = 6.9$ MPa; $M_\infty = 19$; $h = 1.0$ mm.

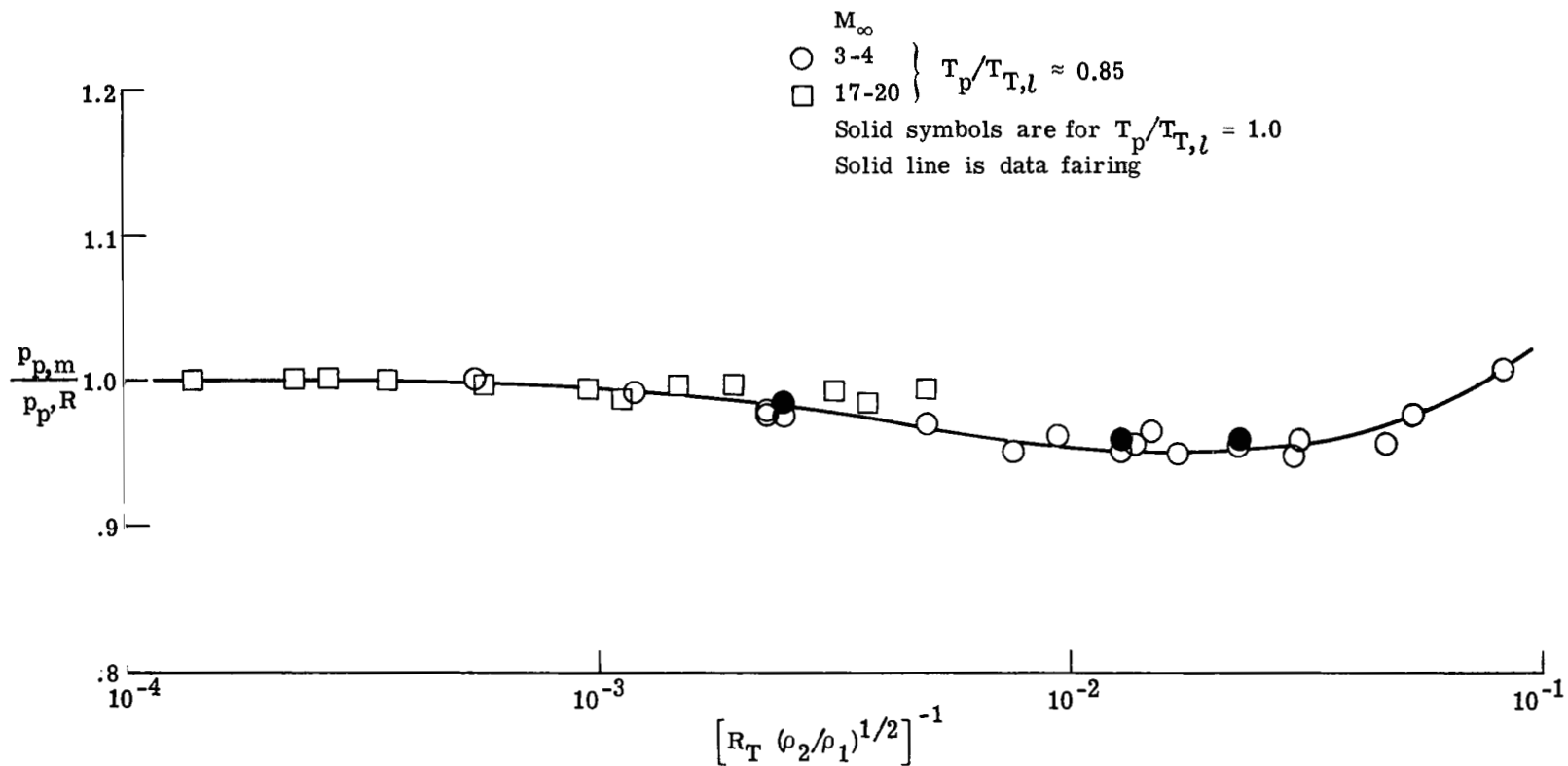


Figure 43.- Viscous and rarefied flow effects on pitot pressure in helium.

1. Report No. NASA TP-1243	2. Government Accession No.	3. Recipient's Catalog No.	
4. Title and Subtitle CHARACTERISTICS OF MACH 10 TRANSITIONAL AND TURBULENT BOUNDARY LAYERS		5. Report Date November 1978	6. Performing Organization Code
		8. Performing Organization Report No. L-12016	10. Work Unit No. 505-06-15-01
7. Author(s) Ralph D. Watson	9. Performing Organization Name and Address NASA Langley Research Center Hampton, VA 23665		11. Contract or Grant No.
12. Sponsoring Agency Name and Address National Aeronautics and Space Administration Washington, DC 20546			13. Type of Report and Period Covered Technical Paper
15. Supplementary Notes Appendix B by Leonard M. Weinstein, Langley Research Center.		14. Sponsoring Agency Code	
16. Abstract Measurements of the mean flow properties of transitional and turbulent boundary layers in helium on 4° and 5° wedges have been made for flows with edge Mach numbers from 9.5 to 11.3, ratios of wall temperature to total temperature of 0.4 to 0.95, and maximum length Reynolds numbers of 100×10^6 . The data include pitot and total-temperature surveys and measurements of heat transfer and surface shear. In addition, with the assumption of local similarity, turbulence quantities such as the mixing length were derived from the mean flow profiles and compared with other data and theory. Low Reynolds number and precursor transition effects were significant factors at these test conditions and were included in finite-difference boundary-layer predictions.			
17. Key Words (Suggested by Author(s)) Hypersonic turbulent boundary layer Pitot and total-temperature data Heat transfer Skin-friction data		18. Distribution Statement Unclassified - Unlimited Subject Category 34	
19. Security Classif. (of this report) Unclassified	20. Security Classif. (of this page) Unclassified	21. No. of Pages 322	22. Price* \$11.75

National Aeronautics and
Space Administration

Washington, D.C.
20546

Official Business

Penalty for Private Use, \$300

SPECIAL FOURTH CLASS MAIL
BOOK

Postage and Fees Paid
National Aeronautics and
Space Administration
NASA-451



2 1 1U,D, 092978 S00903DS
DEPT OF THE AIR FORCE
AF WEAPONS LABORATORY
ATTN: TECHNICAL LIBRARY (SUL)
KIRTLAND AFB NM 87117

NASA

POSTMASTER:

If Undeliverable (Section 158
Postal Manual) Do Not Return
